
Using novel and validated tools to study the
distribution and biosynthesis of brain-derived
neurotrophic factor in the rodent brain

Erin Wosnitzka



A thesis submitted to Cardiff University with the requirements for
the degree of Doctor of Philosophy in the discipline of
Neuroscience

School of Biosciences
Cardiff University

May 2021

In memory of Tracy Sampson

Acknowledgements

I would first like to thank my supervisor, Professor Yves-Alain Barde for his endless enthusiasm for my PhD project. I will always be grateful for the knowledge, advice, and anecdotes you shared with me. I would also like to thank my co-supervisor, Dr. Xincheng Nan, for his unwavering technical support, patience, and belief in my ability. Thank you for the lively debates, laughs, and for always asking the most important questions.

This work would not have been possible without the generous funding of the Cardiff University NMHRI and Boehringer Ingelheim GmbH; I would like to thank them both for making this work possible.

I must also extend huge thanks to Dr. Hayley Dingsdale for generating and purifying the BDNF antibody mAb #9 used in these experiments. Thank you also to Professor Michael Sendtner and colleagues at the University of Würzburg, Germany, for their expert advice on BDNF immunostaining. I would also like to express my gratitude to Dr. Pedro Chacón-Fernández at the Hospital Universitario Virgen Macarena, Spain, for his donation of BDNF-FP plasmids. Thank you also to Eman Amin and Professor John Aggleton at the School of Psychology for their training and advice on animal behaviour experiments. Thanks especially to Eman for completing the Fos immunostaining experiments and subsequent cell counts.

I feel very fortunate to have worked alongside such a talented, driven, and helpful group of people. To every member of the Martinez-Garay, Baudouin and Davies lab – thank you for providing such a productive and positive working environment. I am especially grateful to have worked alongside some incredibly kind and thoughtful individuals: Dr. Laura Cassels, Dr. Hayley Dingsdale, and PhD student Sarah Ateaque - thank you for the endless snacks, laughs, and emotional support.

I am also eternally grateful for my friends in both Bude and Cardiff who have provided unmeasurable support over the past three years. Thank you for always listening to my woes and providing joy and laughter when I needed it most. Finally, I must thank my parents, brother, sister, and partner, Sam. Thank you for always believing in me even when I did not believe in myself - I could never have done this without you.

Summary

Brain-derived neurotrophic factor (BDNF) is a critical modulator of neuronal survival, synaptic transmission, and activity-dependent plasticity. In humans, a single nucleotide polymorphism in the BDNF pro-domain is associated with reduced memory performance, whereas deletion of a single *BDNF* allele results in mental retardation, increased food intake and abnormal weight gain. As the enhancement of BDNF signalling is an attractive therapeutic prospect in the context of brain dysfunction, there is a need for a better understanding of the brain circuitry using BDNF as a quasi-neurotransmitter. The lack of sufficient knowledge about the localisation of BDNF in the brain is largely due to its very low abundance and the lack of reliable tools faithfully reporting its localisation. To circumvent these difficulties, validated BDNF antibodies were used here that reliably detected BDNF expression in the CNS. These antibodies were first used to examine the biosynthesis of the endogenous protein in cultured neurons. The biosynthesis of the wildtype protein was then compared with tagged versions of BDNF using *in vitro* expression systems. These experiments revealed that the addition of large probes widely used in the BDNF field impaired the biological processing and secretion of the mature protein. These *in vitro* experiments also included the validation of a novel *Bdnf* cDNA construct, that was next utilised *in vivo* to generate a viable and fertile mouse model that reports *Bdnf* translation using green fluorescent protein (GFP). Using a novel BDNF localisation strategy, the detection of endogenous BDNF in the neural circuits relevant to spatial memory was also achieved in the rat brain. The contribution of past and present tools toward developing a better understanding of the biology of BDNF in neural circuits is also discussed.

Abbreviations

°C	degrees Celsius
µg	microgram(s)
µl	microlitre(s)
µM	micromolar
µm	micrometre(s)
3'-UTR	3 prime untranslated region
4-AP	4-aminopyridine
5'-UTR	5 prime untranslated region
5HT	5-hydroxytryptamine (serotonin)
aa	amino acid(s)
ABC-HRP	avidin-biotin complex-horseradish peroxidase
AD	anti-depressants
alv	alveus
ANOVA	analysis of variance
AP-1	activator protein-1
AR	antigen retrieval
ASPA	Animals (Scientific Procedures) Act 1986
ATN	anterior thalamic nuclei
AVN	anteroventral nucleus of the thalamus
BaSiC	background and shading correction
BBB	blood-brain barrier
BCA	bicinchoninic assay
<i>BDNF</i>	brain-derived neurotrophic factor (human gene)
<i>Bdnf</i>	brain-derived neurotrophic factor (rodent gene)
BDNF	brain-derived neurotrophic factor

<i>Bdnf</i>^{-/-}	brain-derived neurotrophic factor knock-out
<i>Bdnf</i>^{+/-}	brain-derived neurotrophic factor heterozygote
<i>Bdnf</i>^{+/+}	brain-derived neurotrophic factor wildtype
<i>Bdnf</i> cKO	brain-derived neurotrophic factor conditional knockout
BDNF-GFP	BDNF (tagged with) enhanced green fluorescent protein
BDNF-pHluorin	BDNF (tagged with) super-ecliptic pHluorin
BDNF-mCherry	BDNF (tagged with) mCherry
BDNF-moxVenus	BDNF (tagged with) moxVenus
BDNF-moxGFP	BDNF (tagged with) moxGFP
BDNF-myc-GFP	BDNF (tagged with) myc and enhanced GFP
BDNF-(1-4)myc	BDNF (tagged with) myc
BDNF-P2A-GFP	BDNF (tagged with) a 2a self-cleaving peptide and nuclear-localised enhanced GFP
BDNF-ir	BDNF/pro-peptide immunoreactivity
BMI	body mass index
bp	base pair(s)
BRAF	proto-oncogene B-raf
BSA	bovine serum albumin
CA	cellular aggregate
CA1	cornu ammonis 1
CA1D	dorsal cornu ammonis 1
CA1V	ventral cornu ammonis 1
CA2	cornu ammonis 2
CA3	cornu ammonis 3
CA3D	dorsal cornu ammonis 1
CA3V	ventral cornu ammonis 3
CA4	cornu ammonis 4

cDNA	complementary DNA
CL	cell lysate
CM	conditioned medium
cm	centimetre(s)
CMV	(human) cytomegalovirus
CNS	central nervous system
Cre	cyclic recombinase
C-terminus	carboxyl-terminus
DAB	diaminobenzidine
DAPI	4',6-diamidino-2-phenylindole
DCV	dense core vesicle
ddH₂O	distilled and deionised water
DG	dentate gyrus
DGb	bottom (infralimbic) blade of the dentate gyrus
DGt	top (suprapyramidal) blade of the dentate gyrus
dhc	dorsal hippocampal commissure
DIV	days in vitro
DMEM	Dulbecco's modified Eagle medium
DMEM/F12	Dulbecco's modified Eagle medium/nutrient mixture F12
DMSO	dimethyl sulfoxide
DNA	deoxyribonucleic acid
DRG	dorsal root ganglia
DS	donkey serum
dSub	dorsal subiculum
DTT	dithiothreitol
dysRSC	dysgranular retrosplenial cortex

E	embryonic day
EDTA	ethylenediaminetetraacetic acid
ELISA	enzyme-linked immunosorbent assay
EM	electron microscopy
Emx1	empty spiracles homeobox 1
ER	endoplasmic reticulum
EtBr	ethidium bromide
FACS	fluorescence-activated cell sorting
FBS	foetal bovine serum
FP	fluorescent protein
FRT-FLP	flippase recognition target (sites)-flippase recombination
g	gram(s)
G	gauge
GAPDH	glyceraldehyde 3-phosphate dehydrogenase
GFAP	glial fibrillary acidic protein
GFP	(enhanced) green fluorescent protein
gRSC	granular retrosplenial cortex
GS	goat serum
HA	hemagglutinin
HBSS	Hank's balanced salt solution
HEK293	human embryonic kidney 293
Het/HET	heterozygous
HFS	high frequency stimulation
hil	hilus of the dentate gyrus
Hom/HOM	homozygous
HPF	hippocampal formation

hr	hour
HRP	horseradish peroxidase
ICC	immunocytochemistry
IEG	immediate early gene
IgG	immunoglobulin G
IgY	immunoglobulin Y
IHC	immunohistochemistry
ISH	in situ hybridisation
kbp	kilobasepairs
K_D	dissociation constant
kD	kilodalton(s)
ki/KI	knock-in
K_v	voltage-gated potassium channel
LDCVs	large dense core vesicles
loxP	locus of X(cross)-over in P1
LTD	long-term depression
LTP	long-term potentiation
L-VGCC	L-type voltage gated calcium channel
M	molar
mAb	monoclonal antibody
MAP2	microtubule-associated protein 2
Mapt	microtubule associated protein tau
mBDNF	mature brain-derived neurotrophic factor
MCL	molecular cell layer
MES	2-(n-morpholino)ethanesulfonic acid
mESCs	mouse embryonic stem cells

Met	methionine
MFBs	mossy fibre boutons
mg	milligram(s)
min	minute(s)
MK	megakaryocyte
mm	Millimetre(s)
MMB	medial mammillary bodies
mol	molecular layer
mRNA	messenger ribonucleic acid
MSN	medium spiny neurons
MWM	Morris water maze
n.s.	not significant
ng	nanogram(s)
NGF	nerve growth factor
NLS	nuclear localisation sequence
nM	nanomolar
NMDAR	<i>N</i> -methyl- <i>D</i> -aspartate receptor
NPG	nodose-petrosal ganglion complex
NT-3	neurotrophin-3
NT-4	neurotrophin-4
<i>NTRK2</i>	neurotrophin receptor tyrosine kinase 2 (human TrkB gene)
OCT	optimal cutting temperature compound
P	postnatal day
p	probability value
P2A	2a self-cleaving peptide
p75^{NTR}	p75 neurotrophin receptor

pAb	polyclonal antibody
PBS	phosphate buffered saline
pBDNF	BDNF plasmid
PBS-T	phosphate buffered saline with triton x-100
PC1	proprotein convertase 1
PC7	proprotein convertase 7
PCL	pyramidal cell layer
PCR	polymerase chain reaction
<i>Pcsk1/3</i>	proprotein convertase (subtilisin/kexin type) 1
<i>Pcsk7</i>	proprotein convertase (subtilisin/kexin type) 1
Pen Strep	penicillin streptomycin
PF4	platelet factor 4
PFA	paraformaldehyde
pg	picogram(s)
pir	piriform layer
PLA	proximity ligation assay
PNS	peripheral nervous system
pol	polymorph layer
poly(A)	poly(adenine)
pro-BDNF	Pro-brain-derived neurotrophic factor
Pur	puromycin resistance cassette
RAM	radial arm maze
rBDNF	recombinant brain-derived neurotrophic factor
RIPA	radioimmunoprecipitation assay
rpm	revolutions per minute
rpro-BDNF	recombinant pro-brain derived neurotrophic factor

RSC	retrosplenial cortices
RT	room temperature
RTK	receptor tyrosine kinase
s	second(s)
SCG	superior cervical ganglion
SDS	sodium dodecyl sulphate
SDS-PAGE	sodium dodecyl sulphate-polyacrylamide gel electrophoresis
SEM	standard error of the mean
SEP	super-ecliptic pHluorin
SERCA	sarcoendoplasmic reticulum transport ATPase
SL	stratum lucidum
SM1	stem cell modified-1
SNP	single nucleotide polymorphism
SO	stratum oriens
SR	stratum radiatum
SSRI	selective serotonin reuptake inhibitor
SV40	simian vacuolating virus 40
TAE	tris-aminomethane base, acetic acid and ethylenediaminetetraacetic acid
TBS	tris-buffered saline
TBS-T	tris-buffered saline with 0.1% Tween® 20
TGN	trans-golgi network
TMEM-119	transmembrane protein-119
TNF	tumour necrosis factor
tPA	tissue plasminogen activator
Tris	tris-aminomethane
Trk(A/B/C)	tropomyosin receptor kinase (A/B/C)

<i>TrkB</i>	tropomyosin receptor kinase B (rodent gene)
<i>TrkB</i>^{-/-}	tropomyosin receptor kinase B knockout
UTR	untranslated region
V	volts
Val	valine
w/v	% weight per volume
WAGR	Wilms tumour, aniridia, genitourinary abnormalities and mental retardation
wt/WT	wildtype

Contents

Chapter 1. General Introduction	1
1.1 Overview	1
1.2 The neurotrophins	2
1.2.1 The discovery of nerve growth factor (NGF)	2
1.2.2 The neurotrophin family: NGF, BDNF, NT-3 and NT-4.....	3
1.3 The neurotrophin receptors.....	5
1.3.1 TrkA, TrkB and TrkC.....	5
1.3.2 The p75 neurotrophin receptor (p75 ^{NTR}).....	5
1.4 BDNF	8
1.4.1 Transcriptional regulation of <i>Bdnf</i>	8
1.4.2 BDNF localisation in neuronal and non-neuronal cells	9
1.4.3 BDNF biosynthesis	10
1.4.4 The physiology of BDNF.....	14
1.4.5 BDNF-associated pathophysiology	16
1.5 Research aims.....	19
Chapter 2. Methods and Materials	20
2.1 BDNF plasmids.....	20
2.1.1 WT BDNF	20
2.1.2 BDNF-(1-4)myc and BDNF-myc-eGFP	20
2.1.3 BDNF-GFP and BDNF-P2A-(SV40-NLS)GFP	20
2.1.4 BDNF-SEP (pHluorin).....	20
2.1.5 BDNF-mCherry, BDNF-moxVenus and BDNF-moxGFP	21
2.2 Culture and transfection of HEK293 cells.....	21
2.2.1 Maintenance and culture of HEK293 cells	21
2.2.2 Transfection of HEK293 cells.....	21
2.3 Mouse strains	22
2.3.1 Animal husbandry.....	22
2.3.2 C57BL/6	22

2.3.3	<i>Bdnf</i> knockouts (<i>Bdnf</i> ^{-/-})	22
2.3.4	<i>Bdnf-P2a-Gfp</i> mice	23
2.4	Genotyping	23
2.4.1	DNA extraction and polymerase chain reaction (PCR).....	23
2.4.2	PCR product gel electrophoresis	23
2.5	Rats.....	26
2.5.1	Animal husbandry.....	26
2.6	Rat behavioural paradigm.....	26
2.6.1	Apparatus	26
2.6.2	Animal handling and procedure	28
2.7	Immunohistochemistry (IHC)	29
2.7.1	Paraformaldehyde fixation of rat and mouse brains	29
2.7.2	Tissue sectioning.....	30
2.7.3	Fos staining	30
2.7.4	Antigen retrieval.....	30
2.7.5	Immunofluorescence	31
2.8	Image capture, quantification, and analysis	34
2.8.1	Primary cortical cultures	34
2.8.2	<i>Bdnf-P2a-Gfp</i> brain sections.....	34
2.8.3	Rat brain sections.....	34
2.9	Adult brain dissection.....	37
2.10	Western blotting.....	37
2.10.1	Protein extraction and quantification	37
2.10.2	Gel electrophoresis and membrane transfer	38
2.10.3	Protein detection.....	38
2.10.4	Confirmation of equal protein loading and transfer.....	39
2.11	BDNF enzyme-linked immunosorbent assay (ELISA)	41
2.12	Primary cortical cultures	41
2.12.1	Preparation of culture dishes	41
2.12.2	Tissue dissection	41

2.12.3	Culture of CNS neurons.....	42
2.12.4	Transfection of neuronal cultures.....	42
2.12.5	TrkB phosphorylation assays.....	43
2.13	Immunocytochemistry (ICC)	43
2.13.1	Preparation of coverslips	43
2.13.2	Immunofluorescence	43
2.14	Statistical analyses	46
2.14.1	<i>In vitro</i> experiments	46
2.14.2	<i>Bdnf-P2a-Gfp</i> animals	46
2.14.3	Fos and BDNF-ir in rat brain.....	46
Chapter 3.	Revisiting the processing and localisation of BDNF in neuronal cells.....	47
3.1	Short Introduction	47
3.2	Results	49
3.2.1	Validation of BDNF immunostaining in fixed cells and brain tissue	49
3.2.2	Using monoclonal antibodies to detect changes in endogenous BDNF expression by cultured cells.....	51
3.2.3	Comparing the localisation of overexpressed and endogenous BDNF in cortical cultures.....	53
3.2.4	Validation of a new monoclonal antibody for BDNF western blots	55
3.2.5	Changes to BDNF processing after increased cellular activity	57
3.3	Summary and conclusions.....	59
Chapter 4.	Investigating the biological activity of BDNF fusion proteins	61
4.1	Short introduction	61
4.2	Results	63
4.2.1	Screening cDNA constructs encoding BDNF fusion proteins in HEK293 cells	63
4.2.2	BDNF-GFP fails to be efficiently secreted by HEK293 cells.....	68
4.2.3	Increasing tag lengths compromises the ability of BDNF to phosphorylate TrkB	70
4.2.4	Investigating the cellular distribution of BDNF-fusion proteins in cultured neurons	73

4.3	Summary and conclusions.....	75
Chapter 5.	Characterisation of mice expressing <i>Bdnf-P2a-Gfp</i> instead of <i>Bdnf</i>	78
5.1	Short introduction	78
5.2	Results	79
5.2.1	Generation of the <i>Bdnf-P2a-Gfp</i> mouse.....	79
5.2.2	Phenotypic characterisation of <i>Bdnf-P2a-Gfp</i> littermates.....	81
5.2.3	BDNF levels are unchanged in the hippocampus and cerebral cortex of <i>Bdnf-P2a-Gfp</i> mice	83
5.2.4	Optimising protocols for BDNF and GFP immunostaining on mouse brain sections	85
5.2.5	BDNF immunoreactivity in the hippocampus of <i>Bdnf-P2a-Gfp</i> mice is consistent with BDNF WT animals.....	87
5.2.6	GFP faithfully reports activity dependent increases in BDNF in cultured cortical neurons	91
5.2.7	The extrahippocampal distribution of GFP in the <i>Bdnf-P2a-Gfp</i> brain is consistent with previous <i>Bdnf in-situ</i> hybridisation studies	93
5.2.8	GFP is not expressed by microglial cells.....	95
5.3	Summary and conclusions.....	97
Chapter 6.	Optimising BDNF detection in rat brain circuits in a memory relevant paradigm	99
6.1	Short Introduction	99
6.2	Results	104
6.2.1	mBDNF is the most abundant BDNF protein within rat brain.....	104
6.2.2	Using monoclonal antibodies to improve BDNF immunostaining in rat brain sections	106
6.2.3	Probing rat brain sections using antibodies against BDNF or its pro-peptide result in the same patterns of immunoreactivity	108
6.2.4	BDNF immunoreactivity is markedly enhanced when sections are probed using both BDNF antibodies	110
6.2.5	BDNF-ir was also detectable in the extrahippocampal correlates of memory previously mapped by Fos staining.....	112

6.2.6	Both BDNF and Fos are readily detectable in the hippocampi of animals subjected to a spatial memory task.....	114
6.2.7	Rats performing the spatial memory task failed to show the expected changes in Fos expression	116
6.2.8	No change in BDNF-ir was detected in the hippocampi of animals exposed to spatial learning	118
6.3	Summary and conclusions.....	120
Chapter 7.	General Discussion	122
7.1	Summary of the main findings	122
7.2	Characterising the processing and localisation of BDNF proteins by neuronal cells	122
7.2.1	The limitations of <i>in vitro</i> overexpression systems	123
7.2.2	Understanding the physiological role of pro-BDNF and the cleaved pro-peptide	124
7.3	The biological relevance of BDNF-fusion proteins	126
7.4	The generation of a novel mouse line that reports BDNF translation by the co-expression of GFP	130
7.5	Studying mechanisms of <i>Bdnf</i> regulation within brain	131
7.6	Outlook.....	132

Figures

Figure 1.1. Interactions of the pro- and mature neurotrophins with the Trk receptors and p75 ^{NTR}	6
Figure 1.2. The intracellular processing of mature BDNF by CNS neurons under physiological conditions.	12
Figure 1.3. The biochemical processing of pre-, pro-, and mature BDNF.....	13
Figure 2.1 A scheme representing the two radial arm mazes employed in the rat behavioural paradigm.	27
Figure 2.2 Images from confocal imaging before and after BaSiC correction.	36
Figure 3.1. Validation of BDNF immunostaining in fixed cells and brain tissue.....	50
Figure 3.2. Activity dependent increases in BDNF in cultured cortical neurons.	52
Figure 3.3. Endogenous and vector driven BDNF expression in young neuronal cultures.	54
Figure 3.4. Validation of monoclonal antibody 3C11 for western blot.	56
Figure 3.5. Determining the relative abundance of pro- and mature endogenous BDNF in cultured neurons.	58
Figure 4.1. The processing and secretion of BDNF-fusion proteins by HEK293 cells..	67
Figure 4.2. Further analysis of BDNF-GFP, BDNF-pHluorin and BDNF-P2A-GFP in HEK293 cells.	69
Figure 4.3. Increasing the length of BDNF fusion proteins attenuates their ability to phosphorylate TrkB.....	72
Figure 4.4. Visualising of the distribution of BDNF, GFP and pHluorin in transfected primary neurons.....	74
Figure 4.5. Annotated amino acid sequences of the C-terminal tags of BDNF-GFP, BDNF-pHluorin, and novel construct BDNF-P2A-GFP.....	77
Figure 5.1. Schematics illustrating the insertion of <i>Bdnf-P2a-Gfp</i> into the endogenous <i>Bdnf</i> allele in mouse ESCs (mESCs).	80
Figure 5.2. Early characterisation of <i>Bdnf-P2a-Gfp</i> littermates.....	82

Figure 5.3. Monoclonal antibody 3C11 detects WT BDNF and BDNF-P2A in hippocampal extracts.....	84
Figure 5.4. Probing of BDNF WT brain sections with antibodies against BDNF and GFP.	86
Figure 5.5. BDNF and GFP immunoreactivity in the brains of <i>Bdnf-P2a-Gfp</i> mice.	88
Figure 5.6. GFP immunoreactivity in the <i>Bdnf-P2a-Gfp</i> hippocampus (as used for quantification studies).....	90
Figure 5.7. Activity dependent increases in BDNF and GFP in cortical neurons.....	92
Figure 5.8. Cells translating BDNF in the cerebral cortex of <i>Bdnf-P2a-Gfp</i> mice.	94
Figure 5.9. Microglial cells in the <i>Bdnf-P2a-Gfp</i> cortex do not express detectable levels of GFP.....	96
Figure 6.1. Connectivity between the hippocampus and the extrahippocampal correlates of memory.....	101
Figure 6.2. Western blotting for BDNF proteins in hippocampus of home cage control rats.	105
Figure 6.3. Proposed strategy for enhancing BDNF immunoreactivity in rat brain sections fixed using 4% PFA.	107
Figure 6.4. Localisation of BDNF and its pro-peptide in the hippocampus.....	109
Figure 6.5. Enhanced immunoreactivity of BDNF-containing vesicles in the rodent hippocampus when combining anti-BDNF #9 and anti-pro-peptide 5H8.	111
Figure 6.6. BDNF staining in the extrahippocampal correlates of memory.	113
Figure 6.7. mBDNF/pro-peptide and Fos immunoreactivity in the hippocampus of control rats.	115
Figure 6.8. Fos positive cell counts in the hippocampus of rats performing a spatial memory task.	117
Figure 6.9. A comparison of Fos counts and BDNF-ir in the hippocampus of control versus experimental rats.....	119
Figure 7.1. A comparison of the immunoreactivity of endogenous BDNF with the GFP signal observed in <i>Bdnf-Gfp</i> knock-in mice.	129

Tables

Table 2.1 PCR conditions for the genotyping of mouse strains.....	25
Table 2.2 Primary antibodies used in immunohistochemistry experiments.....	32
Table 2.3 Secondary antibodies used in immunohistochemistry (IHC) experiments....	33
Table 2.4 Primary antibodies used in western blot experiments.....	40
Table 2.5 Secondary antibodies used in western blot experiments.	40
Table 2.6 Primary antibodies used in immunocytochemistry experiments.....	45
Table 2.7 Secondary antibodies used in immunocytochemistry experiments.	45
Table 4.1. BDNF cDNA constructs, their translational products and predicted molecular weights.	64
Table 5.1. Quantification of GFP signal intensity in the hippocampus of <i>Bdnf-P2a-Gfp</i> mice.....	90

Chapter 1. General Introduction

1.1 Overview

Growth factors are secretory proteins typically expressed at low concentrations. They exert their effects by binding to specific receptors on neighbouring cells, which upon activation initiate specific intracellular signalling cascades. One of the most studied growth factors in the central nervous system (CNS) is brain-derived neurotrophic factor (BDNF). It transduces its trophic effects by activating a receptor designated tropomyosin receptor kinase (TrkB). This activation regulates several intracellular processes that are critical for the function of the nervous system, including the regulation of synaptic plasticity. While the relevance of BDNF to brain function is well appreciated, its low abundance in the brains of all vertebrates examined makes its localisation within neurons and their processes challenging. As a result, still little is known about the delineation of neuronal circuits involving BDNF, and its localisation within neurons. To circumvent this problem, multiple studies have resorted to the overexpression of tagged BDNF cDNAs within transfected neurons, whereby its processing and distribution is typically examined through tags added to BDNF's C-terminus. However, the use of tags, especially when attached to small proteins such as BDNF, raises principal questions of whether or not such modifications alter the biochemistry of the tagged protein. Moreover, the distribution of over-expressed proteins using cDNAs needs to be compared to that of the endogenous protein, a challenging task for any factor expressed and active at low concentrations. These challenges are addressed in detail in the following chapters, which also include the validation of a new strategy that aims to report BDNF expression by translation of green fluorescent protein from the same mRNA.

1.2 The neurotrophins

1.2.1 The discovery of nerve growth factor (NGF)

In 1909, Marian L. Shorey made the early observation that the unilateral removal of a limb in the developing chick embryo impairs the development of the sensory and motor neurons that would have innervated that limb (Shorey 1909). A decade later, experiments on urodele larva by Samuel Detwiler showed a similar loss of sensory neurons following limb extirpation, and interestingly, that “hyperplasia” of the same ganglia occurred when ectopic limb buds were transplanted near the developing spinal cord (Hollyday and Hamburger 1976). Both Shorey and Detwiler’s findings were replicated in subsequent work by Viktor Hamburger and Rita Levi-Montalcini, who confirmed a loss of sensory and motor neurons in the spinal cord and dorsal root ganglia (DRG) respectively when wing buds were removed from developing chick embryos (Hamburger 1934; Hamburger and Levi-Montalcini 1949). Concurrently, Elmer Bueker, a PhD student with Hamburger, observed that transplantation of mouse sarcoma line 180 into developing chick embryos diverted the development of sensory and sympathetic axons towards the tumour cells from their physiological targets (Bueker 1948). This observation led Levi-Montalcini to hypothesise that sarcoma cells may secrete a diffusible agent triggering nerve growth. This revolutionary interpretation was soon supported by *in vitro* experiments where cultured DRG cells exhibited neurite outgrowth after incubation with sarcoma line 180 or prepared extracts from line 37 (Levi-Montalcini and Hamburger 1951; Cohen et al. 1954). In 1960, the responsible factor (named nerve growth factor, NGF) was isolated from mouse submandibular gland by Stanley Cohen and Levi-Montalcini, who in quick succession generated an NGF anti-serum that blocked its biological activity. Injections of this anti-serum into murine neonates led to a substantial loss of sympathetic neurons of the superior cervical ganglion (SCG) (Cohen 1960). These key early studies thus demonstrated that specific neuronal subsets, in this case developing sympathetic neurons, require specific diffusible factors during development. Even though the death of developing neurons (later called “naturally occurring cell death”) had already been observed and reported during normal development by Levi-Montalcini and Hamburger, as well as the accentuation of this phenomenon by limb bud extirpation, it took an additional few decades to understand that the main function of NGF was to actually prevent normally occurring cell death (Hamburger et al. 1981). It was then hypothesised, and subsequently demonstrated, that early in development, neurons are generated in excess to ensure that distal tissues are adequately innervated. The localisation of limiting quantities of NGF in tissues innervated by NGF-dependent neurons finally explained the target dependency for survival of

developing neurons. This mechanism ensures that innervation is neither too sparse nor abundant for optimal tissue function in the mature organism (Korsching and Thoenen 1983). A number of experiments in the peripheral nervous system (PNS) have both tested and validated this hypothesis, including the overexpression of NGF solely within target tissues that resulted in the hyperinnervation of the tissue in question (Edwards et al. 1989). Whilst this mechanism is well documented in the PNS and also applies to the non-NGF neurotrophins (see below), it is still unclear whether or not similar mechanisms operate in the CNS under physiological conditions, in the absence of lesion such as axotomy.

1.2.2 The neurotrophin family: NGF, BDNF, NT-3 and NT-4

Clear evidence of NGF's role in PNS development inspired others to identify factors that may exert similar effects in NGF-unresponsive neuronal populations, including CNS neurons. In 1982, a factor of low abundance with the ability stimulate chick DRG outgrowth and survival was isolated from pig brain (Barde et al. 1982), now known as brain-derived neurotrophic factor (BDNF). Whilst BDNF was first purified using a cell survival assay, the sequencing of this novel, biologically active protein indicated a 50% sequence homology with NGF, including a similar spacing of the cysteine residues (Leibrock et al. 1989). BDNF's specificity of action was clearly illustrated following the demonstration that BDNF promoted the survival of nodose ganglion neurons not supported by NGF. Conversely, BDNF could not support the survival of neurons dependent on NGF for survival such as sympathetic neurons. Interestingly, some populations of PNS neurons relied on the additive effects of BDNF and NGF, indicating that each factor induces trophic signalling mechanisms through its own receptor (Lindsay et al. 1985; Leibrock et al. 1989). The identification of closely related sequences in NGF and BDNF greatly facilitated the cloning of related factors. Using primers targeting conserved sequence between these two factors in the polymerase chain reaction (PCR) (Hohn et al. 1990; Jones and Reichardt 1990; Maisonpierre et al. 1990a; Rosenthal et al. 1990) or by homology cloning (Kaisho et al. 1990), two additional members of the neurotrophin family were identified in mammals, neurotrophin-3 (NT-3) and neurotrophin-4 (NT-4). Each secreted mature neurotrophin has a 50% homology in primary sequence, similar isoelectric point (between 9 and 10) and molecular weight (13.2 – 15.9 kD) (Mowla et al. 2001). All four proteins comprise of six cysteine residues conserved in the same relative position, giving rise to three intra-chain disulphide bonds and a cysteine knot structure (McDonald et al. 1991) a new fold subsequently also identified in additional secretory proteins (Sun and Davies, 1995). Their functional diversity arises from peptide loop regions of low sequence similarity which also determines their affinity for each Trk receptor (McDonald et al. 1991; Robinson et al.

2008). In solution, neurotrophins exist as non-covalently bound homodimers, stabilised by large surfaces composed of highly conserved hydrophobic residues (McDonald and Blundell 1991; Holland et al. 1994).

1.3 The neurotrophin receptors

Neurotrophins exert their distinct biological effects by binding to two different classes of transmembrane dependence receptor, the tropomyosin receptor kinase (Trk) receptors and the p75 neurotrophin receptor (p75^{NTR}).

1.3.1 TrkA, TrkB and TrkC

Neurotrophins prevent programmed cell death by activating one of three Trk receptors (Davies 1994). These transmembrane glycoproteins are ~140 kD members of the receptor tyrosine kinase (RTK) family and each share a sequence homology of ~40 – 45% (Ultsch et al. 1999). Each receptor preferentially binds different neurotrophins, as NGF selectively binds to TrkA, BDNF and NT-4 to TrkB, and NT-3 to TrkC (Berkmeier et al. 1991; Lamballe et al. 1991; Squinto et al. 1991; summarised in Figure 1.1). Neurotrophins interact with Trk by their extracellular immunoglobulin-like domain, activating receptor dimerization and the autophosphorylation of tyrosines in their kinase domain (Meakin and Shooter 1991; Urfer et al. 1995). Kinase phosphorylation then enables recruitment of intracellular adapter proteins, coupling receptor-ligand binding to the activation of cascades regulating gene transcription.

1.3.2 The p75 neurotrophin receptor (p75^{NTR})

The 75 kD p75 neurotrophin receptor (p75^{NTR}) was identified by expression cloning by two groups working in parallel and was the first member of the tumour necrosis factor (TNF) receptor superfamily to be identified (Chao et al. 1986; Radeke et al. 1987). Unlike the Trk receptors, p75^{NTR} has no intrinsic enzymatic activity (Yan and Chao 1991; Baldwin et al. 1992). It binds all neurotrophins with nanomolar affinities ($K_D = 10^{-9}$ M) to activate pro-apoptotic or pro-survival signalling cascades, depending on the cellular context (Rodriguez-Tebar et al. 1990; Rodriguez-Tebar et al. 1991; Barrett and Bartlett 1994). Interestingly, the pro-neurotrophins (see below) bind to p75^{NTR} with higher affinity than mature neurotrophins ($K_D = 10^{-11}$ M) (Lee et al. 2001), whereby studies using furin-resistant pro-neurotrophins indicated that all four pro-proteins mediate cell death through p75^{NTR} when co-expressed with Sortilin, thought to act as a death-determining co-receptor governing the pro-apoptotic signal induced by pro-protein-p75^{NTR} interactions (Nykjaer et al. 2004; Teng et al. 2005).

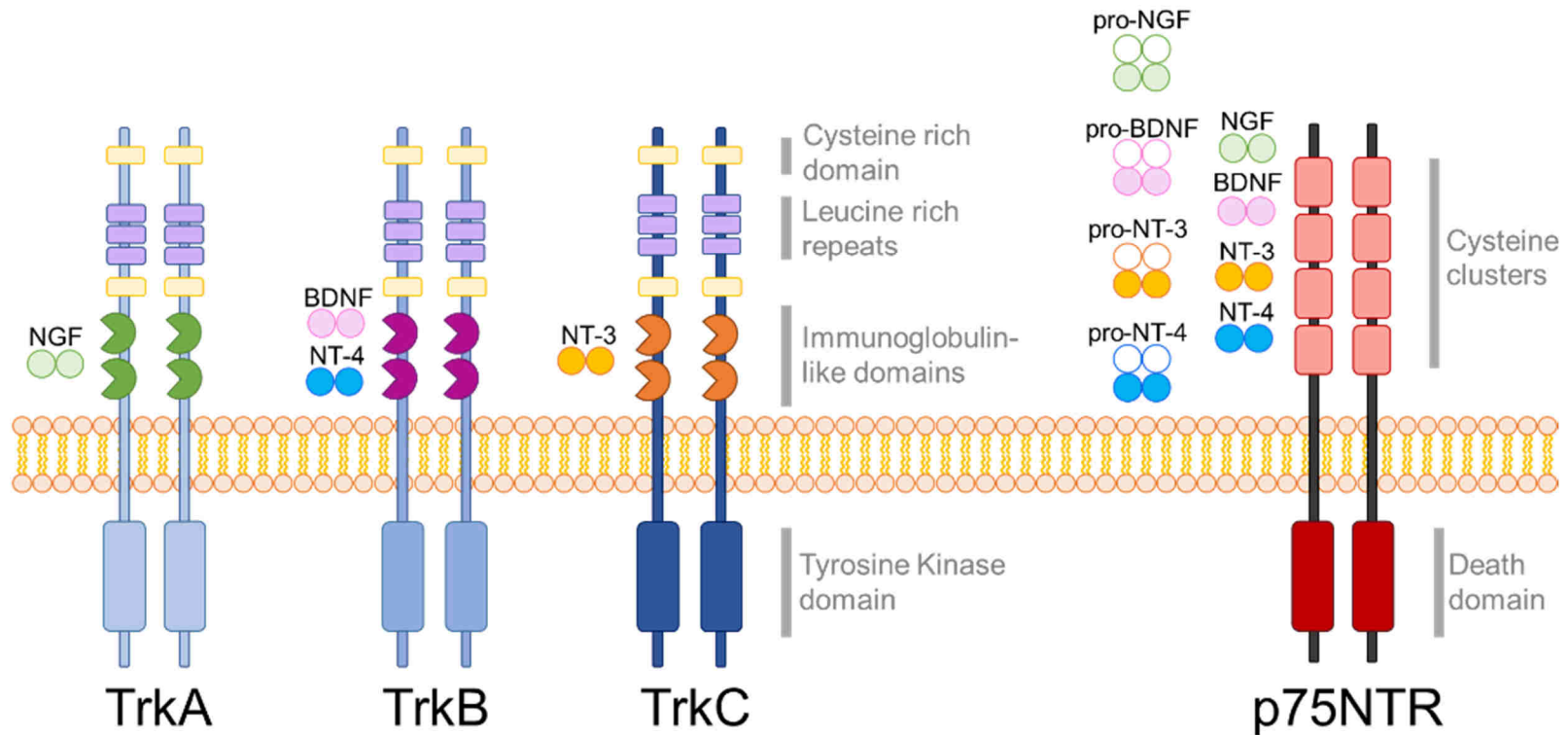


Figure 1.1. Interactions of the pro- and mature neurotrophins with the Trk receptors and p75^{NTR}.

Each Trk receptor comprises an extracellular, transmembrane, and intracellular domain. The extracellular domain comprises two cysteine-rich domains, a leucine-rich repeat and two immunoglobulin-like domains. The mature neurotrophins bind at the immunoglobulin-like domains to activate autophosphorylation at tyrosine residues in their intracellular domains. Mostly, the p75^{NTR} extracellular domain consists mostly of cysteine clusters, shown to form interactions with all pro- and mature neurotrophins. Both the Trk and p75^{NTR} receptors form homodimers but can also form heterodimers at high concentrations. Although its functional significance is not yet fully understood, p75^{NTR} has been shown to induce cell death both with and without ligand binding. TrkA and TrkC can also induce cell death in a similar manner, but TrkB, the BDNF receptor, does not (adapted from Sánchez -Sánchez and Arévalo, 2017).

p75^{NTR} plays an important role in both neuronal survival and programmed cell death. As the nervous system matures it is markedly downregulated in all areas with exception of cholinergic neurons of the basal forebrain (Barrett and Bartlett 1994; Barrett et al. 2005). During development, p75^{NTR} is often, but not always, co-expressed with Trk receptors. In the absence of Trk, p75^{NTR} induces apoptosis even without ligand (Rabizadeh et al. 1993; von Bartheld et al. 1994). In contrast, co-transfection of receptor cDNAs shows that p75^{NTR} interacts with all three RTKs to modulate their affinity and kinase activity, and that neurotrophin induced cell-death is absent in cells co-expressing the ligand's cognate RTK and p75^{NTR} (Rabizadeh et al. 1993; Bibel et al. 1999; Eggert et al. 2000). Interestingly, in the adult brain, p75^{NTR} expression is upregulated in multiple types of neurodegenerative disease. The receptor can bind the toxic β -amyloid peptide characteristic of Alzheimer's Disease ($K_D = 10^{-10}$ M) and is thought to contribute to the Alzheimer's disease-mediated neuronal apoptosis of cholinergic neurons (Yaar et al. 1997).

1.4 BDNF

1.4.1 Transcriptional regulation of *Bdnf*

Early *in situ* hybridisation experiments indicated that in the brain, *Bdnf* and *Ngf* mRNAs are predominantly expressed by neurons, raising the possibility that neuronal activity drives their synthesis (Hofer et al. 1990; Zafra et al. 1990; Zafra et al. 1991). The depolarisation of hippocampal neurons *in vitro* then directly demonstrated that activity-driven increases in *Bdnf* expression occur in a calcium (Ca^{2+})-dependent manner, relying on the actions of *N*-methyl-D-aspartate glutamate receptors (NMDAR) and L-type voltage-gated calcium channels (L-VGCC) (Greer and Greenberg 2008). This increase was also observed *in vivo*, where seizure-related activity resulted in increased *Bdnf* transcription and mRNA levels in the rodent hippocampus (Zafra et al. 1990; Ernfors et al. 1991; Isackson et al. 1991; Ghosh et al. 1994; Castrén et al. 1998).

The current understanding of activity dependent *Bdnf* expression is largely based on the characterisation of the BDNF gene locus by Timmusk, Greenberg and colleagues who showed that the human (*BDNF*) and rodent (*Bdnf*) BDNF gene share eight 5' non-coding exons and one 3' coding exon that contains the open reading frame (ORF) for the pre-protein (Timmusk et al. 1993b; Pruunsild et al. 2007; Greenberg et al. 2009). Across species, each exon is differentially regulated by a unique promoter to produce a transcript containing one of eight 5' untranslated regions (UTR) spliced to the 3' coding sequence. While the functional relevance of each promoter is not yet completely understood, the activity- or stimulus-dependent expression of distinct mRNAs is thought to allow *Bdnf* to exert pleiotropic effects in a diverse range of cell types (Greenberg et al. 2009). In the rodent CNS, exon I and IV containing transcripts are the most strongly expressed following neuronal activity. The first Ca^{2+} -modulated transcription factors to be identified for *Bdnf* promoter I were the Ca^{2+} response element (CaRE) binding protein (CREB) and the upstream stimulatory factor (USF) proteins USF1 and USF2 (Tabuchi et al. 2002). *Bdnf* promoter IV contains three critical cis-responsive elements that are controlled by calcium responsive factor (CaRF), USF1/2, and CREB (Shieh et al. 1998; Tao et al. 1998; Tao et al. 2002). Interestingly, exon II transcripts are also upregulated in response to neuronal activity; however, no Ca^{2+} cis-elements or transcription factors have been identified within the promoter II region (West et al. 2014).

In addition to the activation of different promoters, *Bdnf* transcripts are poly-adenylated at one of two sites in the 3' UTR. This gives rise to two isoforms of mRNAs, harbouring either a long or short poly(A) signal at their 3' end (Timmusk et al. 1993; Aid et al. 2007). The addition of a long or short sequence to the 3'UTR adds yet another layer of regulation

to *Bdnf* expression by determining the stability of newly transcribed mRNAs and their sub-cellular localisation. While several reports claim that short 3' *Bdnf* mRNAs are restricted to the cell soma and long 3' UTRs are transported to dendrites, it remains unclear whether dendritically targeted mRNAs are locally translated to result in the post-synaptic secretion of BDNF, or indeed if BDNF transcripts are localised in dendrites at all (An et al. 2008; Dieni et al. 2012). Indeed, a recent transcriptomic analysis of ribosomes within neuronal soma and neuropil revealed that *Bdnf* mRNAs are in fact preferentially translated in the cell body (Glock et al. 2020).

1.4.2 BDNF localisation in neuronal and non-neuronal cells

Much like other growth factors, understanding the localisation of BDNF has been made exceptionally difficult by its remarkably low abundance within cells. In the brains of both mouse and human, levels of BDNF expression are low at birth but markedly increase during postnatal development (Webster et al. 2002; Baquet et al. 2004). During this period, the spontaneous firing of developing neuronal networks increases BDNF expression in an activity-dependent manner as indicated in the above (Castrén et al. 1992; Timmusk et al. 1993b), enhancing the synaptic plasticity, and thus connectivity, of new neural circuits (Blankenship and Feller 2010). Although the levels significantly drop towards adulthood, *Bdnf* continues to be expressed by the hippocampus, cortex, cerebellum, and amygdala, with the highest levels found in hippocampal neurons (Hofer et al. 1990; Timmusk et al. 1993a; Baquet et al. 2004). In contrast, medium spiny neurons of the striatum do not express detectable levels of its mRNA (Baquet et al. 2004) nor protein (Conner et al. 1997; Yan et al. 1997) but are instead largely dependent on its supply from cortical afferents (Baquet et al. 2005). Astrocytes, oligodendrocytes, and microglial cells of the spinal cord have been shown to upregulate BDNF expression in response to injury (Dougherty et al. 2000), however its synthesis by these cells in brain is yet to be satisfactorily documented.

Despite being a key mediator of synaptic plasticity in both the developing and mature CNS, substantial evidence indicates that the postnatal lethality of *Bdnf*^{-/-} mice does not result from the death of CNS neurons (Gorski et al. 2003a; Rauskolb et al. 2010). Animals are instead thought to die from marked neuronal death in the PNS, including nodose/petrosal ganglion (NPG), a population of cells that relay critical sensory information to the CNS to regulate heart rate, respiration, and blood pressure. During development, these cells rely on BDNF synthesised by the carotid body and arterial baroreceptors, and present with a > 60% reduction in *Bdnf*^{-/-} animals (Ernfors et al. 1994; Erickson et al. 1996; Brady et al. 1999). Both the mRNA and protein have also been detected in smooth muscle (Donovan et al. 1995), heart (Donovan et al. 2000), lung and

kidney (Timmusk et al. 1993a). In rats and humans, BDNF is also expressed by megakaryocytes, the cellular precursor to platelets, in a calcium-dependent manner (Chacón-Fernández et al. 2016). This results in platelet BDNF levels 10 to 100 times higher than that detected in brain (Yamamoto and Gurney 1990; Fujimara et al. 2002). Although its role in blood is not clear, BDNF is speculated to work in conjunction with other platelet-derived factors to stimulate nerve regeneration in the periphery. As platelets have been shown to be activated following exercise (Kestin et al. 1993), fluctuations in serum BDNF levels may play a role in the cognitive benefits of acute or regular physical activity; however, there is no evidence as of yet that BDNF diffuses through the blood-brain barrier (BBB) (Pardridge et al. 1994).

1.4.3 BDNF biosynthesis

Much like other growth factors and hormone precursors, studies of endogenous BDNF indicate that *Bdnf* mRNAs are initially translated into a pre-pro-protein, comprising of an 18 aa signal peptide, 110 aa pro-domain, and a 119 aa mature domain (Leibrock et al. 1989). The signal sequence serves a chaperone function, directing nascent pre-pro-BDNF to the rough endoplasmic reticulum (ER), and is presumably cleaved during ER entry to yield the pro-protein (~32 kD) (Figure 1.3). Here, the pro-domain undergoes N-glycosylation, deemed essential for the proper proteolytic cleavage of the mature protein (Benicky et al. 2019). As is the case with many secreted proteins including growth factors, protein disulphide isomerases are thought to catalyse the formation of disulphide bonds between cysteines of BDNF's mature domain, giving rise to its characteristic cystine knot structure. Pro-BDNF as previously demonstrated with pro-NGF (Suter et al. 1991) is required for the correct folding of the mature domain and its sorting into the secretory pathway. From the ER, N-glycosylated pro-BDNF is translocated to the trans-Golgi network (TGN) where the proteolytic cleavage of di-basic residues liberates mature BDNF (mBDNF; ~14 kD) from its pro-peptide (~17 kD) (Matsumoto et al. 2008). Although overexpression paradigms first suggested that the proprotein convertase 1 (PC1) may be a key regulator of this process (Seidah et al. 1996), reduced levels of mBDNF observed in brains of *Pcsk7* (but not *Pcsk1/3*) knockout mice implicates PC7 as the most likely mediator of pro-domain cleavage within neurons (Wetsel et al. 2013). Along with its pro-peptide, mBDNF is then sorted into the regulatory secretory pathway and transported to axon termini within LDCVs (Wu et al. 2004; Dieni et al. 2012). Here, LDCVs accumulate at the pre-synaptic membrane until exocytosed in response to neuronal activity (Lou et al. 2005). It is now well understood that the activity-dependent release of mBDNF serves as a critical enhancer of synaptic plasticity following binding to and activation of its postsynaptic receptor TrkB (Zakharenko et al. 2003). Interestingly, mBDNF is also thought to act in an autocrine manner to enhance quantal

neurotransmitter release from pre-synaptic terminals (Jovanovic et al. 2000; Tyler and Pozzo-Miller 2001), modulating the plasticity of active synapses in a bidirectional manner. Indeed, the presence of functional pre-synaptic TrkB receptor has been demonstrated (Merighi et al. 2008; Li et al. 2017). By contrast, the functional relevance of the secreted pro-peptide is less clear, though recent findings suggest an involvement in dendritic spine retraction (Guo et al. 2016) and p75^{NTR}-mediated long-term depression (LTD) (Mizui et al. 2015).

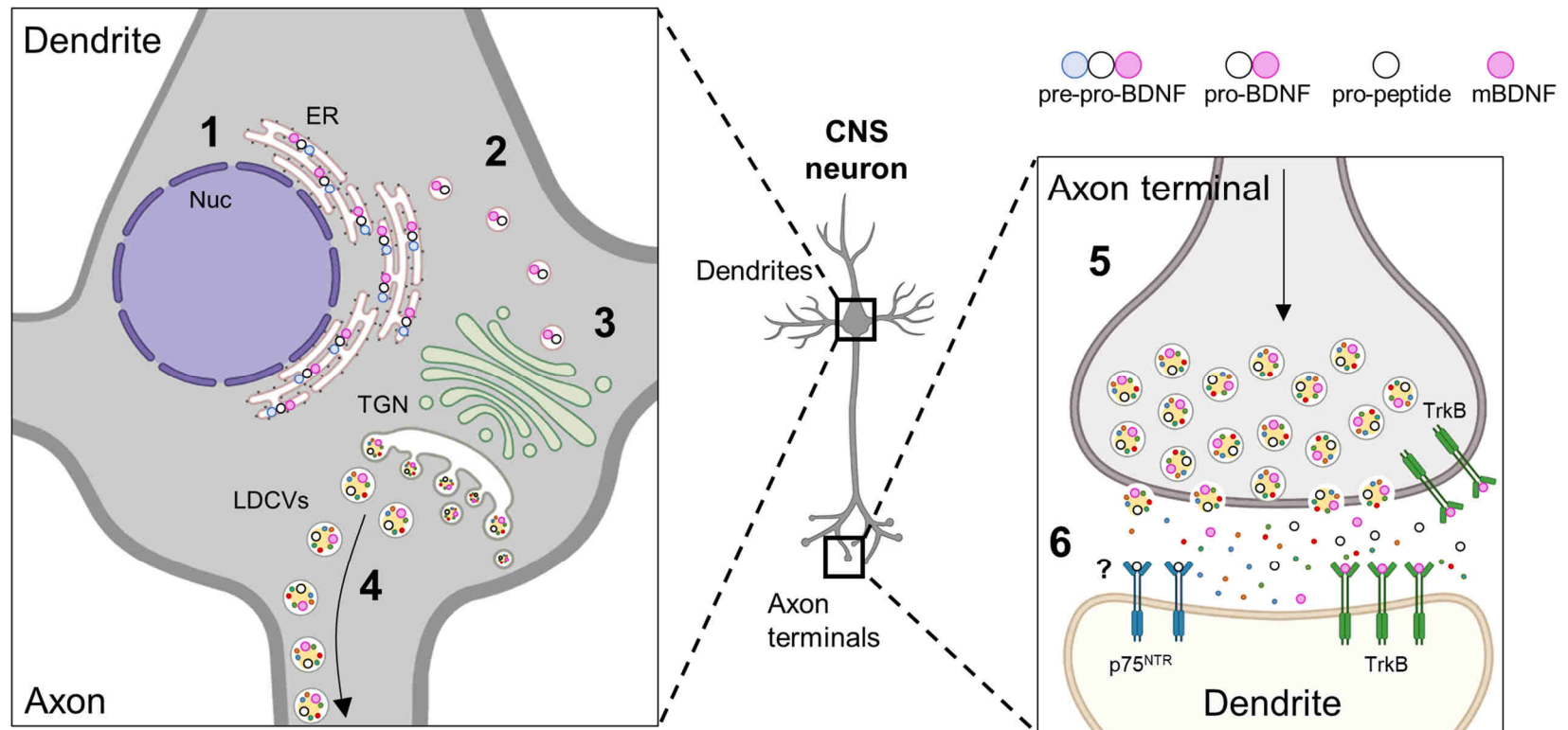


Figure 1.2. The intracellular processing of mature BDNF by CNS neurons under physiological conditions.

Schematic representation of the current understanding of BDNF synthesis and processing by neurons of the CNS. (1) Pre-pro-BDNF is first synthesised and then rapidly cleaved in the ER. (2) The resulting protein, pro-BDNF, is then transported to the trans-Golgi network (TGN) via the endoplasmic-reticulum golgi intermediate compartment where it undergoes N-glycosylation and correct folding. (3) After sorting into either secretory pathway, the pro-domain is cleaved by PC7 or furin within the TGN or vesicles to yield the mature protein. (4) mBDNF and its pro-peptide are then packaged into large dense core vesicles (LDCVs) destined for axon terminals by the regulated secretory pathway. (5) LDCVs then accumulate within presynaptic terminals until their membrane fusion is induced by intracellular or extracellular stimuli. (6) Once released, BDNF preferentially binds to its cognate receptor TrkB on the post-synaptic cell to modulate synaptic plasticity, whereas the significance of pro-peptide-p75NTR interactions still requires further clarification. Adapted from Lu et al. (2005), Cuhna et al. (2010) and Kojima et al. (2019).

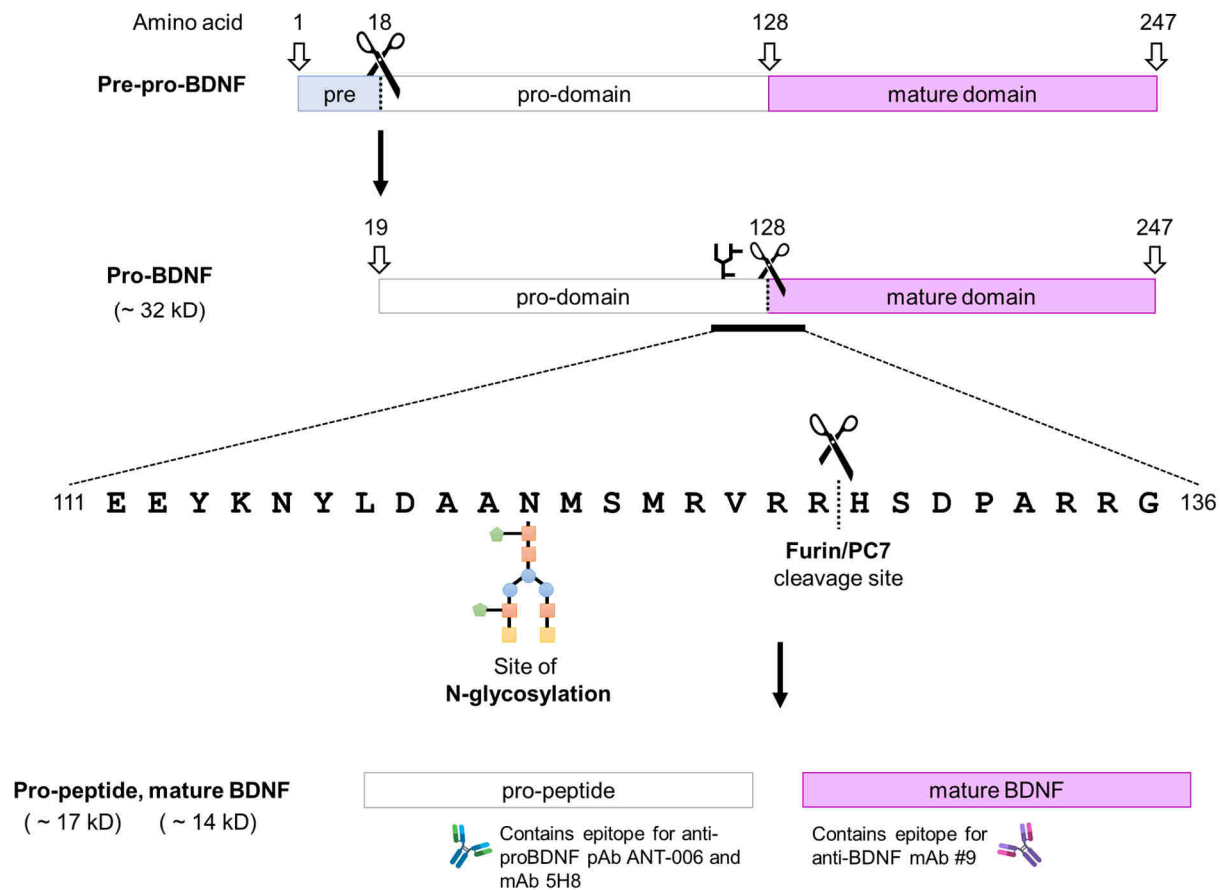


Figure 1.3. The biochemical processing of pre-, pro-, and mature BDNF.

Schematic representation of the proteolytic processing steps of BDNF in the ER and TGN. First, nascent pre-pro-BDNF is rapidly cleaved by ER proteases to yield ~32 kD pro-BDNF. Pro-BDNF is next translocated to the TGN where it undergoes sulfation and N-glycosylation 8 aas prior to the furin/PC7 cleavage site. N-glycosylation then facilitates the proper folding of the mature protein and the correct sorting into either secretory pathway. The pro-peptide (~17 kD) is then efficiently cleaved from the mature protein (~14 kD) by either members of the prohormone convertase (PC) family. Mature BDNF (recognised by mAb #9) and its pro-peptide (recognised by pAb ANT-006 and mAb 5H8) are then packaged into vesicles and translocated to presynaptic terminals for constitutive or stimulus-dependent secretion. Adapted from Dieni et al. (2012) and Benicky et al. (2019).

Biochemical studies performed by Uegaki and colleagues (2017) have also identified a role for the pro-peptide that extends beyond the correct folding and chaperoning of the mature protein. As BDNF and its pro-domain are basic and acidic (with isoelectric points of 9.6 and 5.2, respectively), they are described to interact in an electrostatic manner after cleavage within the acidic environment of intracellular compartments. Interestingly, this complex was shown to be more stable in cells expressing Met BDNF (discussed further below) at both neutral and acidic pH levels. As this strengthened interaction may interfere with the bioavailability of the mature BDNF protein, these findings may better explain the biological underpinnings of the phenotypes of Met carriers than those speculated by Egan et al. (2003).

1.4.4 The physiology of BDNF

1.4.4.1 The role of BDNF during development

BDNF was initially characterised as a survival-promoting molecule for specific neuronal subsets of the PNS not supported by NGF (Barde et al. 1982). This was first observed *in vitro*, where differentiated sensory neurons incubated with BDNF could survive through typical periods of embryonic naturally occurring cell death. These neuronal populations included neurons derived from epidermal placodes not responding to NGF (Davies et al. 1986a; Davies et al. 1986b; Henderson et al. 1993). These initial observations were later confirmed *in vivo* when the injection of purified BDNF into developing quail embryos increased the final neuron number in the nodose and dorsal root ganglia by preventing naturally occurring cell death (Hofer and Barde 1988). The physiological relevance of endogenous BDNF was later confirmed by the generation of mice carrying a homozygous deletion of *Bdnf* (*Bdnf*^{-/-}) that die before reaching 3 weeks of age (Ernfors et al. 1994; Jones et al. 1994). These animals display behavioural abnormalities including spinning and circling movements caused by failed innervation of the inner ear caused by the death of most neurons comprising the vestibular ganglia (Jones et al. 1994). Strikingly, no cell death is observed in the brains or motor neurons of *Bdnf*^{-/-} mice, suggesting that BDNF is not a physiological pro-survival factor for the developing CNS even though it does prevent the death of motoneurons after axotomy in neonatal animals (Sendtner et al. 1992; Yan et al. 1992)

1.4.4.2 The role of BDNF in the postnatal and adult CNS

The early postnatal lethality of mice lacking both *Bdnf* alleles led to the generation of *Bdnf* conditional mutant (*Bdnf* cKO) animals, using a number of Cre drivers, including some expressed in neurons such as *Emx1* or *Tau* (or *Mapt*). Detailed examination of these animals revealed a critical role for BDNF in neuronal differentiation but not for

survival. Thus, mice lacking BDNF in the cerebral cortex as a result of Cre expression in Emx-positive neurons did not show abnormalities in the cerebral cortex but presented with severely shrunk somata in striatal medium spiny neurons (MSNs). Shorter and less branched dendrites were also observed in these cells, as well as the reduced expression of calbindin, parvalbumin and neuropeptide-Y. Cell death was only observed in older animals, indicating that unlike for the PNS, BDNF is not immediately required for the survival of CNS neurons (Gorski et al. 2003a). As this study also confirmed the absence of *Bdnf* expression in the striatum (using a beta-galactosidase reporter under the control of *Bdnf* transcription, see above), these works also confirmed that striatal neurons depend on the anterograde transport of BDNF from projecting cortical neurons (Altar et al. 1997). BDNF is thought to act in a similar manner on developing serotonergic neurons, as mice lacking BDNF in the early postnatal brain mature with behavioural deficits associated with serotonin dysfunction (Jones et al. 1994; Altar et al. 1997; Lyons et al. 1999; Rauskolb et al. 2010).

1.4.4.3 BDNF and synaptic transmission

One of the most studied properties of BDNF is its ability to modulate synaptic transmission. This followed an early report that Lohof et al. (1993) indicating that BDNF and NT-3 potentiate neurotransmitter release at the developing neuro-muscular junction. The early observation that by comparison with other brain areas, *Bdnf* is highly expressed by granule and pyramidal cells of the hippocampus (Hofer et al. 1990) and that neuronal activity further increases the levels of *Bdnf* mRNA (Isackson et al. 1991; Castrén et al. 1992; Dugich-Djordjevic et al. 1992) provided a rationale for the possibility that BDNF may play a role in synaptic plasticity in the hippocampus, a hypothesis that was directly supported by the observation that BDNF applied to hippocampal slices enhances synaptic transmission (Kang and Schuman 1995). Importantly, a critical role for endogenous BDNF was then demonstrated by the observation that slices prepared from animals lacking even just one allele of *Bdnf* showed decreased long term potentiation (LTP) following high-frequency stimulation (HFS) of the Schaffer collateral synapse (Korte et al. 1995). These deficits could be rescued by viral-mediated transfer of *Bdnf* or addition the addition of the recombinant protein (Korte et al. 1995; Korte et al. 1996; Patterson et al. 1996). Similar LTP deficits were later observed after blockade of the signalling cascade using BDNF antibodies or TrkB-IgG constructs, thereby indicating the need for BDNF to be released during the process of LTP induction by high-frequency stimulation of the presynaptic input (Korte et al. 1998; Chen et al. 1999; Kossel et al. 2001). Whilst the role of BDNF in LTP is now firmly established, the molecular mechanisms underpinning these changes are still incompletely understood. They are likely to involve the generation of new spines, known to accompany LTP (Trommald et

al. 1996; Engert and Bonhoeffer 1999; Toni et al. 1999). Following activation of its postsynaptic receptor TrkB, BDNF has also been shown to increase translation of a number of mRNA localised in dendrites by rapamycin-sensitive mechanisms (Tang et al. 2002). Modulation of actin polymerisation and as well as number of changes in postsynaptic compartments have also been reported to accompany LTP (Lin et al. 2005; Kulik et al. 2019).

Although BDNF's role in LTP is now well appreciated, the relative contributions of pre- and post-synaptic BDNF still requires further clarification. While substantial evidence exists for the action of pre-synaptic BDNF in the induction of hippocampal LTP, the potential role of post-synaptic BDNF in LTP maintenance remains a matter of debate (Zakharenko et al. 2003; Jia et al. 2010; Lin et al. 2018). While several reports claim to detect BDNF within CA1 dendrites, the bulk of experiments relied on tagging BDNF with large fluorescent probes, BDNF overexpression, or the use of non-specific antibodies, failing to report the behaviour of the endogenous protein (Tongiorgi et al. 2004; Harward et al. 2016; Leschik et al. 2019). In contrast, studies probing endogenous BDNF using validated antibodies revealed that BDNF is undetectable in dendrites both *in vitro* and *in vivo* (Dieni et al. 2012; Andreska et al. 2014). These findings are supported by a recent analysis of the hippocampal transcriptome and translome, whereby *Bdnf* mRNA transcripts were shown to be preferentially translated by ribosomes of the neuronal soma opposed to dendritic polyribosomes (Lau et al. 2010; Baj et al. 2016; Glock et al. 2020). Together, these results indicate that BDNF is neither synthesised nor released by dendrites in response to neuronal activity, and that pre-synaptic BDNF is more likely the pre-dominant driver of hippocampal LTP.

1.4.5 BDNF-associated pathophysiology

1.4.5.1 BDNF in mood and memory disorders

BDNF can be considered as an “endogenous” neuroprotectant and as a result, it has been associated with a large number of disorders including depression and neurodegenerative diseases. For example, in the forebrain, lower levels of *BDNF* mRNA have been associated with more rapid cognitive decline (Buchman et al. 2016). By contrast, increased hippocampal *Bdnf* expression partly contributes to the mood-alleviating effects of both anti-depressant drugs (ADs) and exercise (Nibuya et al. 1995; Chen et al. 2001; Vaynman et al. 2004; Duman et al. 2008). Indeed, increased BDNF signalling through TrkB has been recently proposed to explain the mode of action of the most commonly used antidepressants (see below). Before the discovery of BDNF synthesis in human megakaryocytes (discussed above), it was widely assumed that

fluctuations in serum BDNF were reflective of those in brain. Serum BDNF was thus frequently used as a biomarker of psychiatric disorders or AD efficacy, despite there being very little evidence of BDNF transfer at the BBB (Pardridge et al. 1994). However, the discovery that megakaryocytes and brain neurons exhibit similarities in the transcriptional regulation of *BDNF* (Chacón Fernández et al. 2016) suggests that there may be common regulators of *BDNF* transcription in neurons and megakaryocytes. Indeed, this may explain the strong correlation between levels of serum BDNF and the degree of mood episodes observed in depressed patients (Polyakova et al. 2015) or the severity of cognitive decline in sufferers of Alzheimer's disease (Laske et al. 2011).

In animal models, BDNF injections into the brain improve both memory performance and depressive-like symptoms (Siuciak et al. 1997; Shirayama et al. 2002; Cirulli et al. 2004); however, the poor pharmacokinetic properties of BDNF call for an alternative means of reproducing this effect within brain. Interestingly, it has been known for some time that the anti-depressive effects of selective serotonin reuptake inhibitors (SSRIs) and ketamine are dependent on the activation of TrkB by endogenous BDNF (Saarelainen et al. 2003; Monteggia et al. 2004; Autry et al. 2011). However, it was only demonstrated very recently that these drugs mediate their effects by potentiating BDNF signalling after binding the TrkB transmembrane domain (Casarotto et al. 2021). This was a particularly striking finding considering that neither SSRIs nor ketamine were developed based on their affinity for this receptor. The demonstration in the same study that AD treatment improves the performance of mice in memory tests suggests that ADs can be used to enhance BDNF-TrkB signalling in both mood and memory disorders. Furthermore, it implicates BDNF and TrkB as attractive therapeutic targets to develop novel classes of drugs to treat illnesses characteristic of disrupted neural plasticity.

1.4.5.2 The Val66Met single nucleotide polymorphism (SNP)

The most studied *BDNF* polymorphism is designated rs6265 and results in the substitution of a valine for a methionine residue in the BDNF pro-domain (Val66Met, rs6265). Observed at a frequency of ~20% in Western populations (Petryshen et al. 2010), carriers have been shown to exhibit mild learning and memory deficits across certain tasks (Egan et al. 2003; Hariri et al. 2003; Cathomas et al. 2010) and reduced hippocampal volumes, a phenotype more commonly associated with depression (Bueller et al. 2006; Frodl et al. 2007; MacQueen et al. 2008). Converging evidence also implicates this polymorphism in bipolar disorder (Neves-Pereira et al. 2002; Sklar et al. 2002), however the biological implications of this amino acid substitution, and how it relates to these phenotypes, remains unclear. Although early studies performed *in vitro* suggested Met BDNF is less efficiently secreted than the Val form (Egan et al. 2003), these conclusions were largely drawn from the over-expression of GFP-tagged Met *Bdnf*.

The shortcomings of this approach are discussed in detail in the subsequent Chapters. As genetic association studies are inefficient for establishing causality, mouse models were also generated in attempt to replicate the situation observed *in vivo*. Interestingly, the first model developed by Chen and colleagues (2006) exhibited anxiety-related behaviours, but not memory deficits, with later results indicating that the steady state levels of hippocampal BDNF were reduced by ~50% for reasons that remain unclear (Bath et al. 2012). However, a notable issue with this model was that the Met version of *Bdnf* includes a linker sequence and a C-terminal poly-histidine tag that is absent in wildtype “controls”. Although an alternative mouse line was later generated that more closely mimics the human situation, studying its behaviours led to somewhat different conclusions, with Met carriers showing enhanced behavioural flexibility (Vandenberg et al. 2018) and increased susceptibility to alcohol addiction (Warnault et al. 2016).

1.4.5.3 BDNF and obesity

Although weak links have also been reported between the *BDNF* Val66Met polymorphism and increased body mass index (BMI) (Beckers et al. 2008; Skledar et al. 2012), more recent work by Sonoyama and colleagues (2020) identified an additional, rare SNP in the BDNF mature domain (referred to as E183K) whereby heterozygous carriers presented with hyperphagia and severe learning difficulties. Furthermore, 100% of individuals suffering with Wilms tumour, aniridia, genitourinary anomalies and mental retardation (WAGR) - resulting from large deletions in chromosome 11 - exhibit childhood obesity when these deletions encompass the *BDNF* gene, a proportion that is reduced to just 20% when *BDNF* was spared from these mutations (Han et al. 2008). These findings were consistent with early reports of *Bdnf*^{+/-} mice and those lacking *Bdnf* expression in postnatal brain, both of which exhibit learning deficits, increased food intake and progressive obesity (Kernie et al. 2000; Rios et al. 2001; Gorski et al. 2003b). As similar phenotypes have also been identified in humans carrying large deletions or SNPs in *NTRK2* (Yeo et al. 2004; Sonoyama et al. 2020), BDNF-TrkB signalling is deemed an attractive therapeutic target for treating obesity and related metabolic disorders.

1.5 Research aims

For most molecules of interest, determining their localisation within cells is a critical step toward understanding their biological function. This also applies to growth factors, as it is otherwise difficult to understand their role and mechanisms of action without the precise knowledge of their cellular origin. This is also of special relevance when considering the cell biology of neurons, given their complex cytoarchitecture and the possibility that growth factors may accumulate in, and be released from dendrites, axon terminals or both. However, for the majority of these factors, remarkably little is known regarding their cellular and sub-cellular localisation, largely because of the technical challenges associated with their low abundance and the high-resolution methods required to localise them.

Given the increasing interest in developing new reagents that selectively increase BDNF levels in disease- and behaviourally relevant brain circuits, the objective of this thesis was to develop and implement reliable tools that allow the detection of BDNF-expressing cells both *in vitro* and *in vivo*. Using monoclonal antibodies, the aim of early experiments was to revisit the biosynthesis and localisation of endogenous BDNF in the mouse CNS. Next, using HEK293 cells and primary neurons, the biochemical processing of WT BDNF was compared to several BDNF reporter constructs, including a novel bicistronic mRNA that reports BDNF translation using GFP as a surrogate marker. Once validated *in vitro*, subsequent experiments aimed to test the functionality of this construct *in vivo*, whereby a novel mouse line was generated that expresses *Bdnf-P2a-Gfp* instead of *Bdnf*. Following the validation of a novel approach to BDNF immunostaining, the aim of the final chapter was to visualise changes in endogenous BDNF levels in a rat model of spatial learning.

Chapter 2. Methods and Materials

2.1 BDNF plasmids

2.1.1 WT BDNF

pCMV6-BDNF was generated by inserting a PCR fragment encoding the full-length mouse *Bdnf* sequence into the Xba1 site of pCMV6-XL3 vector (Hofer et al. 1990) (Addgene plasmid #39857; <http://n2t.net/addgene:39857>; RRID:Addgene_39857).

2.1.2 BDNF-(1-4)myc and BDNF-myc-eGFP

pBDNF-myc was generated by introducing a sequence encoding c-myc into pCMV6-BDNF. Myc was added to the C-terminus of mouse BDNF following deletion of the last 3 amino acids (aa) (Matsumoto et al. 2008). Comparing the amino-acid composition of purified protein and its cDNA sequence suggests that BDNF undergoes carboxyterminal processing, resulting in the loss of its last three aas. Thus, deletion of RGR within this construct prevents the loss of C-terminal myc by proteolytic cleavage (Arginine-Glycine-Arginine; RGR) (Barde et al. 1982; Leibrock et al. 1989; Rodriguez-Tebar et al. 1991).

2.1.3 BDNF-GFP and BDNF-P2A-(SV40-NLS)GFP

BDNF-GFP and BDNF-P2A-GFP expression plasmid was kindly donated by Boehringer Ingelheim GmbH (Biberach an der Riß, Germany). Briefly, a PacI/Ascl restricted gene fragment containing the full mouse *Bdnf* sequence followed by a glycine-serine linker and the sequence for enhanced GFP (GFP) (Zhang et al. 1996) (synthesised at GeneArt, Regensburg, Germany) was ligated into an identically restricted pAAVsc_CMV (Kästle et al. 2018). pBDNF-P2A-nEGFP was then generated by exchanging the BamHI-Ascl fragment from pAAVsc_CMV for BamHI-Ascl gene fragment containing the teschovirus-1 P2A sequence, the SV40 nuclear localisation signal (SV40^{NLS}) (Ray et al. 2015) and the coding sequence of GFP. Insertion of the P2A teschovirus sequence results in the co-translation of 14 kD BDNF-P2A and 27 kD NLS^{SV40}-GFP.

2.1.4 BDNF-SEP (pHluorin)

A plasmid encoding BDNF tagged with super ecliptic pHluorin (SEP) was a gift from Ryohei Yasuda (Addgene plasmid #83955; <http://n2t.net/addgene:83955>; RRID:Addgene_83955) (Harward et al. 2016). This construct encodes CMV-HA-BDNF-Flag with SEP added to the 3' end to yield HA-BDNF-FLAG-SEP (from here on in referred to as pBDNF-pHluorin).

2.1.5 BDNF-mCherry, BDNF-moxVenus and BDNF-moxGFP

Plasmids encoding BDNF-mCherry, BDNF-moxVenus and BDNF-GFP were kindly donated by Dr. Pedro Chacón-Fernández (Hospital Universitario Virgen Macarena, Seville, Spain). Using restriction sites Nhe1 and BamHI, the full-length mouse BDNF sequence was added to vectors pmCherry N1 (Clontech Laboratories Inc., CA, plasmid #632523), pmoxGFP (gifted by Erik Snapp, Addgene plasmid #68068; <http://n2t.net/addgene:68070>; RRID:Addgene_68070) and moxVenus (gifted by Erik Snapp, Addgene plasmid #68068; <http://n2t.net/addgene:68068>; RRID:Addgene_68068).

2.2 Culture and transfection of HEK293 cells

2.2.1 Maintenance and culture of HEK293 cells

HEK293 cells were thawed in a water bath tempered to 37°C and resuspended in warmed cellular aggregate (CA) media (Gibco™ Dulbecco's modified Eagle medium (DMEM) supplemented with 10% Gibco™ foetal bovine serum (FBS), Gibco™ GlutaMAX™ and Gibco™ MEM non-essential amino acid solution (all Thermo Fisher Scientific, MA, USA). Cells were then washed by centrifugation at 1000 rpm for 2 min and resuspended in 10 ml fresh media and re-plated. Cultures were maintained on 100 mm Nunc™ culture dishes (VWR, PA, USA) at 37°C and 5% CO₂ until reaching 80% confluency. To passage, cells were gently washed with Gibco™ phosphate buffered saline (PBS) and incubated with Gibco™ 0.05% Trypsin-EDTA (both Thermo Fisher Scientific) for 2 min at 37°C. After halting the reaction with 9 ml CA media, cells were washed at 1000 rpm for 2 min and resuspended in the required volume of fresh media for re-plating. Alternatively, cells destined for storage were resuspended in 2 ml CA media supplemented with 10% dimethyl sulfoxide (DMSO) (Sigma-Aldrich, MO, USA) and frozen in a Thermo Scientific™ Mr. Frosty™ Freezing container at -80°C (Thermo Fisher Scientific) before transferring to liquid nitrogen tanks on dry ice.

2.2.2 Transfection of HEK293 cells

HEK293 cells were re-plated onto 6-well Thermo Scientific™ Nunc™ cell-culture treated multi-dishes (Thermo Fisher Scientific) coated with 0.5 mg/ml poly-L-lysine (Sigma-Aldrich) 24 hr prior to transfection. Across experiments, transfections were performed on cultures at ~80% confluency. Transfections were performed using 2 µg of the indicated cDNAs (see Section 2.1) combined with 4 µl of Invitrogen™ Lipofectamine 2000™ Transfection Reagent diluted in Gibco™ Opti-MEM™ medium (all Thermo Fisher

Scientific). After 5 hr, the medium was replaced with N2B27 medium (consisting of equal volumes of Dulbecco's Modified Eagle Medium (DMEM)/F12 and Neurobasal™-A medium, 1% B27 supplement, 1% GlutaMAX™, 1% penicillin-streptomycin (Pen Strep) (all Gibco™, Thermo Fisher Scientific) and 75 µg/ml bovine serum albumin (BSA, Sigma-Aldrich) to analyse secretory proteins by SDS-PAGE. Cells were then cultured for 24 hr to allow for adequate protein expression. While the transfection efficiency of pBDNF and pBDNF-myc could not be visualised, the successful transfection of BDNF reporter constructs was confirmed by the inspection of fluorescing cells. To control for low protein expression resulting from poor transfection, only plates presenting with ~80% transfection efficiency across wells were progressed for protein analysis. Collected conditioned media and protein extracts were then subsequently analysed using BDNF western blot or ELISA.

2.3 Mouse strains

2.3.1 Animal husbandry

The breeding of mice and all associated procedures followed the guidelines of the Home Office Animals (Scientific Procedures) Act (ASPA) 1986 and Cardiff University Ethical Review Board. Mice were housed in a 12 hr light/dark cycle with access to food and water ad libitum. Litters were weaned between 3 and 5 weeks of age (dependent on strain) into same-sex, mixed genotype cages with up to 4 littermates. Individual animals were distinguished from cage mates by distinct ear notches collected for genotyping.

2.3.2 C57BL/6

8-week-old JAX™ C57BL/6 mice were purchased from Charles River Laboratories (MA, USA) and habituated for 7 days before use in timed matings or colony maintenance. Upon arrival, non-littermate males were housed individually to prevent territorial aggressiveness and related stress or injury.

2.3.3 *Bdnf* knockouts (*Bdnf*^{-/-})

Colonies of *Bdnf* heterozygotes (*Bdnf*^{+/-}) were maintained by crossing mice carrying a cyclic recombinase transgene (*Cre*) under the control of the human CMV promoter (*CMV-Cre*) with mice carrying one floxed *Bdnf* allele, whereby the *Bdnf* coding exon, exon IX, is flanked by loxP sites (*Bdnf*^{+/*lox*}) (Rauskolb et al. 2010). This results in the Cre-mediated deletion of a single *Bdnf* allele and viable *Bdnf*^{+/-} offspring. *Bdnf*^{+/-} parents were then placed in breeding pairs to generate *Bdnf*^{-/-} offspring at the predicted

Mendelian ratio. Consistent with previous findings, *Bdnf*^{-/-} pups failed to survive beyond 3 weeks of age (Ernfors et al. 1994; Jones et al. 1994).

2.3.4 *Bdnf-P2a-Gfp* mice

Bdnf-P2a-Gfp knock-in animals were generated by Taconic Biosciences (Leverkusen, Germany) and kindly donated by Boehringer Ingelheim GmbH. Animals were generated using a targeting strategy based on the NCBI transcript NM_0091048139.1 and Ensembl gene ID ENSMUSG0000004842 in which exon II contains the complete *Bdnf* coding region.

After FLP-FRT mediated recombination of the puromycin resistance cassette in targeted embryonic stem cells (mESCs) (for more details, see Chapter 5), ESCs were injected into blastocysts and implanted within the uterus pseudo-pregnant C57BL/6J mice. The offspring was then continually crossed with C57BL/6J to reduce the likelihood of off-target mutations and maintained on the same background throughout. *Bdnf-P2a-Gfp* animals were born at the expected Mendelian ratios when generated from heterozygous breeding pairs, with WT, Het and Hom animals all surviving beyond 12 months old.

2.4 Genotyping

2.4.1 DNA extraction and polymerase chain reaction (PCR)

DNA was extracted from ear notches using the PCR BIO Rapid Extract Kit™ (PCR Biosystems, UK) according to the manufacturer's instructions. For extraction of DNA, ear biopsies were incubated in 100 µl reaction mix for 30 min on a ThermoMixer (Eppendorf, Stevenage, UK) adjusted to 60°C and 1100 rpm. Following a subsequent 10 min at 95°C, each lysate was diluted in 400 µl ddH₂O and centrifuged for 1 min at 15,000 rpm. DNA lysates were then stored at -20°C until required for PCR.

The PCR was carried out in 20 µl of reaction mix containing 10 µl MasterMix (PCR Biosystems), 0.1 µl of forward and reverse primers and 9.8 µl ddH₂O. PCR reaction cycles were completed using a T100 Thermal Cycler (Bio-Rad, CA, USA) (for primers and PCR conditions, see Table 2.1). All PCR products were either used immediately in gel electrophoresis or stored at 4°C for a maximum of 48 hr.

2.4.2 PCR product gel electrophoresis

After completion of the thermocycler programme, PCR products were loaded into 2% w/v Invitrogen™ UltraPure™ agarose (Thermo Fisher Scientific) gels supplemented with 5 µl ethidium bromide (EtBr) per 100 ml. Gels were submerged in TAE buffer (40 mM

Tris, 20 mM acetic acid and 1 mM EDTA in ddH₂O, pH 8.0) and run at 120 V for 45 min or until the expected bands (see Table 2.1) were clearly separated.

Table 2.1 PCR conditions for the genotyping of mouse strains.

Target(s)	Forward Primer (5' → 3')	Reverse Primer (5' → 3')	PCR program			Product size (bp)
<i>Bdnf</i> (WT) <i>Bdnf-P2a-Gfp</i> (FRT remnant)	CTTGTGATTCTTGGTCAGCC	TGGGCTAACCAGTGAGACCC	{ 95°C 95°C 60°C 68°C 4°C	{ 5 min 30 s 30 s 1 min 10 min	35 cycles	Wildtype <i>Bdnf</i> 235 bp <i>Bdnf-P2a-Gfp</i> 310 bp
<i>Bdnf</i> (WT) <i>loxP-Bdnf-loxP</i>	GTTGCGTAAGCTGTCTGTGCACTGTGC	CAGACTCAGAGGGCACTTTGATGGCTTG TCCGAGCCTTCCTTTAGGAATGTCTC	{ 95°C 95°C 60°C 68°C 4°C	{ 5 min 30 s 30 s 1 min 10 min	40 cycles	Wildtype <i>Bdnf</i> 629 bp <i>loxP-Bdnf-loxP</i> 1.5 kbp
<i>CMV-Cre</i>	GGTTATGCGGCGGATCCGAAAAGAAA	ACCCGGCAAAACAGGTAGTTATTCGGATCA	{ 95°C 95°C 58.5°C 68°C 4°C	{ 3 min 30 s 30 s 4 min 30 s 5 min	35 cycles	<i>CMV-Cre</i> transgene 381 bp

2.5 Rats

2.5.1 Animal husbandry

The maintenance of rat colonies and their use in behavioural experiments were performed within the guidelines of the Home Office Animals (Scientific Procedures) Act (ASPA) 1986 and approved by the Cardiff University Ethical Review Board. 24 8-week-old Lister-Hooded rats were purchased from Charles River Laboratories and housed in cages of 3. Rats were housed in a 12 hr light/dark cycle with access to food and water *ad libitum* until required for behavioural experimentation.

2.6 Rat behavioural paradigm

2.6.1 Apparatus

Behavioural tasks were carried out in an 8-arm radial arm maze (Olton and Samuelson 1976) consisting of an octagonal central platform (34 cm diameter) with 8 equally spaced radial arms (87 cm long, 10 cm wide). The base of the maze was made of white painted wood whereas the arms were made of clear acrylic (24 cm high). Access to individual arms from the central platform was managed by acrylic guillotine doors (12 cm high) attached to a pulley system controlled by the experimenter. The distal end of each arm contained a food well (2 cm diameter, 0.5 cm deep) baited with sucrose pellets by the experimenter between trials. Two mazes of this kind were installed in separate rooms with unique spatial cues of different colours, patterns, contrasts, and shapes (Figure 2.1).

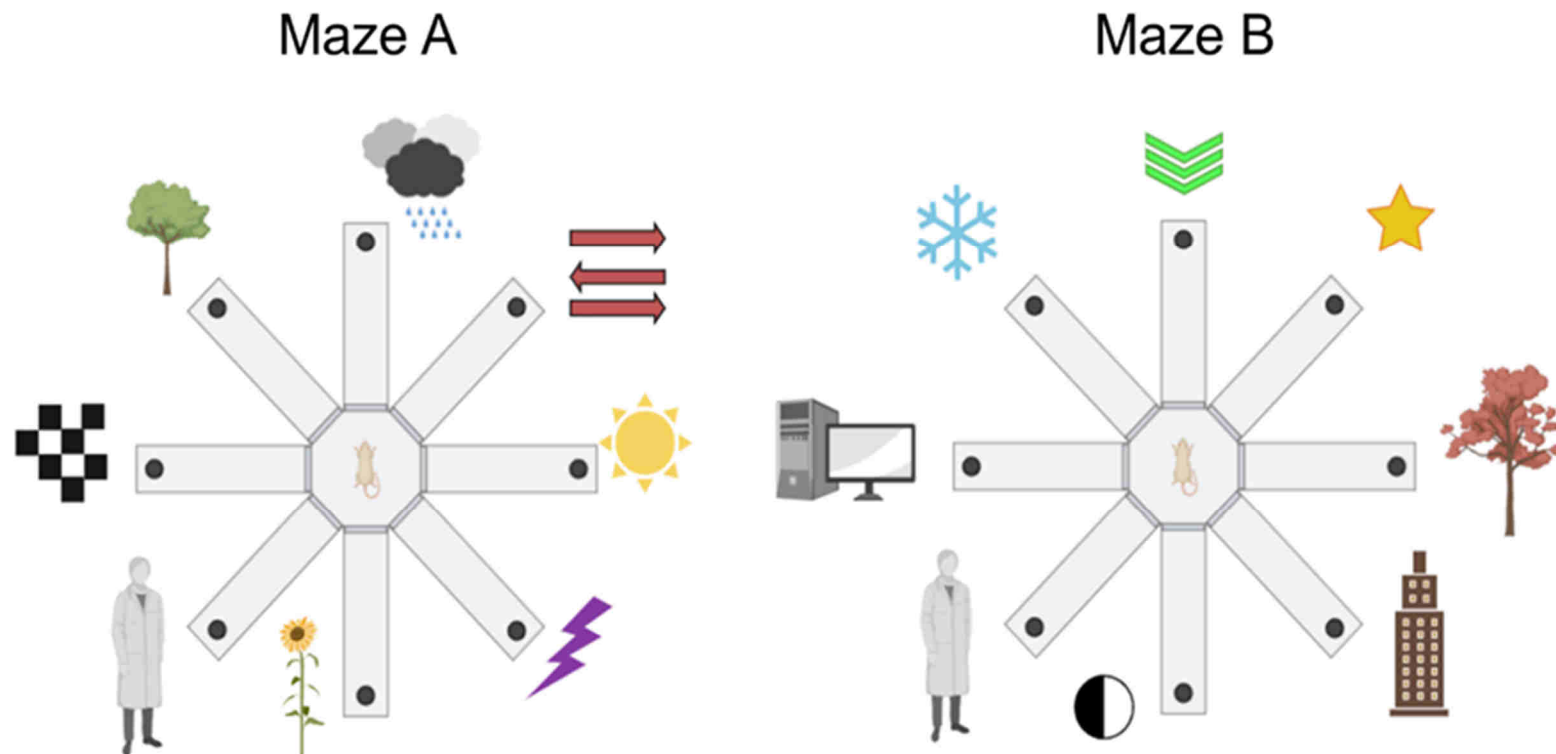


Figure 2.1 A scheme representing the two radial arm mazes employed in the rat behavioural paradigm.

During the training phase, control and experimental animals were accustomed to the spatial memory task in separate mazes (Maze A and Maze B, respectively). Each maze was placed within its own room and surrounded by several visual stimuli in the form of coloured images attached to surrounding walls. On test day, experimental animals performed the spatial learning paradigm in a novel maze (Maze A), whereas control animals remained in their original training setting (also Maze A). Grey lines surrounding the octagonal platform represent guillotine doors attached to a pulley system controlled by the experimenter. Black dots at the end of each arm represent the shallow wells baited with one sucrose pellet per trial. Schematic made using BioRender.

2.6.2 Animal handling and procedure

One week prior to training, animals were placed on a food-restricted diet. Their weight was recorded every other day and was not permitted to drop below 85% of their free-feeding weight. Two days before entering the maze, rats were introduced to sucrose pellets (used as the task reward) within their home cages.

2.6.2.1 Habituation

Throughout the experiments, multiple measures were put in place to control for changes in *c-fos* or *Bdnf* expression induced by unrelated stimuli. During the food restriction period, animals were handled by the experimenter for approx. 2 min per day. The same experimenter conducted all handling and training to avoid the upregulation of genes associated with novel social interactions.

Rats were familiarised with the maze and aluminium travelling box for a minimum of 5 days prior to training. Rats were also placed in the aluminium box between trials, allowing the experimenter to rebait the maze. On day 1, rats were added to the maze in pairs and encouraged to freely explore. All 8 doors of the maze were open and sucrose pellets were scattered along both arms and wells of each maze. On days 2 and 3, animals were encouraged to explore individually to retrieve rewards from wells only. On the remaining days, rats were placed in the centre of the maze, and the experimenter began to mimic the trial by opening and closing all 8 doors. During this time, arms were continuously baited. Once animals became familiar with waiting 5 s at the central platform between arm visits, the next behavioural training stage commenced.

2.6.2.2 Behavioural training

To reduce gene expression resulting from unrelated sensory stimuli, rats were placed alone within standard housing cages in a dark and quiet room for 30 min before and 2 hr after maze training.

For the next 6 days, half of the behavioural cohort (hereinafter referred to as the 'experimental group', $n = 12$ rats) was trained to perform the spatial memory task. The aim was to retrieve single sucrose pellets from all 8 radial arms, using external spatial cues as a guide. At the start of each trial, a rat was placed on the central platform of the maze. After 5 s, all 8 guillotine doors were opened, giving the animal a full choice of arms to visit. Upon entering their choice of arm, the guillotine door was closed until the rat retrieved and consumed the pellet from the well at the far end. The door was then re-opened, allowing the rat to return to the centre. Before having access to their next choice of arm, animals were held at the central platform for 5 s. Repeat visits to the same arm

within a trial were recorded as a visit error. This process was repeated until the animal visited all 8 arms. At the end of the trial, rats were placed in the aluminium travelling box while the experimenter re-baited the maze. During the training-phase, each rat performed the task for 20 min per day for 6 days.

In parallel, the second half of the behavioural cohort (from now on referred to as the 'control group', $n = 12$ rats) was trained to run between the central platform and a single arm of the maze. Across trials, the number of runs replicated their 'yoked' experimental counterpart, thus matching their motor behaviour while receiving the same number of sucrose rewards. All other experimental conditions remained the same.

2.6.2.3 The spatial memory task

Experimental animals and controls were trained simultaneously to undergo testing and perfusion on day 7. As before, animals were kept in dark conditions 30 min before completing the behavioural paradigm. Each experimental animal and their yoked control were tested at the same time of day across pairs. For the final task, experimental animals were introduced to a novel room containing new spatial cues. As before, they were given 20 min to perform as many trials of the maze as possible and their performance, including visit errors, was recorded. As before, controls completed the same number of runs as their paired experimental counterparts but down a single arm of a familiar maze. 2 hr after completing the task, animals were perfused for the analysis of brains by immunohistochemistry.

2.7 Immunohistochemistry (IHC)

2.7.1 Paraformaldehyde fixation of rat and mouse brains

3-4 month old mice and rats were heavily sedated by intraperitoneal injections of 0.1/1 ml Euthatal® pentobarbital sodium (Merial Animal Health, Woking, UK) and then transcardially perfused with warmed PBS followed by ice-cold Thermo Fisher™ Pierce™ Formaldehyde (PFA, Thermo Fisher Scientific) in PBS. Across experiments, both PBS and PFA solutions were corrected to pH 6.0 using HCl. To be optimal for BDNF and Fos IHC, rat brains were perfused using 4% PFA. Sections required for BDNF IHC were then progressed onto a heat-based antigen retrieval (AR) step (described below) before further processing. Although this method also proved effective for achieving BDNF immunostaining in mouse tissues, perfusion with 2% PFA was preferred as AR proved incompatible with BDNF/GFP co-staining (likely due to the heat-sensitive nature of the GFP protein). Interestingly, this change in PFA % markedly improved the sensitivity of both stainings (data not shown).

After perfusion and their subsequent dissection, brains were post-fixed at room temperature (RT) for 1 hr and then cryoprotected in 30% w/v sucrose solution overnight at 4°C. The next day, mouse brains were embedded in OCT compound (VWR) and stored at -80°C until required, whereas rat brains were sectioned prior to storage.

2.7.2 Tissue sectioning

OCT-embedded mouse brains were sectioned using a cryostat (CLM3050 S, Leica Biosystems, Milton Keynes, UK) into 30 µm coronal sections and then immediately processed for IHC. After overnight sucrose cryoprotection, rat brains were sectioned into a 1:4 series using a freezing microtome (8000 sledge microtome, Bright Instruments, Luton, UK) and stored long-term in cryoprotectant (for 1 L: 30% w/v sucrose, 1% w/v polyvinylpyrrolidone, 300 ml ethylene glycol (all Sigma-Aldrich) and 500 ml PBS) at -20°C.

2.7.3 Fos staining

Rat sections used for Fos staining were first incubated in peroxidase blocking solution (0.3% H₂O₂ in PBS with 0.2% Triton X-100; 0.2% PBS-T) for 10 min on a rotating shaker to inhibit endogenous peroxidase activity. After 4 washes in 0.2% PBS-T for 10 min, sections underwent blocking in 3% goat serum (GS) (Sigma-Aldrich) in 0.2% PBS-T for 1 hr at RT. Tissues were then incubated in rabbit polyclonal c-Fos antibody (Sigma-Aldrich) (1:5000 in PBS-T) for 24 hr at RT. The next day, sections were washed 4 times for 10 min in 0.2% PBS-T and incubated in biotinylated goat anti-rabbit secondary antibody (Vector Laboratories, CA, USA) (1:200 in 0.2% PBS-T) with 1.5% GS for 2 hr at RT. Sections were then washed 4 times in 0.2% PBS-T and processed using a VECTASTAIN® Elite avidin-biotinylated horse radish peroxidase complex (ABC-HRP) Kit (Vector Laboratories) in 0.2% PBS-T for 1 hr at RT. Finally, sections were washed 4 times for 10 min in 0.2% PBS-T and 2 times for 10 min in Tris non-saline (TNS) buffer (0.05 M Tris in ddH₂O). The ABC-HRP reaction was visualised using a diaminobenzidine (DAB) substrate kit (Vector Laboratories) until the desired degree of staining was achieved, whereby the reaction was stopped by washing with ice-cold TNS buffer for 20 s. Processed sections were mounted on gelatine-coated slides, dehydrated using 70%, 90% and 100% alcohol and then cover-slipped.

2.7.4 Antigen retrieval

Prior to pro-peptide/BDNF immunostaining, tissues fixed in 4% PFA underwent an antigen retrieval (AR) step involving a 20 min incubation in citrate buffer (10 mM citric acid (Sigma-Aldrich) in PBS, corrected to pH 6.0 with NaOH) heated to 80°C. These

sections were then cooled to RT before further processing. Due to the incompatibility of GFP immunostaining with heat-based AR, this step was avoided for the majority of experiments involving mouse tissues, which were instead fixed using 2% PFA (described above).

2.7.5 Immunofluorescence

Sections were added to blocking solution (PBS supplemented with 0.1% Triton-X100 (Sigma-Aldrich) (PBS-T), 3% donkey serum (DS) and 4% bovine serum albumin (BSA); both Sigma-Aldrich)) for 1 hr on a circular shaker. Sections were then incubated with primary antibodies (see Table 2.2) diluted in blocking solution overnight at 4°C. The following day, sections were washed twice in PBS-T for 10 min, and once in PBS for 10 min before fluorescently labelled secondary antibodies (see Table 2.3) diluted in blocking solution were added for 1 hr at RT. From this point onward, sections were kept in the dark whenever possible. Samples were then washed for 10 min in PBS-T and incubated in DAPI (1:4000 dilution in PBS) for 30 min. Afterwards, sections were washed once more in PBS and mounted onto Thermo Scientific™ Superfrost Plus™ glass slides (Thermo Fisher Scientific). Once dry, coverslips were mounted using DAKO mounting medium (Agilent Technologies, CA, USA) and were left to set overnight at RT.

Table 2.2 Primary antibodies used in immunohistochemistry experiments.

Primary antibody	Isotype	Clonality	Manufacturer	Catalogue #	Working dilution
anti-BDNF-#9	mouse IgG _{2b}	monoclonal	see Kolbeck <i>et al.</i> (1999)	-	1:1000
anti-c-Fos	Rabbit IgG	polyclonal	Sigma-Aldrich	ABE457	1:5000
anti-GFAP	goat IgG	polyclonal	Abcam (Cambridge, UK)	ab53554	1:500
anti-GFP*	chicken IgY	polyclonal	Abcam	ab13970	1:1000
anti-MAP2	chicken IgY	polyclonal	Abcam	ab92434	1:5000
anti-pro-BDNF (clone 5H8)	mouse IgG ₁	monoclonal	Santa Cruz (Texas, USA)	#sc-65514	1:1000
anti-pro-BDNF	rabbit IgG	polyclonal	Alamone Labs (Jerusalem, Israel)	#ANT-006	1:1000
anti-TMEM119	rabbit IgG	monoclonal	Abcam	ab209064	1:500
anti-Tau	rabbit IgG	polyclonal	Abcam	ab64193	1:5000

*This antibody also cross reacts with fluorescent proteins derived from *Aequoria victoria*, such as pHluorin.

Table 2.3 Secondary antibodies used in immunohistochemistry (IHC) experiments.

Secondary antibody	Host	Species reactivity	Manufacturer	Catalogue #	Working dilution
Invitrogen™ Alexa Fluor 555-conjugated anti- mouse	donkey	mouse IgG	Thermo Fisher Scientific	#A-31570	1:500
Invitrogen™ Alexa Fluor 488-conjugated anti-chicken	goat	chicken IgY	Thermo Fisher Scientific	#A-11039	
Invitrogen™ Alexa Fluor 647-conjugated anti-chicken	goat	chicken IgY	Thermo Fisher Scientific	#A-21449	
Invitrogen™ Alexa Fluor 647-conjugated anti-rabbit	goat	rabbit IgG	Thermo Fisher Scientific	#A-21245	
Invitrogen™ Alexa Fluor 555-conjugated anti-rabbit	goat	rabbit IgG	Thermo Fisher Scientific	#A-32732	
Goat anti-rabbit IgG H&L (Alexa Fluor® 405)	goat	Rabbit IgG	abcam	ab175652	

2.8 Image capture, quantification, and analysis

2.8.1 Primary cortical cultures

To investigate protein expression following cDNA transfection or 4-AP treatment, neuronal cultures (see below for details) were imaged at 20 or 63 × using the Z-stack function of a LSM 780 confocal microscope. For analysis of activity-induced changes to BDNF and GFP expression, 20 × images were converted to maximum intensity projections using FIJI/ImageJ (Schindelin et al. 2012). Neurons were then selected by their MAP2 and β -III tubulin positive somas and measured for BDNF or GFP staining using the ‘Oval selection’ and ‘Measure’ functions of the same software.

2.8.2 *Bdnf-P2a-Gfp* brain sections

For counts of GFP positive cells in *Bdnf-P2a-Gfp* hippocampi, sections were captured as tile scans using a 63 × oil immersion and processed using FIJI/ImageJ and CellProfiler™ (McQuin et al. 2018). For each image, masks were created using FIJI/ImageJ to focus the automated analyses onto the granule cells of dentate gyrus and pyramidal cells of CA1, CA2 and CA3. To detect GFP expression within individual cells, the CellProfiler™ pipeline was first optimised to recognise individual nuclei by DAPI fluorescence under the IdentifyPrimaryObjects module. GFP staining within nuclei was then measured using MeasureObjectIntensity and categorised into custom-defined bins according to their staining intensity. These bins were determined and labelled by the program user as “Below Threshold”, “Light”, “Moderate”, “Heavy” or “Very Heavy”.

2.8.3 Rat brain sections

2.8.3.1 Imaging and quantification of BDNF/pro-peptide immunoreactivity

To detect BDNF/pro-peptide immunoreactivity in neuronal layers of the hippocampus, sections were imaged at 63 × using the automated tile scan function of an LSM 780 confocal microscope. Fluorescence images captured at high magnification were consistently affected by shading or vignetting, caused by differences in brightness intensity from the centre of the optical axis to the outer edges. This noticeably degrades image quality by causing discontinuities within individual tiles, resulting in a grid-like shading pattern across the stitched image. As this could significantly compromise the downstream analysis of BDNF immunoreactivity, an illumination correction of each image was performed using BaSiC, a plug-in for FIJI/ImageJ (Peng et al. 2017) (Figure 2.2). BDNF/pro-peptide immunoreactivity was selected and quantified in neuronal layers

of the hippocampus using the 'polygon selection' and 'Measure' tools of FIJI/ImageJ. During the quantification procedure, the experimenter remained blind to the experimental conditions. A minimum of 4 sections were analysed per brain area per animal. Across sections, BDNF immunoreactivity was normalised to the fluorescence signal observed in 10 nuclei per neuronal layer of the hippocampus.

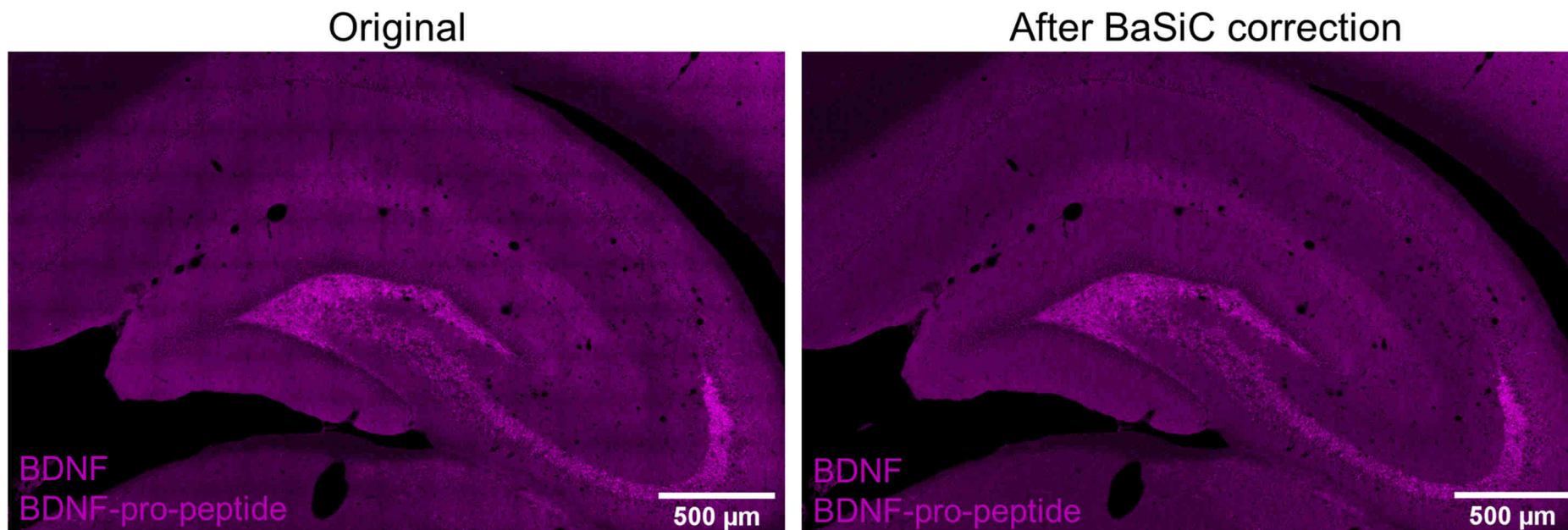


Figure 2.2 Images from confocal imaging before and after BaSiC correction.

The original stitched tile scan of the rat hippocampus captured at 63 × shows discontinuities across individual tiles, resulting in a grid-like pattern across the final image (left panel). The same image corrected using BaSiC (right panel) allows for the same image to be stitched without discontinuities at tile borders.

2.8.3.2 Fos cell counts

As the brain sections from both control and experimental animals were randomly selected, and brain regions matched in both total area and cell density, automated cell counting was deemed appropriate as opposed to reporting a percentage of positive cells per subregion of the hippocampus. Digital images were captured at 5 × using an Olympus DP70 camera linked to a Leica DMRB microscope. To avoid experimenter bias, cells positive for c-Fos were counted using ANALYSIS[^]D software (Soft-Imaging Systems; Olympus, Southend, UK). Throughout the counting procedure, the experimenter was blind to the group conditions. Cells were counted in areas following identification of their nuclei (determined by a mean ferret (measure of particle size) of 4 – 20 μm) and a greyscale staining intensity above that of background, with a minimum of 4 sections quantified per animal.

2.9 Adult brain dissection

Adult mice were culled by cervical dislocation, or pups by decapitation, in accordance with Home Office Animals (Scientific Procedures) Act (ASPA) 1986. Brains were immediately dissected on a pre-chilled metal block to remove the cortex, hippocampus, hypothalamus, and cerebellum. All subregions were then weighed, snap-frozen on dry ice and then stored at –80°C.

2.10 Western blotting

2.10.1 Protein extraction and quantification

Brain tissues, cultured HEK293 cells and cortical neurons were lysed in ice-cold RIPA buffer (50 mM Tris-HCl, 150 mM NaCl, 1 mM ethylenediaminetetraacetic acid (EDTA), 0.1% sodium dodecyl sulphate (SDS), 0.2% sodium deoxycholate, and 1% Triton X-100) supplemented with phosphatase and protease inhibitor cocktail mixes, 10 μM phenanthroline monohydrate, 10 mM amino hexanoic acid, 10 μg/ml aprotinin, and 2 mM sodium orthovanadate (NaOV) (all Sigma-Aldrich). Brain tissues were immediately dissociated using homogenising pestles and further triturated with a 25 G needle and syringe. After 20 min on ice, all samples were centrifuged at 15,000 rpm at 4°C for 15 min. Supernatants were then kept at -80°C until required for further analysis.

The protein concentration of lysates was determined using a Thermo Scientific™ Pierce™ BCA Protein Assay Kit (Thermo Fisher Scientific) according to the manufacturer's instructions. Protein samples were diluted between 1:20 – 1:100 in

ddH₂O and prepared in triplicates. Both samples and BSA standards (25 - 2000 µg/ml) were incubated in working reagent for 30 min at 37°C. Next, absorbances were recorded on a FLUOstar® Omega microplate reader (BMG Labtech, Aylesbury, UK) and the protein concentration of each sample estimated using the calibrated BSA standard curve.

2.10.2 Gel electrophoresis and membrane transfer

Supernatants and lysates were incubated for 10 min at 70°C in LDS buffer (0.74 mM lithium dodecyl sulphate (LDS), 106 mM Tris HCl, 141 mM Tris Base, 0.51 mM EDTA, 1.1 M Glycerol, 0.22 mM Coomassie Brilliant Blue G and 0.175 mM Phenol Red (all Sigma-Aldrich), pH 8.5) and 50 mM Invitrogen™ dithiothreitol (DTT, Thermo Fisher Scientific). After a brief centrifugation at 4000 rpm, samples were loaded into either 10- or 15-well Invitrogen™ NuPAGE™ Novex 4 - 12% Bis-Tris gels (Thermo Fisher Scientific) in running buffer (50 mM Tris base, 50 mM 2-(N-morpholino)ethanesulfonic acid (MES), 1 mM EDTA, and 0.1% SDS) and run for 1 hr 15 min at 120 V. For blots requiring BDNF quantification, recombinant BDNF (rBDNF) standards (Regeneron/Amgen) between 18.75 and 600 pg were run alongside to create calibration curves as appropriate.

Proteins were transferred onto Amersham™ Protran™ nitrocellulose membranes (0.2 µm) (Cytiva) using a Trans-Blot semi-dry transfer system (Biorad). Gels and membranes were sandwiched between two sheets of Thermo Scientific™ Pierce™ Western Blotting Filter Paper (Thermo Fisher Scientific) soaked in transfer buffer (25 mM Bis-Tris, 25 mM Bicine, 1 mM EDTA and 20% methanol; all Sigma-Aldrich) and transferred over 1 hr at 17 V.

2.10.3 Protein detection

After washing once in PBS, the successful transfer and equal loading of proteins was determined by incubating membranes with Ponceau S (Sigma-Aldrich) solution (5% w/v in 1 M acetic acid) for 10 s. Only membranes indicative of near equal protein loading were proceeded to the next stage of the immunoblot procedure. Membranes were washed briefly with ddH₂O and incubated for 1 hr minimum in blocking buffer (5% skimmed milk powder (Bio-Rad) and 1% BSA in Tris-buffered saline with 0.1% TWEEN® 20 detergent (all Sigma-Aldrich); TBS-T). Membranes were then incubated in primary antibodies (detailed in Table 5) diluted in blocking buffer overnight at 4°C. The next day, membranes were washed three times for 10 min in TBS-T and incubated with secondary antibodies for 1 hr at RT (Table 6). After three 20 min washes in TBS-T, blots were developed using 1 ml WesternBright ECL HRP Substrate (Advansta Inc., CA, USA).

Bands were visualised and imaged using a ChemiDoc MP Imaging System and quantified using ImageLab software (both Bio-Rad).

2.10.4 Confirmation of equal protein loading and transfer

The equal loading and transfer of proteins was confirmed by re-probing blots with antibodies against house-keeping proteins glyceraldehyde 3-phosphate dehydrogenase (GAPDH; for HEK293 cells) and β -actin (neuronal cultures and brain tissues). Where these reagents were not available, protein transfer was visualised using a Ponceau S stain as previously described.

Table 2.4 Primary antibodies used in western blot experiments.

Primary antibody	Isotype	Clonality	Manufacturer	Catalogue #	Working dilution
anti-BDNF (clone 3C11)	mouse IgG ₁	monoclonal	Icosagen (Tartu, Estonia)	#327-100	1:2000
anti-GAPDH	chicken IgY	polyclonal	Abcam	ab15822	1:5000
anti-GFP	chicken IgY	polyclonal	Abcam	ab13970	1:2000
anti-pro-BDNF (clone 5H8)	mouse IgG ₁	monoclonal	Santa-Cruz	#sc-65514	1:1000
anti- β -actin	goat IgG	polyclonal	Abcam	ab8229	1:5000
anti-phospho-TrkA (Tyr675/675) / TrkB (Tyr706/707)	rabbit IgG	monoclonal	Cell Signalling Technology (MA, USA)	#4621	1:2000

Table 2.5 Secondary antibodies used in western blot experiments.

Secondary antibody	Host	Species reactivity	Manufacturer	Catalogue #	Working dilution
anti-chicken IgY H&L (HRP)	goat	Chicken IgY	Abcam	ab6877	1:2000
anti-goat IgG-HRP	mouse	goat IgG	Santa Cruz	sc-2354	
anti-mouse IgG (H+L), HRP conjugate	goat	mouse IgG	Promega	#W4021	
Invitrogen™ anti-mouse IgG1 secondary antibody, HRP	goat	mouse IgG1	Thermo Fisher Scientific	#PA1-74421	
anti-rabbit IgG (H+L), HRP conjugate	goat	rabbit IgG	Promega	#W4011	

2.11 BDNF enzyme-linked immunosorbent assay (ELISA)

Brain extracts used in the BDNF ELISA were prepared in RIPA buffer as described (see Section 2.10.1) but in absence of SDS. Lysates were diluted 1:10, 1:20, and 1:40 in ddH₂O for their BDNF concentrations to fit the assay's working range.

Measurements of BDNF in adult brain were performed using the sandwich ELISA protocol described in Naegelin et al. (2018). To ensure detection of mature BDNF only, monoclonal antibodies detecting antigens exclusive to the mature peptide were used, namely biotin conjugated mAb BDNF-#1 and horseradish peroxidase (HRP)-conjugated mAb BDNF-#9 (Kolbeck et al. 1999). Thermo Scientific™ Pierce™ 96-well NeutrAvidin™-coated high-capacity plates (Thermo Fisher Scientific) were incubated for 2 hr at RT with 13 mg/ml mAb BDNF-#1 in phosphate buffer (0.1 M KH₂PO₄, 0.1 M Na₂HPO₄ and 0.1% Triton X-100 in ddH₂O). After washing three times with blocking buffer (1% BSA (Sigma-Aldrich) in phosphate buffer), 150 µl phosphate buffer was added to plates along with 50 µl of samples or recombinant BDNF standards (Regeneron/Amgen) diluted in blocking buffer (0.24 – 25 ng/ml). Plates were then left for 3 hr at RT on a rotating shaker set to 130 rpm. After three washes in phosphate buffer, BDNF protein was detected by incubating plates with 1 mg/ml HRP-conjugated mAb BDNF-#9 in blocking buffer for another 3 hr at RT with shaking. Following 3 more washes with phosphate buffer, BM Chemiluminescence ELISA Substrate (POD) (Roche, Basel, Switzerland) was added according to the manufacturer's instructions and chemiluminescence immediately measured using a FLUOstar® Omega microplate reader.

2.12 Primary cortical cultures

2.12.1 Preparation of culture dishes

To ensure cell adhesion, dishes were incubated with sterile-filtered 0.5 mg/ml Poly-L-lysine (Sigma-Aldrich) for a minimum of 4 hr at 37°C. Dishes were then washed twice with Gibco™ sterile ddH₂O (Thermo Fisher Scientific) and left to dry in a laminar flow hood. Once dry, their lids were replaced to prevent over-drying. Dishes were stored short-term in the tissue culture hood or kept for up to 7 days when stored at 4°C.

2.12.2 Tissue dissection

To obtain embryonic cortices, homozygous *Bdnf-P2a-Gfp* or C57BL6/J mice were placed into timed breedings. Successful matings were confirmed by inspection of vaginal plugs

the morning after pairing, considered embryonic day 0.5 (E0.5). On either E14.5 (for transfection and TrkB phosphorylation assays) or E17.5 (for BDNF immunocytochemistry), pregnant dams were culled by cervical dislocation and embryos dissected out into ice-cold Gibco™ PBS (Thermo Fisher Scientific). Pups were decapitated using scissors, and heads gently washed in PBS to remove excess blood. After brain extraction, cortices were carefully dissected from their surrounding tissues (including the meninges) and were placed into ice-cold Gibco™ Hanks' Buffered Salt Solution (HBSS, Thermo Fisher Scientific).

2.12.3 Culture of CNS neurons

Cortices were minced with scissors before being transferred to a 50 ml Falcon tube (STARLAB, Milton Keynes, UK) containing 1 mg/ml trypsin (Worthington Biochemical Corp., NJ, USA) in HBSS. The tissue was incubated in a water bath tempered to 37°C for 15 – 20 min before the reaction was halted by supplementation with 1 mg/ml soybean inhibitor (Sigma-Aldrich) and 50 µg/ml DNase 1 (Roche). After gentle mixing, trypsinised cells were fully dissociated using a 5 ml serological pipette and centrifuged for 5 min at 1400 rpm. Pellets were resuspended in 10 ml plating media (DMEM supplemented with 10% foetal bovine serum (FBS), 1% GlutaMAX™ and 1% Pen Strep; all Gibco™, Thermo Fisher Scientific) and counts estimated using a NucleoCounter® NC-100™ (Chemomtec, Allerød, Denmark) and plated into 12- or 24-well plates (for protein analysis or transfection and immunocytochemistry, respectively). After 3 hr in plating media, neurons were maintained in primary neuronal media (Neurobasal™-A medium supplemented with 2% SM1 neuronal supplement (Stem Cell Technologies, Cambridge, UK), 1% GlutaMAX™ and 1% Pen Strep) with half medium changes twice weekly.

2.12.4 Transfection of neuronal cultures

Neurons were plated at high density on pre-treated coverslips (see Section 2.13.1) coated in poly-L-lysine (Sigma-Aldrich) within 12-well Thermo Scientific™ Nunc™ cell-culture treated multi-dishes (Thermo Fisher Scientific) 5 days prior to transfection. Transfections were performed using 2 µg of the indicated cDNAs (see Section 2.1) combined with 4 µl of Invitrogen™ Lipofectamine 2000™ Transfection Reagent diluted in Gibco™ Opti-MEM™ medium (all Thermo Fisher Scientific). After 5 hr, the media were replaced with primary neuronal media. All neurons were cultured for 24 hr after transfection before undergoing PFA fixation for ICC. As previously described for HEK293 cells, the efficacy of transfection was confirmed by the visual inspection of fluorescing neurons. Only plates presenting with ~5% transfection efficiency across wells (due to poor transfectability of neurons) were progressed for ICC analysis.

2.12.5 TrkB phosphorylation assays

To test the potency of various BDNF fusion proteins on BDNF's cognate receptor, TrkB, cultures of primary cortical neurons were prepared as previously described. Prior to treatment, cells were washed once with Neurobasal™-A medium to aid clearance of endogenous Trk phosphorylation. After it was discovered that E17.5 7DIV cultures exhibit high levels of phosphorylation even after washing, cultures were instead prepared from pups at E14.5 and treated on DIV5, where levels of endogenous BDNF expression were shown to be much lower (see Chapters 3 and 4). After ~15 min, the media were removed and cells incubated with BDNF fusion proteins standardised to 6.5 or 25 ng/ml using a BDNF ELISA. After 15 min, cells were then washed using ice-cold PBS supplemented with 2 mM NaOV to inhibit phosphatase activity. Cells were then lysed for western blot as previously described.

2.13 Immunocytochemistry (ICC)

2.13.1 Preparation of coverslips

Neurons for immunocytochemistry or transfection experiments were cultured on pre-treated 13 mm or 16 mm diameter cover glass (VWR) (for 24- or 12-well plates respectively). To remove greasy residues, coverslips were incubated in nitric acid at RT overnight and then brought to neutral pH following repeat washes in ddH₂O. Coverslips were next incubated in 1 M HCl at 45°C for 4 hr. After neutralising again with ddH₂O, coverslips were washed in absolute ethanol for 1 hr and dried on filter paper. To maintain sterility, coverslips were autoclaved and immediately stored in absolute ethanol. 6 hr prior to the plating of cells, coverslips were removed from ethanol and placed within wells of either 12- or 24-well Thermo Scientific™ Nunc™ cell-culture treated multi-dishes (Thermo Fisher Scientific) and left to dry. Coverslips were then treated with poly-L-lysine as previously described.

2.13.2 Immunofluorescence

One day after transfection or treatment with 4-AP, cells cultured on coverslips were retained within plates for both fixation and staining procedures. After the media were discarded, cells were washed once in ice-cold PBS and immediately fixed with 4% PFA for 10 min on ice. No AR step was required for these experiments. After fixation, coverslips were washed three times with PBS-T (PBS with 0.1% Triton X-100) for 5 min at RT, and then blocked in ICC blocking solution (PBS-T supplemented with 3% DS and 1% BSA). Cells were then incubated in primary antibodies (see Table 2.6) diluted in ICC

blocking solution overnight at 4°C. The next day, cells were washed once with PBS and twice with PBS-T, each for 5 min at RT. Secondary antibodies (Table 2.7) diluted in ICC blocking solution were then added for 1 hr at RT. Cells were washed once for 5 min in PBS-T and subsequently incubated in DAPI (1:4000 dilution in PBS) for no longer than 30 min. Coverslips were then mounted onto slides (VWR) using Dako mounting medium and left to dry in the dark at RT.

Table 2.6 Primary antibodies used in immunocytochemistry experiments.

Primary antibody	Isotype	Clonality	Manufacturer	Catalogue #	Working dilution
anti-BDNF-#9	mouse IgG2b	monoclonal	see Kolbeck et al. (1999)	-	1:1000
anti-pro-BDNF (clone 5H8)	mouse IgG1	monoclonal	Santa Cruz	#sc-65514	
anti-GFP	chicken IgY	polyclonal	abcam	ab13970	
anti-MAP2	chicken IgY	polyclonal	abcam	ab92434	1:5000
anti-Tau	rabbit IgG	polyclonal	abcam	ab64193	

Table 2.7 Secondary antibodies used in immunocytochemistry experiments.

Secondary antibody	Host	Species reactivity	Manufacturer	Catalogue #	Working dilution
Invitrogen™ Alexa Fluor 555-conjugated anti- mouse	donkey	mouse IgG	Thermo Fisher Scientific	#A-31570	1:500
Invitrogen™ Alexa Fluor 488-conjugated anti-chicken	goat	chicken IgY	Thermo Fisher Scientific	#A-11039	
Invitrogen™ Alexa Fluor 647-conjugated anti-chicken	goat	chicken IgY	Thermo Fisher Scientific	#A-21449	
Invitrogen™ Alexa Fluor 647-conjugated anti-rabbit	goat	rabbit IgG	Thermo Fisher Scientific	#A-21245	
Invitrogen™ Alexa Fluor 555-conjugated anti-rabbit	goat	rabbit IgG	Thermo Fisher Scientific	#A-32732	

2.14 Statistical analyses

Data were analysed using Microsoft Excel 2013 and SPSS Statistics ® 26 (IBM, New York, USA). Across experiments, the normal distribution of data sets was first confirmed using a Shapiro-Wilk Test. When appropriate, the homogeneity of variances was also assessed using Levene's test. The details of significant results are reported in the main text, whereas further details of all statistical analyses can be found in Appendix I.

2.14.1 *In vitro* experiments

Upregulation of BDNF and GFP expression in wildtype and *Bdnf-P2a-Gfp* cortical cultures was analysed using a 2-tailed Mann-Whitney U test, as the assumptions of normal distribution and homogeneity of variances were violated in both cases.

The levels of BDNF-fusion protein secreted into the HEK293 cell media were analysed using an Independent Samples Kruskal-Wallis test. As BDNF-pHluorin failed to meet the assumption of normal distribution, and all values were relative to the degree of secretion shown by WT (considered to be secreted at 100% efficiency), an ANOVA could not be used. Pairwise comparisons were then performed using a Dunn-Bonferroni for pairwise comparisons, with significance deemed as $p < 0.0083$.

As all datasets passed the assumption of normal distribution, differences in relative phosphorylation, the activation of TrkB by BDNF fusion proteins was compared against that of BDNF-myc (considered to induce maximal phosphorylation, 100%) using a One-Sample *t*-test. Pairwise comparisons were then performed using a Dunn-Bonferroni correction, whereby significance was met when $p < 0.0125$.

2.14.2 *Bdnf-P2a-Gfp* animals

To compare the body weights of *Bdnf-P2a-Gfp* mice, a Kruskal-Wallis test was used with a Dunn-Bonferroni post-hoc test for pairwise comparisons; a significant change in body weight was deemed by $p < 0.025$. Levels of BDNF were compared to those of WT animals using a One-Sample *t*-test.

2.14.3 Fos and BDNF-ir in rat brain

To compare changes in hippocampal subfield Fos counts and BDNF-ir between groups, parametric data were analysed using a Two-Tailed Student's *t*-test and non-parametric data using the two-tailed Mann-Whitney U-test. Data sets with normal distribution that violated the assumption of homogeneity of variance were analysed using Welch's *t*-test.

Chapter 3. Revisiting the processing and localisation of BDNF in neuronal cells

3.1 Short Introduction

Neurons are highly polarised cells that typically present with a single axon and several dendrites. Their complex morphology relies on sophisticated yet incompletely understood mechanisms to sort organelles and proteins into their relevant compartments, processes that are also critical for synaptic maturation, signalling, and plasticity. While the biological effects of BDNF in CNS function are now widely recognised, there is still limited understanding of how the endogenous protein is processed and secreted from neurons. This is mainly due to the technical limitations associated with the very low abundance of BDNF in the adult brain, as initially reported by Barde and colleagues (1982) and confirmed many years later by independent methods (Matsumoto et al. 2008).

To circumvent these difficulties, overexpressing the *Bdnf* cDNA in neuronal cultures prepared from embryonic cortex or hippocampus became a widely used technique for studying the cell biology of BDNF. Although these studies proved particularly useful for identifying the biochemical relevance of the neurotrophins' highly conserved pro-domain (Suter et al. 1991; Benicky et al. 2019), they also brought considerable confusion to the field. For instance, studies overexpressing BDNF tagged with fluorescent proteins led to the conclusion that both pro- and mature BDNF (mBDNF) are preferentially transported to, and released from dendrites (Goodman et al. 1996; Kojima et al. 2001; Adachi et al. 2005; Dean et al. 2009; Matsuda et al. 2009; Harward et al. 2016), contradicting former evidence of mBDNF's intracellular processing and anterograde transport by neurons studied *in situ* (Altar et al. 1997; Conner et al. 1997; Matsumoto et al. 2008; Dieni et al. 2012). Others used similar methods to demonstrate the physiological secretion of pro-BDNF (Pang et al. 2004; Nagappan et al. 2009), contradicting the results of pulse-chase experiments characterising endogenous pro-BDNF as an intracellularly cleaved, short-lived biosynthetic intermediate comprising just ~10% of total BDNF found within neurons (Matsumoto et al. 2008). However, the relevance of over-expression paradigms for studying neurotrophin biology is yet to be satisfactorily documented, a technically challenging endeavour complicated by late availability of reliable BDNF antibodies. Nearly all commercially available antibodies lack the appropriate validation using tissues lacking the *Bdnf* gene, resulting in weak or non-specific signals when used for immunohistochemistry or western blot. This proved especially problematic for biochemical studies of mature protein processing, with artefactual signals commonly

appearing between 28 – 32 kD, the predicted molecular weight of pro-BDNF (Matsumoto et al. 2008).

As there is still considerable confusion regarding the processing and localisation of the mature BDNF protein, the aim of this chapter was to revisit the biosynthesis of endogenous BDNF in neurons. Using monoclonal antibodies against BDNF, the processing and localisation of BDNF was revisited. To ascertain whether overexpression of the wildtype *Bdnf* gene reflects the distribution of the endogenous protein, high resolution microscopy was used to determine the localisation of BDNF in primary cortical neuronal cultures. Using tissues lacking the BDNF gene, a novel antibody was validated for detecting BDNF within brain and cultured neuron lysates. This antibody was then used to characterise BDNF processing after increased cellular activity, specifically the relative abundance of the pro- and mature protein in both neuronal cells. These results also provide a basis for the validation of the BDNF cDNA constructs introduced and discussed in the following chapters.

3.2 Results

3.2.1 Validation of BDNF immunostaining in fixed cells and brain tissue

As specific BDNF immunostaining using anti-BDNF mAb #9 (Kolbeck et al. 1999) has been reported previously in both fixed cells (Andreska et al. 2014) and brain tissues (Dieni et al. 2012; Andreska et al. 2020), it was first tested whether these data could be independently reproduced. To this end, E17.5 DIV11 cortical cultures and adult brain sections were prepared for BDNF ICC and IHC respectively. To control for immunofluorescence caused by non-specific binding of the secondary antibody to endogenous mouse IgGs, mAb #9 was omitted from experiments performed in parallel (Figure 3.1A and B, left panels).

Consistent with previous findings, cultured neurons probed with mAb #9 presented with strong, punctate BDNF signals mostly confined to their somas (Figure 3.1A, right panels). Distinct patterns of immunoreactivity were also observed on brain sections, with the strongest BDNF signals observed in the mossy fibre boutons and pyramidal cell layer of hippocampal CA3 (Figure 3.1B, right panels). In both cases, immunoreactivity resulting from mAb #9 binding was clearly distinguishable from non-specific staining generated by the secondary Ab (Figure 3.1A and B, left panels).

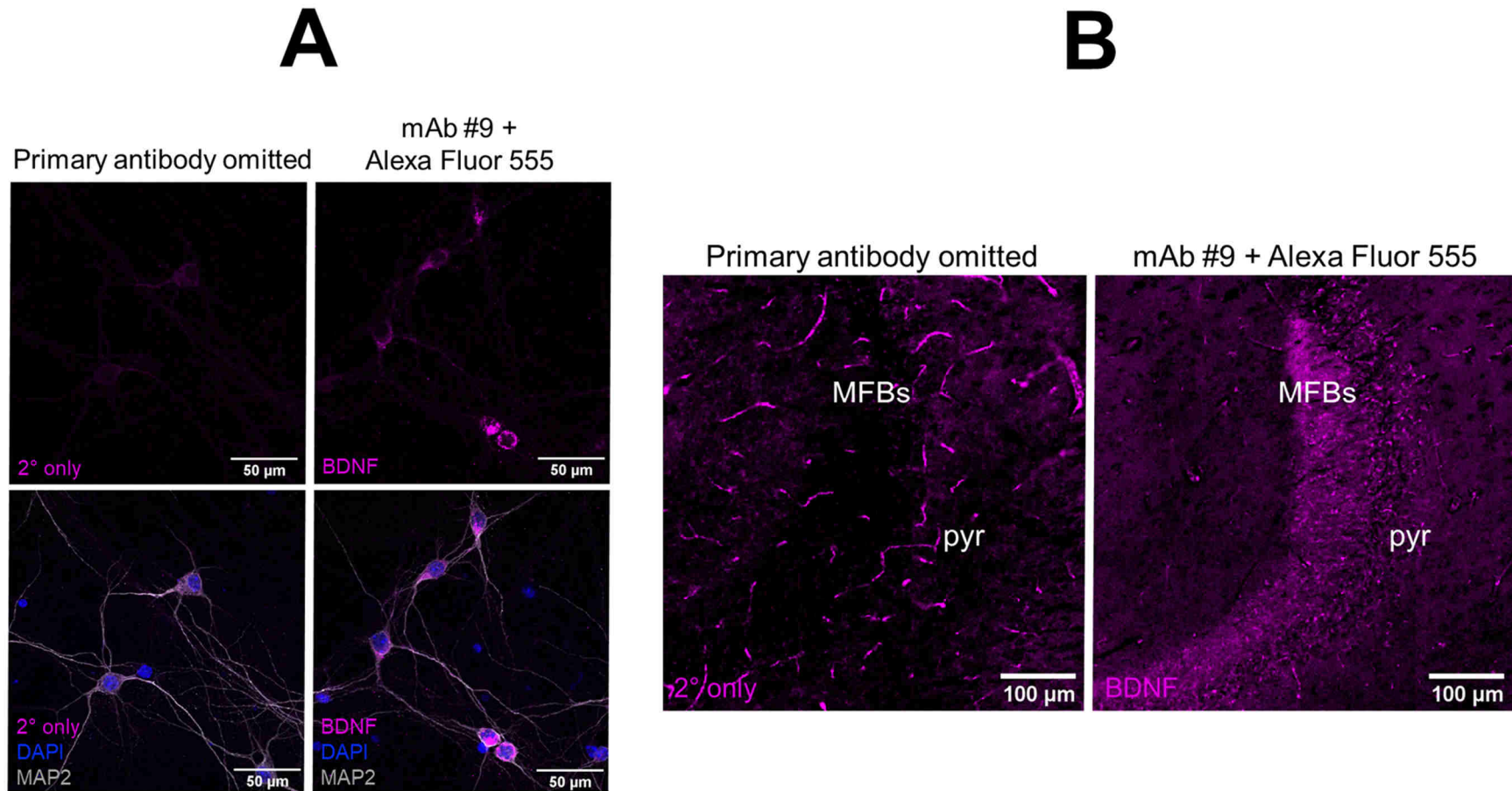


Figure 3.1. Validation of BDNF immunostaining in fixed cells and brain tissue.

High power images of BDNF immunoreactivity in E17.5 DIV11 cortical neurons (**A**) and adult brain sections fixed using 4% PFA (**B**). In (**A**), note the complete loss of punctate signals with omission of the primary antibody (left panels). In (**B**), note the high level of background staining resulting from interactions of the secondary antibody with vascular-like structures known to be rich in endogenous immunoglobulins (left panel). Representative images from $n = 2$ experiments.

3.2.2 Using monoclonal antibodies to detect changes in endogenous BDNF expression by cultured cells

It was next investigated whether changes in endogenous BDNF expression are detectable in the same neuronal culture system. Using the same BDNF ICC protocol as previously described (see above), primary neurons were probed using mAb #9 and also a primary antibody against neuronal marker β -III tubulin. Confocal images captured at low magnification (left panels) revealed that the majority of neurons expressed low levels of BDNF under standard conditions (Figure 3.2A). Punctate BDNF staining was predominantly confined to cell somas, however imaging performed at a higher magnification (Figure 3.2A, right panel) also revealed sparse, punctate BDNF labelling within β -III tubulin-positive projections.

In parallel, neurons from the same preparation were incubated on DIV10 with 1 mM 4-aminopyridine (4-AP), a blocker of voltage-gated K^+ channels (K_v) and known enhancer of neuronal excitability (Hue et al. 1976; Kirsch and Drewe 1993). After 24 hr of treatment, BDNF immunoreactivity markedly increased in both neuronal somas and their immediate projections (Figure 3.2B) while also maintaining the punctate staining pattern observed under standard conditions (Figure 3.2A). Quantification of the BDNF signals observed under both conditions revealed that neurons showed an almost three-fold increase in BDNF immunoreactivity within their cell bodies following treatment with 4-AP (Figure 3.2C; $U = 1060$ and $p = 5.57 \times 10^{-33}$).

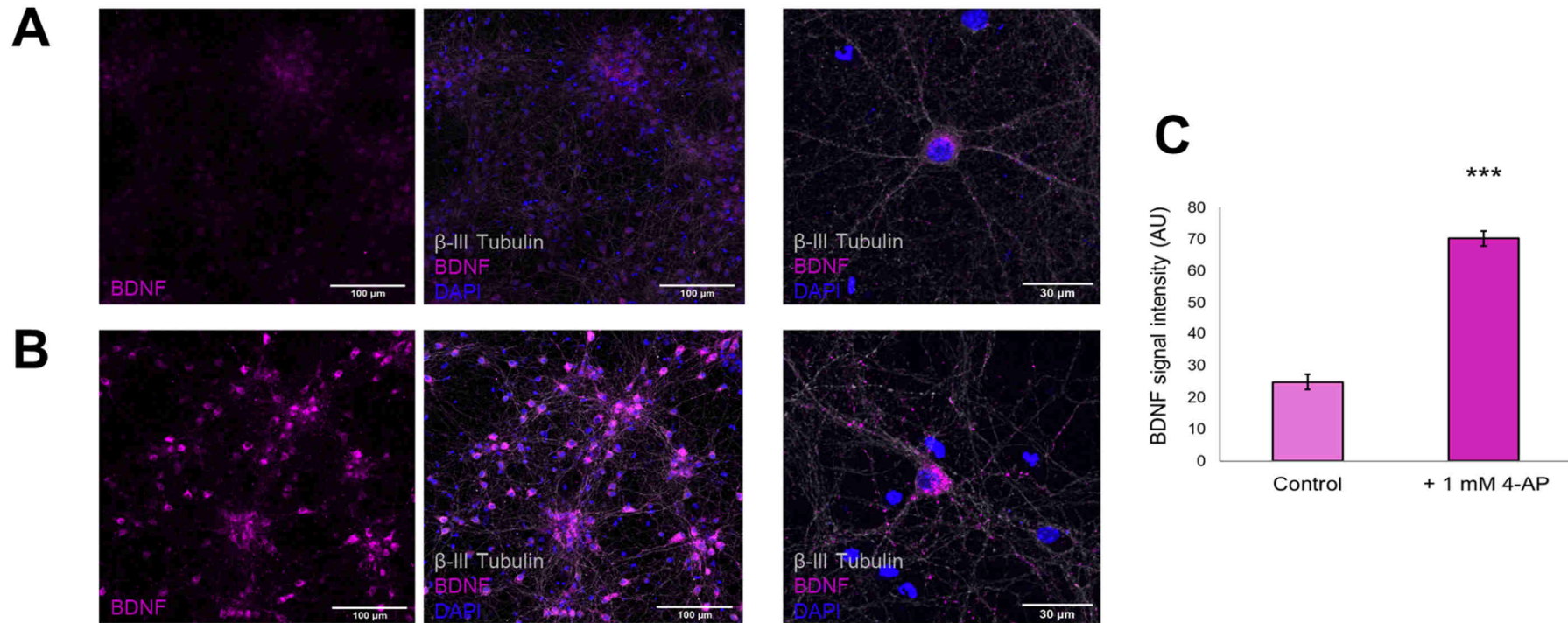


Figure 3.2. Activity dependent increases in BDNF in cultured cortical neurons.

BDNF immunoreactivity in E17.5 DIV11 cortical cultures at low (left panels) and high (right panel) magnification. In untreated cells (**A**), note that BDNF staining is mainly confined to neuronal soma(s) with only a very light distribution of puncta within β -III tubulin-positive projections. In cells treated with 4-AP (**B**), note the increased, but still punctate, BDNF signal within both the soma(s) and projections. Representative images from $n = 3$ culture experiments. (**C**) Quantification of BDNF immunoreactivity in control and 1 mM 4-AP treated cultures. 127 cells analysed per condition. *** indicates $p < 0.001$ ($p = 5.57 \times 10^{-33}$).

3.2.3 Comparing the localisation of overexpressed and endogenous BDNF in cortical cultures

The successful visualisation of endogenous BDNF in late-stage neuronal cultures (Figure 3.1 and Figure 3.2) raised the question of whether vector-driven BDNF expression faithfully reports the subcellular localisation of the endogenous protein. As moderate levels of endogenous BDNF were detectable in E17.5 neurons at DIV11, cultures were instead prepared from the E15.5 cortex and transfected after DIV5, in-line with previous BDNF over-expression experiments (Goodman et al. 1996; Hartmann et al. 2001; Egan et al. 2003; Dean et al. 2009). All cells were then prepared for BDNF ICC as previously described.

To first determine whether young neurons express detectable levels of endogenous BDNF, no-transfection control cells were analysed at high magnification for BDNF immunoreactivity (Figure 3.3A). After DIV6, very light BDNF staining was detectable within some neuronal somas and their early MAP2-positive projections, but not in distal processes (Figure 3.3A, left panel). As observed in E17.5 cultures, the addition of 1 mM 4-AP (Figure 3.3A, right panel) markedly increased BDNF immunoreactivity within cell bodies, but in contrast failed to increase the abundance of puncta within processes.

BDNF immunoreactivity in age-matched cells overexpressing the WT *Bdnf* cDNA (Hofer et al. 1990) (Figure 3.3B) was then compared with those solely expressing the endogenous protein (Figure 3.3A). During the imaging procedure, transfected neurons were easily identified by their abnormally high levels of BDNF expression, often resulting in the clustering of signals within distal projections (Figure 3.3B). In contrast to the no-transfection controls, BDNF's typical punctate staining pattern was lost from the cell body, but still partially present within both early and late neuronal processes. Aggregate-like BDNF immunoreactivity was also frequently found within the nuclear compartment, contrasting with the lack of BDNF observed within nuclei of both E15.5 and E17.5 culture experiments.

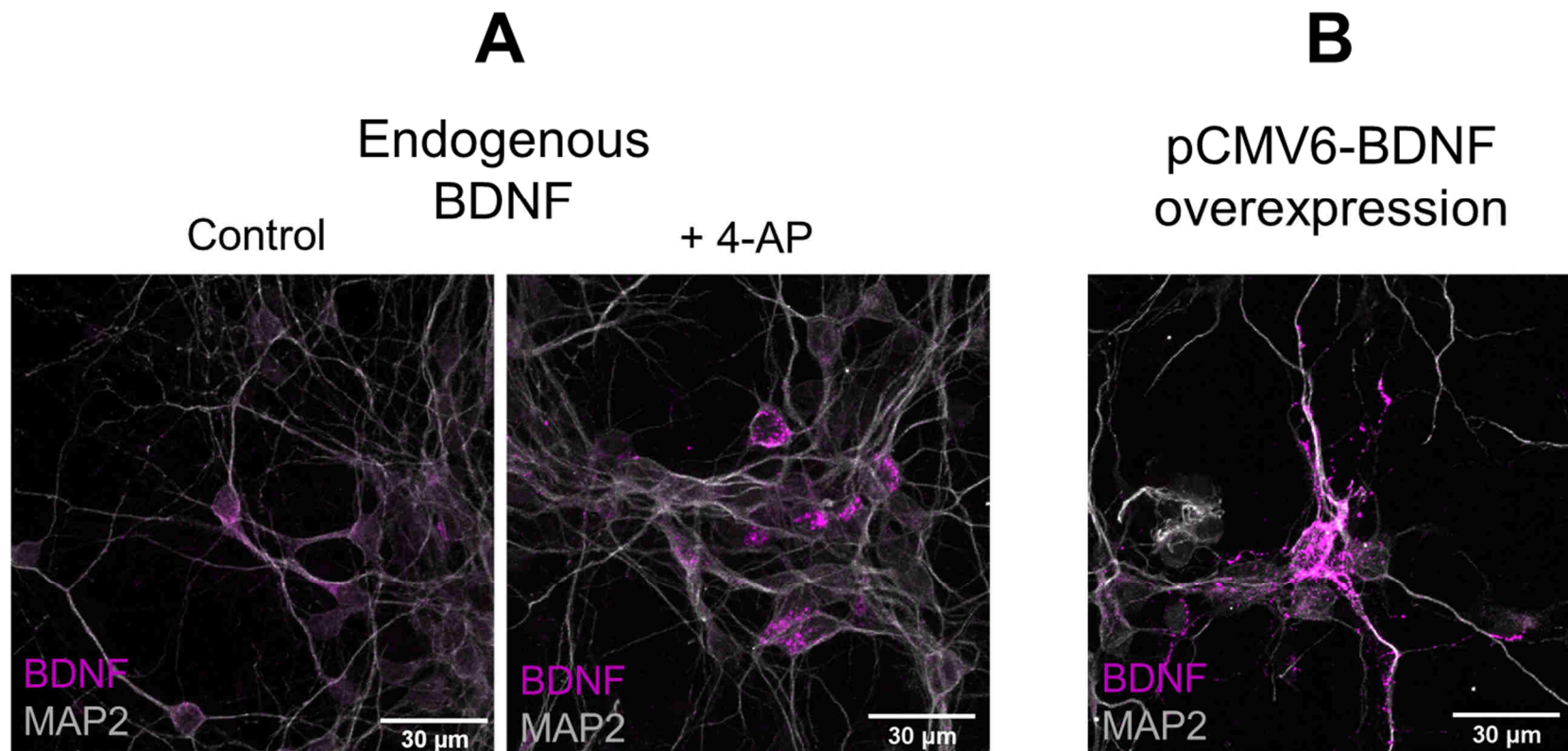


Figure 3.3. Endogenous and vector driven BDNF expression in young neuronal cultures.

(A) Endogenous BDNF expression under control conditions (left panel) and after treatment with 1 mM 4-AP (right panel) in E15.5 DIV5 cortical cultures. Note the absence of BDNF in distal neuronal projections even following prolonged activation. (B) Overexpression of the BDNF cDNA in a neuron of the same age. Note the widespread localisation of BDNF both within MAP2-positive projections and the cell nucleus. Representative images from $n = 2$ culture experiments, 20 neurons imaged per condition.

3.2.4 Validation of a new monoclonal antibody for BDNF western blots

Anti-BDNF mAb #9 has proven to work exceptionally well in immunostaining studies (Dieni et al. 2012), ELISA (Naegelin et al. 2018), BDNF immunoprecipitation (Matsumoto et al. 2008), and as a functional blocker of BDNF-TrkB signalling (Kossel et al. 2001) but fails to recognise BDNF on western blot. An alternative monoclonal antibody developed by Icosagen however had recently been shown to recognise both human and rat BDNF stored in megakaryocytes and platelets (Chacón Fernández et al. 2016). To determine whether this antibody also recognises BDNF within brain lysates, western blots were performed on tissue prepared from P7 *Bdnf* wildtype (WT), heterozygous (Het) and knockout animals and then probed using monoclonal antibody 3C11 (Figure 3.4). To confirm the equal loading of protein across lanes, the membrane was simultaneously probed using a polyclonal antibody against β -actin.

The detection of mAb 3C11 binding revealed bands at ~14 kD, the molecular weight of mature BDNF (mBDNF), in both *Bdnf* WT and Het lysates (Figure 3.4, upper panel). The specificity of this signal was confirmed by absence of the same band in KO lysates, and the appearance of the same band in lanes corresponding to 150 and 300 pg of recombinant BDNF. Consistent with previous findings (Matsumoto et al. 2008), a band corresponding to pro-BDNF was absent in extracts from both WT and Het brain; however, an ambiguous band at a similar molecular weight (~30 kD) was present in all brain lysates.

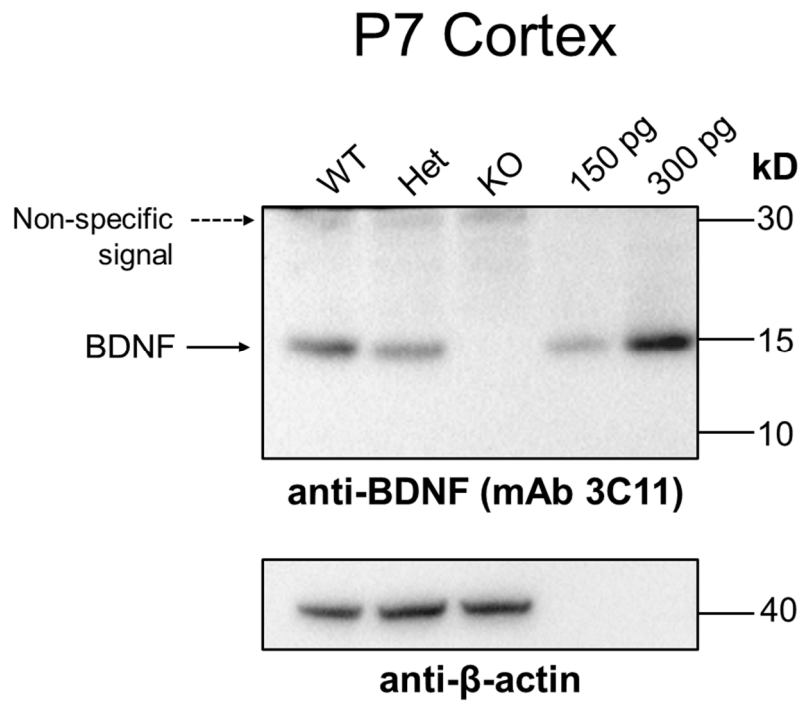


Figure 3.4. Validation of monoclonal antibody 3C11 for western blot.

Western blotting of brain lysates prepared from *Bdnf* wildtype (WT), heterozygous (Het) and knock-out (KO) littermates probed with mAb 3C11 (upper panel) and anti-β-actin (lower panel). Note the absence of a ~14 kD band in KO lysates, confirming the reliable detection of endogenous BDNF in both WT and Het animals. Note the non-specific signal detected in lysates at ~30 kD (dashed arrow) and the absence of a signal corresponding to pro-BDNF in all lysates. 150 pg and 300 pg recombinant BDNF used as a positive control. 10 μg protein loaded per lane; equal protein loading confirmed by probing the same membrane with antibodies against β-actin. *n* = 2 animals used per genotype.

3.2.5 Changes to BDNF processing after increased cellular activity

The successful visualisation of endogenous BDNF by ICC (Figure 3.2 and Figure 3.3) raised the question of whether activity-driven changes in BDNF expression can be further analysed by western blot. As little is known about the true capacity of neurons to process pro-BDNF, E17.5 cortical cultures, were prepared as previously described but treated with either 1 or 10 mM of 4-AP on DIV10. Whereas 1 mM 4-AP treatment was expected to increase BDNF levels by near 3-fold (Figure 3.2), the effects of using a higher, excitotoxic dose of 4-AP on BDNF expression remained unknown.

First, the analysis of cultures by BDNF ICC revealed changes to both BDNF distribution and the appearance of cells treated with 10 mM 4-AP (Figure 3.5A, right panels). Unlike those in control and 1mM 4-AP conditions (Figure 3.5A, left and centre panels, respectively) neurons treated with 10 mM 4-AP formed dense, cellular aggregates, likely resulting from glutamatergic excitotoxicity. Interestingly, BDNF immunoreactivity remained largely absent from MAP2-positive projections, suggesting the failed sorting of BDNF into its appropriate secretory pathway.

Next, the probing of cell lysates and conditioned media by western blot revealed that mAb 3C11 detects pro-BDNF and mBDNF in the lysates of both treated and untreated cells (CL) (Figure 3.5B). As observed by ICC, cultures incubated with 1 mM 4-AP showed substantial increases in BDNF, including an increased abundance of its pro-protein. Reduced amounts of pro- and mBDNF were also detected in cells treated with 10 mM 4-AP, indicating an attenuated synthesis and/or processing of the mature protein. The quantification of bands by densitometric analysis (Figure 3.5C) revealed that pro-BDNF comprises just 9.66% (± 2.42) of neuronal BDNF under control conditions, consistent with previous findings (Matsumoto et al. 2008). This proportion was shown to slightly increase following 24 hr treatment with 1 mM 4-AP (12.83% ± 3.53), however cultures exposed to 10 mM 4-AP presented with a striking increase of pro-BDNF, making up 53.73% (± 3.67).

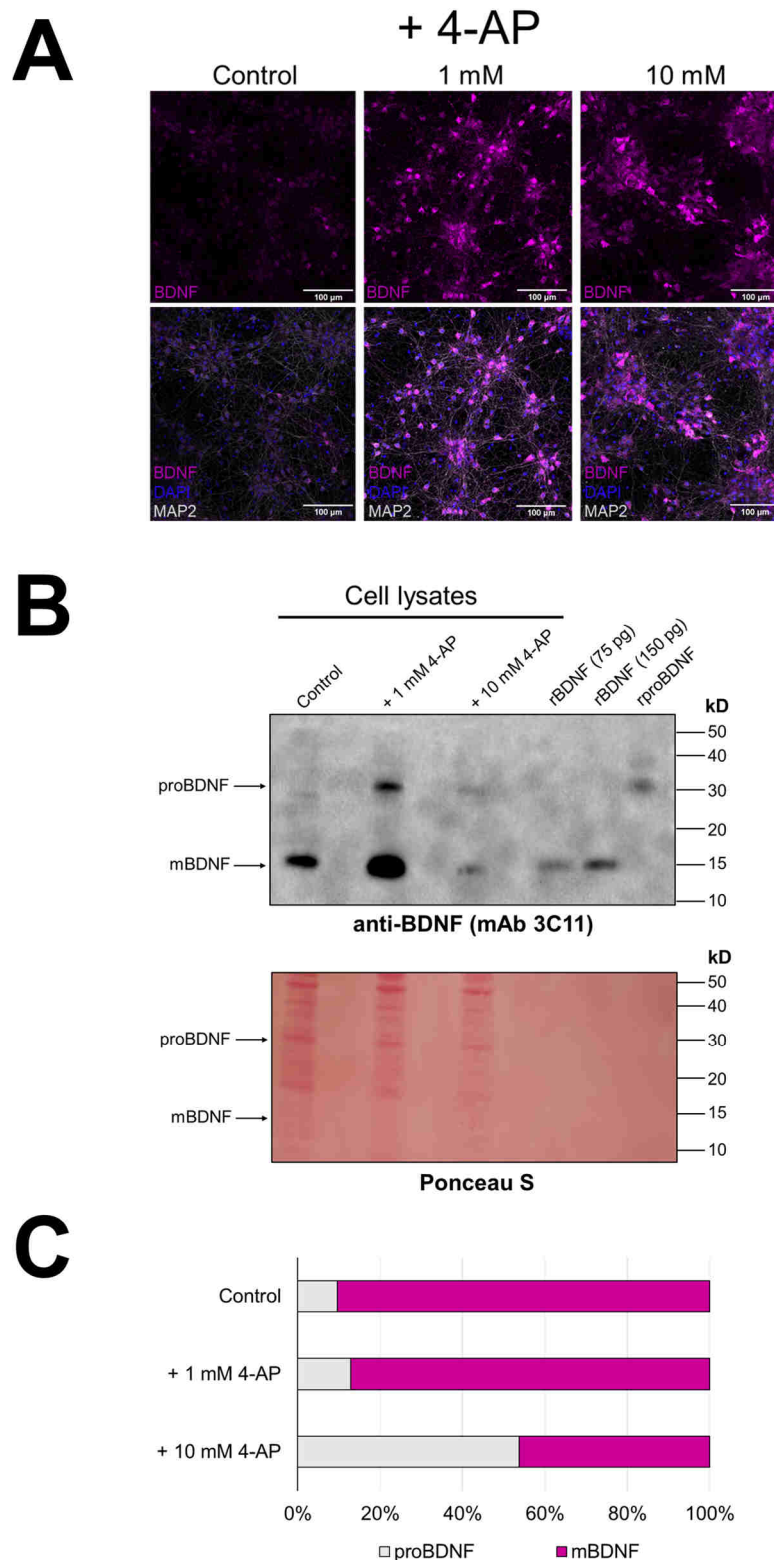


Figure 3.5. Determining the relative abundance of pro- and mature endogenous BDNF in cultured neurons.

(A) Low power images of WT E18 DIV11 cortical cultures incubated for 24 hr with the indicated concentrations of 4-aminopyridine (4-AP). Note the clustering of somas and the loss of puncta between cells after treatment 10 mM 4-AP (right panels). Representative images from $n = 3$ culture experiments. (B) Western blotting for BDNF proteins in the neuronal lysates (CL) and conditioned media (CM) of untreated (control) and 4-AP treated neurons. Note the rapid processing of pro-BDNF to mature BDNF (mBDNF) within lanes corresponding to no treatment and 1 mM 4-AP. Serial dilutions of rBDNF (150 – 9 pg) were used as positive controls. (C) Percentage of pro-BDNF and mBDNF in each lane of (B) quantified by densitometric analysis. Bars represent the mean percentages recorded from $n = 3$ culture experiments.

3.3 Summary and conclusions

This chapter summarises results related to the endogenous BDNF biosynthesis by neurons of the CNS. Together, these results re-define the processing and localisation of the *endogenous* BDNF, thus providing a basis for the understanding of the functionality and relevance of the BDNF cDNA constructs examined in the following chapters.

Probing established cortical cultures with monoclonal antibodies against the mature domain revealed that endogenous BDNF is detectable at steady-state levels within neuronal soma and their projections (Figure 3.2), agreeing with super-high resolution *in vitro* studies of hippocampal neurons (Andreska et al. 2014). The abundance of endogenous BDNF was shown to increase near 3-fold after 24 hr of depolarisation, demonstrating that activity-dependent changes in BDNF expression are detectable within neurons. Low level endogenous expression was also observed in younger cultures whereby immunoreactivity was confined to cell soma, even after 4-AP treatment (Figure 3.3A). Interestingly, overexpressing the *Bdnf* cDNA in cells from the same culture preparation resulted in a different localisation of BDNF, including its accumulation within nuclei (Figure 3.3B). This suggests that neurons of this age lack the adequate machinery to cope with high levels of BDNF expression, resulting in aberrant localisation of the mature protein. This is important to consider when interpreting previous conclusions of BDNF localisation and secretion, many of which were inferred from the transfection of plasmids encoding tagged versions of BDNF into young neuronal cultures (Goodman et al. 1996; Hartmann et al. 2001; Dean et al. 2009; Orefice et al. 2013).

The western blotting of brain lysates using anti-BDNF mAb 3C11 resulted in a specific band at ~14 kD, the predicted weight of mBDNF (Figure 3.4). It was also proven to recognise activity dependent changes in pro- and mBDNF levels in both cortical (Figure 3.5B) and megakaryocyte cultures (Chacón-Fernández et al. 2016). The absence of a band corresponding to pro-BDNF in cells kept under standard conditions supports previous findings that pro-BDNF is rapidly processed into the mature protein, comprising less than ~10% of total BDNF found within cell lysates (Matsumoto et al. 2008; Chacón-Fernández et al. 2016). Although others have argued that pro-BDNF can be secreted physiologically to be cleaved extracellularly by tPA, plasmin, or metalloprotease-7 (Pang et al. 2004; Nagappan et al. 2009; Yang et al. 2009), this late-stage cleavage is more likely to acting as a compensatory mechanism to avoid the apoptotic effects of pro-BDNF-p75^{NTR} (and sortilin) interactions in cases where pro-BDNF fails to be intracellularly cleaved. This does not exclude that under pathological conditions, pro-

BDNF may be released from dead cells, which could explain results published by other groups using culture conditions likely to be toxic for neurons, including the use of mitotic inhibitors (see Yang et al. 2009).

Chapter 4. Investigating the biological activity of BDNF fusion proteins

4.1 Short introduction

Since the cloning of green fluorescent protein from *Aequorea victoria* (Prasher et al. 1992; Chalfie et al. 1994), fluorescent proteins (FPs) have become indispensable tools for studying the spatial and temporal patterns of gene expression *in vivo*. The fusion of such probes to molecules of interest allows for the generation of tools that facilitate the tracing of their subcellular localisation and transport by live imaging experiments. This also holds true for BDNF, whereby the transient overexpression of BDNF-GFP and -pHluorin have been used to study its trafficking and release from neurons (Hartmann et al. 2001; Dean et al. 2009; Matsuda et al. 2009; Harward et al. 2016). However, with FPs being about twice the size of a BDNF monomer, this raises a question of whether the biological activity of BDNF is affected by the fusion of such comparatively large probes. Indeed, it has long been known that interactions between FPs can lead to the formation of aggregates within cells, perturbing the targeting or function of proteins of interest (Zhang et al. 1996; Lauf et al. 2001; Shaner et al. 2004). One must also consider that BDNF exists as a homodimer in solution (Kolbeck et al. 1994) and that the oxidising conditions of the secretory pathway – required for the correct folding of mature BDNF – can induce non-native disulfide bonding in FPs, contributing to their misfolding and potential aggresome formation (Costantini and Snapp 2013; Costantini et al. 2015). By contrast, replacing *Bdnf* with myc- or hemagglutinin-tagged versions of the *Bdnf* gene allowed the generation of healthy and viable animals (Matsumoto et al. 2008; Yang et al. 2009), suggesting that small tags can be added to BDNF without interfering with post-natal survival, given that the synthesis of biologically active and secreted BDNF is a requirement for the survival of mice beyond 3-weeks-of-age (Ernfors et al. 1994; Jones et al. 1994). The aim of this chapter was to investigate using *in vitro* systems whether the biological activity of BDNF is retained when large tags are fused at its C-terminus. These experiments revisit in particular the processing of both BDNF-GFP and BDNF-pHluorin previously used by others to explore various aspects of BDNF's biology *in vitro* (see above). Novel constructs were also tested in this Chapter, whereby BDNF was fused to mCherry, moxVenus, or moxGFP, fluorescent proteins that were previously optimised by others to prevent misfolding or aggregation (Shaner et al. 2004; Costantini et al. 2015). As BDNF-myc had been shown previously to replicate the biology of the wildtype protein, the suitability of BDNF-myc-GFP was also tested. Inspired by previous works on the BRAF oncogene (van Veen et al. 2016), a novel approach was also tested

that allows BDNF and GFP to be co-translated from a single bicistronic mRNA (hereinafter referred to as BDNF-P2A-GFP). Insertion of a 22 aa P2A sequence between the coding sequence for BDNF and GFP causes a break in the polypeptide chain during translation, resulting in the generation of BDNF-P2A and GFP as separate proteins. To determine whether BDNF's functionality becomes increasingly compromised by lengthening the tag at its C-terminus, experiments were performed in parallel that study its processing, secretion, and potency at the endogenous TrkB receptor after the adding of multiple copies of the epitope tag, myc. The main conclusions resulting from the data detailed in this Chapter have been published in a short report (see Wosnitzka et al. 2020).

4.2 Results

4.2.1 Screening cDNA constructs encoding BDNF fusion proteins in HEK293 cells

To assess the biological processing of tagged BDNF proteins, cDNAs encoding BDNF fused to various tags (listed in Table 4.1) were introduced into plasmid vectors and expressed in transfected HEK293 cells. As accumulating evidence suggests that HEK293 cells are also of neural crest ectodermal origin yet are more easily transfected than neurons (Shaw et al. 2002; Lin et al. 2014), these cells were considered a reasonable *in vitro* model for studies of neuronal BDNF processing. Expression of each cDNA in these cells was under regulatory control of the human CMV promoter/enhancer sequence, resulting in the constitutive overexpression of proteins. Note that the molecular weight of proteins was as predicted from its cDNA sequence (see Chapter 2 for more details).

Table 4.1. BDNF cDNA constructs, their translational products and predicted molecular weights.

Plasmid	Translation product(s)				Predicted molecular weight (kDa)			
					pre/proBDNF protein	mature BDNF protein	epitope/ fluorescent protein	
pBDNF (Hofer et al. 1990)	pre	pro-peptide	BDNF		28.1	14.0	-	
pBDNF-myc (Matsomoto et al. 2008)	pre	pro-peptide	BDNF	myc	29.3	15.2	1.2	
pBDNF-2myc	pre	pro-peptide	BDNF	myc myc	30.5	16.4	2.4	
pBDNF-3myc	pre	pro-peptide	BDNF	myc myc myc	31.7	17.6	3.6	
pBDNF-4myc	pre	pro-peptide	BDNF	myc myc myc myc	32.9	18.8	4.8	
pBDNF-mCherry	pre	pro-peptide	BDNF	mCherry	54.8	40.7	26.7	
pBDNF-moxVenus	pre	pro-peptide	BDNF	moxVenus	55.0	40.9	26.9	
pBDNF-moxGFP	pre	pro-peptide	BDNF	moxGFP	55.0	40.9	26.9	
pBDNF-GFP	pre	pro-peptide	BDNF	GFP	55.2	41.1	27.1	
pBDNF-SEP (Yasuda et al. 2009)	pre	pro-peptide	BDNF	FLAG pHluorin	57.1	43.0	29.0	
pBDNF-P2A-NLS-GFP	pre	pro-peptide	BDNF	P2A	30.3	16.2	2.2 (P2A)	24.0 (GFP)
	+							

Probing HEK293 cell lysates with antibodies against BDNF and its pro-peptide revealed that the majority of immunoreactive material migrates as pro-BDNF glycosylated to different degrees (Figure 4.1A and B, left panels). The abundance of pro-BDNF is expected to result from cDNA-driven overexpression of *Bdnf* overwhelming the processing capacity of transfected HEK293 cells. In the lysates of cells expressing pBDNF-mCherry, -moxVenus, -moxGFP and -mycGFP, the pro-protein was shown to be atypically processed, likely corresponding to its early degradation by intracellular proteases (Figure 4.1B, left panel). In contrast, the maturation of BDNF-P2A was shown to closely resemble that of BDNF and BDNF-myc, indicating the addition of the P2A tag does not measurably interfere with pro-domain cleavage.

Western blotting of the conditioned media revealed that BDNF-P2A is also secreted at comparable levels to BDNF and BDNF-myc (Figure 4.1A and B, right panels). As observed in cell lysates, the upward shift of both the pro- and mature protein indicates that the P2A tag remains attached even after secretion. Except for BDNF-GFP, all other BDNF fusion proteins were readily detectable in the conditioned media. This was also true for their respective pro-proteins although their detection was limited by the presence of a large BSA band at ~60 kD.

A

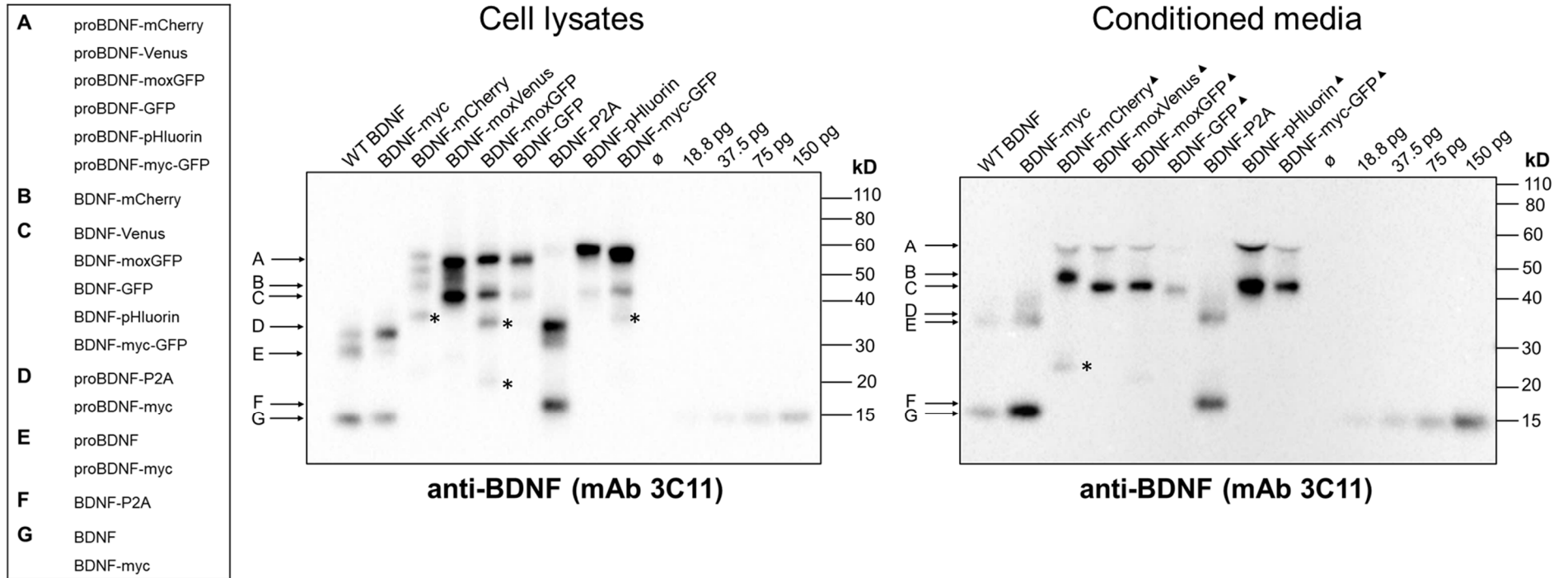


Figure 4.1. The processing and secretion of BDNF-fusion proteins by HEK293 cells (continued on the next page).

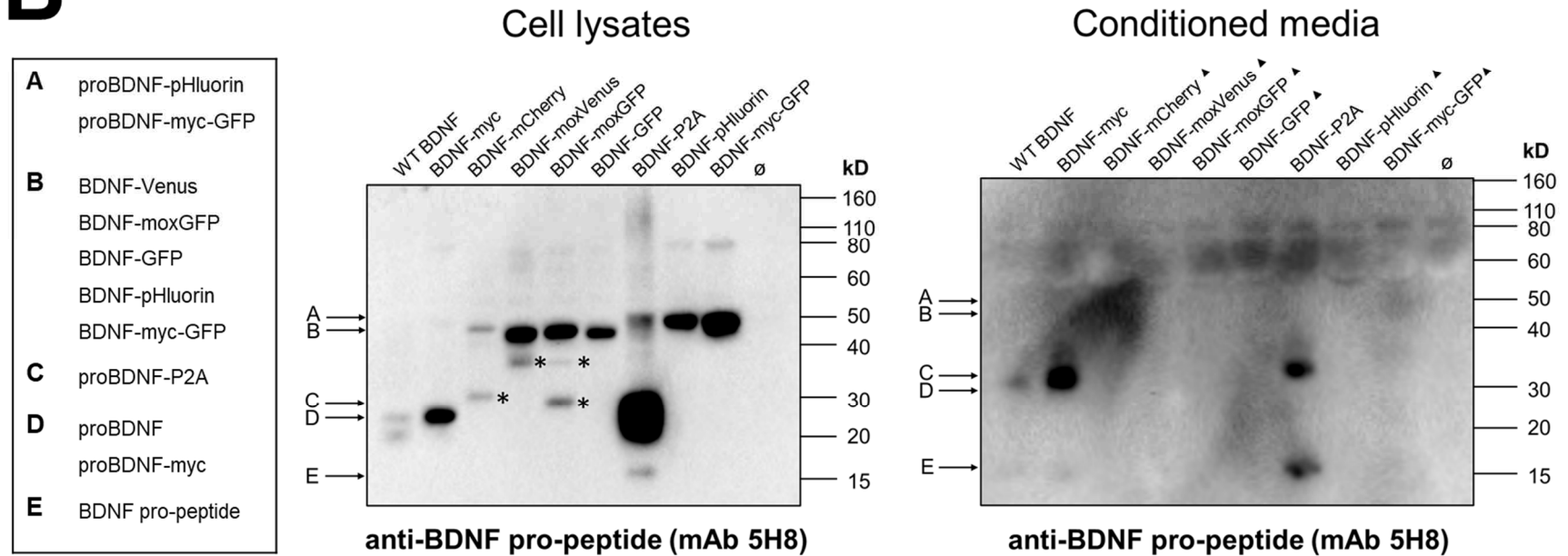
B

Figure 4.1. The processing and secretion of BDNF-fusion proteins by HEK293 cells.

Western blot analysis of cell lysates and conditioned media using monoclonal antibodies against BDNF (**A**, previous page) and its pro-peptide (**B**). Cells were transfected with the indicated plasmids and processed after 24 hr. A plasmid encoding WT BDNF or rBDNF (18.8 – 150 pg, only used in **A**) was used as positive controls. ø, no transfection control. * indicates atypical proteolytic processing of the pro- or mature protein; ▲ indicates a 5 × loading volume of conditioned media. In blots corresponding to the conditioned media (right panels), note that the detection of pro-proteins was compromised by a large band corresponding to BSA (~60 kD).

4.2.2 BDNF-GFP fails to be efficiently secreted by HEK293 cells

As BDNF-mCherry, -moxVenus, -moxGFP and -myc-GFP were shown to be atypically processed by HEK293 cells, their respective cDNA constructs were omitted from further transfection studies. As BDNF-GFP and BDNF-pHluorin have been used extensively in the literature to study the trafficking, localisation, and secretion of BDNF (Hartmann et al. 2001; Kojima et al. 2001; Harward et al. 2016), their biological similarity to the wildtype protein was further analysed by western Blot.

After the confirmation of equal protein loading using antibodies against protein GAPDH (Figure 4.2A), the secretion of each fusion protein was compared to that of WT BDNF. The densitometric analysis of blots (as shown in Figure 4.2B) revealed the attenuated secretion of BDNF-GFP, where the mature protein was secreted at levels 85% (± 8.37) lower than the wildtype protein ($t = -13.500$, $p = 0.002$) (Figure 4.2B and C). In contrast, no significant difference was observed in the secretion of BDNF-pHluorin ($t = -6.143$, $p = 0.180$), or BDNF-P2A ($t = -7.357$, $p = 0.070$).

The re-probing of blots using antibodies against GFP revealed that BDNF-GFP and BDNF-pHluorin also undergo slight degradation, liberating small amounts of fluorophore from the BDNF protein (Figure 4.2B). In line with the previous detection of a band corresponding to cleaved BDNF-P2A (Figure 4.2A), GFP was shown to accumulate as a single band in cells transfected with the pBDNF-P2A-NLS-GFP construct. In addition, the absence of GFP in the corresponding conditioned media suggests that GFP is successfully retained, avoiding the secretory pathway utilised by the cleaved BDNF-P2A protein.

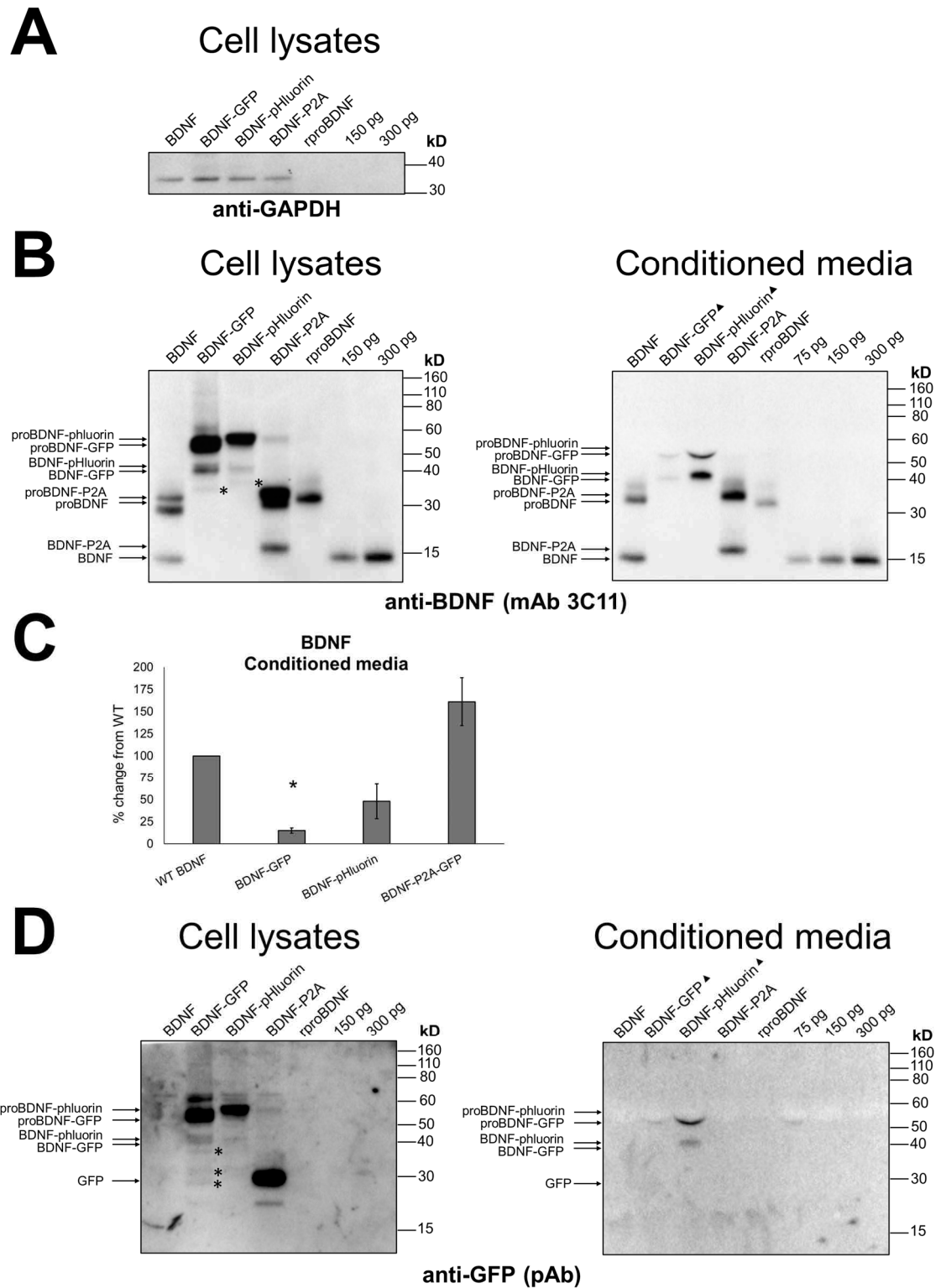


Figure 4.2. Further analysis of BDNF-GFP, BDNF-pHluorin and BDNF-P2A-GFP in HEK293 cells.

Western blotting of HEK293 cell lysates (left panels) and conditioned media (right panels) using antibodies against GAPDH (loading control, **A**), BDNF (**B**), and GFP (**D**). Note that 3 × more conditioned media was loaded from cells transfected with BDNF-GFP or BDNF-pHluorin, indicated by ▲. On blots, * indicates atypical proteolytic processing of proteins. rpro-BDNF and rBDNF (75 – 300 pg) were used as positive controls. (**C**) Densitometric analysis of (**B**, right panel). Bars represent the % secretion of each fusion protein when compared to the WT protein ± SEM. * indicates $p < 0.008$ ($p = 0.002$).

4.2.3 Increasing tag lengths compromises the ability of BDNF to phosphorylate TrkB

Given that BDNF-P2A-GFP is *processed* in a similar manner to the wildtype protein, it was important to next investigate whether the P2A tag (22 aa) added to BDNF's C-terminus compromises its ability to activate its cognate receptor, TrkB. To further test whether receptor phosphorylation is directly affected by the length of tag at BDNF's C-terminus, the potency of BDNF proteins carrying large C-terminal tags, including 1-4 repeats of the epitope myc tag (10, 20, 30 or 40 aa), were compared to that of BDNF-P2A (Matsumoto et al. 2008; Dieni et al. 2012).

First, the conditioned medium from HEK293 cells transfected with pBDNF, pBDNF-GFP and pBDNF-P2A-NLS-GFP were collected and then standardised using a BDNF ELISA (data not shown). Their ability to phosphorylate TrkB was then tested by incubating primary cultures of E17.5 7DIV mouse cortical neurons with 6.5 ng/ml of each protein, a concentration limited by the poor secretory characteristics of BDNF-GFP (see above). After confirmation of equal protein loading using Ponceau S, the immunoblotting of membranes using antibodies recognising phosphorylated Trk receptors revealed comparable levels of phosphorylation induced by WT BDNF and BDNF-P2A (Figure 4.3A). Although levels of phosphorylation induced by BDNF-GFP appeared comparable to the no treatment control (indicated by \emptyset), only limited conclusions could be drawn from these studies due to high levels of basal phosphorylation, likely caused by endogenous BDNF expression in cultures of this age (see Chapter 3). To circumvent these difficulties, younger neuronal cultures were utilised for further Trk phosphorylation experiments, whereby the expression of endogenous BDNF was expected to be much lower (see Chapter 3).

To test the effect of increasing tag length on the phosphorylation of TrkB, HEK293 cells were also transfected with plasmids encoding BDNF fused to 1-4 copies of myc. The amount of BDNF-myc, -2myc, -3myc, -4myc and -P2A in their conditioned media was then also standardised using a BDNF ELISA (data not shown). TrkB phosphorylation was then tested by incubating E14.5 neurons on DIV5 with 25 ng/ml of each BDNF protein. After confirmation of equal protein loading using antibodies against β -actin, immunoblotting the membrane using a monoclonal antibody against phosphorylated Trk receptors revealed that receptor activation was successfully induced by all BDNF proteins, albeit with decreasing efficiency as a function of tag length (Figure 4.3B and C). In particular, activation of TrkB was shown to be significantly reduced by BDNF-3myc ($t(5) = -5.329$, $p = 0.003$) or BDNF-4myc ($t(5) = -5.047$, $p = 0.004$), whereas no significant decrease in phosphorylation was observed for BDNF-2myc ($t(6) = -0.631$, $p = 0.551$) or

BDNF-P2A ($t(2) = -0.747, p = 0.533$). In contrast to previous experiments using E17.5 DIV7 neurons, no endogenous phosphorylation was observed in these cultures under control conditions.

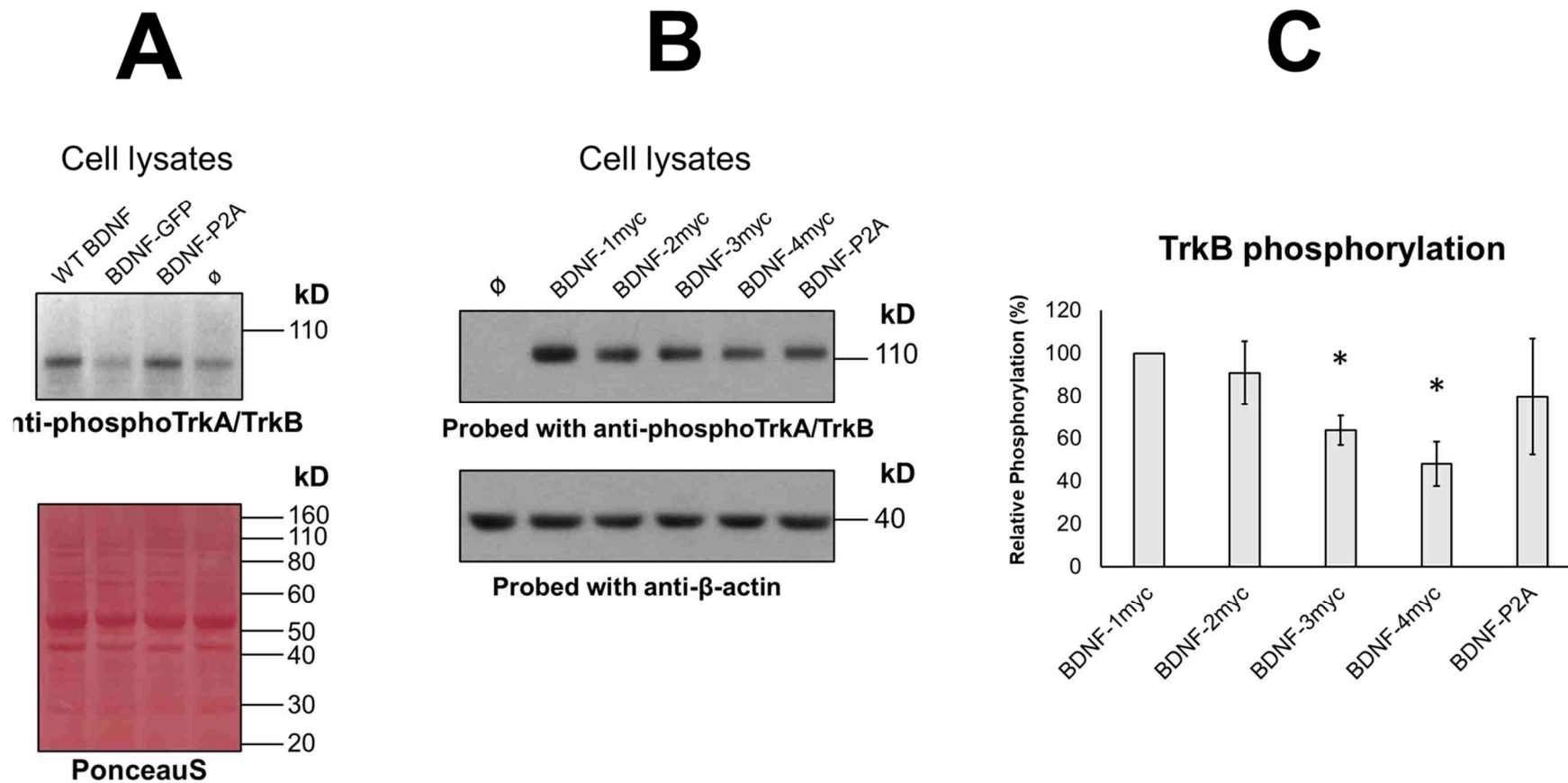


Figure 4.3. Increasing the length of BDNF fusion proteins attenuates their ability to phosphorylate TrkB.

(A) Western blotting of E17.5 DIV 7 neuronal lysates following 15 min treatment with conditioned media containing 6.5 ng/ml of the indicated proteins. \emptyset indicates conditioned medium from non-transfected HEK293 cells. PonceauS used as a loading control. (B) Western blot of E14.5 DIV5 neuronal lysates following 15 min treatment with conditioned media containing 25 ng/ml of the indicated proteins. β -actin used as a loading control. (C) Densitometric analysis of (B). Bars represent the % phosphorylation induced by each protein when compared with BDNF-myc, \pm SEM. * indicates $p < 0.0125$ (BDNF 3-myc, $p = 0.003$; BDNF-4myc, $p = 0.004$). With thanks to Xinsheng and Jeff Nan at Cardiff University who generated the results shown in (B) and (C).

4.2.4 Investigating the cellular distribution of BDNF-fusion proteins in cultured neurons

As HEK293 cells lack the dedicated secretory pathway found in neurons, BDNF fusion proteins were then transfected into E14.5 DIV5 cortical cultures. Using antibodies against BDNF combined with high power imaging, it was next investigated whether the fluorescent probes GFP and pHluorin faithfully report the cellular localisation of BDNF. As the GFP sequence of pBDNF-P2A-GFP is preceded by a nuclear localisation sequence (NLS), it was also tested whether this was functional when expressed by neuronal cells.

As previously shown (see Chapter 3), overexpression of the WT protein resulted in strong BDNF immunoreactivity across both neuronal soma and their early processes (Figure 4.4A). This however was not the case for BDNF-GFP or BDNF-pHluorin, where the bulk of BDNF-immunoreactivity was limited to the cell soma (Figure 4.4B and C, respectively). High magnification imaging of early neurites also showed the separation of GFP or pHluorin fluorescence from BDNF-positive puncta, indicating that a fraction of each fluorescent protein becomes separated from BDNF's C-terminus (indicated by arrows in i and ii).

The localisation of BDNF-P2A however (bottom panels) closely matched the distribution of the wild-type protein (top panels), with intense labelling of both neuronal soma and early projections (Figure 4.4A). GFP on the other hand was detected almost solely in the nucleus, confirming the functionality of its nuclear localisation sequence.

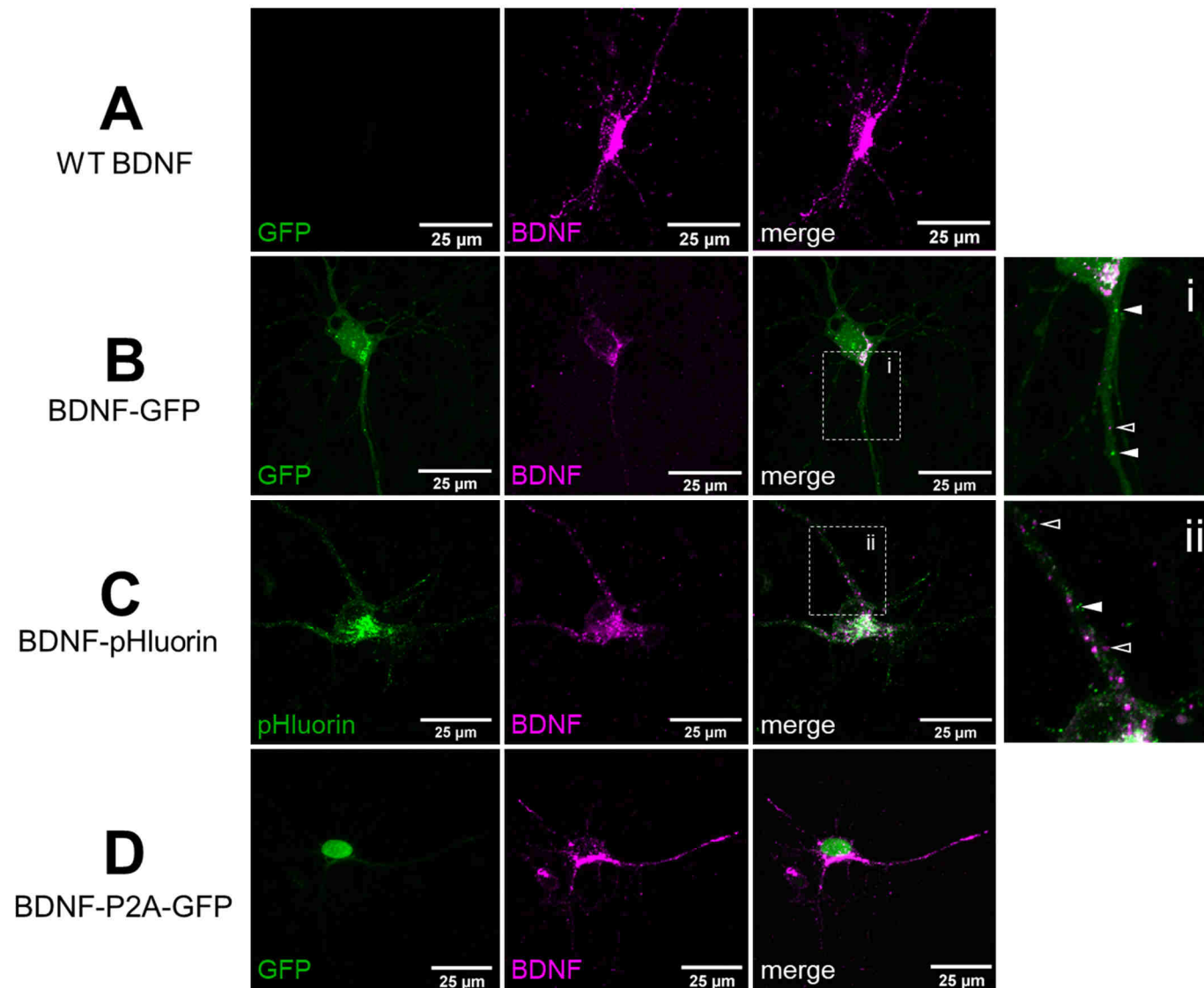


Figure 4.4. Visualising of the distribution of BDNF, GFP and pHluorin in transfected primary neurons.

E14.5 cultures on DIV6, 24 hr after transfection with plasmids encoding WT BDNF, BDNF-GFP, BDNF-pHluorin and BDNF-P2A-GFP. Cells were stained using antibodies against BDNF, whereas GFP and pHluorin were detected by innate fluorescence. Note that the bulk of BDNF is detected in the perisomal region in areas likely corresponding to the ER or Golgi apparatus. In neurons transfected with BDNF-GFP and BDNF-pHluorin, note the separation of GFP fluorescence (green, white arrowheads) from BDNF immunoreactivity (magenta, empty arrowheads) within both nuclei and proximal neuronal processes (i and ii, respectively).

4.3 Summary and conclusions

This chapter demonstrates the functionality of a novel BDNF cDNA construct that reports the expression of BDNF by the co-translation of GFP. The transfection of pBDNF-P2A-NLS-GFP into HEK293 cells and primary neurons (Figure 4.2 and Figure 4.4 respectively) revealed the biosynthesis of BDNF-P2A and GFP as distinct products. BDNF-P2A was shown to closely replicate the biological activity of the wildtype protein and BDNF-myc, suggesting it may be suitable for use *in vivo*. Although animal models have been previously generated that allow for the detection of the BDNF protein by tagging its C-terminus with short epitope tags recognised by myc or HA antibodies (Matsumoto et al. 2008; Yang et al. 2009), the replacement of the *Bdnf* with this novel construct will facilitate the isolation of cells actively expressing *Bdnf* through the sorting of GFP positive nuclei, facilitating not only the characterisation of *Bdnf* expressing cells in the CNS but the generation of new reagents that can directly modulate *Bdnf* expression, such as 4-AP (see Chapter 3).

The western blot analyses of proteins synthesised in HEK293 cells detailed in this Chapter exposed multiple problems associated with the processing of BDNF when fused to large fluorescent probes. Whilst these problems were not necessarily unexpected, it is surprising that such constructs have been extensively used in a number of previous publications, without detailed validation of the constructs ((Hartmann et al. 2001; Kojima et al. 2001; Egan et al. 2003; Dean et al. 2009; Harward et al. 2016). In particular, the pro-proteins of BDNF-mCherry, -moxVenus, -moxGFP and -myc-GFP all underwent premature degradation (Figure 4.1A and B) and this was also the case for BDNF-GFP and -pHluorin, albeit to a lesser extent (Figure 4.2). Transfection of pBDNF-GFP and -pHluorin into primary cultures (Figure 4.4) also indicated that this cleavage occurs in neurons, supported by previous evidence of a cleavage site located at BDNF's C-terminus (Rodriguez-Tebar et al. 1991) (Figure 4.5). The atypical processing of BDNF-GFP was also inferred from analysing the conditioned media of HEK293 cells, whereby secretion of the mature protein was dramatically reduced (Figure 4.1 and Figure 4.3). Although this was not the case for BDNF-pHluorin, analysis of their amino acid sequence reveals a FLAG linker in BDNF-pHluorin which may improve the flexibility and thus activity of the mature protein (highlighted in Figure 4.5). However, as the degree of transfection was not formally quantified, it should be considered that lower levels of BDNF in the conditioned medium may instead reflect poor transient expression of the respective constructs in comparison to pBDNF. However, this seems unlikely considering comparable levels of the pro- and mature protein were detected across cell lysates (Figure 4.2B, left panel).

In vitro studies of BDNF constructs with multiple copies of myc added to BDNF's c-terminus further suggests that there is limited scope to adding extended tags to BDNF while preserving its biological activity. Indeed, the notable decrease in TrkB phosphorylation by BDNF-3myc and -4myc (Figure 4.3B and C) suggests that caution should be exerted when generating large fusion constructs, as they would seem unlikely to sufficiently phosphorylate TrkB. Although accumulating evidence suggests that HEK293 cells are more similar to neurons than first described (Shaw et al. 2002; Lin et al. 2014), these cells do not contain the regulatory secretory pathway utilised by neurons to mediate BDNF's activity-dependent release. Follow-up experiments should therefore be performed in neurons matured *in vitro* or *in vivo* to determine the relevance of these findings.

A BDNF-GFP

RGRGSGMVSKGEELFTGVVPILVELDGDVNGHKFSVSGEGEGDATYGKLTLKFICTTGKLPVPWPTLVTTLTYGVQCFSRYPDHMKQHDFFKSAMPEGYVQERTI
FFKDDGNYKTRAEVKFEGDTLVNRIELKGIDFKEDGNILGHKLEYNYNSHNVYIMADKQKNGIKVNFKIRHNIEDGSVQLADHYQQNTPIGDGPVLLPDNHYLST
QSALSKDPNEKRDHMLLEFVTAAGITLGMDELYK

B BDNF-pHluorin

RGRGSDYKDDDDKSKGEELFTGVVPILVELDGDVNGHKFSVSGEGEGDATYGKLTLKFICTTGKLPVPWPTLVTTLTYGVQCFSRYPDHMKRHDFFKSAMPEGYV
QERTIFFKDDGNYKTRAEVKFEGDTLVNRIELKGIDFKEDGNILGHKLEYNNDHQVYIMADKQKNGIKANFKKIRHNIEDGGVQLADHYQQNTPIGDGPVLLPD
NHYLFTTSTLSKDPNEKRDHMLLEFVTAAGITHGMDELYK

C BDNF-P2A-GFP

RGRGSGATNFSLLKQAGDVEENPGPPKKKRKMVSKGEELFTGVVPILVELDGDVNGHKFSVSGEGEGDATYGKLTLKFICTTGKLPVPWPTLVTTLTYGVQCFS
RYPDHMKQHDFFKSAMPEGYVQERTIFFKDDGNYKTRAEVKFEGDTLVNRIELKGIDFKEDGNILGHKLEYNYNSHNVYIMADKQKNGIKVNFKIRHNIEDGSVQ
LADHYQNTPIGDGPVLLPDNHYLSTQSALSKDPNEKRDHMLLEFVTAAGITLGMDELYK

Figure 4.5. Annotated amino acid sequences of the C-terminal tags of BDNF-GFP, BDNF-pHluorin, and novel construct BDNF-P2A-GFP.

A schematic detailing the C-terminal tags fused to the mouse BDNF sequence (last 3 aas shown in magenta). BDNF-GFP (A) comprises of BDNF fused to a short linker sequence (GSG, black underline) immediately followed by that of enhanced green fluorescent protein (GFP, double green underline). BDNF-pHluorin (B), (first published by Yasuda et al. 2009) contains a FLAG linker sequence (GSDYKDDDDK, underlined) followed by the aa sequence for super ecliptic pHluorin (SEP, strong green underline). Novel BDNF construct BDNF-P2A-GFP (C) contains BDNF again followed by a short linker (GSG, black underline) followed by aa sequence for P2A (blue highlight). Scissors indicate the P2A self-cleavage site, found between a C-terminal glycine (G) and proline (P) of the 2A peptide. eGFP (double green underline) is preceded by the SV40 nuclear localisation sequence (PKKKRKM, grey highlight), facilitating the translocation of nascent eGFP to the cell nucleus.

Chapter 5. Characterisation of mice expressing *Bdnf-P2a-Gfp* instead of *Bdnf*

5.1 Short introduction

Correlations between impaired synaptic plasticity and neuronal dysfunction suggest that BDNF may be an attractive target for the treatment of nervous system disorders. In particular, there is an increasing appreciation for the notion that both fast- and slow-acting antidepressants involve the BDNF-TrkB pathway (Björkholm and Monteggia 2016; Casarotto et al. 2021), raising the question of whether increasing levels of the endogenous ligand may exert beneficial effects *in vivo*. Due to the problems associated with detecting endogenous BDNF (discussed in Chapter 3), such questions call for the design of a new mouse model that facilitates the identification of cells that actively translate the *Bdnf* mRNA.

Having established the suitability of the BDNF-P2A-GFP construct with regard to the biosynthesis and secretion of BDNF and the co-translation of GFP (see Chapter 4), this chapter describes the generation of a novel mouse model where the *Bdnf* protein coding sequence is replaced with the reporter construct BDNF-P2A-NLS-GFP (hereinafter referred to as *Bdnf-P2a-Gfp*). The viability of *Bdnf-P2a-Gfp* hetero- and homozygotes was initially assessed by confirming the fertility of both male and female mice and monitoring the genotypes of animals observed at birth. As previous reports indicated that BDNF-TrkB signalling plays a critical role in the regulation of food intake (Lyons et al. 1999; Kernie et al. 2000), the body weights of animals, maintained in mixed genotype housing, were monitored throughout. The biosynthesis and localisation of BDNF-P2A in these mice was also compared to wildtype mice by western blot and immunohistochemical analyses. The experiments also included cultures of neurons isolated from *Bdnf-P2a-Gfp* mice, and testing whether the activity dependent expression of GFP replicates the fold change observed for that of *Bdnf*, whereby both proteins are expressed from the same gene locus and mRNA construct. Last, GFP signals in the adult hippocampus and cerebral cortex were analysed at high magnification and compared to previous reports of *Bdnf* expression. The characterisation of this mouse model has been published in a short report (see Wosnitzka et al. 2020).

5.2 Results

5.2.1 Generation of the *Bdnf-P2a-Gfp* mouse

Bdnf-P2a-Gfp mice were kindly generated by our colleagues at Boehringer Ingelheim GmbH and Taconic Biosciences. First, a construct encoding *Bdnf-P2a-Gfp* was targeted to the wildtype *Bdnf* allele (Figure 5.1A) in mouse embryonic stem cells (mESCs) by transient transfection. This target construct encoded the entire coding region of *Bdnf* preceded by a puromycin resistance sequence (Pur) flanked by two short Flippase (*Flp*) recognition target (*FRT*) sites in intron I (Figure 5.1B). Cultures were then treated with antibiotics to identify cells that had successfully integrated the construct, whereby cells expressing *Bdnf-P2a-Gfp* have a resistance to puromycin. After the identification of successfully targeted cells, the *in vitro* transient expression of *Flp* allowed for the successful deletion of the puromycin resistance cassette, resulting in a redundant *FRT* site in a non-conserved region of the *Bdnf* locus. ESCs containing the resulting construct (Figure 5.1C) were then injected into blastocysts and implanted into the uterus of surrogate pseudo-pregnant mice. Chimeric offspring were then continuously bred on a C57BL/6 background until germline transmission of the *Bdnf-P2a-Gfp* allele was confirmed by PCR. Upon the generation of heterozygotes, the mouse colony was then rapidly expanded by *in vitro* fertilisation and shipped to Cardiff for generation of a new cohort. Subsequent generations of *Bdnf-P2a-Gfp* animals were maintained on the C57BL/6 background also used for animals wild-type for *Bdnf* expression.

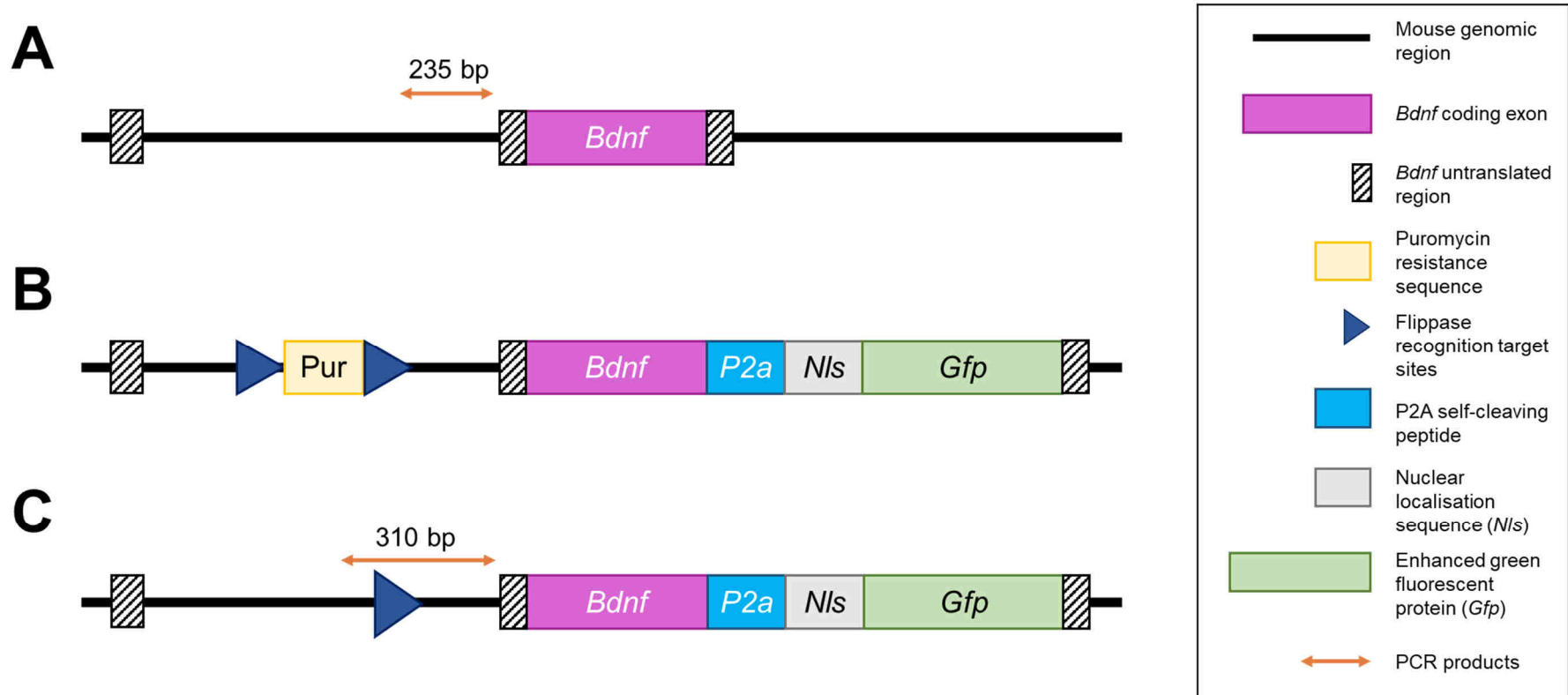


Figure 5.1. Schematics illustrating the insertion of *Bdnf-P2a-Gfp* into the endogenous *Bdnf* allele in mouse ESCs (mESCs).

(A) The wildtype mouse *Bdnf* allele targeted in mESCs. (B) The initial *Bdnf-P2a-Gfp* target construct, including a puromycin resistance cassette flanked by two FRT sites for selection of successfully targeted cells. (C) The same construct as (B) after FLP-FRT mediated recombination *in vitro*. Orange arrows indicate the PCR products resulting from primer hybridisation with the wildtype (A) or knock-in (C) allele. With thanks to Michael Schuler (Boehringer Ingelheim) who designed the *Bdnf-P2a-Gfp* target construct and performed the initial targeting of ESCs, and to Taconic Biosciences for generating these animals.

5.2.2 Phenotypic characterisation of *Bdnf-P2a-Gfp* littermates

To genotype litters of the *Bdnf-P2a-Gfp* colony, primer pairs were generated that flank an unconserved sequence in intron 1 of WT *Bdnf* (see Figure 5.1A and C). As this region contains the remnants of FRT-FLP recombination sites in *Bdnf-P2a-Gfp* mice, PCR amplification of their DNA resulted in bands at 235 and 310 bp, corresponding to the WT and knock-in (KI) allele respectively (Figure 5.2A). The analysis of 8 litters born from heterozygous breeding pairs revealed that both heterozygous and homozygous animals were born at the expected Mendelian ratio (Figure 5.2B).

Although these mice were also shown to be viable and fertile, the monitoring of their body weights revealed that both heterozygous and homozygous *Bdnf-P2a-Gfp* males significantly gained weight in the later stages of adulthood ($t = -22.142$, $p = 0.023$ and $t = -26.685$, $p = 0.018$, respectively) (Figure 5.2C). Interestingly, females were spared from this phenotype, showing no significant change to body weight. Despite the dramatic change observed in the body weight of males, *Bdnf-P2a-Gfp* animals otherwise displayed no overt phenotypes, having a life span of > 1 year when maintained in standard animal housing (data not shown).

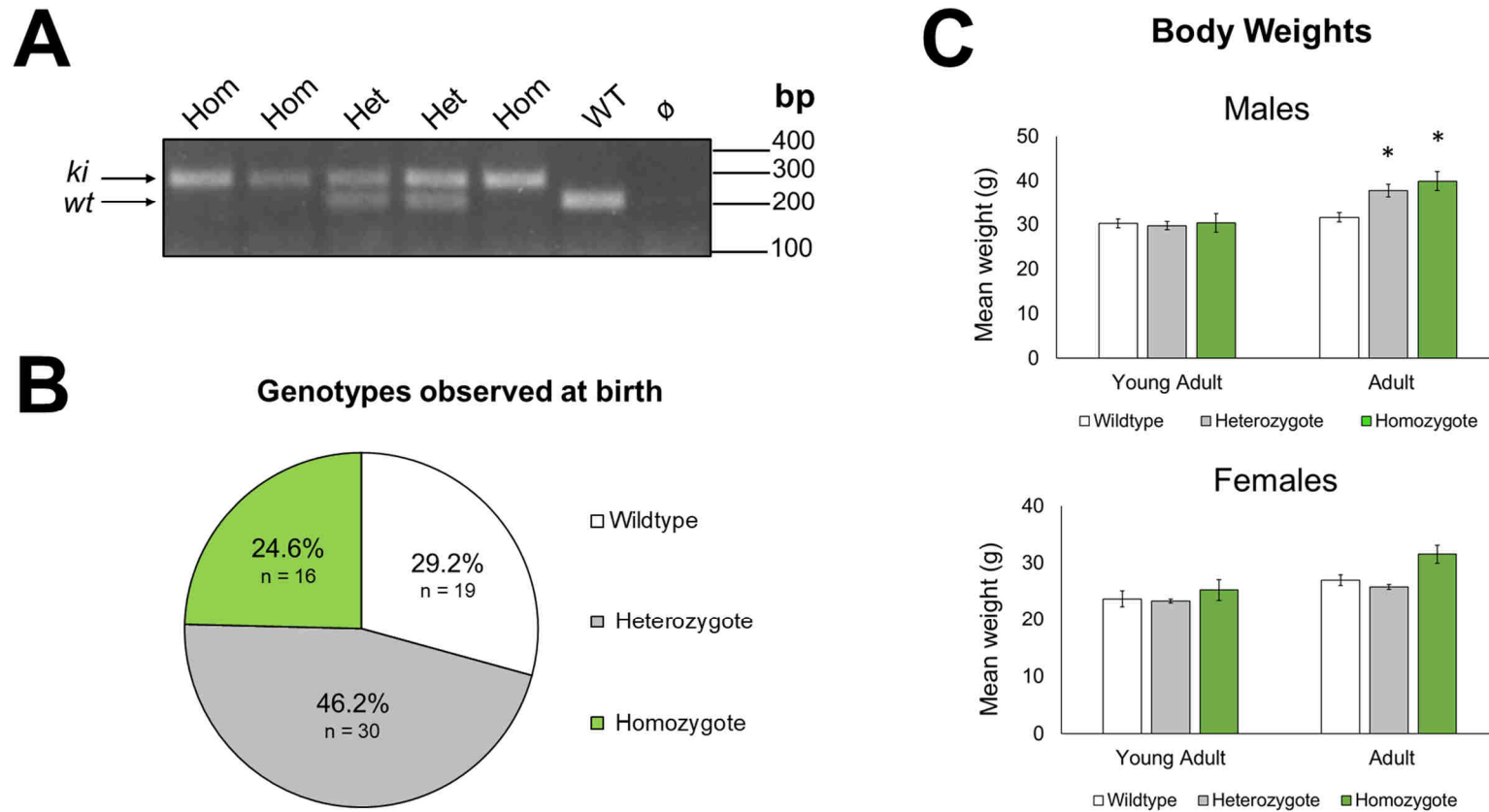


Figure 5.2. Early characterisation of *Bdnf-P2a-Gfp* littermates.

(A) Representative results from the genotyping of *Bdnf-P2a-Gfp* littermates. Note the presence of two bands at 235 bp and 310 bp, corresponding to the wildtype and knock-in allele, respectively. \emptyset represents no DNA control. (B) Percentage of genotypes observed across 66 animals born from 8 litters. (C) Body weights of young adult (3- to 4-month-old) and adult (6- to 7-month-old) male and female *Bdnf-P2a-Gfp* mice. Data are mean \pm SEM. * indicates $p < 0.01$ ($p = 0.010$ and $p = 0.0017$ for heterozygous and homozygous males, respectively). $n > 9$ animals analysed per age category and genotype.

5.2.3 BDNF levels are unchanged in the hippocampus and cerebral cortex of *Bdnf-P2a-Gfp* mice

As *Bdnf*^{+/-} mice also exhibit progressive obesity (Lyons et al. 1999), this raised a question of whether this weight gain resulted from reduced BDNF levels in *Bdnf-P2a-Gfp* mice. To compare BDNF levels between littermates, protein extracts were prepared from the adult (6- to 7-month-old) hippocampus and cortex and analysed by western blot (Figure 5.3). Due to the limited availability of homozygous mice, animals of both sexes were included in this analysis. The probing of hippocampal lysates with monoclonal antibody 3C11 first revealed that BDNF retains the P2A tag at its C-terminus, demonstrated by an upward shift in BDNF proteins observed in both heterozygous and homozygous animals (Figure 5.3A), consistent with previous findings (see Chapter 4). Prolonging the exposure of the blot also revealed bands corresponding to both pro-BDNF and pro-BDNF-P2A, both of which were observed at notably lower levels than the mature protein. A large non-specific band was also detected at ~54 kD, likely resulting from the binding of secondary antibodies to IgG light chains expressed within brain. After the normalisation of protein loading using antibodies against β -actin (data not shown), a comparison of BDNF levels between *Bdnf-P2a-Gfp* littermates revealed no significant difference in the cortex or hippocampus of hetero- or homozygous mice (Figure 5.3B).

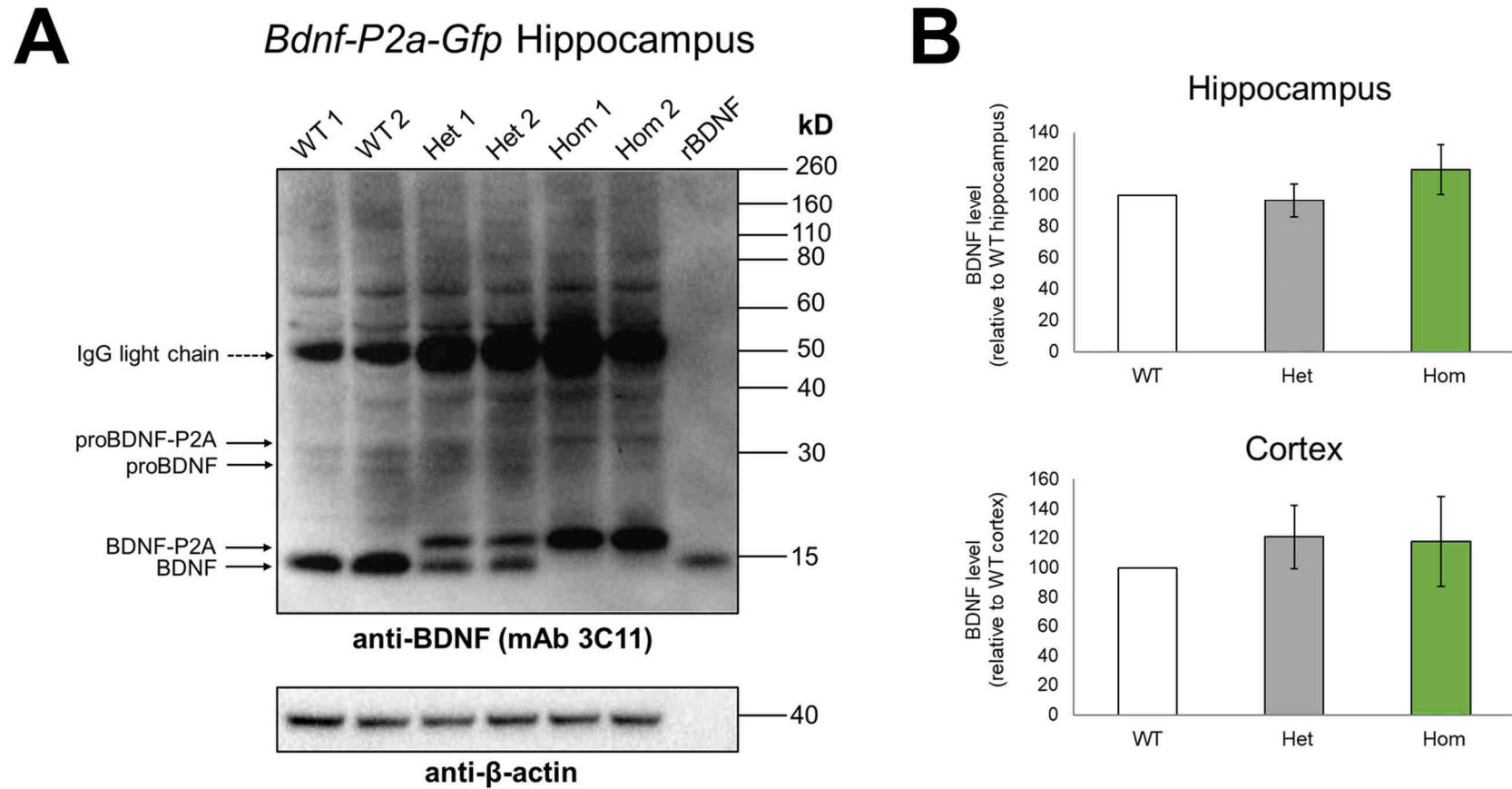


Figure 5.3. Monoclonal antibody 3C11 detects WT BDNF and BDNF-P2A in hippocampal extracts.

(A) Western blot analysis of adult wildtype (WT), *Bdnf-P2a-Gfp* heterozygous (Het) and homozygous (Hom) brain lysates; two animals shown per genotype. Note the shift in molecular weight of BDNF-P2A, and the faint bands corresponding to pro-BDNF or pro-BDNF-P2A in all lysates (upper panel). 75 µg rBDNF used as a positive control. 10 µg protein loaded per lane; equal loading confirmed by probing the same membrane with anti-β-actin (lower panel). (B) Levels of mature BDNF protein in *Bdnf-P2a-Gfp* mice relative to WT littermates, as determined by western blot. $n = 6$ and $n = 3$ lysate preparations analysed per genotype for the hippocampus and cortex, respectively.

5.2.4 Optimising protocols for BDNF and GFP immunostaining on mouse brain sections

As GFP fluorescence proved undetectable in animals carrying one or two copies of the *Bdnf-P2a-Gfp* gene, it was next tested whether GFP expression could be visualised using antibodies against GFP. As it was soon discovered that GFP IHC was incompatible with the antigen retrieval required for BDNF immunostaining (see Methods), brains were instead fixed using 2% PFA to avoid over-fixation.

Low power imaging of *Bdnf-P2a-Gfp* sections probed using polyclonal antibodies against GFP revealed populations of GFP-positive cells across the cerebral cortex, with the most dense labelling observed across the hippocampal formation (Figure 5.4A, right panel). The specificity of this staining was confirmed by the parallel staining of tissues prepared from *Bdnf* WT mice Figure 5.4. Probing of BDNF WT brain sections with antibodies against BDNF and GFP (Figure 5.4A, left panel).

As it was desirable to label both GFP and BDNF in brain sections prepared from *Bdnf-P2a-Gfp* mice, it was next tested whether BDNF IHC was compatible with this newly optimised GFP staining protocol. To this end, brain sections from *Bdnf* WT mice were fixed using 2% PFA and then probed using mAb anti-BDNF #9 as previously described (see Chapter 3). Surprisingly, the change in fixation conditions also dramatically improved BDNF immunoreactivity, particularly in the neuronal layers of the dentate gyrus (Figure 5.4B) and CA3 (Figure 5.4C).

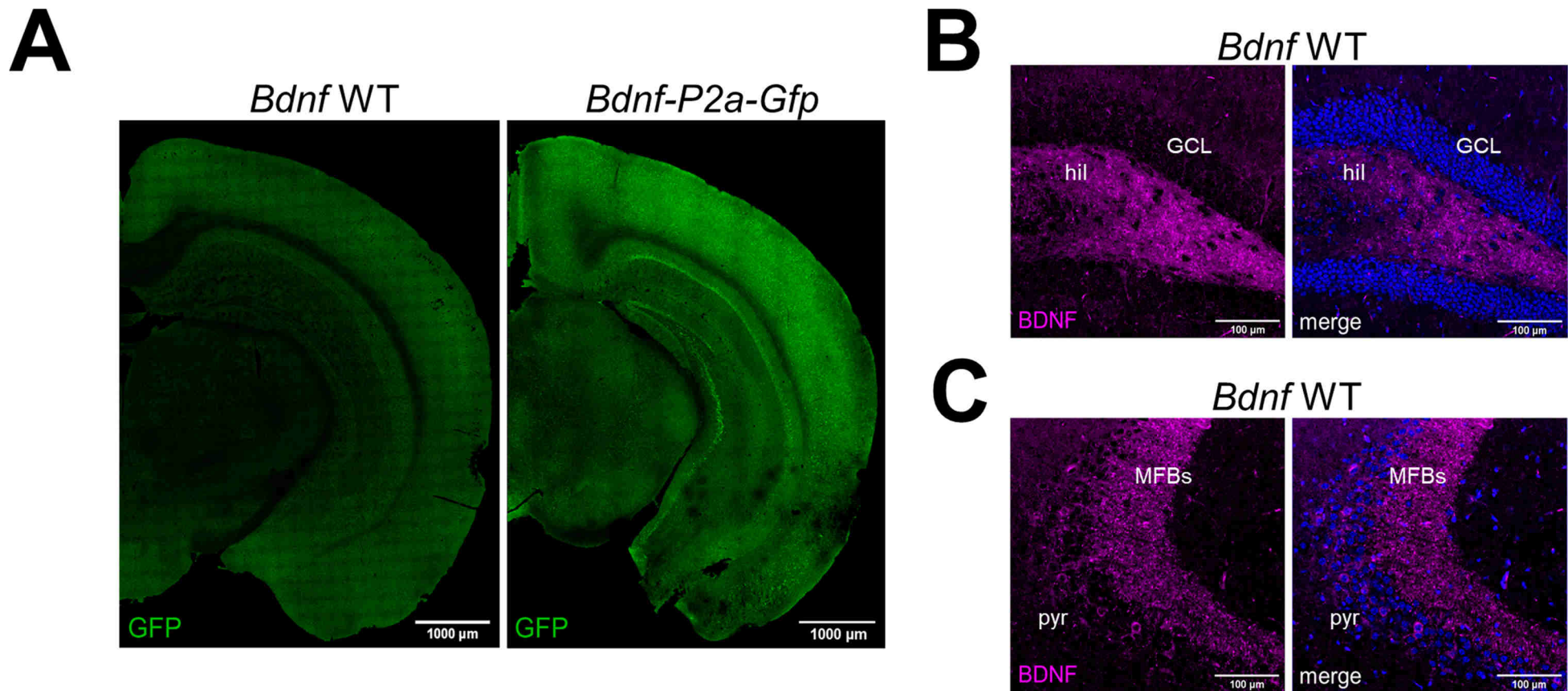


Figure 5.4. Probing of BDNF WT brain sections with antibodies against BDNF and GFP.

(A) Low power image of *Bdnf* WT (left panel) and *Bdnf-P2a-Gfp* homozygote brain sections fixed using 2% PFA and probed using polyclonal antibodies against GFP. Note the global absence of immunofluorescence in WT brain and the strong labelling of the hippocampal neuronal layers and cerebral cortex in *Bdnf-P2a-Gfp* mice. High magnification images of the *Bdnf* WT dentate gyrus (DG) (B) and CA3 region (C) fixed using 2% PFA and probed using mAb anti-BDNF #9 and the nuclear marker DAPI. Note the intense BDNF immunoreactivity shown in the hilus of the DG and mossy fibre terminals of CA3.

5.2.5 BDNF immunoreactivity in the hippocampus of *Bdnf-P2a-Gfp* mice is consistent with BDNF WT animals

Using monoclonal antibodies against BDNF, it was next determined whether the distribution of BDNF-P2A in the brains of *Bdnf-P2a-Gfp* mice was comparable to the wildtype protein. Coronal brain sections were prepared from 3-month-old *Bdnf-P2a-Gfp* mice and probed using monoclonal antibodies against BDNF and GFP.

The imaging of sections immunostained for BDNF, GFP and the nuclear marker DAPI revealed that the distribution of BDNF-P2A within brain fell in line with previous reports of BDNF localisation (Conner et al. 1997; Yan et al. 1997; Dieni et al. 2012) (Figure 5.5). Although BDNF immunoreactivity was detected at low levels within neuronal soma, the protein was shown to accumulate in both the hilar regions of the dentate gyrus (DG) (Figure 5.5A) and the mossy fibre terminals of CA3 (Figure 5.5B). GFP immunoreactivity was also observed in most cells residing in the neuronal layers of the DG and CA3, but to varying degrees. Further high-power imaging of these cells revealed that GFP signals were largely confined to neuronal nuclei and their somas, whereas BDNF remained exclusively within cell bodies and their early projections (i and ii, indicated by white arrowheads).

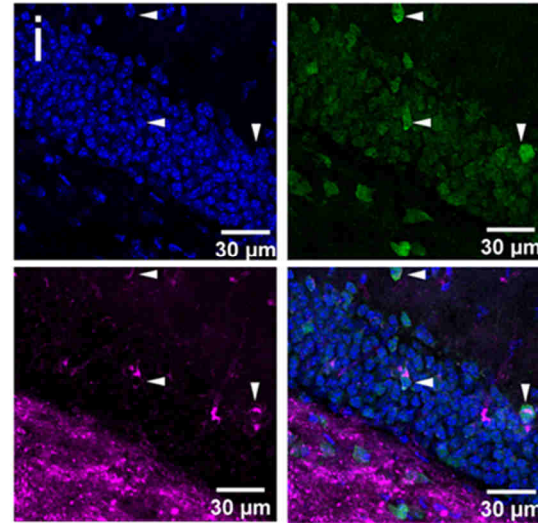
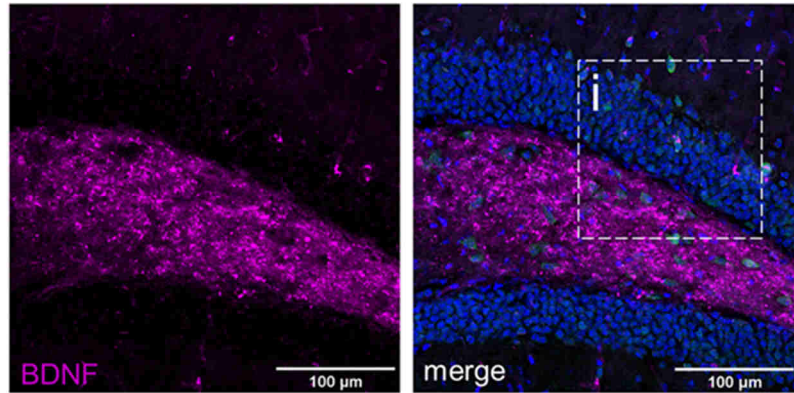
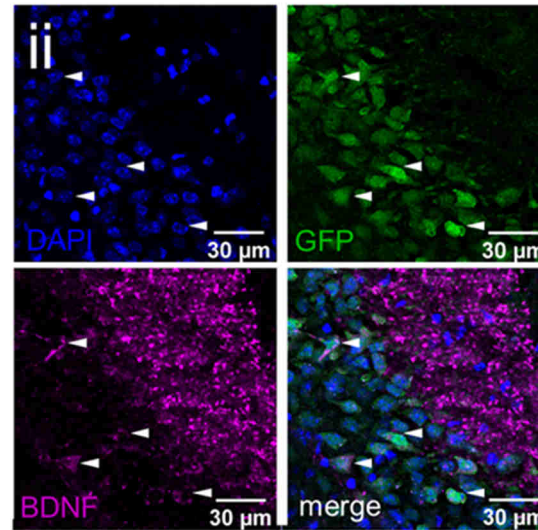
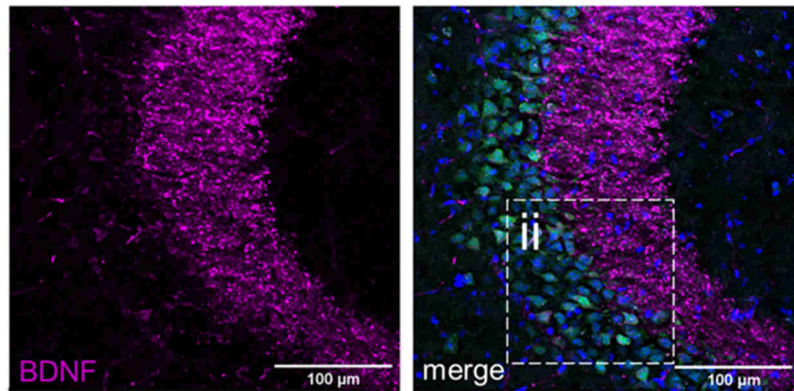
A

Figure 5.5. BDNF and GFP immunoreactivity in the brains of *Bdnf-P2a-Gfp* mice.

High magnification images of the adult *Bdnf-P2a-Gfp* dentate gyrus (DG) (**A** and **i**) and CA3 region (**B** and **ii**) stained with antibodies against GFP and BDNF, and the nuclear marker DAPI. Note the intense immunoreactivity for BDNF in the hilus of the DG and mossy fibre terminals of CA3, but not GFP. High expressing BDNF and GFP neurons indicated by white arrow heads. Representative images from the analysis of $n = 4$ animals, 4 sections analysed per animal.

B

Further analysis of the GFP signal in the *Bdnf-P2a-Gfp* hippocampus revealed that GFP (and thus BDNF) was translated by all neuronal layers, but at differing levels (Figure 5.6). The quantification of these GFP signals in multiple animals revealed that the highest proportion of heavily or very heavily labelled cells were found in hippocampal CA3, making up 6.15% (± 1.45) and 17.58 (± 2.64) of cells, respectively. In contrast, the highest proportion of lightly labelled cells were found in CA1 (65.43%, ± 7.38), shortly followed by CA2 (57.25% ± 7.65) and the DG (55.26% ± 6.33). Interestingly, across subregions, less than 10% of nuclei contained GFP signals at the level considered as background, suggesting that the vast majority of cells actively translate *Bdnf-P2a-Gfp* mRNAs.

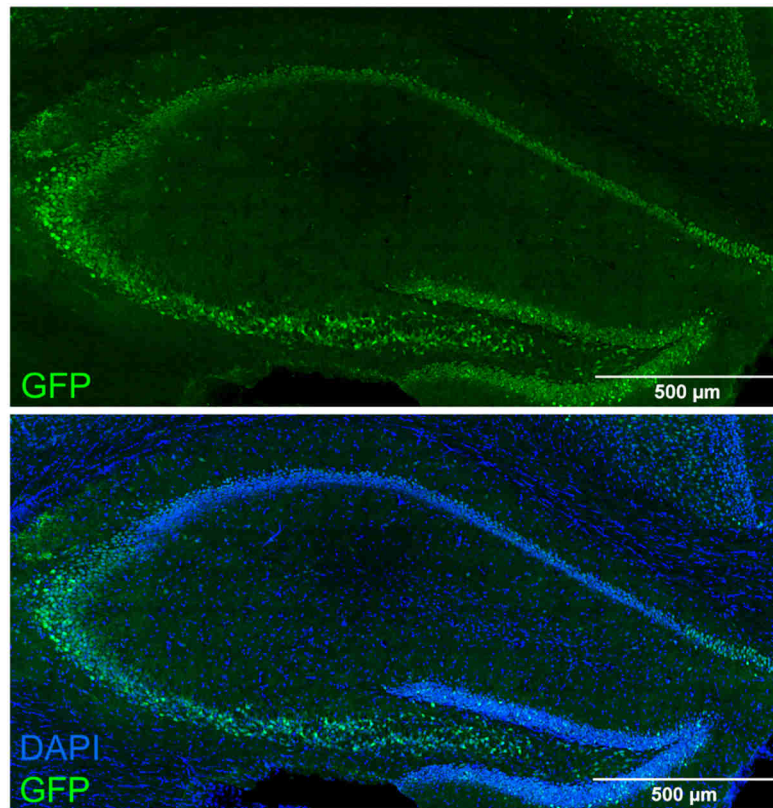


Figure 5.6. GFP immunoreactivity in the *Bdnf-P2a-Gfp* hippocampus (as used for quantification studies).

Representative images of the *Bdnf-P2a-Gfp* sections used to quantify GFP signals in the adult hippocampus. Note that the majority of GFP immunoreactivity was confined within neuronal layers of the CA1, CA2, and CA3, but to varying degrees.

Table 5.1. Quantification of GFP signal intensity in the hippocampus of *Bdnf-P2a-Gfp* mice.

Region	Proportions of GFP-positive cells				
	Background	Light	Moderate	Heavy	Very Heavy
DG	5.37%	55.26%	32.08%	6.66%	0.64%
SEM	1.79%	6.33%	5.05%	2.95%	0.24%
CA1	4.11%	65.43%	24.25%	5.39%	0.81%
SEM	1.33%	7.38%	5.43%	3.47%	0.69%
CA2	5.52%	57.25%	26.69%	9.93%	0.61%
SEM	1.55%	7.65%	4.96%	3.90%	0.26%
CA3	6.96%	31.50%	37.82%	17.58%	6.15%
SEM	0.92%	4.11%	2.05%	2.64%	1.45%

Automated cell counts were based on DAPI stained nuclei in the granule cell layer of the dentate gyrus and the pyramidal layers of CA1, 2 and 3. Values represent the percentage of cells expressing differing levels of GFP. Values obtained from sections taken from $n = 3$ 3 month old *Bdnf-P2a-Gfp* homozygous mice, 5 sections analysed per animal. All analysed sections fell between Bregma coordinates -1.355 and -2.880, regions identified using images from the Allen Brain Atlas.

5.2.6 GFP faithfully reports activity dependent increases in BDNF in cultured cortical neurons

After establishing that BDNF and GFP were successfully translated as separate proteins in neurons overexpressing the *Bdnf-P2a-Gfp* cDNA (see Chapter 4), this raised the question of whether this was also the case in neuronal cultures prepared from *Bdnf-P2a-Gfp* mice. To establish the localisation of BDNF and GFP in these cells, E17.5 cortical cultures were maintained until DIV11 and then processed for immunocytochemistry. To determine whether the distribution of BDNF or GFP changed after activity-dependent increases in *Bdnf-P2a-Gfp* expression, neurons from the same preparation were also treated with 4-AP (as previously described, see Chapter 3).

Probing cultures with antibodies against BDNF, GFP, and neuronal marker Tau revealed that the distribution of BDNF-P2A was indistinguishable from wildtype BDNF in both treated and untreated cells (Figure 5.7A). As observed in brain (Figure 5.5), GFP immunoreactivity was largely confined in neuronal nuclei and had very limited overlap with BDNF-P2A. The specificity of this signal was confirmed by probing WT neurons with the same GFP antibodies, that resulted in no detectable immunoreactivity.

The quantification of BDNF and GFP immunoreactivity revealed that much like endogenous BDNF, BDNF-P2A levels increase by near three-fold following treatment with 4-AP (Figure 5.7B, $U = 564$, $p = 1.271 \times 10^{-24}$). Surprisingly, GFP levels were also shown to significantly increase but by less than 2-fold (Figure 5.7B, $U = 621$, $p = 2.519 \times 10^{-23}$), likely resulting from the increased half-life of GFP when compared to that of BDNF.

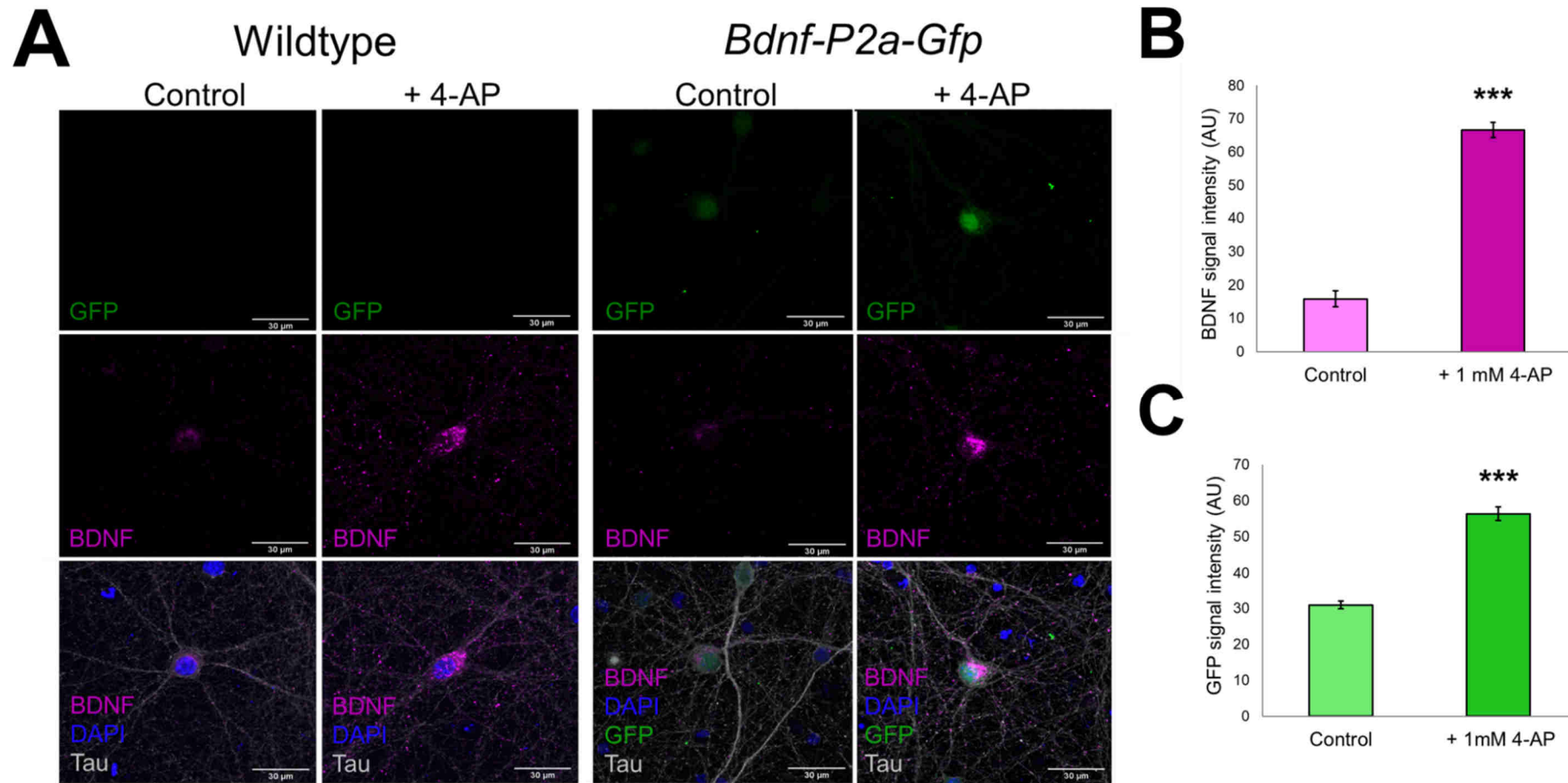


Figure 5.7. Activity dependent increases in BDNF and GFP in cortical neurons.

(A) High power images of WT (left panels) and *Bdnf-P2a-Gfp* homozygous (right panels) neurons stained with antibodies against BDNF (mAb #9), GFP, Tau and nuclear marker DAPI. After 24 hr treatment with 1 mM 4-AP, note the increased presence of BDNF puncta in both the cell bodies and the surrounding projections, and the accompanying increase in GFP within nuclei. Representative images from $n = 3$ culture experiments. (B) Quantification of the increased BDNF and GFP fluorescence in *Bdnf-P2a-Gfp* cultures following 4-AP treatment. *** indicates $p < 0.001$ ($p = 1.271 \times 10^{-24}$ and 2.519×10^{-23} for BDNF and GFP, respectively).

5.2.7 The extrahippocampal distribution of GFP in the *Bdnf-P2a-Gfp* brain is consistent with previous *Bdnf in-situ* hybridisation studies

Coronal brain sections prepared from *Bdnf-P2a-Gfp* homozygous mice were then further examined for GFP immunoreactivity in wider brain areas. As reliable data visualising *Bdnf* expression outside of the hippocampus remain limited, results were compared to data generated from *in situ* hybridisation studies from the Allen Brain Atlas ([Gene Detail :: Allen Brain Atlas: Mouse Brain \(brain-map.org\)](https://www.brain-map.org/gene-detail/Bdnf)).

Confocal imaging of adult brain sections revealed patterns of GFP immunoreactivity that closely mimicked patterns reported by the Allen Brain Atlas *Bdnf* ISH study. GFP-positive nuclei were detectable in multiple regions of the cerebral cortex (Figure 5.8). In the somatosensory area (Figure 5.8A), varied GFP labelling was detected in layers II/III, V and VI, but was largely absent from layers I and IV. Strong GFP immunoreactivity was also detected in cells of the piriform cortices, namely in the pyramidal layers and endopiriform nuclei (Figure 5.8B) and within the basolateral nucleus of the amygdala (Figure 5.8C). In line with previous findings, GFP (and thus *Bdnf*) expression was entirely absent from the striatum.

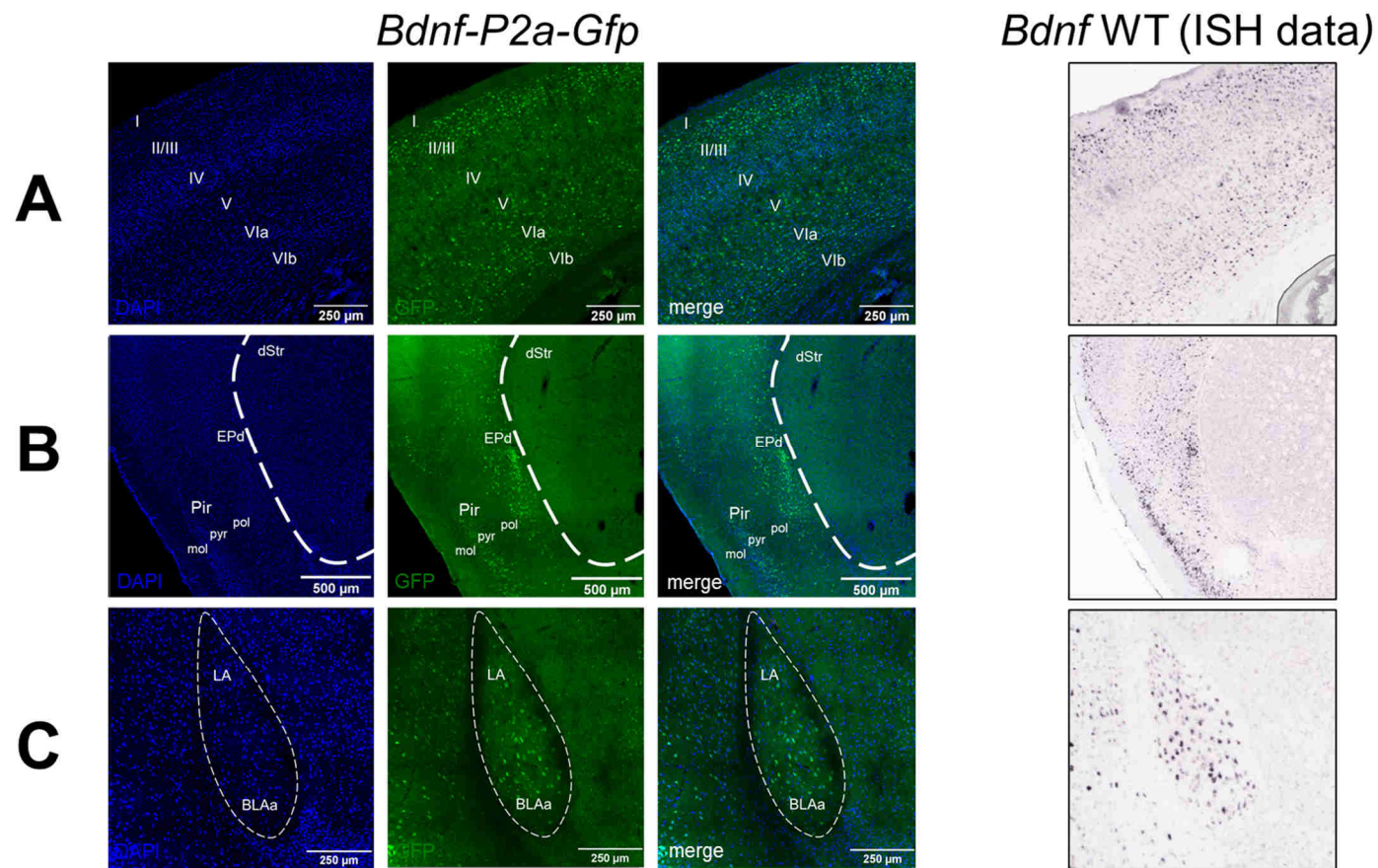


Figure 5.8. Cells translating BDNF in the cerebral cortex of *Bdnf-P2a-Gfp* mice.

GFP immunostaining in the brains of 3-month-old homozygous *Bdnf-P2a-Gfp* mice, including the primary somatosensory area (**A**), the striatum and piriform cortex (**B**) and the amygdalar nuclei (**C**) (left panels). Note the reduced number of GFP positive nuclei in cortical layer IV (**A**) dorsal striatum in (**B**). Representative images from the study of $n = 6$ mice, 3 sections studied per animal. Right panels show ISH data for *Bdnf* in the P56 mouse brain taken from the Allen Brain Atlas. Note the similarities in staining pattern for GFP and the *Bdnf* mRNA between left and right panels respectively. dStr, dorsal striatum; EPd, dorsal endopiriform nucleus; Pir, piriform cortex; mol, molecular layer of Pir, pyr, pyramidal layer of Pir, pol, polymorph layer of Pir; LA, lateral amygdalar nucleus; BLAa, Basolateral amygdalar nucleus, anterior part.

5.2.8 GFP is not expressed by microglial cells

As previous studies also indicate that *Bdnf* is expressed by microglial cells (Pankhurst et al. 2013; Habib et al. 2016), *Bdnf-P2a-Gfp* brain sections were also probed using a knock-out validated mAb against transmembrane protein 119 (TMEM-119), a marker of non-activated microglia (Bennett et al. 2016). High magnification analysis of the cerebral cortex revealed that GFP levels did not exceed that of background levels in TMEM-119-positive cells across layers I-VI (Figure 5.9, indicated by white arrowheads). These cells however were often found in close proximity to, or forming connections with large, neuron-like cells, many of which contained with high levels of GFP within their nuclei.

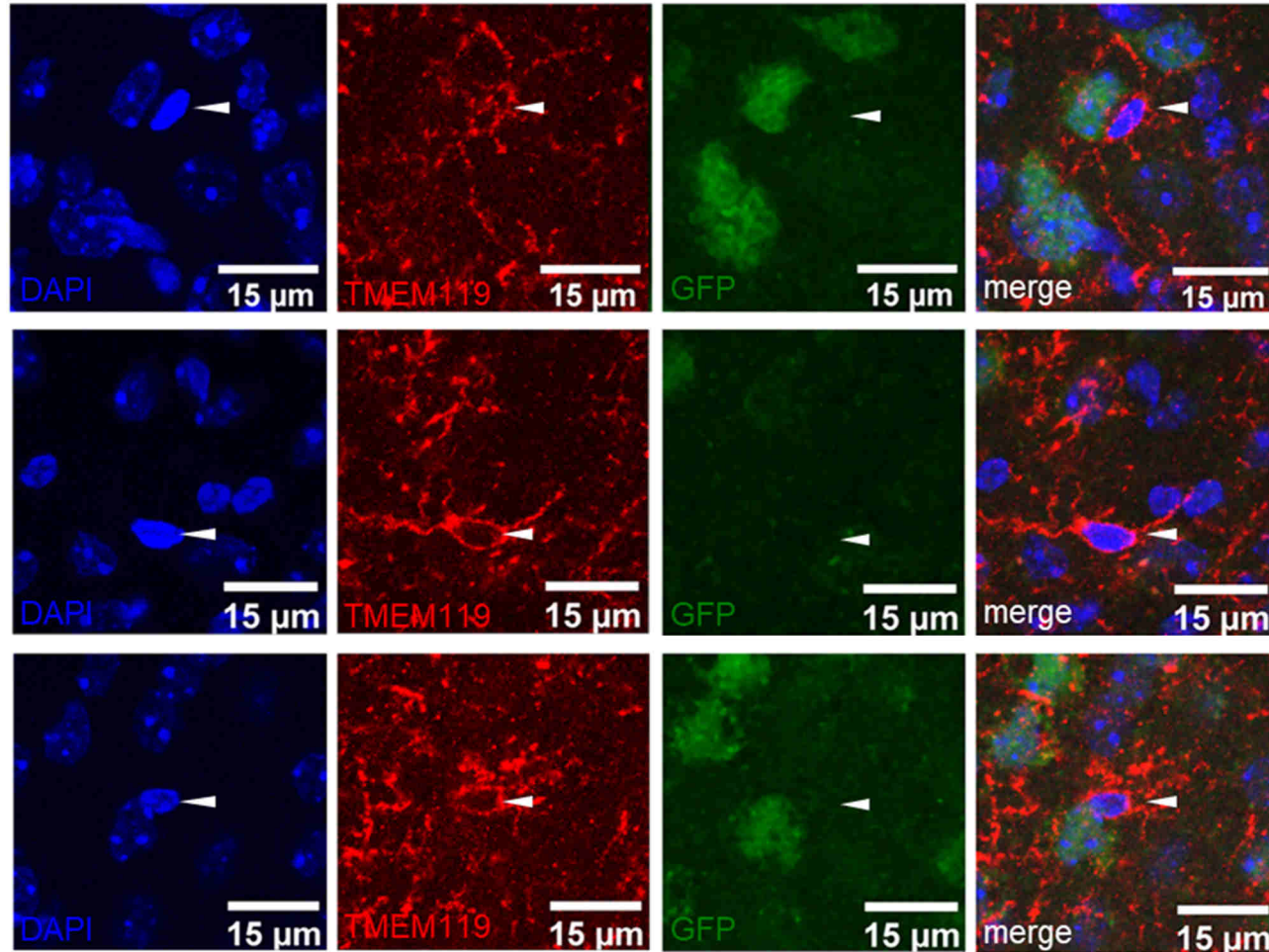


Figure 5.9. Microglial cells in the *Bdnf-P2a-Gfp* cortex do not express detectable levels of GFP.

TMEM119-positive microglial cells (indicated by white arrow heads) in the cerebral cortex of 3-month-old homozygous *Bdnf-P2a-Gfp* animals. Note the close proximity of microglia to GFP-positive cells, most likely resembling glutamatergic neurons. Representative images from the examination of $n = 2$ mice, 3 sections studied per animal.

5.3 Summary and conclusions

This chapter reports the characterisation of a novel mouse model that expresses *Bdnf-P2a-Gfp* under the regulatory elements of endogenous *Bdnf*. Mice carrying either one or two copies of the knock-in allele proved both viable and fertile, although progressive postnatal obesity was frequently observed in males (Figure 5.2). This phenotype is consistent with previous studies of BDNF deficient mice (Kernie et al. 2000; Rios et al. 2001; Unger et al. 2007); however, western blot analyses of the brain homogenates of *Bdnf-P2a-Gfp* hetero- and homozygotes revealed that BDNF levels remained comparable to their wildtype littermates (Figure 5.3). Although it was previously shown that TrkB phosphorylation by BDNF-P2A did not significantly differ from wildtype BDNF when used at high concentrations *in vitro* (see Chapter 4), it is plausible that the P2A tag at BDNF's C-terminus may chronically reduce the activation of TrkB *in vivo*, impairing the function of circuits that regulate food intake behaviours in these mice.

The confocal imaging of brain sections prepared from *Bdnf-P2a-Gfp* homozygotes revealed that the distribution of BDNF-P2A replicated that of the wildtype, myc- or hemagglutinin-tagged protein (Conner et al. 1997; Yan et al. 1997; Yang et al. 2009; Dieni et al. 2012). This was also the case in primary neuronal cultures, where high magnification imaging revealed a punctate-like staining pattern matching that observed in wildtype cells (Figure 5.7). Perhaps not unexpectedly, given the very low levels of BDNF within brain, GFP could only be visualised once brain sections were probed using GFP antibodies. Nonetheless, the levels of innate fluorescence are likely to be sufficient to be detected by FACS analysis. Nuclear-localised GFP successfully reported the level of *Bdnf* translation within both brain sections and in cultured cells (Figure 5.5 and Figure 5.7); however, the quantification of immunoreactivity before and after 4-AP treatment demonstrated a lower fold-change in GFP signal intensity when compared to BDNF-P2A (Figure 5.7C), most likely resulting from the different half-lives and cellular fates of each protein. A more in-depth analysis of GFP signals in the intact adult hippocampus (summarised in Table 5.1) revealed that the majority of neurons translated the *Bdnf-P2a-Gfp* mRNA at readily detectable, albeit different levels, with the largest proportion of heavily labelled cells found in CA3 (Figure 5.6). This contrasts with recent hippocampal single cell RNA-seq data (Habib et al. 2016), where *Bdnf* mRNAs were detected at the highest level in the DG (search *Bdnf* at: [Single Cell Portal \(broadinstitute.org\)](https://singlecell.broadinstitute.org)). This kind of discrepancy may result from the differing post-transcriptional regulation of *Bdnf* mRNAs in the various cell types of the hippocampus, given the multi-level regulation of *Bdnf* transcripts in both mouse and human neurons (West et al. 2014). Such results highlight the importance of following up transcriptomic analyses with studies of protein

biosynthesis in cells of interest. The detection of GFP-positive nuclei in distinct cortical layers, the amygdaloid nucleus and piriform cortex (Figure 5.8) were consistent with *Bdnf* studies performed in both rat (Wetmore et al. 1990; Conner et al. 1997) and mouse (Hofer et al. 1990). The lack of such signals in the dorsal striatum also agreed with previous findings (Baquet et al. 2004) and will prove a useful intra-section negative control in future studies of *Bdnf* translation within these mice. Interestingly, the probing of tissues using a thoroughly validated monoclonal antibody against microglial marker TMEM-119 showed that microglial cells did not express GFP above background (Figure 5.9). Although this observation agreed with a previous RNAseq analysis of microglia isolated from brain (Bennett et al. 2016) it contradicts previous works that describe a role for microglia-derived BDNF in the modulation of synaptic plasticity (Pankhurst et al. 2013).

Together, these results indicate that *Bdnf* translation can be monitored by virtue of a novel construct that synthesises BDNF and GFP as two functionally distinct proteins. Using this model, cells translating different levels of *Bdnf* can be sorted by level of GFP (and thus BDNF) translation, aiding the characterisation of cells that provide BDNF in both disease- and behaviourally relevant brain circuitries. In particular, it is now possible to perform single cell transcriptomics as a function of BDNF protein levels in FACS isolated neurons and nuclei. This new mouse line may also prove useful for the development of drugs designed to increase the levels of endogenous BDNF in cell populations of interest, such as those implicated in depression that are currently targeted using fast- and slow-acting anti-depressants (Björkholm and Monteggia 2016; Casarotto et al. 2021).

Chapter 6. Optimising BDNF detection in rat brain circuits in a memory relevant paradigm

6.1 Short Introduction

The first genes to be transcribed in response to neuronal activity are members of the immediate early gene (IEG) family. Their identification provided evidence that cells can immediately and rapidly respond to activity by dynamically altering gene transcription (Greenberg and Ziff 1984; Milbrandt 1987; Lyford et al. 1995). These transcripts function either as regulatory transcription factors controlling the expression of target genes or else serve as immediate effectors of cellular function. One of the most extensively studied neuronal IEGs is proto-oncogene *c-fos*. Its respective protein, Fos, heterodimerises with members of the Jun family to form activator protein 1 (AP-1), a transcription factor implicated in LTP maintenance, structural changes to the synapse and the formation of new memories (Abraham et al. 1993; Sanyal et al. 2002). Under basal conditions, *c-fos* transcription is remarkably low, however expression of its mRNA rapidly peaks 30- to 60-minutes after activity-dependent transcription. Much like other IEGs the *c-fos* mRNA are short-lived and degraded within minutes, whereas the half-life of the protein is longer, lasting around 90-minutes within nuclei and remaining detectable for up-to 4 hours post-stimulus (Sariban et al. 1988; Hughes et al. 1992; Zangenehpour and Chaudhuri 2002).

Early studies of the intact brain showed that IEG expression is markedly upregulated in the hippocampal formation during hippocampus-dependent memory tasks including the radial arm maze, novel object recognition and contextual fear conditioning (Guzowski et al. 1999; Vann et al. 2000b; Hall et al. 2001). The analysis of Fos expression proved an exceptionally useful surrogate marker of neuronal activity, aiding the identification cell populations and circuits involved in specific behaviours and exposure to different environmental contexts (Greenberg and Ziff 1984; Hughes et al. 1992; Kovács 1998; Barros et al. 2015). This was especially informative in models of spatial learning, where the analysis of *c-fos* expression revealed the critical involvement of extrahippocampal networks in working or reference memory. These include unidirectional or reciprocal connections between the hippocampus and the retrosplenial cortex (RSC), anterior thalamic nuclei (ATN), mammillary bodies (MBs), entorhinal cortex, and subicular regions (for a summary of these networks, see Figure 6.1) (Vann et al. 2000a; Vann et al. 2000b; Santín et al. 2003; Pothuizen et al. 2009; Albasser et al. 2010). Their circuit connectivity and contribution were behaviourally confirmed after surgically or genetically ablating inputs from each area, most of which led to marked deficits in memory

acquisition or recall (Bannerman et al. 2001; Vann and Aggleton 2003,2005; Albasser et al. 2007; Nelson et al. 2015; Nelson et al. 2020).

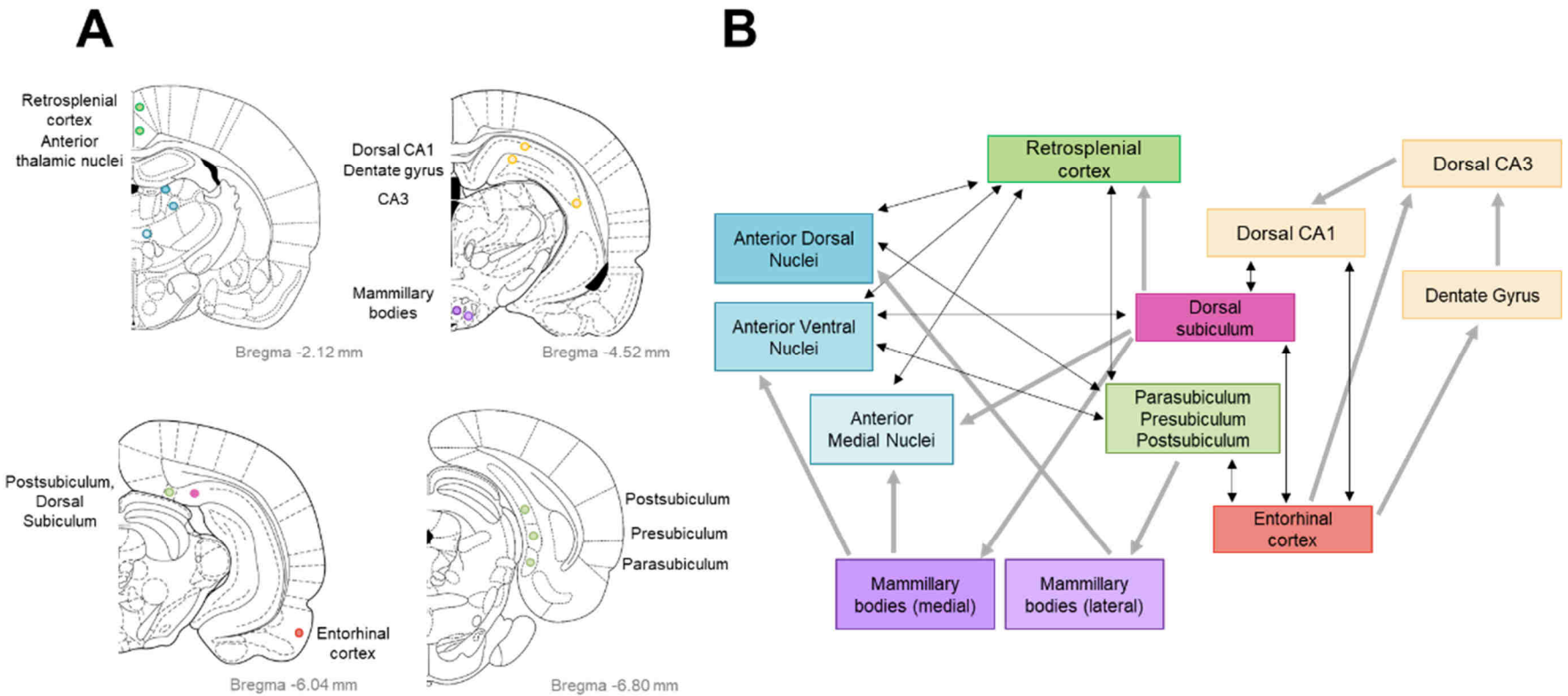


Figure 6.1. Connectivity between the hippocampus and the extrahippocampal correlates of memory.

(A) Coronal illustrations of the adult rat brain labelled with brain areas of interest (taken from Paxino and Watson, 1998). (B) A schematic of circuit connectivity between the rat hippocampus, subicular areas, retrosplenial cortex and medial diencephalon understood to govern spatial and episodic memory. Grey arrows represent unidirectional projections, black arrows indicate a reciprocal connection between areas (scheme adapted from Nelson et al. 2020).

Increased neuronal activity within intact brain circuits also results in the increased expression of *Bdnf* mRNAs. Early studies demonstrated that *Bdnf* expression is markedly increased following multiple types of artificially induced seizure (Zafra et al. 1990; Ernfors et al. 1991; Isackson et al. 1991), electrically stimulated LTP (Patterson et al. 1992), and exposure to light as a sensory input (Castrén et al. 1992). An early *in vivo* study also indicated that *Bdnf* mRNA levels are regulated by neuronal activity in the developing chick visual system (Herzog et al. 1994). These findings were supported by limited BDNF immunostaining studies, where the probing of rat brain using BDNF polyclonal antibodies or anti-serum revealed similar increases in the BDNF protein after periods of increased neuronal activity (Hofer et al. 1990; Nawa et al. 1995; Conner et al. 1997; Yan et al. 1997; Rudge et al. 1998). Although these data confirmed that *Bdnf* expression is indeed driven by increased excitatory input, changes to BDNF protein levels within behaviourally relevant brain circuits is yet to be visualised. This is mainly due to its exceptionally low abundance of the endogenous protein and the limited availability of specific and sensitive BDNF monoclonal antibodies. Yet there are indications for the functional relevance of BDNF and its receptor TrkB in specific behavioural paradigms, such as those requiring new memory formation. In rodent models of spatial memory, the hippocampal expression of *Bdnf* was shown to positively correlate with increased spatial learning in rats trained in either the radial arm maze (RAM) or the Morris water maze (MWM) (Mizuno et al. 2000; Silhol et al. 2007). Across both tasks, the intra-hippocampal administration of BDNF was shown to enhance performance, whereas genetic knockdown of *Bdnf* markedly impaired both working and reference memory (Cirulli et al. 2004; Koponen et al. 2004; Heldt et al. 2007; Nakajo et al. 2008). In mice, the pharmacological or genetic ablation of TrkB similarly impaired both hippocampal LTP and maze performance, suggesting that both nascent BDNF and TrkB play a critical role in memory formation (Minichiello et al. 1999; Minichiello et al. 2002; Mizuno et al. 2003). Indeed, these data are also supported by human studies, whereby carriers of the *BDNF* Val66Met polymorphism exhibit a reduced performance in hippocampus-dependent memory tasks (Egan et al. 2003).

The aim of this chapter was to optimise a novel immunostaining protocol for visualising BDNF within rat brain. Unlike Fos, only very recently were behaviour-related changes in BDNF expression visualised within a mouse model of learning (Andreska et al. 2020). However, achieving reliable detection of BDNF in the rat, by far the preferred rodent model for behavioural studies, remains exceptionally difficult due to the lack of rigorous control tissue, including that with region-specific deletions of BDNF. By using monoclonal antibodies against the mature protein and its pro-sequence previously validated in *Bdnf* KO mice (Kolbeck et al. 1999; Rauskolb et al. 2010), BDNF containing structures were successfully detected in memory-relevant brain areas. In addition, an attempt was made

to quantify changes in BDNF expression within the brains of rats subject to the radial arm maze task (Olton and Samuelson 1976). This chapter reports a novel means of detecting BDNF in fixed brain tissue, whereby two BDNF antibodies are used simultaneously to enhance both the specificity and intensity of BDNF immunoreactivity.

6.2 Results

6.2.1 mBDNF is the most abundant BDNF protein within rat brain

Previous western blot analyses of cultured neurons (see Chapter 3) and brain lysates (Matsumoto et al. 2008) have shown that mBDNF is the predominant BDNF isoform found in the mouse hippocampus, comprising ~90% of total BDNF. However, a similar analysis was yet to be performed on rats. To this end, hippocampal lysates from home cage control animals were analysed by western blot to determine the relative abundance of pro- and mature BDNF in the rat hippocampus.

The probing of hippocampal lysates using mAb 3C11 revealed that mBDNF is the predominant BDNF moiety found in the rat hippocampus (Figure 6.2). As observed in mouse, the pro-protein was only detectable after the prolonged exposure of blots, supporting previous evidence that proBDNF undergoes rapid processing to yield the mature protein and its cleaved pro-peptide (not shown).

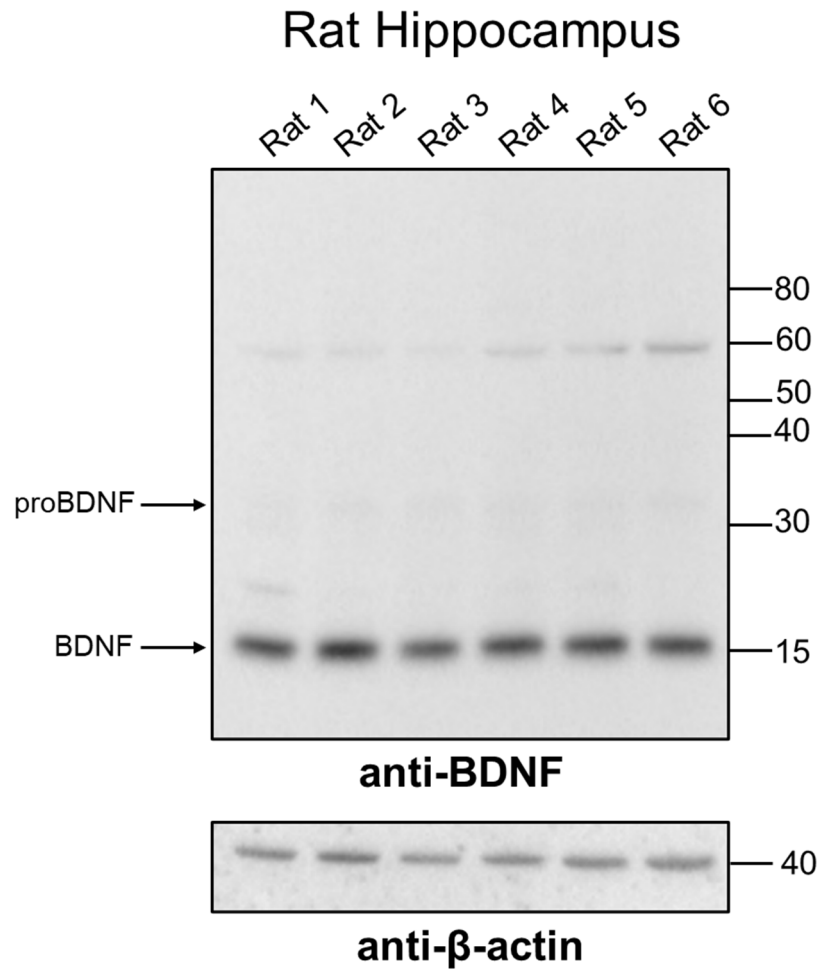


Figure 6.2. Western blotting for BDNF proteins in hippocampus of home cage control rats.

Western blot analysis of adult rat hippocampal lysates. Note the near complete absence of a band corresponding to proBDNF (~32 kD) and the accumulation of protein at the molecular weight of the mature protein (~14 kD). Note that mAb 3C11 does not recognise the cleaved pro-peptide expected to accumulate at ~ 17 kD. 10 µg protein loaded per lane; equal loading of protein confirmed by probing the same membrane with antibodies against β-actin. Hippocampal lysates prepared from $n = 6$ rats, representative image from $n = 3$ experiments.

6.2.2 Using monoclonal antibodies to improve BDNF immunostaining in rat brain sections

It was next investigated whether BDNF could be detected in rat brain using immunohistochemistry, as previously achieved in mouse sections (see Chapter 5). However, as rats were perfused using 4% PFA – the strength of fixative required for optimal Fos immunostaining (Eman Amin, personal communication) – this raised questions of how BDNF immunodetection could be improved when brains were fixed using a PFA concentration two-fold higher than what proved optimal for mouse brain (2% PFA; see Methods).

Using thoroughly validated monoclonal antibodies (mAbs) against BDNF and its pro-peptide, Dieni and colleagues (2012) demonstrated by western blot and immuno-EM that mBDNF and its cleaved pro-peptide are equally abundant in hippocampal neurons, mostly co-localising in cell bodies and the pre-synaptic terminals of the mossy fibre projection pathway. As these data strongly suggest that BDNF and its pro-peptide remain associated after cleavage, this inspired the design of a novel BDNF staining approach, whereby antibodies against the mature and pro-peptide are used in combination to enhance the detection of BDNF-containing structures within brain (see Figure 6.3).

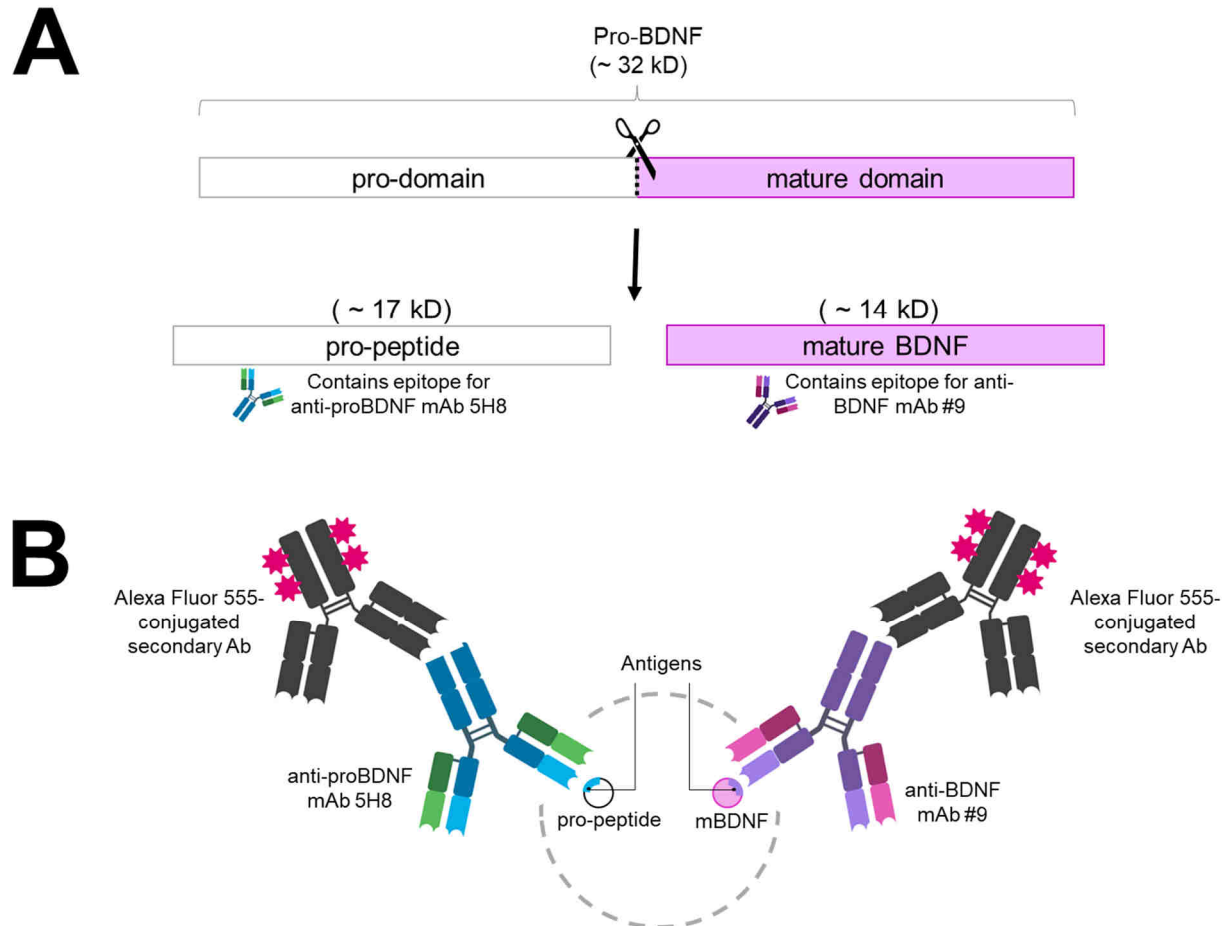


Figure 6.3. Proposed strategy for enhancing BDNF immunoreactivity in rat brain sections fixed using 4% PFA.

(**A**) Schematic representation of BDNF maturation from proBDNF. proBDNF is rapidly cleaved by furin or PC7 to yield the cleaved pro-peptide (~ 17 kD) and the mature protein (~14 kD). Both products – shown to exist at near equal concentrations - are then packaged into LDCVs and translocated to pre-synaptic terminals for secretion. (**B**) Proposed method for improving BDNF immunoreactivity in rat brain sections. Note that mAb #9 and 5H8 recognise unique epitopes on BDNF and its cleaved pro-peptide respectively, allowing the double-labelling of BDNF-containing structures. Dashed line denotes subcellular organelles known to contain BDNF, i.e. the ER, TGN, or LDCVs. Adapted from Dieni et al. (2012), (**B**) made using Biorender.

6.2.3 Probing rat brain sections using antibodies against BDNF or its pro-peptide result in the same patterns of immunoreactivity

To independently confirm whether mBDNF and its cleaved pro-peptide indeed share distribution patterns in rat brain, immunohistochemistry was first performed using either monoclonal antibodies against mature BDNF or its pro-sequence in IHC. Sections prepared from home cage control rats were incubated with either anti-BDNF #9 (7 µg/ml) or anti-pro-BDNF 5H8 (0.2 µg/ml) and then visualised using the same secondary antibody. Across experiments, the parameters used for microscopic imaging also remained unchanged.

High power imaging revealed that both mBDNF and its pro-peptide were readily detectable within brain and had a matching distribution across the hippocampus (Figure 6.4). As shown for BDNF in mouse (see Chapter 5), both proteins were detectable in the mossy fibre projection pathway, namely in the dentate gyrus (DG) granule cell somas, its hilar region, and the mossy fibre terminals of CA3. Strong immunoreactivity was also detected in the cell bodies of pyramidal CA3 neurons and to a lesser extent in CA1. Despite being utilised at different concentrations (see above), a comparable degree of staining was achieved across experiments, likely resulting from the different affinity of each antibody to their respective epitope.

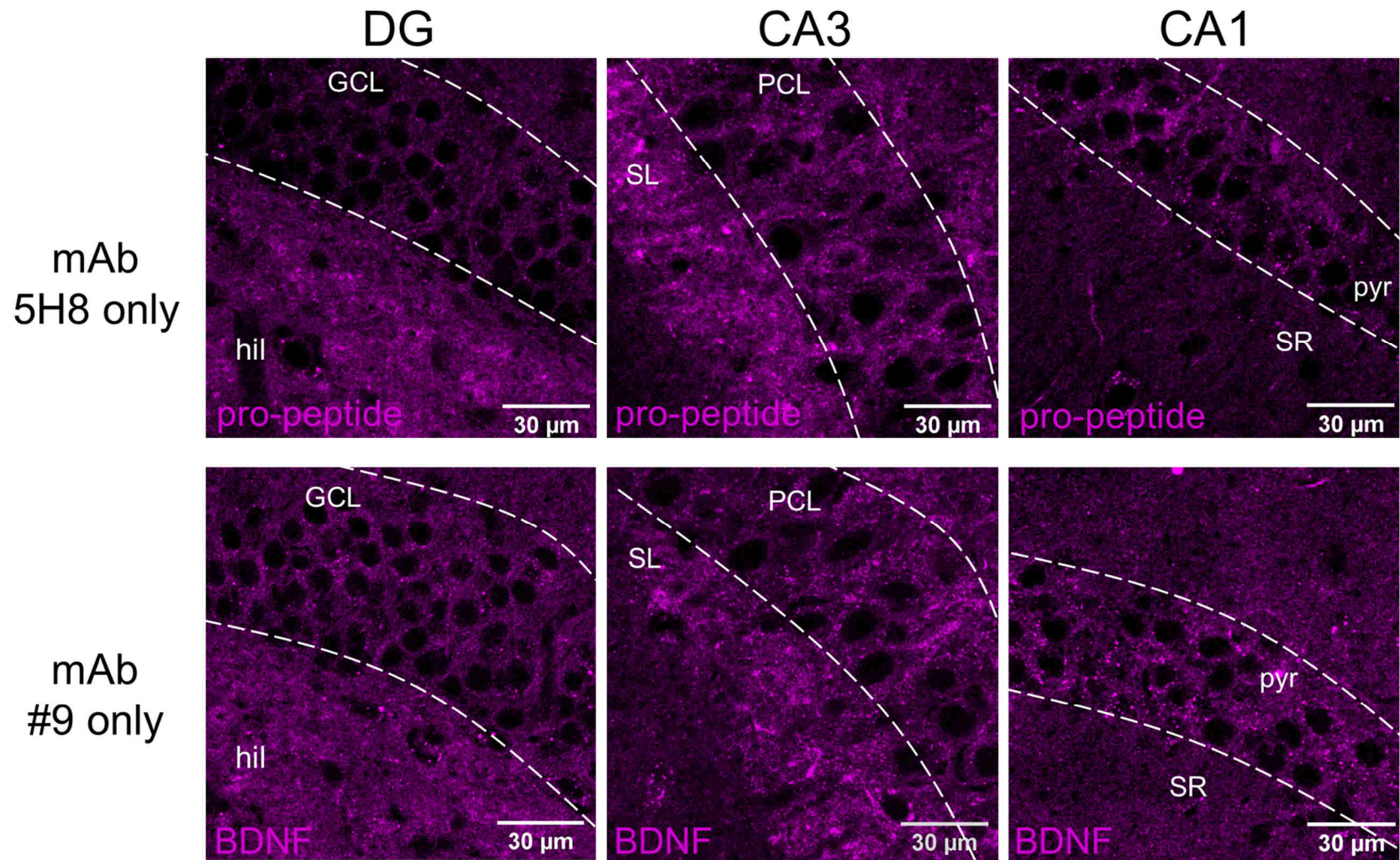


Figure 6.4. Localisation of BDNF and its pro-peptide in the hippocampus.

High magnification images of the rat hippocampus stained with antibodies against mBDNF (mAb #9) or its pro-peptide (mAb 5H8). Note the intense immunoreactivity for both proteins in the hilus of the DG and the SL of CA3. $n = 3$ animals analysed; 4 sections per animal. CA3, cornu ammonis 3; CA1, cornu ammonis 1; DG, dentate gyrus; GCL, granule cell layer; hil, hilus; MCL, molecular cell layer; PCL, pyramidal cell layer; SL, stratum lucidum; SR, stratum radiatum.

6.2.4 BDNF immunoreactivity is markedly enhanced when sections are probed using both BDNF antibodies

After confirmation that staining with mAb #9 or mAb 5H8 results in the same pattern of immunoreactivity, both antibodies were used in combination to test whether this strategy can markedly improve the detection of BDNF-containing structures within brain. Using the same concentrations of antibodies as described previously (see above), brain sections were incubated with both mAb #9 (isotype mouse IgG2) and mAb 5H8 (isotype mouse IgG1). The binding of both Abs was then visualised using a fluorophore-conjugated secondary antibody that recognising both IgG isotypes (see Methods).

A comparison of this method (Figure 6.7B, lower panels) with the use of mAb #9 alone (Figure 6.7B, upper panels) revealed that staining with both Abs markedly enhanced immunoreactivity across the dorsal and ventral hippocampus, particularly improving visualisation of BDNF-containing structures in the DG hilar region (Figure 6.5), CA3 stratum lucidum (SL) and CA3 pyramidal cell layer (PCL) (Figure 6.7B).

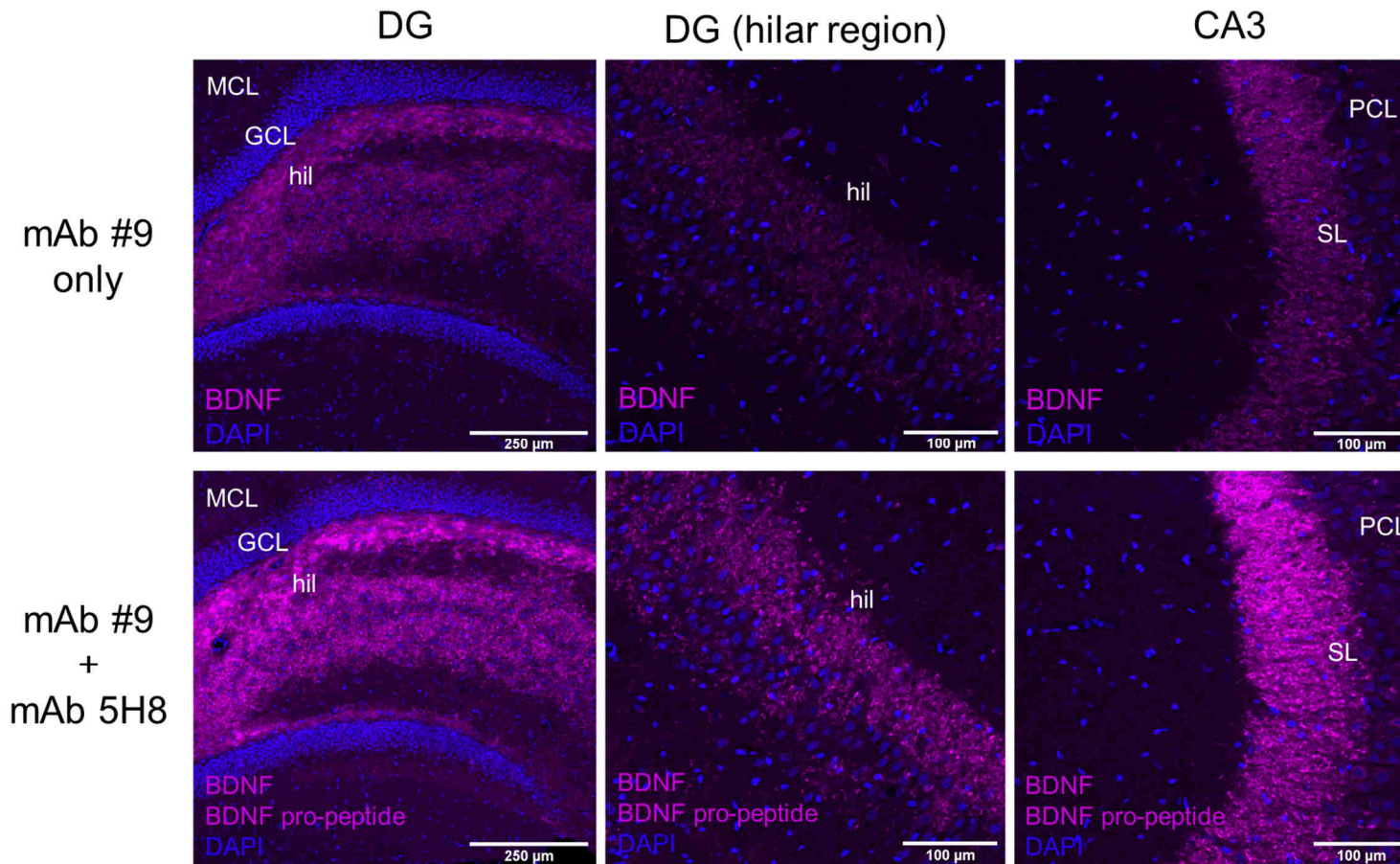


Figure 6.5. Enhanced immunoreactivity of BDNF-containing vesicles in the rodent hippocampus when combining anti-BDNF #9 and anti-pro-peptide 5H8.

Representative low power images of BDNF (upper panels) and BDNF/pro-peptide staining (lower panels) in the dorsal hippocampus. Note the enhancement of the signal when two BDNF antibodies are used in combination and detected using a common secondary antibody. Note that the choice of secondary antibody, its working concentration, and imaging conditions remained consistent throughout. $n = 3$ animals analysed per group, 4 sections per animal. DG, dentate gyrus; CA3, cornu ammonis 3; CA1, cornu ammonis 1; GCL, granule cell layer; hil, hilus; MCL, molecular cell layer; PCL, pyramidal cell layer; SL, stratum lucidum.

6.2.5 BDNF-ir was also detectable in the extrahippocampal correlates of memory previously mapped by Fos staining

After validating the combined use of monoclonal antibodies in the hippocampus, BDNF expression was next examined in the extrahippocampal brain areas implicated in spatial learning. Using reports of Fos expression as a guide, cell populations of both cortical- and subcortical-hippocampal connections (summarised in Figure 6.1) were studied at high magnification to ascertain whether BDNF could modulate the plasticity of these circuits in an activity-dependent manner.

Consistent with early BDNF localisation data generated using BDNF anti-serum or polyclonal antibodies (Conner et al. 1997; Yan et al. 1997), BDNF/pro-BDNF immunoreactivity (BDNF-ir) was readily detectable in cells of the retrosplenial cortices (RSC), medial diencephalon and dorsal subiculum (dSub) (Figure 6.6). In the RSC, BDNF-ir was most abundant in the dysgranular cell layer, although light staining was also detected in cells of the granular region. In the anteroventral nucleus of the thalamus (AVN) and the medial mammillary bodies (MMB), most cells contained BDNF-positive puncta within their soma, although vesicular-like staining was also seen between cells, likely corresponding to BDNF in axonal projections. In contrast, the dSub contained fewer labelled cells with less BDNF in the surrounding neuropil.

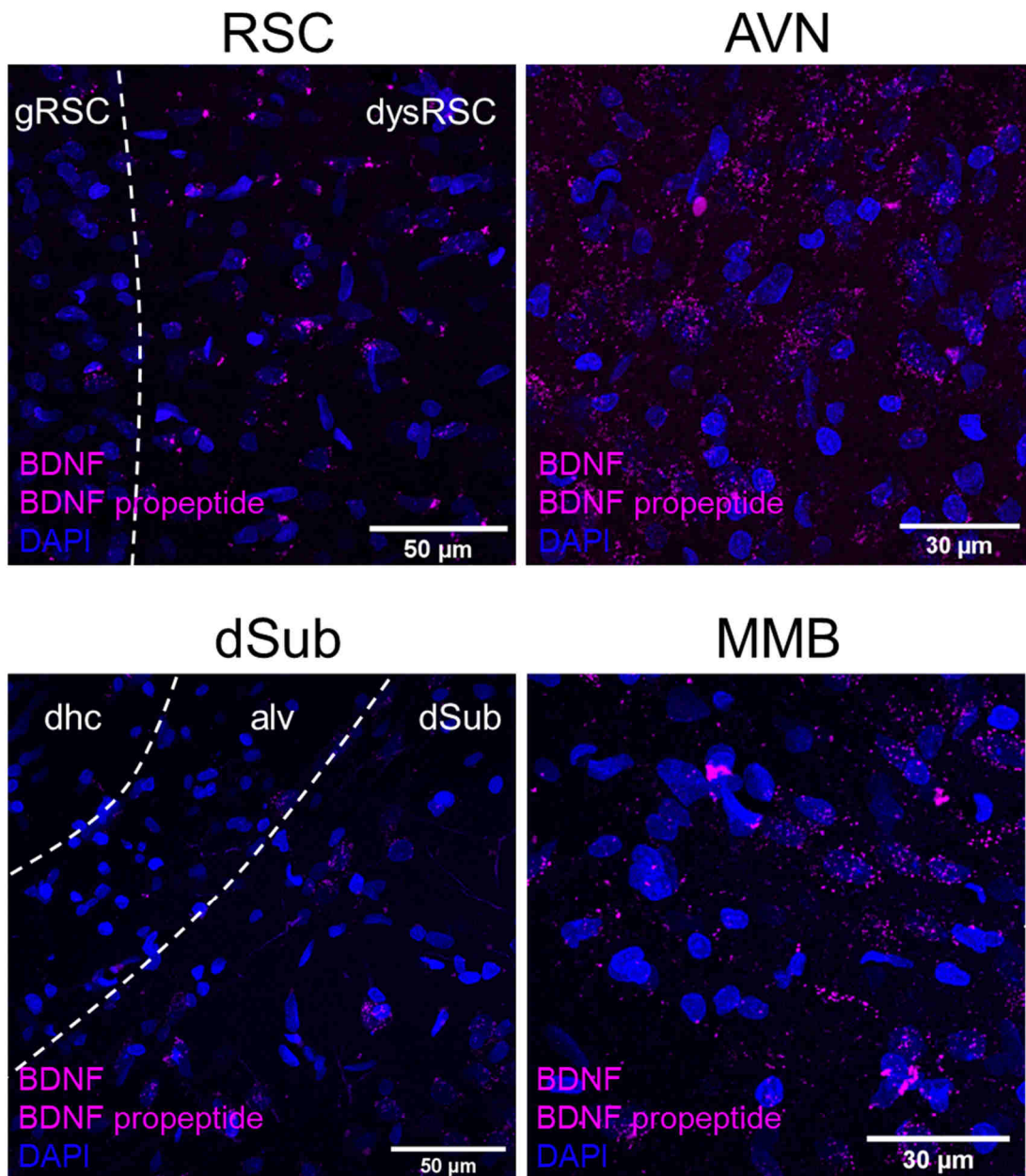


Figure 6.6. BDNF staining in the extrahippocampal correlates of memory.

BDNF-containing subcellular structures were readily detectable in neuron-like cell bodies belonging to the anterior thalamic nuclei, mammillary bodies, retrosplenial cortex and dorsal subiculum. In both the AVN and MMB, note the presence of puncta between cell bodies, likely corresponding to BDNF in axonal projections. Dotted lines represent boundaries between anatomical regions. Analysis of $n = 6$ rats, minimum of $n = 4$ sections analysed per animal. RSC, retrosplenial cortex; AVN, anteroventral nucleus of the thalamus; dSub, dorsal subiculum (pyramidal layer); MMB, medial mammillary bodies; gRSC, granular retrosplenial cortex; dysRSC, dysgranular retrosplenial cortex; alv, alveus; dhc, dorsal hippocampal commissure.

6.2.6 Both BDNF and Fos are readily detectable in the hippocampi of animals subjected to a spatial memory task

After confirmation that this staining technique enhanced BDNF-ir in brain sections prepared from multiple animals, mBDNF and pro-peptide IHC was performed on the brains of rats subject to a hippocampus-dependent spatial memory task (for more details, see Methods). The study included two groups: the first was trained to use allocentric visual cues to learn and complete a standard 8-arm radial arm maze task (hereinafter referred to as the 'experimental group'). The second was trained to visit a single arm the same number of times as their task-performing counterpart, matching both their motor behaviour and the number of rewards retrieved (from now on referred to as the 'control group'). On the final day of training, the experimental group was forced to perform the same task in a new room, navigating through the maze using new novel cues. The control group remained in a familiar room, performing matched single-arm visits as before.

Sections from both groups were also incubated with a polyclonal antibody against Fos, used as a surrogate marker of neuronal activity associated with spatial processing. As per previous findings, Fos immunoreactivity was predominantly confined to cell nuclei in all neuronal layers of the hippocampus (Figure 6.7C), with the highest number of labelled cells found in CA3 and CA1 (in rostral and caudal brain, respectively). Interestingly, a notable difference was detected between the DG suprapyramidal and infrapyramidal blades, whereby suprapyramidal granule cells exhibited markedly higher numbers of Fos-positive nuclei even under control conditions. In-line with BDNF immunoreactivity, no discernible differences in any brain areas were observed in Fos staining between control and experimental animals (data not shown).

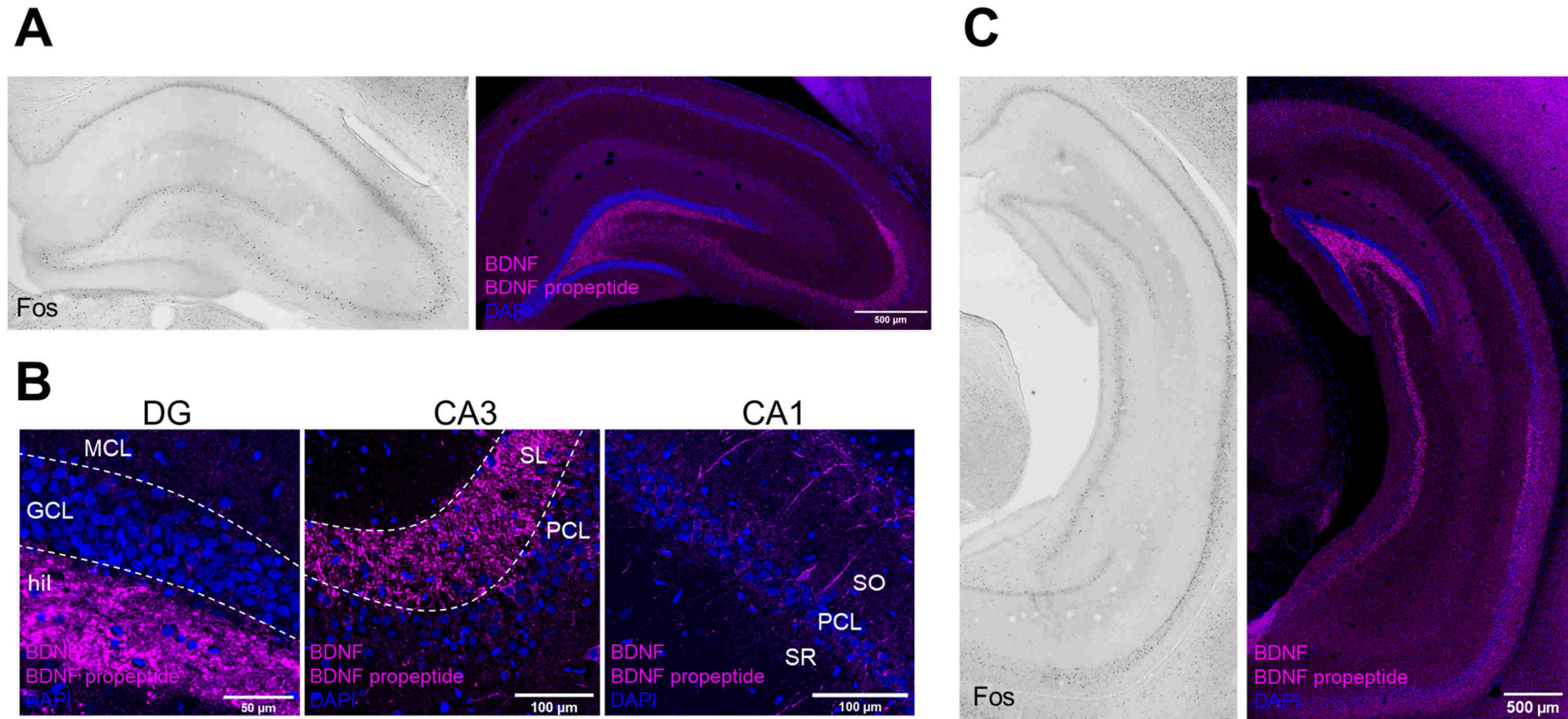


Figure 6.7. mBDNF/pro-peptide and Fos immunoreactivity in the hippocampus of control rats.

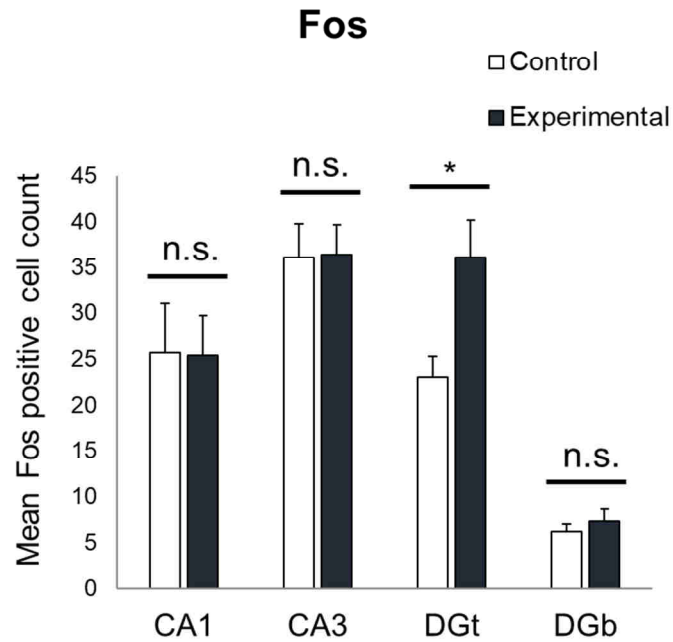
(A) Representative image of Fos (left panel) and BDNF/pro-peptide (right panel) immunofluorescence in the rostral rat hippocampus. (B) High magnification images of BDNF and pro-peptide staining in the dorsal hippocampus. Note the presence of an enhanced signal in the neuronal layers of the DG and CA3 and the CA3 SL. (C) Representative images of Fos (left panel) and mBDNF/pro-peptide (right panel) in the caudal hippocampus. For Fos, $n = 12$ animals analysed per group, BDNF $n = 6$ animals analysed per group. Minimum of $n = 4$ sections analysed per animal. CA3, cornu ammonis 3; CA1, cornu ammonis 1; DG, dentate gyrus; GCL, granule cell layer; hil, hilus; MCL, molecular cell layer; PCL, pyramidal cell layer; SL, stratum lucidum; SO, strata oriens; SR, strata radiatum.

6.2.7 Rats performing the spatial memory task failed to show the expected changes in Fos expression

To determine whether the animals subject to the spatial memory task exhibited spatial learning, Fos-positive cell counts were performed in the hippocampus within neuronal layers of the DG, CA3 and CA1. Fos counts in the dorsal (septal) and ventral (temporal) hippocampus were counted separately due to functional differences running along the dorsal-ventral axis that translates to the posterior-anterior axis within humans (Strange et al. 2014). In rodents, the dorsal hippocampus is implicated in spatial navigation and learning, whereas the ventral region mediates anxiety-related behaviours (Moser et al. 1993; Moser et al. 1995; Moser and Moser 1998; Bannerman et al. 1999; Bannerman et al. 2003; Strange et al. 2014). In agreement with previous IEG studies, increased Fos expression in the dorsal hippocampus was therefore considered a confirmation of spatial learning in this experiment. Fos changes in the DG suprapyramidal (top) and infrapyramidal (bottom) blades were recorded separately due to accumulating evidence of their functional and structural asymmetry (Scharfman et al. 2002).

Fos-positive cell counts were taken from the dorsal and ventral hippocampus of coronal sections prepared from rats performing the spatial memory task (experimental group, $n = 12$) and their yoked controls (control group, $n = 12$) (Figure 6.8). Surprisingly, no significant increase in Fos expression was seen in either dorsal CA1 ($t(22) = 0.38$, $p = 0.97$) or CA3 ($t(22) = 0.58$, $p = 0.954$) in the experimental group. A significant increase was recorded for the DG suprapyramidal blade (DGt) ($t(17.02) = -2.721$, $p = 0.015$), however the increase in the infralimbic blade (DGb) failed to reach significance ($t(22) = -0.691$, $p = 0.497$). As expected, no changes in Fos expression were observed across the ventral hippocampus in either the control or experimental group.

Rostral Hippocampus



Caudal Hippocampus

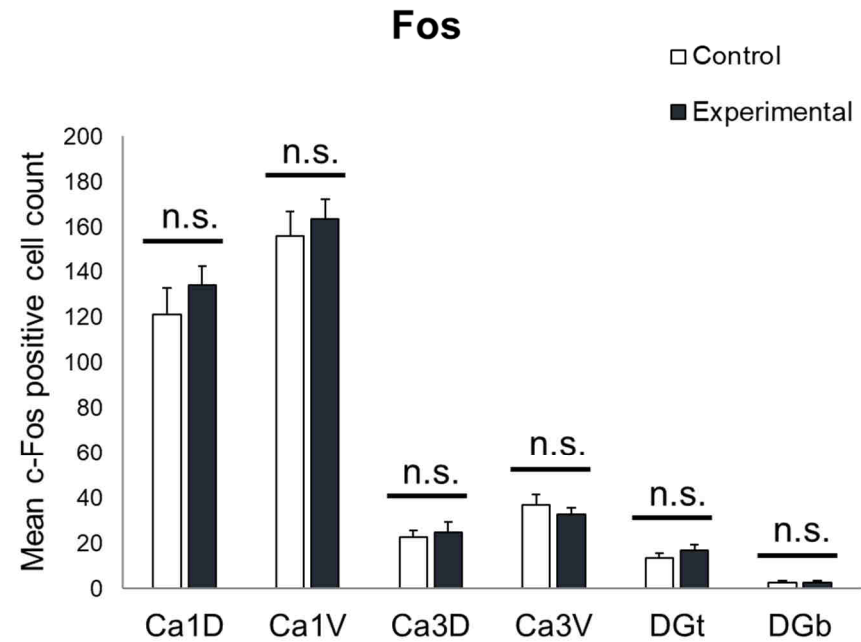


Figure 6.8. Fos positive cell counts in the hippocampus of rats performing a spatial memory task.

Values represent the mean number of Fos-positive cells for each experimental group \pm SEM. Note a significant increase in Fos expression in the top blade of the dorsal DG. $n = 12$ animals analysed per group (full cohort), minimum 4 sections per animal. * indicates $p < 0.05$ ($p = 0.015$); n.s., not significant. CA1, cornu ammonis 1; CA3, cornu ammonis 3; DGt, top blade of the dentate gyrus; DGb, bottom blade of the dentate gyrus; Ca1D, dorsal CA1; Ca1V, ventral CA1; Ca3D, dorsal CA3; Ca3V, ventral CA3.

6.2.8 No change in BDNF-ir was detected in the hippocampi of animals exposed to spatial learning

To ascertain whether there were differences in BDNF levels between rats performing the spatial memory task and their yoked controls, BDNF/pro-peptide immunoreactivity (see Methods, hereafter referred to as BDNF-ir) was quantified in the neuronal somas of the dorsal and ventral hippocampus (Figure 6.9). As per previous findings, BDNF-ir was detected in all subregions, with the highest intensity found in the cell bodies of both rostral and caudal CA1 and CA3 (Figure 6.9A and B). In parallel with Fos, no significant change in BDNF-ir was detected in dorsal CA1 or CA3 in animals performing the spatial memory task ($U = 10.0$, $p = 0.200$ and $t(10) = 1.233$, $p = 0.246$, respectively). In contrast to the increase of Fos expression in the DG suprapyramidal blade (DGt) of experimental animals ($t(5.735) = -2.080$, $p = 0.033$), no changes BDNF-ir were observed in either the suprapyramidal ($t(10) = 1.188$, $p = 0.262$) or infrapyramidal blade ($t(10) = 1.165$, $p = 0.271$) of experimental rats. As expected, and in-line with Fos, no differences in BDNF-ir were detected across the ventral hippocampus in either group.

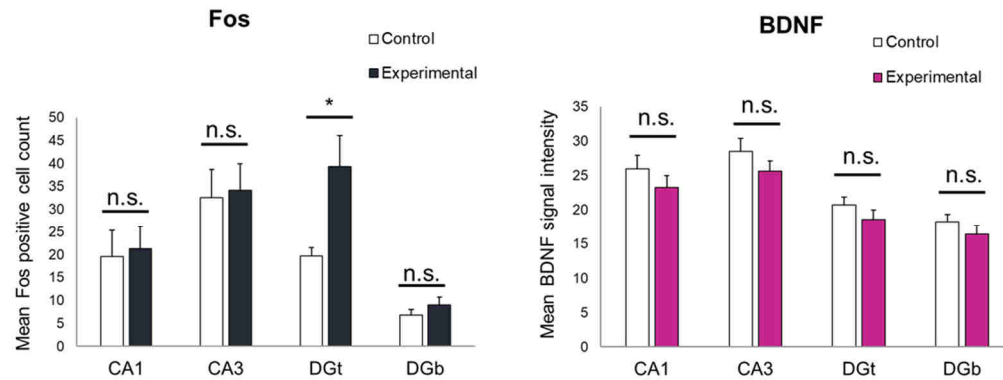
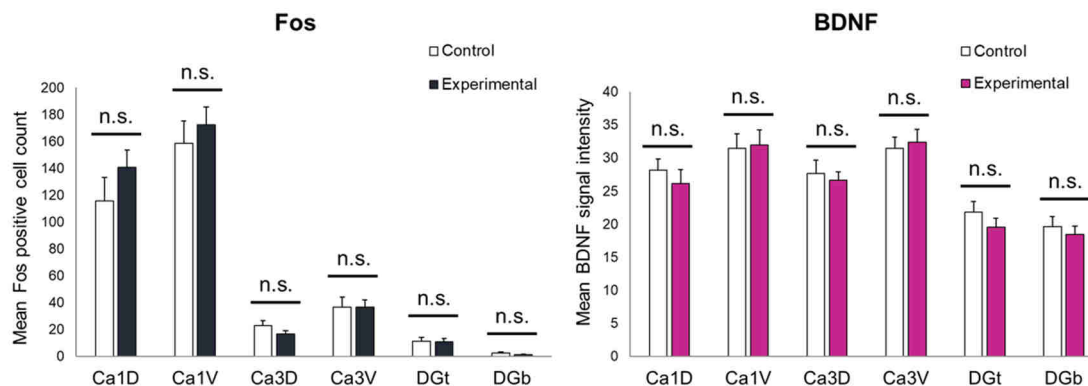
A**Rostral Hippocampus****B****Caudal Hippocampus**

Figure 6.9. A comparison of Fos counts and BDNF-ir in the hippocampus of control versus experimental rats.

Quantification of Fos positive cells and BDNF-ir in the rostral (**A**) and caudal (**B**) hippocampus of rats performing the spatial memory task and yoked controls. Values represent the mean number of Fos-positive cells or mean BDNF-immunoreactivity for each experimental group \pm SEM. With exception of Fos counts in DGt, no significant changes were observed in the expression of Fos or BDNF between experimental animals and their yoked controls. $n = 6$ animals analysed per group, minimum 4 sections per animal. * indicates $p < 0.05$ ($p = 0.033$); n.s., not significant. CA1, cornu ammonis 1; CA3, cornu ammonis 3; DGt, top blade of the dentate gyrus; DGb, bottom blade of the dentate gyrus; CA1D, dorsal CA1; CA1V, ventral CA1; CA3D, dorsal CA3; CA3V, ventral CA3.

6.3 Summary and conclusions

This chapter includes the successful detection of a low abundance protein by probing tissues with two well-validated monoclonal antibodies. The enhanced signal intensity achieved by pairing these probes (Figure 6.5) allowed for strong and specific BDNF staining to be achieved. The distribution of the endogenous protein observed in all brain sections agreed with historic rat studies, mouse lines carrying tagged versions of BDNF, and mouse sections probed using mAb #9 (Figure 6.4 and Figure 6.7) (Conner et al. 1997; Yan et al. 1997; Yang et al. 2009; Dieni et al. 2012; Andreska et al. 2020). Furthermore, anatomical patterns of BDNF expression matched closely with the GFP-positive populations observed in the *Bdnf-P2a-Gfp* mouse hippocampus reported earlier in this Thesis (see Chapter 5). This was also true for BDNF found in the extrahippocampal correlates of memory (Figure 6.6), suggesting that BDNF may indeed function as a modulator of plasticity in the medial-diencephalic, cortical, and parahippocampal circuits implicated in learning. Furthermore, the optimisation of BDNF staining in mouse tissues (see Chapter 5) suggests that BDNF detection in rat brain could be further improved by modifying the PFA fixation protocol, a development that would significantly benefit future studies of activity-dependent BDNF expression in rodent models of behaviour. Indeed, a similar approach has already been utilised by Andreska and colleagues (2020) to visualise the changes in cortical BDNF expression associated with motor learning.

Unexpectedly, there was no significant difference in the Fos expression profile of rats performing the spatial memory task when compared with controls, with exception of the suprapyramidal blade of the dentate gyrus (Figure 6.8). Matching Fos positive cell counts in the ventral hippocampus of control and experimental animals confirmed that the experimental protocol was adequately designed to control for Fos expression induced by anxiety or emotionally significant stimuli (Figure 6.9). Still, for no known reason, Fos counts in the dorsal hippocampus were abnormally high in controls when compared to studies of comparable design (Wan et al. 1999; Vann et al. 2000b; Pothuizen et al. 2009). To delineate changes in Fos expression induced by maze performance opposed to external, unrelated stimuli, the addition of a home cage control group may have helped explaining the unexpectedly high Fos counts recorded under control conditions (Aggleton, personal communication). Unfortunately, the COVID-19 pandemic prevented the later addition of an additional cohort.

Although the expected changes in Fos expression were not observed between groups, there were clear differences between the expression patterns of Fos and BDNF across hippocampal subregions. In both the dorsal and ventral hippocampus, the highest

number of Fos positive cells were localised to CA1, whereas BDNF was most abundant in the somas of CA3 neurons (Figure 6.9). This implies that expression of Fos or BDNF may undergo further regulation independent of activity- or Ca^{2+} -modulated transcription (Sheng et al. 1990; Tao et al. 1998; Tao et al. 2002). For instance, it is well appreciated that the unique instability of the *c-fos* mRNA and protein allows for the transient and rapid modulation of transcription in response to a wide range of environmental stimuli (Shyu et al. 1991; Ferrara et al. 2003). In contrast, the half-lives of *Bdnf* transcripts harbouring short or long 3'-UTRs have been measured at ~20 and 130 minutes respectively (Castrén et al. 1998), potentially outliving *c-fos* mRNAs by 2 hours (Hughes et al. 1992). Although the half-life of its protein is yet to be determined, the packing of BDNF within DCVs at the Golgi apparatus protects it from degradation while ensuring successful transportation to distal presynaptic compartments (Dieni et al. 2012). This likely extends its lifespan beyond that of Fos, a nuclear protein that is rapidly degraded to achieve transient bouts of gene expression (Curran et al. 1984). In order to further delineate functional differences in *Bdnf* and *c-fos* expression in the context of spatial memory, future experiments should aim to achieve BDNF and Fos immunostaining in the same brain sections to identify potential differences in their activity-dependent expression by distinct neuronal subsets.

Chapter 7. General Discussion

7.1 Summary of the main findings

The main objective of this thesis was to use well-validated tools to characterise a novel mouse model that uses GFP as a surrogate marker of BDNF expression within brain circuits utilising BDNF as a quasi-neurotransmitter. First, monoclonal antibodies were used to revisit the biosynthesis of wildtype, endogenous BDNF in neuronal cultures. Consistent with previous findings from our laboratory (Matsumoto et al. 2008; Dieni et al. 2012), BDNF was shown to be predominantly stored in its mature form both in brain and neuronal culture extracts. Activity-dependent increases in *Bdnf* expression were readily detectable *in vitro*, whereas an increased abundance of the uncleaved BDNF precursor, i.e., pro-BDNF, was only detectable during excitotoxic conditions. High-power imaging of these neurons revealed a distinct staining pattern for BDNF notably different to that observed in transfected neurons overexpressing the *Bdnf* cDNA. As tagged versions of BDNF have been extensively used in the literature, the processing and secretion of wildtype BDNF was also compared to that of BDNF fusion proteins. These experiments demonstrated that the addition of large tags to BDNF's C-terminus significantly attenuates its biosynthesis, secretion, and ability to phosphorylate TrkB, whereas the new BDNF-P2A-GFP bicistronic mRNA construct was demonstrated to faithfully report *Bdnf* translation using GFP tagged with a nuclear localisation signal. The knock-in of this construct into the mouse *Bdnf* locus resulted in the generation of viable and fertile animals exhibiting a distribution of BDNF-P2A comparable to wildtype BDNF in both brain sections and primary cultures, with levels of GFP also reflecting that of BDNF. An improved immunostaining technique was also described for rat brain, allowing the visualisation of BDNF in circuits involved in spatial memory. These findings are discussed in the context of a large number of previous studies attempting to address the important question of the cellular and sub-cellular distribution of BDNF in the rodent brain.

7.2 Characterising the processing and localisation of BDNF proteins by neuronal cells

Growth factors are highly bioactive molecules acting at very low concentrations, thus raising significant technical challenges when attempting to localise them in cells and tissues. Using invertebrate species with smaller genomes, such as *D. melanogaster* and *C. elegans*, cells expressing growth factors are typically identified using reporter constructs, whereby the corresponding promoters drive the expression of reporters such

as GFP. However, unlike many other growth factors, neurotrophins have not been identified in these species, with the exception of the *Drosophila* neurotrophins (DNTs), a group of distantly related proteins acting through the Toll-like receptors (Delotto and Delotto 1998; Mizuguchi et al. 1998; Parker et al. 2001; Gay and Gangloff 2007). Even when using sensitive immunofluorescent techniques to study their expression by mammalian tissues, it is exceedingly difficult to clearly distinguish between subcellular compartments including axon terminals and dendrites, given that spines are typically engulfed by presynaptic terminals (Harris and Weinberg 2012). Currently, only high-resolution techniques such as immuno electron microscopy (immuno EM) can accurately determine the subcellular localisation of these factors *in situ*. Indeed, this approach was successfully used by Dieni and colleagues (2012) to visualise both mature BDNF in presynaptic LDCVs at the DG-CA3 synapse using well-validated gold-labelled antibodies and brain tissues lacking BDNF as a negative control.

7.2.1 The limitations of *in vitro* overexpression systems

While overexpression studies may aid in the detection of molecules of interest, their suitability for studying protein localisation remains questionable. Indeed, using these techniques to study BDNF distribution has led to conflicting results regarding its trafficking and release. For instance, the overexpression of *Bdnf* in both heterologous (Lee et al. 2001; Mowla et al. 2001) and neuronal cells (Pang et al. 2004; Nagappan et al. 2009) results in a detectable secretion of pro-BDNF, not observed in studies asking the same question centred on the endogenous protein (Matsumoto et al. 2008). Using constructs encoding tagged versions of BDNF, others reported its release from dendrites (Hartmann et al. 2001; Dean et al. 2009; Matsuda et al. 2009), despite extensive evidence of its anterograde transport within brain (Altar et al. 1997; Conner et al. 1997; Baquet et al. 2004; Dieni et al. 2012).

Using similar *in vitro* expression systems to those described above, the results in this thesis highlight the limitations of these methods for studying BDNF's biology in mammalian cells. In Chapter 4, high power imaging of transfected cortical neurons revealed that cellular distribution of BDNF is markedly perturbed when overexpressed from its cDNA, potentially explaining the dendritic localisation observed by others (Hartmann et al. 2001; Dean et al. 2009; Matsuda et al. 2009). Using HEK293 cells, it was also shown that abnormally high levels of pro-BDNF are a common feature of overexpression experiments. This supports previous observations reported by Mowla and colleagues (1999), whereby both pro- and mature BDNF were atypically secreted in a constitutive manner when overexpressed by hippocampal neurons. This is most likely

a result of the use of strong promoters such as CMV leading to the saturation of the processing capacity of neurons, resulting in the accumulation of pro-BDNF and its secretion. This is consistent with the results of the only BDNF pulse-chase experiment to date, whereby the conversion of endogenous pro-BDNF to mBDNF was shown to occur entirely in neurons, with no secretion of pro-BDNF into the surrounding culture medium (Matsumoto et al. 2008). These results were challenged in a subsequent study using neurons cultured in the presence of anti-mitotic agents to prevent the growth of non-neuronal cells, whereby the detection of pro-BDNF in the medium can be attributed to the death of neurons caused by the mitotic inhibitor used (Oorschot 1989; Yang et al. 2009).

Independent of cDNA overexpression, it is also important to consider whether dissociated neuronal cultures – widely used to study protein trafficking and secretion – truly reflect the situation *in vivo*. Neurons have a complex cytoarchitecture, whereby their structure naturally impacts their function. In both the developing and mature CNS, this structure is dynamically regulated by extracellular signals from other cell types, including in particular from differentiated astrocytes that have different properties from those matured *in vitro* (Cahoy et al. 2008; Foo et al. 2011). It is thus likely that these critical synaptogenic cues are absent in dissociated neuronal culture systems. In addition, the difficulties associated with maintaining long-term CNS cultures resulted in most studies on BDNF trafficking being performed with neurons at < 21 DIV, despite the fact that sub-cellular structures such as spines take several weeks to develop (Goodman et al. 1996; Brigadski et al. 2005; Dean et al. 2009; Matsuda et al. 2009). Indeed, previous reports indicate that neurons require between 3 and 4 weeks in culture to form typical axons and dendrites (Papa et al. 1995; Sahu et al. 2019), and that spine formation is dependent on co-culture with glial cells (Banker 1980; Pfrieder and Barres 1997).

7.2.2 Understanding the physiological role of pro-BDNF and the cleaved pro-peptide

7.2.2.1 pro-BDNF

Much like NGF that is also first synthesised as a precursor protein (Suter et al. 1991; Rattenholl et al. 2001), the generation of pro-BDNF is essential for the formation of disulphide bonds that are in turn essential for the correct folding of mBDNF. The discovery that these precursors bind p75^{NTR} to a higher affinity than mature neurotrophins (Lee et al. 2001) led to speculation that secreted pro-neurotrophins may serve physiological functions beyond the folding of their mature domain. Indeed, in cultured cells, recombinant pro-NGF and pro-BDNF have been shown to induce process

retraction and neuronal apoptosis through p75^{NTR} when co-expressed with sortilin (Lee et al. 2001; Nykjaer et al. 2004; Teng et al. 2005). These findings were supported by follow-up *in vivo* studies where mice expressing a single allele of cleavage-resistant pro-BDNF exhibited a reduced arborisation of hippocampal dendrites and enhanced LTD at Schaffer collateral synapses (Yang et al. 2014).

However, to determine the true physiological relevance of these findings, it is first critical to accurately report the relative proportion of pro-BDNF in neuronal cells. Thus far, answering this question has been hindered significantly by a lack of reliable BDNF antibodies. Although mAb #9 exhibits a high degree of sensitivity across immunostaining, immunoprecipitation (Matsumoto et al. 2008), and ELISA experiments (Naegelin et al. 2018; Dingsdale et al. 2021), its inability to recognise BDNF moieties on western blot called for the validation of an alternative antibody. The comparatively late availability of a monoclonal antibody designated mAb 3C11 allowed for the unambiguous detection of both pro- and mBDNF on western blot and was also validated by a lack of signal in the cortical lysates of *Bdnf*^{-/-} mice. This antibody will prove an essential tool for future studies of BDNF biosynthesis by cells of the CNS. Indeed, it has already been used to reveal critical aspects of BDNF processing by human and rat megakaryocytes (Chacón Fernández et al. 2016).

Using mAb 3C11, the analysis of lysates prepared from cortical cultures (Chapter 3) and adult brain tissues (Chapter 5 and 6) revealed that endogenous pro-BDNF comprises just ~10% of total BDNF detected in brain neurons, confirming previous findings (Rauskolb et al. 2010, Dieni et al. 2012). Although these results largely disagree with data generated using the now discontinued pAb N-20 (Santa Cruz), several reports using this antibody or others of questionable specificity (see for example mAb EPR1292, abcam) illustrated the presence of non-specific signals on western blots with molecular weights roughly corresponding to that of pro-BDNF (Michalski and Fahnstock 2003; Teng et al. 2005). Interestingly, the proportion of pro-BDNF remained stable after increased physiological activity, but not in excitotoxic culture conditions, whereby its proportion increased to over 50%. These data suggest that the accumulation and release of pro-BDNF only may prove relevant in the context of lesioned cells. This is an important finding considering that cleavage-resistant pro-BDNF negatively modulates synaptic transmission and cell survival (Teng et al. 2005; Woo et al. 2005). As p75^{NTR} levels have also been shown to increase at sites of nerve injury or in cases of neurodegenerative disease (Mufson and Kordower 1992; Dowling et al. 1999; Roux et al. 1999; Lowry et al. 2001; Beattie et al. 2002), these results indicate that pro-BDNF-p75^{NTR} interactions may be a significant driver of apoptotic signalling in pathologies characteristic of increased cell death.

7.2.2.2 The BDNF pro-peptide

Although BDNF's role in brain function is now widely appreciated, very little is still known about possible roles of its cleaved pro-peptide beyond an essential role in assisting folding before cleavage. This is partly due to its poor detectability, whereby the pro-peptide is typically washed away on western blots and requires glutaraldehyde fixation to the membrane to be detected (Dieni et al. 2012), a result later confirmed by Anastasia et al. (2013). A better understanding of the biological functions of the cleaved peptide is important and various scenarios have been proposed, also in view of the human Val66Met polymorphism (see for example Anastasia et al. 2013 and Giza et al. 2018).

Using well-validated antibodies in immuno-EM, Dieni and colleagues (2012) visualised the storage of the BDNF pro-peptide within presynaptic LDCVs of the hippocampal mossy fibre projection pathway. These findings are supported by data presented in Chapter 3, where a PLA confirmed the colocalization of the pro-peptide and mBDNF in subcellular structures. As signals in this assay are only generated by the exceptionally close proximity of targets, it should also be considered whether these proteins interact after cleavage. Indeed, a recent study by Uegaki and colleagues (2017) demonstrated a stable electrostatic interaction between the pro-peptide and mBDNF under acidic conditions resembling that of intracellular vesicles. Strikingly, under both acidic and neutral conditions - tentatively replicating that of LDCVs and the extracellular space, respectively - this interaction was shown to strengthen significantly when involving the Met pro-peptide. It is thus conceivable that this interaction reduces the bioavailability of BDNF, resulting in the Val66Met phenotypes reported by others (Neves-Pereira et al. 2002; Egan et al. 2003; Bueller et al. 2006)

7.3 The biological relevance of BDNF-fusion proteins

As it is now well established that the “trophic” properties of BDNF are localised in its carboxy terminal half, it should in principle be possible to tag BDNF's N-terminus, given that previous studies reported that partially processed, glycosylated BDNF retains its biological activity (Kolbeck et al. 1994). These data showed that the replacement of a single arginine by lysine at the site of pro-domain cleavage (see Introduction) unexpectedly resulted in the generation of a biologically active BDNF moiety that carries a 19 aa extension at its N-terminus. However, further experiments inspired by this finding revealed that the replacement of this extension with short epitope tags (such as myc or HA) impaired the biological activity of the mature protein (Johanes Klose, PhD Thesis, Munich, 1998). It was soon found that BDNF only remained functional when such small tags were added to BDNF's C-terminus, of which led to the successful generation of

viable animals expressing *Bdnf-Myc* or *Bdnf-HA* from the endogenous *Bdnf* locus presenting with no observable phenotype (Matsumoto et al. 2008; Yang et al. 2009).

A number of published studies have also used much longer probes to investigate the trafficking of BDNF in cultured neurons or brain slices. These experiments typically involved the overexpression of constructs encoding *Bdnf* fused to a fluorescent protein at its C-terminus, such as enhanced GFP (GFP) or its pH-sensitive counterpart pHluorin. Such studies concluded that BDNF is released from neurons constitutively or in an activity-dependent manner (Hartmann et al. 2001; Kohara et al. 2001; Kojima et al. 2001; Brigadski et al. 2005; Dean et al. 2009; Matsuda et al. 2009). Whereas others using the same methodology reported that BDNF is transported in a bidirectional fashion, with some groups claiming that it is preferentially sorted into dendritic shafts and spines (Edelmann et al. 2015; Harward et al. 2016). However, as described in Chapter 4, studying these constructs in HEK293 cells revealed that the fusion of these probes to BDNF significantly impairs its biological processing. When fused to optimised probes mCherry, moxVenus, and moxGFP, the BDNF pro-protein underwent early degradation, resulting in multiple BDNF moieties not observed during biosynthesis of the wildtype protein. The similar degradation of BDNF-myc-GFP further indicates that the addition of large FPs interferes with pro-protein processing, as these abnormalities are also not observed with BDNF-myc, a tagged construct previously implemented *in vivo* (Matsumoto et al. 2008). Interestingly, in both HEK293 cells and neurons, both BDNF-GFP and BDNF-pHluorin were atypically processed, resulting in their partial degradation and the attenuated secretion of BDNF-GFP. Although the potency of these proteins was not determined, follow-up experiments utilising subsequent additions of myc tags suggests that adding lengthy tags to BDNF's C-terminus attenuates its ability to phosphorylate TrkB. A review of the corresponding publications reporting these constructs suggests that neither BDNF-GFP nor BDNF-pHluorin were thoroughly tested for their biological activity, although Matsuda et al. (2009) did attempt this in the supplementary material of their publication. However, their results remain unconvincing due to their reliance on a BDNF antiserum that was not thoroughly validated. A more recent study by Leschik et al. (2019) attempted to generate a mouse line expressing *Bdnf-Gfp* in place of the wildtype gene. A close look of this report indicated that ~50% of homozygotes were not viable, with the survival of the remaining half potentially explained by the cleavage of GFP from BDNF, which would explain their documented localisation of alleged BDNF that largely contradicts reports of the endogenous protein (Figure 7.1). As it has been previously noted that BDNF purified from pig brain lacks 3 aa from its C-terminus when compared to the aa sequence predicted from its cDNA, it is conceivable that GFP may have been cleaved from BDNF's C-terminus in these animals by virtue of

cleavage at this site. This would explain the survival of some of these animals until adulthood, and the localisation of GFP as a product separated from BDNF.

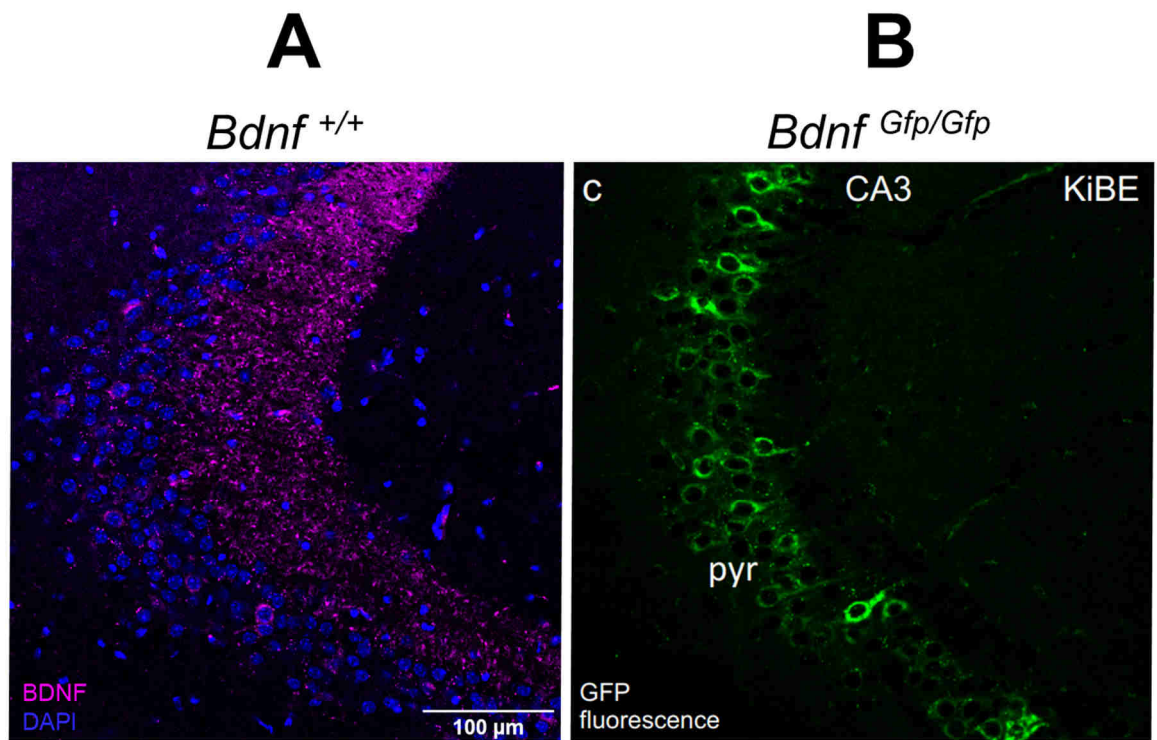


Figure 7.1. A comparison of the immunoreactivity of endogenous BDNF with the GFP signal observed in *Bdnf-Gfp* knock-in mice.

(A) High power imaging of endogenous BDNF-ir in the hippocampal CA3 region of *Bdnf*^{+/+} mice. (B) The GFP signal observed by Leschik and colleagues (2019) in homozygous *Bdnf-Gfp* knock-in mice (KiBE). Note the presence of GFP fluorescence in the CA3 cell bodies, but the total lack of signal in the adjacent mossy fibre terminals (taken from Leschik et al. 2019).

7.4 The generation of a novel mouse line that reports BDNF translation by the co-expression of GFP

To better understand the mechanisms regulating *Bdnf* expression within brain, it is desirable to use methods that visualise its transcription using reporter proteins such as GFP. The feasibility of these approaches has been demonstrated by previous studies, where vectors encoding the regulatory sequences of *Bdnf* were used to drive reporter expression *in vivo* (Guillemot et al. 2007; Koppel et al. 2009; Fukuchi et al. 2017). Detectable levels of fluorescence were also achieved by inserting the coding sequences of reporter proteins within activity-dependent exons of *Bdnf* (Singer et al. 2018). Together, these results indicate that the *Bdnf* promoters are strong enough to drive the expression of fluorescent proteins to levels allowing the visualisation and sorting of *Bdnf*-expressing cells. However, given the mounting evidence for the presence of regulatory processes occurring downstream of transcription (Vogel and Marcotte 2012; Buccitelli and Selbach 2020), a better model was needed to faithfully report the degree of BDNF translation by monitoring GFP as surrogate and proportional marker. This thesis describes an attempt to achieve this goal by validating a novel bicistronic mRNA construct reporting the levels of BDNF translation by the co-translating GFP. The functionality of this mRNA was first tested in cultured cells, where BDNF-P2A and GFP were shown to be successfully translated as two functionally distinct, biologically active proteins. Further biochemical analyses of pBDNF-P2A-NLS-GFP translation products revealed that the P2A sequence remains attached to BDNF without interfering with either its processing or secretion. Similar to myc- and HA- tagged versions of the protein (Matsumoto et al. 2008; Yang et al. 2009), this remnant tag may in future prove useful for detecting BDNF using 2A antibodies, but at the time of writing only two are commercially available. In mice, the replacement of the *Bdnf* coding sequence with *Bdnf-P2a-Gfp* resulted in the generation of both viable and fertile animals. In the hippocampus, BDNF-P2A and GFP presented with distinct patterns of immunoreactivity, indicating their successful translation into separate and differentially processed proteins. The distribution of BDNF-P2A matched earlier reports of the endogenous protein (Conner et al. 1997; Yan et al. 1997; Dieni et al. 2012), whereas GFP was shown to accumulate within the nuclei of cells known to actively transcribe the *Bdnf* mRNA (Hofer et al. 1990; Wetmore et al. 1990; Gorski et al. 2003a). Although GFP expression was only detectable once enhanced using GFP antibodies, its low fluorescence more likely results from the exceptionally low level of *Bdnf* expression occurring *in vivo* opposed to the impaired folding of the GFP polypeptide chain. Indeed, overexpression of the pBDNF-P2A-NLS-GFP construct in cultured neurons resulted in a GFP signal that was easily detected by low-power fluorescence microscopy (data not shown). Together, these data validate the

use of this bicistronic mRNA strategy for studying growth factor expression *in vivo*. Furthermore, use of the same strategy by van Veen and colleagues (2016) to visualise sites of *Braf* oncogene expression in developing mice suggests that this approach may be applied to a range of biological questions. Progressive obesity was observed in *Bdnf-P2a-Gfp* homozygous males beyond 6 months of age. Weight gain is well-recognised as a BDNF “hypomorphic” phenotype (Kernie et al. 2000; Rios et al. 2001; Unger et al. 2007), whereby no measurable differences in steady state BDNF levels were observed in the brains of knock-in mice. Furthermore, the relative abundance of pro- and mature-BDNF was shown to be unchanged compared to that of their wildtype littermates, indicating no change to the bioavailability of mBDNF within brain. However, it appears likely that the addition of P2A to BDNF’s C-terminus results in the submaximal activation of TrkB over extended periods *in vivo*, resulting in a progressive impairment of feeding-related brain circuits. Although this interpretation seems to contradict the results of the *in vitro* TrkB phosphorylation assay in Chapter 4, it is likely that the comparatively high concentration of BDNF used in these experiments may have masked critical differences in the potency of BDNF-P2A when compared to the wildtype protein. To test this hypothesis, the level of TrkB phosphorylation may be compared between the brains of *Bdnf-P2a-Gfp* animals and their wildtype littermates, with a focus on the brain areas associated with feeding behaviours. Although no additional hypomorphic phenotypes (see Introduction) were observed at the time of writing, future users of this mouse strain may need to further test for unexpected phenotypes, especially when using aged animals.

7.5 Studying mechanisms of *Bdnf* regulation within brain

As post-mitotic cells, neurons continuously adapt throughout their lifetime in response to a large variety of stimuli. Their functional plasticity is highly dependent on the regulated transcription of gene products whereby the disruption of such mechanisms may progressively lead to cognitive decline. The increasing evidence that BDNF exerts both neuro-protective and anti-depressive effects by modulating synaptic plasticity makes it a particularly attractive drug target. However, its poor pharmacokinetic properties including short half-life and unfavourable diffusion characteristics as a small, highly-charged protein (Barde et al. 1982) calls for alternative means of increasing BDNF levels within brain. To achieve this, a better understanding of the regulatory mechanisms governing the expression of BDNF is desirable. While it has long been appreciated that *Bdnf* transcription markedly increases during learning (Hall et al. 2000; Mizuno et al. 2000; Silhol et al. 2007), changes in the level of protein expression have been exceedingly difficult to appreciate. The experiments described in Chapter 6 summarise an attempt to

achieve this goal in the brains of rats subjected to the RAM task. By combining the use of two well-validated antibodies against BDNF and its pro-peptide, BDNF-containing structures were successfully visualised in both the hippocampal and extrahippocampal correlates of memory. These data revealed striking differences between the hippocampal expression profiles of Fos and BDNF, a surprising, but relevant finding considering that both genes undergo activity- and Ca²⁺-dependent transcriptional regulation within neurons (Sheng et al. 1990; Tao et al. 1998; Tao et al. 2002). As rats are the preferred animal model for studying behaviour relevant to human conditions, this staining technique will prove useful for identifying neuronal circuits reliant on activity-dependent BDNF expression for functional plasticity. Although no significant change in BDNF expression was observed in rats performing the RAM task, this can be attributed to multiple factors. As changes in Fos expression did not match that observed by others using similar paradigms (Wan et al. 1999; Vann et al. 2000b; Pothuizen et al. 2009), it seems unlikely that in this particular set of experiments, learning-dependent changes in BDNF would have been detected. It is also conceivable that the change in maze surroundings may itself have been enough to induce hippocampal BDNF expression (Novkovic et al. 2015; Gualtieri et al. 2017). However, such subtle changes may have been masked by the already high levels of expression in each subregion observed in the experiments in question. In future studies, this methodology would need to be adapted and may prove more useful for studying BDNF-dependent in plasticity in populations with lower basal levels of BDNF expression. This type of approach was recently implemented by Andreska and colleagues (2020) who were able to show increased BDNF expression in cortico-striatal projection neurons essential for motor learning.

7.6 Outlook

While the present study details the need for sensitive and specific BDNF immunostaining techniques to accurately report the localisation of the endogenous protein, this type of approach has a limited scope for characterising the identity of cells actively translating the *Bdnf* mRNA within brain. To circumvent these difficulties, the *Bdnf-P2a-Gfp* mouse was generated and subsequently characterised. After confirming that the pattern of GFP immunoreactivity matched previous reports of *Bdnf* expression within brain, *in vitro* experiments examined whether the level of GFP reliably reports the degree of *Bdnf* translation. The treatment of *Bdnf-P2a-Gfp* cortical cultures with potassium channel inhibitor 4-AP demonstrated that like BDNF, GFP levels increased in an activity-dependent manner. Cultures prepared from these mice will therefore prove a useful, high throughput screening tool for the development of new drugs designed to enhance *Bdnf* expression not only in neurons but in any other cell cultures prepared from primary

tissues of interest. Indeed, a similar approach was recently used to identify a novel, CREB-dependent inducer of neuronal *Bdnf* transcription from a library of herbal extracts (Fukuchi et al. 2019). However, as GFP fluorescence proved undetectable in *Bdnf-P2a-Gfp* brain neurons, this model is expected to be unsuitable for live cell-imaging studies of BDNF translation.

While it is also widely accepted that *Bdnf* mRNAs are largely upregulated in response to neuronal activity *in vivo* (Zafra et al. 1990; Ernfors et al. 1991, Isackson et al. 1991; Castrén et al. 1992), the respective changes in protein expression are yet to be satisfactorily documented, with the exception of limited immunostaining studies in rodent models of seizure (Rudge et al. 1998). Utilising *Bdnf-P2a-Gfp* mice in similar paradigms would help clarify whether activity-induced increases in *Bdnf* transcription result in increased levels of BDNF protein. Indeed, combining such experiments with transcriptomic analyses would help elucidate the potential role of 3' UTRs in *Bdnf* translation (Tongiorgi et al. 2004), and whether this can be process can be modulated using pharmacological agents such as ketamine (Monteggia et al. 2013).

Studying changes in GFP expression in distinct neuronal subsets may also bring new insights into the brain circuitries utilising BDNF as a critical modulator of circuit plasticity, such as the extrahippocampal correlates of memory described in Chapter 6. Furthermore, as levels of GFP expression should be sufficient to achieve fluorescence activated cell sorting (FACS), single cell transcriptomics can now be envisaged to characterise the molecular profile of these neurons as a function of BDNF protein levels. When combined with epigenome sequencing (reviewed in Armand et al. 2021), this type of approach will help identifying regulators of *Bdnf* transcription in context of specific behaviours, aging and diseases (West et al. 2014). Such experiments would also help clarify the mechanisms of pre-existing drugs such as Fingolimod, a modulator of the sphingosine-1 phosphate receptor described to cross the BBB to increase BDNF levels (Deogracias et al. 2012).

References

Abraham, W. C., Mason, S. E., Demmer, J., Williams, J. M., Richardson, C. L., Tate, W. P., Lawlor, P. A. and Dragunow, M. (1993). Correlations between immediate early gene induction and the persistence of long-term potentiation. *Neuroscience* **56**:717–727.

Adachi, N., Kohara, K. and Tsumoto, T. (2005). Difference in trafficking of brain-derived neurotrophic factor between axons and dendrites of cortical neurons, revealed by live-cell imaging. *BMC Neuroscience* **6**:42.

Albasser, M. M., Poirier, G. L. and Aggleton, J. P. (2010). Qualitatively different modes of perirhinal-hippocampal engagement when rats explore novel vs. familiar objects as revealed by c-Fos imaging. *European Journal of Neuroscience* **31**(1):134-147.

Albasser, M. M., Poirier, G. L., Warburton, E. C. and Aggleton, J. P. (2007). Hippocampal lesions halve immediate-early gene protein counts in retrosplenial cortex: distal dysfunctions in a spatial memory system. *European Journal of Neuroscience* **26**:1254–1266.

Altar, C. A., Cai, N., Bliven, T., Juhasz, M., Conner, J. M., Acheson, A. L., Lindsay, R. M. and Wiegand, S. J. (1997). Anterograde transport of brain-derived neurotrophic factor and its role in the brain. *Nature* **389**(6653):856–860.

An, J. J., Gharami, K., Liao, G. - Y., Woo, N. H., Lau, A. G., Vanevski, F., Torre, E. R., Jones, K. R., Feng, Y., Lu, B. and Xu, B. (2008). Distinct role of long 3' UTR BDNF mRNA in spine morphology and synaptic plasticity in hippocampal neurons. *Cell* **134**(1):175–187.

Anastasia, A., Deinhardt, K., Chao, M. V., Will, N. E., Irmady, K., Lee, F. S., Hempstead, B. L. and Bracken, C. (2013). Val66Met polymorphism of BDNF alters prodomain structure to induce neuronal growth cone retraction. *Nature Communications* **4**:2490.

Andreska, T., Aufmkolk, S., Sauer, M. and Blum, R. (2014). High abundance of BDNF within glutamatergic presynapses of cultured hippocampal neurons. *Frontiers in Cellular Neuroscience* **8**(107).

Andreska, T., Rauskolb, S., Schukraft, N., Lüningschrör, P., Sasi, M., Signoret-Genest, J., Behringer, M., Blum, R., Sauer, M., Tovote, P. and Sendtner, M. (2020). Induction of BDNF expression in layer II/III and layer V neurons of the motor cortex is essential for motor learning. *The Journal of Neuroscience* **40**(33):6289–6308.

Armand, E.J., Li, J., Xie, F., Luo, C. and Mukamel, E. A. (2021). Single-cell sequencing of brain cell transcriptomes and epigenomes. *Neuron* **109**(1):11-26.

Autry, A. E., Adachi, M., Nosyreva, E., Na, E. S., Los, M. F., Cheng, P. F., Kavalali, E. T. and Monteggia, L. M. (2011). NMDA receptor blockade at rest triggers rapid behavioural antidepressant responses. *Nature* **475**(7354):91–95.

Baj, G., Pinhero, V., Vaghi, V. and Tongiorgi, E. (2016). Signaling pathways controlling activity-dependent local translation of BDNF and their localization in dendritic arbors. *Journal of Cell Science* **129**(14):2852-2864.

Baldwin, A. N., Bitler, C. M., Welcher, A. A. and Shooter, E. M. (1992). Studies on the structure and binding properties of the cysteine-rich domain of the rat low affinity nerve growth factor receptor (p75^{NGFR}). *The Journal of Biological Chemistry* **267**(12):8352-8359.

Banker, G. A. (1980). Trophic interactions between astroglial cells and hippocampal neurons in culture. *Science* **209**(4458):809–810.

Bannerman, D. M., Grubb, M., Deacon, R. M. J., Yee, B. K., Feldon, J. and Rawlins, J. N. P. (2003). Ventral hippocampal lesions affect anxiety but not spatial learning. *Behavioural Brain Research* **139**(1-2):197-213.

Bannerman, D. M., Yee, B. K., Good, M. A., Heupel, M. J., Iversen, S. D. and Rawlins, J. N. (1999). Double dissociation of function within the hippocampus: a comparison of dorsal, ventral and complete hippocampal cytotoxic lesions. *Behavioural Neuroscience* **113**(6):1170-1188.

Bannerman, D. M., Yee, B. K., Lemaire, M., Wilbrecht, L., Jarrard, L., Iversen, S. D., Rawlins, J. N. P. and Good, M. A. (2001). The role of the entorhinal cortex in two forms of spatial learning and memory. *Experimental Brain Research* **141**(3):281-303.

Baquet, Z. C., Gorski, J. A. and Jones, K. R. (2004). Early striatal dendrite deficits followed by neuron loss with advanced age in the absence of anterograde cortical brain-derived neurotrophic factor. *Journal of Neuroscience* **24**(17):4250-4258.

Baquet, Z. C., Bickford, P. C. and Jones, K. R. (2005). Brain-derived neurotrophic factor is required for the establishment of the proper number of dopaminergic neurons in the substantia nigra pars compacta. *Journal of Neuroscience* **25**(26):6251-6259.

Barde, Y. A., Edgar, D. and Thoenen, H. (1982). Purification of a new neurotrophic factor from mammalian brain. *The EMBO Journal* **1**(5):549-553.

Barrett, G. L. and Bartlett, P. F. (1994). The p75 nerve growth factor receptor mediates survival or death depending on the stage of sensory neuron development. *Proceedings of the National Academy of Sciences of the United States of America* **91**(14):6501-6505.

Barrett, G. L., Greferath, U., Barker, P. A., Trieu, J. and Bennie, A. (2005). Co-expression of the p75 neurotrophin receptor and neurotrophin receptor-interacting melanoma antigen homolog in the mature rat brain. *Neuroscience* **133**(2):381-392.

Barros, V. N., Mundim, M., Galindo, L. T., Bittencourt, S., Porcionatto, M. and Mello, L. E. (2015). The pattern of c-Fos expression and its refractory period in the brain of rats and monkeys. *Frontiers in Cellular Neuroscience* **9**:72.

Bath, K. G., Jing, D. Q., Dincheva, I., Neeb, C. C., Pattwell, S. S., Chao, M. V., Lee, F. S. and Ninan, I. (2012). BDNF Val66Met impairs fluoxetine-induced enhancement of adult hippocampus plasticity. *Neuropsychopharmacology* **37**(5):1297–1304.

Beattie, M. S., Harrington, A. W., Lee, R., Kim, J. Y., Boyce, S. L., Longo, F. M., Bresnahan, J. C., Hempstead, B. and Yoon, S. K. (2002). ProNGF induces p75-mediated death of oligodendrocytes following spinal cord injury. *Neuron* **36**(3):375–386.

Beckers, S., Peeters, A., Zegers, D., Mertens, I., Gaal, L. V. and Van Hul, W. (2008). Association of the BDNF Val66Met variation with obesity in women. *Molecular Genetics and Metabolism* **95**(1-2):110-112.

Benicky, J., Sanda, M., Brnakova Kennedy, Z. and Goldman, R. (2019). N-Glycosylation is required for secretion of the precursor to brain-derived neurotrophic factor (proBDNF) carrying sulfated LacdiNAc structures. *The Journal of Biological Chemistry* **294**(45):6816-16830.

Bennett, M. L., Bennett, F. C., Liddelow, S. A., Ajami, B., Zamanian, J. L., Fernhoff, N. B., Mulinyawe, S. B., Bohlen, C. J., Adil, A., Tucker, A., Weissman, I. L., Chang, E. F., Li, G., Grant, G. A., Gephart, M. G. H. and Barres, B. A. (2016). New tools for studying microglia in the mouse and human CNS. *Proceedings of the National Academy of Sciences of the United States of America* **113**(12):E1738–E1746.

Berkemeier, L. R., Winslow, J. W., Kaplan, D. R., Nikolics, K., Goeddel, D. V. and Rosenthal, A. (1991). Neurotrophin-5: A novel neurotrophic factor that activates trk and trkB. *Neuron* **7**(5):857–866.

Bibel, M., Hoppe, E. and Barde, Y. A. (1999). Biochemical and functional interactions between the neurotrophin receptors trk and p75NTR. *The EMBO Journal* **18**(3):616-622.

Björkholm, C. and Monteggia, L. M. (2016). BDNF – a key transducer of antidepressant effects. *Neuropharmacology* **102**:72–79.

Blankenship, A. G. and Feller, M. B. (2010). Mechanisms underlying spontaneous patterned activity in developing neural circuits. *Nature Reviews Neuroscience* **11**(1):18-29.

Brady, R., Zaidi, S. I., Mayer, C. and Katz, D. M. (1999). BDNF is a target-derived survival factor for arterial baroreceptor and chemoafferent primary sensory neurons. *The Journal of Neuroscience* **19**(6):2131-2142.

Brigadski, T., Hartmann, M., and Lessman, V. (2005). Differential vesicular targeting and time course of synaptic secretion of the mammalian neurotrophins. *Journal of Neuroscience* **25**(33):7601-7614.

Buccitelli, C. and Selbach, M. (2020). mRNAs, proteins and the emerging principles of gene expression control. *Nature Reviews Genetics* **21**(10):630-644.

Buchman, A. S., Yu, L., Boyle, P. A., Schneider, J. A., De Jager, P. L. and Bennett, D. A. (2016). Higher brain BDNF gene expression is associated with slower cognitive decline in older adults. *Neurology* **86**(8):735-741.

Bueker, E. D. (1948). Implantation of tumors in the hind limb field of the embryonic chick and the developmental response of the lumbosacral nervous system. *The Anatomical Record*. **102**(3):369-389.

Bueller, J. A., Aftab, M., Sen, S., Gomez-Hassan, D., Burmeister, M. and Zubieta, J. K. (2006). BDNF Val66Met allele is associated with reduced hippocampal volume in healthy subjects. *Biological Psychiatry* **59**(9):812-815.

Burnouf, T., Kuo, Y. P., Blum, D., Burnouf, S. and Su, C. Y. (2011). Human platelet concentrates: a source of solvent/detergent-treated highly enriched brain-derived neurotrophic factor. *Transfusion* **52**(8):1721-1728.

Cahoy, J. D., Emery, B., Kaushal, A., Foo, L. C., Zamanian, J. L., Christopherson, K. S., Xing, Y., Lubischer, J. L., Krieg, P. A., Krupenko, S. A., Thompson, W. J. and Barres, B. A. (2008). A transcriptome database for astrocytes, neurons, and oligodendrocytes: a new resource for understanding brain development and function. *The Journal of Neuroscience* **28**(1):264–278.

Casarotto, P. C., Girysh, M., Fred, S. M., Kovaleva, V., Moliner, R., Enkavi, G. and Biojone, C., Cannarozzo, C., Sahu, M. D., Kaurinkoski, K., Brunello, C. A., Steinzeig, A., Winkel, F., Patil, S., Vestring, S., Serchov, T., Diniz, C. R. A. F., Laukkanen, L., Cardon, I., Antila, H., Rog, T., Piepponen, T., Bramham, C. R., Normann, C., Lauri, S. E., Saarma, M., Vattulainen, I. and Castrén E. (2021). Antidepressant drugs act by directly binding to TRKB neurotrophin receptors. *Cell* **184**(5):1299–1313.

Castrén, E., Berninger, B., Leingärtner, A. and Lindholm, D. (1998). Regulation of brain-derived neurotrophic factor mRNA levels in hippocampus by neuronal activity. *Progress in Brain Research* **117**:57-64.

Castrén, E., Zafra, F., Thoenen, H. and Lindholm, D. (1992). Light regulates expression of brain-derived neurotrophic factor mRNA in rat visual cortex. *Proceedings of the National Academy of Sciences of the United States of America* **89**(20):9444-9448.

Cathomas, F., Vogler, C., Euler-Sigmund, J. C., de Quervain, D. J. F. and Papassotiropoulos, A. (2010). Fine-mapping of the brain-derived neurotrophic factor (BDNF) gene supports an association of the Val66Met polymorphism with episodic memory. *The International Journal of Neuropsychopharmacology* **13**(8):975-980.

Chacón-Fernández, P., Säuberli, K., Colzani, M., Moreau, T., Ghevaert, C. and Barde, Y. A. (2016). Brain-derived neurotrophic factor in megakaryocytes. *The Journal of Biological Chemistry* **291**(19):9872-9881.

Chalfie, M., Tu, Y., Euskirchen, G., Ward, W. W. and Prasher, D. C. (1994). Green fluorescent protein as a marker for gene expression. *Science* **263**(5148):802-805.

Chao, M. V., Bothwell, M., Ross, A. H., Koprowski, H., Lanahan, A. A., Buck, C. R. and Sehgal, A. (1986). Gene transfer and molecular cloning of the human NGF receptor. *Science* **232**(4749):518-521.

Chen, B., Dowlatshahi, D., MacQueen, G. M., Wang, J. F. and Young, L. T. (2001). Increased hippocampal BDNF immunoreactivity in subjects treated with antidepressant medication. *Biological Psychiatry* **50**(4):260-265.

Chen, Z. Y., Jing, D., Bath, K. G., Ieraci, A., Khan, T., Siao, C. J., Herrera, D. G., Toth, M., Yang, C., McEwen, B. S., Hempstead, B. L. and Lee, F. S. (2006). Genetic variant BDNF (Val66Met) polymorphism alters anxiety-related behavior. *Science* **314**(5796):140-143.

Cirulli, F., Berry, A., Chiarotti, F. and Alleva, E. (2004). Intrahippocampal administration of BDNF in adult rats affects short-term behavioral plasticity in the Morris water maze and performance in the elevated plus-maze. *Hippocampus* **14**(7):802-807.

Cohen, S. (1960). Purification of a nerve-growth promoting protein from the mouse salivary gland and its neuro-cytotoxic antiserum. *Proceedings of the National Academy of Sciences of the United States of America* **46**(3):302-311.

Cohen, S., Levi-Montalcini, R. and Hamburger, V. (1954). A nerve growth-stimulating factor isolated from sarcomas 37 and 180. *Proceedings of the National Academy of Sciences of the United States of America* **40**(10):1014-1018.

Conner, J. M., Lauterborn, J. C., Yan, Q., Gall, C. M. and Varon, S. (1997). Distribution of brain-derived neurotrophic factor (BDNF) protein and mRNA in normal adult rat CNS: evidence for anterograde axonal transport. *The Journal of Neuroscience* **17**(7):2295-2313.

Costantini, L. M., Baloban, M., Markwardt, M. L., Rizzo, M., Guo, F., Verkhusha, V. V. and Snapp, E. L. (2015). A palette of fluorescent proteins optimized for diverse cellular environments. *Nature Communications* **6**:7670.

Costantini, L. M. and Snapp, E. L. (2013). Fluorescent proteins in cellular organelles: serious pitfalls and some solutions. *DNA and Cell Biology* **32**(11):622-627.

Curran, T., Miller, A. D., Zokas, L. and Verma, I. M. (1984). Viral and cellular fos proteins: a comparative analysis. *Cell* **36**(2):259-268.

Davies, A. M., Thoenen, H. and Barde, Y. A. (1986a). The response of chick sensory neurons to brain-derived neurotrophic factor. *The Journal of Neuroscience* **6**(7):1897-1904.

Davies, A. M. (1994). Neurotrophic factors: switching neurotrophin dependence. *Current Biology* **4**(3):273-276.

Davies, A. M., Thoenen, H. and Barde, Y. A. (1986b). Different factors from the central nervous system and periphery regulate the survival of sensory neurones. *Nature* **319**(6053):497-499.

Dean, C., Liu, H., Dunning, F. M., Chang, P. Y., Jackson, M. B. and Chapman, E. R. (2009). Synaptotagmin-IV modulates synaptic function and long-term potentiation by regulating BDNF release. *Nature Neuroscience* **12**(6):767-776.

Delotto, Y. and Delotto, R. (1998). Proteolytic processing of the Drosophila Spätzle protein by easter generates a dimeric NGF-like molecule with ventralising activity. *Mechanisms of Development* **72**(1-2):141-148.

Deogracias, R., Yazdani, M., Dekkers, M. P. J., Guy, J., Ionescu, M. C. S., Vogt, K. E. and Barde, Y. A. (2012). Fingolimod, a sphingosine-1 phosphate receptor modulator, increases BDNF levels and improves symptoms of a mouse model of Rett Syndrome. *Proceedings of the National Academy of Sciences* **109**(35):14230-14235.

Dieni, S., Matsumoto, T., Dekkers, M., Rauskolb, S., Ionescu, M. S., Deogracias, R., Gundelfinger, E. D., Kojima, M., Nestel, S., Frotscher, M. and Barde, Y. A. (2012). BDNF and its pro-peptide are stored in presynaptic dense core vesicles in brain neurons. *Journal of Cell Biology* **196**(6):775–788.

Dingsdale, H., Nan, X., Garay, S. M., Mueller, A., Sumption, L. A., Chacón-Fernández, P., Martínez-Garay, I., Ghevaert, C., Barde, Y. A. and John, R. A. (2021). The placenta protects the fetal circulation from anxiety-driven elevations in maternal serum levels of brain-derived neurotrophic factor. *Translational Psychiatry* **11**(1):62.

Donovan, M. J., Lin, M. I., Wiegand, P., Ringstedt, T., Kraemer, R., Hahn, R., Wang, S., Ibañez, C. F., Rafii, S. and Hempstead, B. L. (2000). Brain-derived neurotrophic factor is an endothelial cell survival factor required for intramyocardial vessel stabilisation. *Development* **127**(21):4531-4540.

Donovan, M. J., Miranda, R. C., Kraemer, R., McCaffrey, T. A., Tessarollo, L., Mahadeo, D., Sharif, S., Kaplan, D., Tsoulfas, P., Parada, L., Toran-Allerand, C. D., Hajjar, D. P., and Hempstead, B. L. (1995). Neurotrophin and neurotrophin receptors in vascular smooth muscle cells. *The American Journal of Pathology* **147**(2):309-324.

Dougherty, K. D., Dreyfus, C. F. and Black, I. B. (2000). Brain-derived neurotrophic factor in astrocytes, oligodendrocytes, and microglia/macrophages after spinal cord injury. *Neurobiology of Disease* **7**(6):574-585.

Dowling, P., Ming, X., Raval, S., Husar, W., Cascaccia-Bonnet, P., Chao, M., Cook, S. and Blumberg, B. (1999). Up-regulated p75^{NTR} neurotrophin receptor on glial cells in MS plaques. *Neurology* **58**(8):1676-1682.

Dugich-Djordjevic, M. M., Tocco, G., Willoughby, D. A., Najm, I., Pasinetti, G., Thompson, R. F., Baudry, M., Lapchak, P. A. and Hefti, F. (1992). BDNF mRNA expression in the developing rat brain following kainic acid-induced seizure activity. *Neuron* **8**(6):1127-1138.

Duman, C. H., Schlesinger, L., Russell, D. S. and Duman, R. S. (2008). Voluntary exercise produces antidepressant and anxiolytic behavioral effects in mice. *Brain Research* **1199**:148-158.

Edelmann, E., Cepeda-Prado, E., Frank, M., Lichtenecker, P., Brigadski, T. and Lessmann, V. (2015). Theta burst firing recruits BDNF release and signalling in postsynaptic CA1 neurons in spike-timing-dependent LTP. *Neuron* **86**:1041-1054.

Edwards, R. H., Rutter, W. J. and Hanahan, D. (1989). Directed expression of NGF to pancreatic beta cells in transgenic mice leads to selective hyperinnervation of the islets. *Cell* **58**(1):161-170.

Egan, M. F., Kojima, M., Callicott, J. H., Goldberg, T. E., Kolachana, B. S., Bertolino, A., Zaitsev, E., Gold, B., Goldman, D., Dean, M., Lu, B. and Weinberger, D. R. (2003). The BDNF Val66Met polymorphism affects activity-dependent secretion of BDNF and human memory and hippocampal function. *Cell* **112**(2):257-269.

Eggert, A., Sieverts, H., Ikegaki, N. and Brodeur, G. M. (2000). p75 mediated apoptosis in neuroblastoma cells is inhibited by expression of TrkA. *Medical and Pediatric Oncology* **35**(6):573-576.

Engert, F. and Bonhoeffer, T. (1999). Dendritic spine changes associated with hippocampal long-term synaptic plasticity. *Nature* **399**(6731):66-70.

Erickson, J. T., Conover, J. C., Borday, V., Champagnat, J., Barbacid, M., Yancopoulos, G. and Katz, D. M. (1996). Mice lacking brain-derived neurotrophic factor exhibit visceral sensory neuron losses distinct from mice lacking NT4 and display a severe developmental deficit in control of breathing. *The Journal of Neuroscience* **16**(17):5361-5371.

Ernfors, P., Bengzon, J., Kokaia, Z., Persson, H. and Lindvall, O. (1991). Increased levels of messenger RNAs for neurotrophic factors in the brain during kindling epileptogenesis. *Neuron* **7**(1):165-176.

Ernfors, P., Lee, K. F. and Jaenisch, R. (1994). Mice lacking brain-derived neurotrophic factor develop with sensory deficits. *Nature* **368**(6467):147-150.

Lynette, L. C., Allen, N., Bushong, E. A., Ventura, P. B., Chung, W. S., Zhou, L., Cahoy, J. D., Daneman, R., Zong, H., Ellisman, M. H. and Barres, B. (2011). Development of a method for the purification and culture of rodent astrocytes. *Neuron* **71**(5):799–811.

Fredriksson, S., Gullberg, M., Jarvius, J., Olsson, C., Pietras, K., Gústafsdóttir, S. M., Östman, A. and Landegren, U. (2002). Protein detection using proximity-dependent DNA ligation assays. *Nature Biotechnology* **20**:473–477.

Frodl, T., Schüle, C., Schmitt, G., Born, C., Baghai, T., Zill, P., Bottlender, R., Rupprecht, R., Bondy, B., Reiser, M., Möller, H. J. and Meisenzahl, E. M. (2007). Association of the brain-derived neurotrophic factor Val66Met polymorphism with reduced hippocampal volumes in major depression. *Archives of General Psychiatry* **64**(4):410.

Fujimara, H., Altar, C. A., Chen, R., Nakamura, T., Kambayashi, J., Sun, B. and Tandon, N. N. (2002). Brain-derived neurotrophic factor is stored in human platelets and released by agonist stimulation. *Thrombosis and Haemostasis* **87**(4):728-734.

Fukuchi, M., Izumi, H., Mori, H., Kiyama, M., Otsuka, S., Maki, S., Maehata, Y., Tabuchi, A., and Tsuda, M. (2017). Visualizing changes in brain-derived neurotrophic factor

(BDNF) expression using bioluminescence imaging in living mice. *Scientific Reports* **7**(1):4949.

Fukuchi, M., Okuno, Y., Nakayama, H., Nakano, A., Mori, H., Mitazaki, S., Nakano, Y., Toume, K., Jo, M., Takasaki, I., Watanabe, K., Shibahara, N., Komatsu, K., Tabuchi, A. and Tsuda, M. (2019). Screening inducers of neuronal BDNF gene transcription using primary cortical cell cultures from BDNF-luciferase transgenic mice. *Scientific Reports* **9**(1):11833.

Gay, N. J. and Gangloff, M. (2007). Structure and function of Toll receptors and their ligands. *Annual Review of Biochemistry* **76**:41-165.

Ghosh, A., Carnahan, J. and Greenberg, M. E. (1994). Requirement for BDNF in activity-dependent survival of cortical neurons. **263**(5153):1618-1623.

Giza, J. I., Kim, J., Meyer, H. C., Anastasia, A., Dincheva, I., Zheng, C. I., Lopez, K., Bains, H., Yang, J., Bracken, C., Liston, C., Jing, D., Hemstead, B. L. and Lee, F. S. (2018). The BDNF Val66Met prodomain disassembles dendritic spines altering fear extinction circuitry and behaviour. *Neuron* **99**(1):163-178.

Glock, C., Biever, A., Tushev, G., Bartnik, I., Nassim-Assir, B., tom Dieck, S and Schuman, E. M. (2020). The mRNA translation landscape in the synaptic neuropil. *bioRxiv*, doi: <https://doi.org/10.1101/2020.06.09.141960>

Goodman, L. J., Valverde, J., Lim, F., Geschwind, M. D., Federoff, H. J., Geller, A. I. and Hefti, F. (1996). Regulated release and polarized localization of brain-derived neurotrophic factor in hippocampal neurons. *Molecular and Cellular Neurosciences* **7**(3):222-238.

Gorski, J. A., Zeiler, S. R., Tamowski, S. and Jones, K. R. (2003a). Brain-derived neurotrophic factor is required for the maintenance of cortical dendrites. *The Journal of Neuroscience* **23**(17):6856-6865.

Gorski, J. A., Balogh, S. A., Wehner, J. M. and Jones, K. R. (2003b). Learning deficits in forebrain-restricted brain-derived neurotrophic factor mutant mice. *Neuroscience* **121**(2):341-354.

Greenberg, M. E., Xu, B., Lu, B. and Hempstead, B. L. (2009). New insights in the biology of BDNF synthesis and release: implications in CNS function. *The Journal of Neuroscience* **29**(41):12764-12767.

Greenberg, M. E. and Ziff, E. B. (1984). Stimulation of 3T3 cells induces transcription of the c-fos proto-oncogene. *Nature* **311**(5985):433-438.

Greer, P. L. and Greenberg, M. E. (2008). From synapse to nucleus: calcium-dependent gene transcription in the control of synapse development and function. *Neuron* **59**(6):846-860.

Gualtieri, F., Brégère, C., Laws, G. C., Armstrong, E. A., Wylie, N. J., Moxham, T. T., Guzman, R., Boswell, T. and Smulders, T. V. (2017). Effects of environmental enrichment on Doublecortin and BDNF expression along the dorso-ventral axis of the dentate gyrus. *Frontiers in Neuroscience* **11**:488.

Guillemot, F., Cerutti, I., Auffray, C. and Devignes, M. D. (2007). A transgenic mouse model engineered to investigate human brain-derived neurotrophic factor in vivo. *Transgenic Research* **16**(2):223-237.

Guo, J., Ji, Y., Ding, Y., Jiang, W., Sun, Y., Lu, B. and Nagappan, G. (2016). BDNF pro-peptide regulates dendritic spines via caspase-3. *Cell Death & Disease* **7**(6):e2264.

Guzowski, J. F., McNaughton, B. L., Barnes, C. A. and Worley, P. F. (1999). Environment-specific expression of the immediate-early gene Arc in hippocampal neuronal ensembles. *Nature Neuroscience* **2**(12):1120-1124.

Habib, N., Li, Y., Heidenreich, M., Swiech, L., Avraham-Davidi, I., Trombetta, J. J., Hession, C., Zhang, F. and Regev, A. (2016). Div-Seq: Single-nucleus RNA-Seq reveals dynamics of rare adult newborn neurons. *Science* **353**(6302):925–928.

Hall, J., Thomas, K. L., and Everitt, B. J. (2000). Rapid and selective induction of BDNF expression in the hippocampus during contextual learning. *Nature Neuroscience* **3**(6):533-535.

Hall, J., Thomas, K. L. and Everitt, B.J. (2001). Cellular imaging of Zif268 expression in the hippocampus and amygdala during contextual and cued fear memory retrieval: selective activation of hippocampal CA1 neurons during the recall of contextual memories. *The Journal of Neuroscience* **21**(6):2186-2193.

Hamburger, V. (1934). The effects of wing bud extirpation on the development of the central nervous system in chick embryos. *Journal of Experimental Zoology* **68**(3):449-494.

Hamburger, V. (1993). The history of the discovery of the nerve growth factor. *Journal of Neurobiology* **24**(7):893-897.

Hamburger, V., Brunso-Bechtold, J. K. and Yip, J. W. (1981). Neuronal death in the spinal ganglia of the chick embryo and its reduction by nerve growth factor. *The Journal of Neuroscience* **1**(1):60-71.

Hamburger, V. and Levi-Montalcini, R. (1949). Proliferation, differentiation and degeneration in the spinal ganglia of the chick embryo under normal and experimental conditions. *Journal of Experimental Zoology* **111**(3):457-501.

Han, J. C., Liu, Q. R., Jones, M., Levinn, R. L., Menzie, C. M., Jefferson-George, K. S., Adler-Wailes, D. C., Sanford, E. L., Lacbawan, F. L., Uhl, G. R., Rennert, O. M. and Yanovski, J. A. (2008). Brain-derived neurotrophic factor and obesity in the WAGR syndrome. *New England Journal of Medicine* **359**(9):918-927.

Hariri, A. R., Goldberg, T. E., Mattay, V. S., Kolachana, B. S., Callicott, J. H., Egan, M. F. and Weinberger, D. R. (2003). Brain-derived neurotrophic factor Val66Met polymorphism affects human memory-related hippocampal activity and predicts memory performance. *The Journal of Neuroscience* **23**(17):6690-6694.

Harris, K. M. and Weinberg, R. J. (2012). Ultrastructure of synapses in the mammalian brain. *Cold Spring Harbor Perspectives in Biology* **4**(5):a005587.

Hartmann, M., Heumann, R. and Lessmann, V. (2001). Synaptic secretion of BDNF after high-frequency stimulation of glutamatergic synapses. *The EMBO Journal* **20**(21):5887-5897.

Harward, S. C., Hedrick, N. G., Hall, C. E., Parra-Bueno, P., Milner, T. A., Pan, E., Laviv, T., Hempstead, B. L., Yasuda, R. and McNamara, J. O. (2016). Autocrine BDNF-TrkB signalling within a single dendritic spine. *Nature* **538**(7623):99-103.

Heldt, S. A., Stanek, L., Chhatwal, J. P. and Ressler, K. J. (2007). Hippocampus-specific deletion of BDNF in adult mice impairs spatial memory and extinction of aversive memories. *Molecular Psychiatry* **12**(7):656-670

Henderson, C. E., Camu, W., Mettling, C., Gouin, A., Poulsen, K., Karihaloo, M., Ruilamas, J., Evans, T., McMahon, S. B., Armanini, M. P., Berkmeier, L., Phillips, H. S., and Rosenthal, A. (1993). Neurotrophins promote motor neuron survival and are present in embryonic limb bud. *Nature* **363**(6426):266-270.

Herzog, K. H., Bailey, K. and Barde, Y.A. (1994). Expression of the BDNF gene in the developing visual system of the chick. *Development* **120**(6):1643-1649.

Hofer, M., Pagluisi, S. R., Hohn, A., Leibrock, J. and Barde, Y. A. (1990). Regional distribution of brain-derived neurotrophic factor mRNA in the adult mouse brain. *The EMBO Journal* **9**(8):2459-2464.

Hofer, M. M. and Barde, Y. A. (1988). Brain-derived neurotrophic factor prevents neuronal death in vivo. *Nature* **331**(6153):261-262.

Hollyday, M. and Hamburger, V. (1976). Reduction of the naturally occurring motor neuron loss by enlargement of the periphery. *Journal of Comparative Neurology* **170**(3):311-320.

Hue, B., Pelhate, M., Callec, J. J. and Chanelet, J. (1976). Synaptic transmission in the sixth ganglion of the cockroach: action of 4-aminopyridine. *Journal of Experimental Biology* **65**(3):517-527.

Hughes, P., Lawlor, P. and Dragunow, M. (1992). Basal expression of Fos, Fos-related, Jun, and Krox 24 proteins in rat hippocampus. *Molecular Brain Research* **13**(4):355-357.

Isackson, P. J., Huntsman, M. M., Murray, K. D. and Gall, C. M. (1991). BDNF mRNA expression is increased in adult rat forebrain after limbic seizures: Temporal patterns of induction distinct from NGF. *Neuron* **6**(6):937-948.

Jia, Y., Gall, C. M. and Lynch, G. (2010). Presynaptic BDNF promotes postsynaptic long-term potentiation in the dorsal striatum. *The Journal of Neuroscience* **30**(43):14440-14445.

Jones, K. R., Fariñas, I., Backus, C. and Reichardt, L. F. (1994). Targeted disruption of the BDNF gene perturbs brain and sensory neuron development but not motor neuron development. *Cell* **76**(6):989-999.

Jovanovic, J. N., Czernik, A. J., Fienberg, A. A., Greengard, P. and Sihra, T. S. (2000). Synapsins as mediators of BDNF-enhanced neurotransmitter release. *Nature Neuroscience* **3**(4):323-329.

Kang, H. and Schuman, E. M. (1995). Long-lasting neurotrophin-induced enhancement of synaptic transmission in the adult hippocampus. *Science* **267**(5204):1658-1662.

Kernie, S. G., Liebl, D. J. and Parada, L. F. (2000). BDNF regulates eating behaviour and locomotor activity in mice. *The EMBO Journal* **19**(6):1290-1300.

Kestin, A. S., Ellis, P. A., Barnard, M. R., Errichetti, A., Rossner, B. A. and Michelson, A. D. (1993). Effect of strenuous exercise on platelet activation state and reactivity. *Circulation* **88**:1502-1511.

- Kirsch, G. E. and Drewe, J. A. (1993). Gating-dependent mechanism of 4-aminopyridine block in two related potassium channels. *Journal of General Physiology* **102**(5):797-816.
- Kohara, K., Kitamura, A., Morishima, M. and Tsumoto, T. (2001). Activity-dependent transfer of brain-derived neurotrophic factor to postsynaptic neurons. *Science* **291**(5512):2419-2423.
- Kojima, M., Takei, N., Numakawa, T., Ishikawa, Y., Suzuki, S., Matsumoto, T., Katoh-Semba, R., Nawa, H., and Hatanaka, H. (2001). Biological characterisation and optical imaging of brain-derived neurotrophic factor-green fluorescent protein suggest an activity dependent local release of brain-derived neurotrophic factor in neurites of cultured hippocampal neurons. *Journal of Neuroscience Research* **64**(1):1-10.
- Kolbeck, R., Bartke, I., Eberle, W. and Barde, Y. A. (1999). Brain-derived neurotrophic factor levels in the nervous system of wild-type and neurotrophin gene mutant mice. *Journal of Neurochemistry* **72**(5):1930-1938.
- Kolbeck, R., Jungbluth, S. and Barde, Y. A. (1994). Characterisation of neurotrophin dimers and monomers. *European Journal of Biochemistry* **225**(3):995-1003.
- Koponen, E., Vöikar, V., Riekkö, R., Saarelainen, T., Rauramaa, T., Rauvala, H., Taira, T. and Castrén, E. (2004). Transgenic mice overexpressing the full-length neurotrophin receptor trkB exhibit increased activation of the trkB-PLC γ pathway, reduced anxiety, and facilitated learning. *Molecular and Cellular Neuroscience* **26**(1):166–181.
- Koppel, I., Aid-Pavlidis, T., Jaanson, K., Sepp, M., Pruunsild, P., Palm, K. and Timmusk, T. (2009). Tissue-specific and neural activity-regulated expression of human BDNF gene in BAC transgenic mice. *BMC Neuroscience* **10**:68.
- Korsching, S. and Thoenen, H. (1983). Nerve growth factor in sympathetic ganglia and corresponding target organs of the rat: correlation with density of sympathetic innervation. *Proceedings of the National Academy of Sciences of the United States of America* **80**(11):3513-3516.
- Korte, M., Carroll, P., Wolf, E., Brem, G., Thoenen, H. and Bonhoeffer, T. (1995). Hippocampal long-term potentiation is impaired in mice lacking brain-derived neurotrophic factor. *Proceedings of the National Academy of Sciences* **92**(19):8856-8860.
- Korte, M., Griesbeck, O., Gravel, C., Carroll, P., Staiger, V., Thoenen, H. and Bonhoeffer, T. (1996). Virus-mediated gene transfer into hippocampal CA1 region restores long-term potentiation in brain-derived neurotrophic factor mutant mice. *Proceedings of the National Academy of Sciences of the United States of America* **93**(22):12547-12552.

- Korte, M., Kang, H., Bonhoeffer, T. and Schuman, E. (1998). A role for BDNF in the late-phase of hippocampal long-term potentiation. *Neuropharmacology* **37**(4-5):553-559.
- Kossel, A. H., Cambridge, S. B., Wagner, U. and Bonhoeffer, T. (2001). A caged Ab reveals an immediate/instructive effect of BDNF during hippocampal synaptic potentiation. *Proceedings of the National Academy of Sciences* **98**(25):14702-14707.
- Kovács, K.J. (1998). Invited review c-Fos as a transcription factor: a stressful (re)view from a functional map. *Neurochemistry International* **33**(4):287-297.
- Kulik, Y. D., Watson, D. J., Cao, G., Kuwajima, M. and Harris, K. M. (2019). Structural plasticity of dendritic secretory compartments during LTP-induced synaptogenesis. *eLife* **8**:e46356.
- Kästle, M., Kistler, B., Lamla, T., Bretschneider, T., Lamb, D., Nicklin, P. and Wyatt, D. (2018). FKBP51 modulates steroid sensitivity and NFκB signalling: A novel anti-inflammatory drug target. *European Journal of Immunology* **48**(11):1904-1914.
- Lamballe, F., Klein, R. and Barbacid, M. (1991). TrkC, a new member of the trk family of tyrosine protein kinases, is a receptor for neurotrophin-3. *Cell* **66**(5):967-979.
- Laske, C., Stellos, K., Hoffmann, N., Stransky, E., Straten, G., Eschweiler, G. W. and Leyhe, T. (2011). Higher BDNF serum levels predict slower cognitive decline in Alzheimer's disease patients. *The International Journal of Neuropsychopharmacology* **14**(3):399-404.
- Lau, A. G., Irier, H. A., Gu, J., Tian, D., Ku, L., Liu, G., Xia, M., Fritsch, B., Zheng, J. Q., Dingledine, R., Xu, B., Lu, B. and Feng, Y. (2010). Distinct 3'UTRs differentially regulate activity-dependent translation of brain-derived neurotrophic factor (BDNF). *Proceedings of the National Academy of Sciences of the United States of America* **107**(36):15945-15950.
- Lauf, U., Lopez, P. and Falk, M. M. (2001). Expression of fluorescently tagged connexins: a novel approach to rescue function of oligomeric DsRed-tagged proteins. *FEBS Letters* **498**(1):11-15.
- Lee, R., Kermani, P., Teng, K. K. and Hempstead, B. L. (2001). Regulation of cell survival by secreted proneurotrophins. *Science* **294**(5548):1945-1948.
- Leibrock, J., Lottspeich, F., Hohn, A., Hofer, M., Hengerer, B., Masiakowski, P., Thoenen, H. and Barde, Y. A. (1989). Molecular cloning and expression of brain-derived neurotrophic factor. *Nature* **341**(6238):149-152.

Leschik, J., Eckenstaler, R., Endres, T., Munsch, T., Edelmann, E., Richter, K., Kobler, O., Fischer, K. D., Zuschratter, W., Brigadski, T., Lutz, B. and Lessmann, V. (2019). Prominent postsynaptic and dendritic exocytosis of endogenous BDNF vesicles in BDNF-GFP knock-in mice. *Molecular Neurobiology* **56**(10):6833-6855.

Levi-Montalcini, R. and Hamburger, V. (1951). Selective growth stimulating effects of mouse sarcoma on the sensory and sympathetic nervous system of the chick embryo. *Journal of Experimental Zoology* **116**(2):321-361.

Li, Y., Wang, D., Li, Y., Chu, H., Zhang, L., Hou, M., Jiang, X., Chen, Z., Su, B., and Sun, T. (2017). Pre-synaptic TrkB in basolateral amygdala neurons mediates BDNF signaling transmission in memory extinction. *Cell Death & Disease* **8**(7):e2959.

Lin, B., Kramár, E. A., Bi, X., Brucher, F. A., Gall, C. M. and Lynch, G. (2005). Theta stimulation polymerizes actin in dendritic spines of hippocampus. *The Journal of Neuroscience* **25**(8):2062-2069.

Lin, P. Y., Kavalali, E. T. and Monteggia, L. M. (2018). Genetic dissection of presynaptic and postsynaptic BDNF-Trkb signaling in synaptic efficacy of CA3-CA1 synapses. *Cell Reports* **24**(6):1550-1561.

Lin, Y. C., Boone, M., Meuris, L., Lemmens, I., Van Roy, N., Soete, A., Reumers, J., Moisse, M., Plaisance, S., Drmanac, R., Chen, J., Speleman, F., Lambrechts, D., Van de Peer, Y., Tavernier, J. and Callewaert, N. (2014). Genome dynamics of the human embryonic kidney 293 lineage in response to cell biology manipulations. *Nature Communications* **5**:4767.

Lohof, A. M., Ip, N. Y. and Poo, M. M. (1993). Potentiation of developing neuromuscular synapses by the neurotrophins NT-3 and BDNF. *Nature* **363**(6427):350-353.

Lou, H., Kim, S. K., Zaitsev, E., Snell, C. R., Lu, B. and Loh, Y. P. (2005). Sorting and activity-dependent secretion of BDNF require interaction of a specific motif with the sorting receptor carboxypeptidase E. *Neuron* **45**(2):245-255.

Lowry, K. S., Murray, S., Mclean, C. A., Talman, P., Mathers, S., Lopes, E. C. and Cheema, S. S. (2001). A potential role for the p75 low-affinity neurotrophin receptor in spinal motor neuron degeneration in murine and human amyotrophic lateral sclerosis. *Amyotrophic Lateral Sclerosis and Other Motor Neuron Disorders* **2**(3):127-134.

Ludwig, M. and Stern, J. (2015). Multiple signalling modalities mediated by dendritic exocytosis of oxytocin and vasopressin. *Philosophical Transactions of the Royal Society of London B: Biological Sciences* **370**(1672):20140182.

Lyford, G. L., Yamagata, K., Kaufmann, W. E., Barnes, C. A., Sanders, L. K., Copeland, N. G., Gilbert, D. J., Jenkins, N. A., Lanahan, A. A. and Worley, P. F. (1995). *Arc*, a growth factor and activity-regulated gene, encodes a novel cytoskeleton-associated protein that is enriched in neuronal dendrites. *Neuron* **14**(2):433-445.

Lyons, W. E., Mamounas, L. A., Ricaurte, G. A., Coppola, V., Reid, S. W., Bora, S. H., Wihler, C., Koliatsos, V. E. and Tessarollo, L. (1999). Brain-derived neurotrophic factor-deficient mice develop aggressiveness and hyperphagia in conjunction with brain serotonergic abnormalities. *Proceedings of the National Academy of Sciences of the United States of America* **96**(26):15239-15244.

MacQueen, G. M., Yucel, K., Taylor, V. H., Macdonald, K. and Joffe, R. (2008). Posterior hippocampal volumes are associated with remission rates in patients with major depressive disorder. *Biological Psychiatry* **64**(10):880-883.

Matsuda, N., Lu, H., Fukata, Y., Noritake, J., Gao, H., Mukherjee, S., Nemoto, T., Fukata, M. and Poo, M. M. (2009). Differential activity-dependent secretion of brain-derived neurotrophic factor from axon and dendrite. *Journal of Neuroscience* **29**(45):14185-14198.

Matsumoto, T., Rauskolb, S., Polack, M., Klose, J., Kolbeck, R., Korte, M. and Barde, Y. A. (2008). Biosynthesis and processing of endogenous BDNF: CNS neurons store and secrete BDNF, not pro-BDNF. *Nature Neuroscience* **11**(2):131-133.

McQuin, C., Goodman, A., Chernyshev, V., Kametsky, L., Cimini, B. A., Karhohs, K. W., Doan, M., Ding, L., Rafelski, S. M., Thirstup, D., Wiegand, W., Singh, S., Becker, T., Caicedo, J. C. and Carpenter, A. E. (2018). CellProfiler 3.0: Next-generation image processing for biology. *PLOS Biology* **16**:e2005970.

Meakin, S. O. and Shooter, E. M. (1991). Tyrosine kinase activity coupled to the high-affinity nerve growth factor-receptor complex. *Proceedings of the National Academy of Sciences of the United States of America* **88**(13):5862-5866.

Merighi, A., Bardoni, R., Salio, C., Lossi, L., Ferrini, F., Prandini, M., Zonta, M., Gustincich, S. and Carmignoto, G. (2008). Presynaptic functional TrkB receptors mediate the release of excitatory neurotransmitters from primary afferent terminals in lamina II (substantia gelatinosa) of postnatal rat spinal cord. *Developmental Neurobiology* **68**(4):457-475.

Michalski, B. and Fahnstock, M. (2003). Pro-brain-derived neurotrophic factor is decreased in parietal cortex in Alzheimer's disease. *Molecular Brain Research* **111**(1-2):148-154.

Milbrandt, J. (1987). A nerve growth factor-induced gene encodes a possible transcriptional regulatory factor. *Science* **238**(4828):797-799.

Minichiello, L., Calella, A. M., Medina, D. L., Bonhoeffer, T., Klein, R. and Korte, M. (2002). Mechanism of TrkB-mediated hippocampal long-term potentiation. *Neuron* **36**(1):121-137.

Minichiello, L., Korte, M., Wolfner, D., Kühn, R., Unsicker, K., Cestari, V., Rossi-Arnaud, C., Lipp, H. P., Bonhoeffer, T. and Klein, R. (1999). Essential role for TrkB receptors in hippocampus-mediated learning. *Neuron* **24**(2):401-414.

Mizuguchi, K., Parker, J. S., Blundell, T. L. and Gay, N. J. (1998). Getting knotted: a model for the structure and activation of Spätzle. *Trends in Biochemical Sciences* **23**(7):239-242.

Mizui, T., Ishikawa, Y., Kumanogoh, H., Lume, M., Matsumoto, T., Hara, T., Yamawaki, S., Takahashi, M., Shiosaka, S., Itami, C., Uegaki, K., Saarma, M. and Kojima, M. (2015). BDNF pro-peptide actions facilitate hippocampal LTD and are altered by the common BDNF polymorphism Val66Met. *Proceedings of the National Academy of Sciences of the United States of America* **112**(23):E3067-E3074.

Mizuno, M., Yamada, K., He, J., Nakajima, A. and Nabeshima, T. (2003). Involvement of BDNF receptor TrkB in spatial memory formation. *Learning & Memory* **10**(2):108-115.

Mizuno, M., Yamada, K., Olariu, A., Nawa, H. and Nabeshima, T. (2000). Involvement of brain-derived neurotrophic factor in spatial memory formation and maintenance in a radial arm maze test in rats. *The Journal of Neuroscience* **20**(18):7116-7121.

Monteggia, L. M., Barrot, M., Powell, C. M., Berton, O., Galanis, V., Gemelli, T., Meuth, S., Nagy, A., Greene, R. W. and Nestler, E. J. (2004). Essential role of brain-derived neurotrophic factor in adult hippocampal function. *Proceedings of the National Academy of Sciences of the United States of America* **101**(29):10827-10832.

Moser, E., Moser, M. B. and Andersen, P. (1993). Spatial learning impairment parallels the magnitude of dorsal hippocampal lesions, but is hardly present following ventral lesions. *The Journal of Neuroscience* **13**(9):3916-3925.

Moser, M. B. and Moser, E. I. (1998). Functional differentiation in the hippocampus. *Hippocampus* **8**(6):608-619.

Moser, M. B., Moser, E. I., Forrest, E., Andersen, P. and Morris, R. G. (1995). Spatial learning with a minislab in the dorsal hippocampus. *Proceedings of the National Academy of Sciences of the United States of America* **92**(21):9697-9701.

Mowla, S. J., Farhadi, H. F., Pareek, S., Atwal, J. K., Morris, S. J., Seidah, N. G. and Murphy, R. A. (2001). Biosynthesis and post-translational processing of the precursor to brain-derived neurotrophic factor. *The Journal of Biological Chemistry* **276**(16):12660-12666.

Mowla, S. J., Pareek, S., Farhadi, H. F., Petrecca, K., Fawcett, J. P., Seidah, N. G., Morris, S. J., Sossin, W. S. and Murphy, R. A. (1999). Differential sorting of nerve growth factor and brain-derived neurotrophic factor in hippocampal neurons. *The Journal of Neuroscience* **19**(6):2069-2080.

Mufson, E. J. and Kordower, J. H. (1992). Cortical neurons express nerve growth factor receptors in advanced age and Alzheimer disease. *Proceedings of the National Academy of Sciences of the United States of America* **89**(2):569-573.

Naegelin, Y., Dingsdale, H., Säuberli, K., Schädelin, S., Kappos, L. and Barde, Y. A. (2018). Measuring and validating the levels of brain-derived neurotrophic factor in human serum. *eNeuro* **5**(2):ENEURO.0419-0417.

Nagappan, G., Zaitsev, E., Senatorov, V. V., Yang, J., Hempstead, B. L. and Lu, B. (2009). Control of extracellular cleavage of proBDNF by high frequency neuronal activity. *Proceedings of the National Academy of Sciences of the United States of America* **106**(4):1267-1272.

Nakajo, Y., Miyamoto, S., Nakano, Y., Xue, J. H., Hori, T. and Yanamoto, H. (2008). Genetic increase in brain-derived neurotrophic factor levels enhances learning and memory. *Brain Research* **1241**:103-109.

Nawa, H., Carnahan, J. and Gall, C. (1995). BDNF protein measured by a novel enzyme immunoassay in normal brain and after seizure: partial disagreement with mRNA levels. *European Journal of Neuroscience* **7**(7):1527-1535.

Nelson, A. J. D., Hindley, E. L., Pearce, J. M., Vann, S. D. and Aggleton, J. P. (2015). The effect of retrosplenial cortex lesions in rats on incidental and active spatial learning. *Frontiers in Behavioral Neuroscience* **9**:11.

Nelson, A. J. D., Kinnavane, L., Amin, E., O'Mara, S. M. and Aggleton, J. P. (2020). Deconstructing the direct reciprocal hippocampal-anterior thalamic pathways for spatial learning. *The Journal of Neuroscience* **40**(36):6978-6990.

Neves-Pereira, M., Mundo, E., Muglia, P., King, N., Macciardi, F. and Kennedy, J. L. (2002). The brain-derived neurotrophic factor gene confers susceptibility to bipolar disorder: evidence from a family-based association study. *The American Journal of Human Genetics* **71**(3):651-655.

Nibuya, M., Morinobu, S. and Duman, R. (1995). Regulation of BDNF and TrkB mRNA in rat brain by chronic electroconvulsive seizure and antidepressant drug treatments. *The Journal of Neuroscience* **15**(11):7539-7547.

Novkovic, T., Mittmann, T. and Manahan-Vaughan, D. (2015). BDNF contributes to the facilitation of hippocampal synaptic plasticity and learning enabled by environmental enrichment. *Hippocampus* **25**(1):1-15.

Nykjaer, A., Lee, R., Teng, K. K., Jansen, P., Madsen, P., Nielsen, M. S., Jacobsen, C., Kliemannel, M., Schwarz, E., Willnow, T. E., Hempstead, B. L. and Petersen, C. M. (2004). Sortilin is essential for proNGF-induced neuronal cell death. *Nature* **427**(6977):843-848.

Olton, D. S. and Samuelson, R. J. (1976). Remembrance of places passed: Spatial memory in rats. *Experimental Psychology: Animal Behavior Processes* **2**(2):97-116.

Oorschot, D. E. (1989). Effect of fluorodeoxyuridine on neurons and non-neuronal cells in cerebral explants. *Experimental Brain Research* **78**(1):132-138.

Orefice, L. L., Waterhouse, E. G., Partridge, J. G., Lalchandani, R. R., Vicini, S. and Xu, B. (2013). Distinct roles for somatically and dendritically synthesized brain-derived neurotrophic factor in morphogenesis of dendritic spines. *Journal of Neuroscience* **33**(28):11618-11632.

Pang, P. T., Teng, H. K., Zaitsev, E., Woo, N. T., Sakata, K., Zhen, S., Teng, K. K., Yung, W.H., Hempstead, B.L. and Lu, B. (2004). Cleavage of proBDNF by tPA/plasmin is essential for long-term hippocampal plasticity. *Science* **306**(5695):487-491.

Pankhurst, C. N., Yang, G., Ninan, I., Savas, J. N., Yates III, J. R., Lafaille, J. J., Hempstead, B. L., Littman, D. R. and Gan, W. B. (2013). Microglia promote learning-dependent synapse formation through brain-derived neurotrophic factor. *Cell* **155**(7):1596-1609.

Papa, M., Bundman, M., Greenberger, V. and Segal, M. (1995). Morphological analysis of dendritic spine development in primary cultures of hippocampal neurons. *The Journal of Neuroscience* **15**(1):1-11.

Pardridge, W. M., Kang, Y. S. and Buciak, J. L. (1994). Transport of human recombinant brain-derived neurotrophic factor (BDNF) through the rat blood brain barrier *in vivo* using vector-mediated peptide drug delivery. *Pharmaceutical Research* **11**(5):738-746.

Parker, J. S., Mizuguchi, K. and Gay, N. J. (2001). A family of proteins related to Spätzle, the Toll receptor ligand, are encoded in the Drosophila genome. *Proteins: Structure, Function, and Bioinformatics* **45**(1):71-80.

Patterson, S. L., Abel, T., Deuel, T. A., Martin, K. C., Rose, J. C. and Kandel, E. R. (1996). Recombinant BDNF rescues deficits in basal synaptic transmission and hippocampal LTP in BDNF knockout mice. *Neuron* **16**(6):1137-1145.

Patterson, S. L., Grover, L. M., Schwartzkroin, P. A. and Bothwell, M. (1992). Neurotrophin expression in rat hippocampal slices: a stimulus paradigm inducing LTP in CA1 evokes increases in BDNF and NT-3 mRNAs. *Neuron* **9**(6):1081-1088.

Peng, T., Thorn, K., Schroeder, T., Wang, L., Theis, F. J., Marr, C. and Navab, N. (2017). A BaSiC tool for background and shading correction of optical microscopy images. *Nature Communications* **8**:14836.

Petryshen, T. L., Sabeti, P. C., Aldinger, K. A., Fry, B., Fan, J. B., Schaffner, S. F., Waggoner, S. G., Tahl, A. R. and Sklar, P. (2010). Population genetic study of the brain-derived neurotrophic factor (BDNF) gene. *Molecular Psychiatry* **15**(8):810-815.

Pfrieger, F. W. and Barres, B. A. (1997). Synaptic efficacy enhanced by glial cells *in vitro*. *Science* **277**(5332):1684-1687.

Polyakova, M., Stuke, K., Schuemberg, K., Mueller, K., Schoenknecht, P. and Schroeter, M. L. (2015). BDNF as a biomarker for successful treatment of mood disorders: A systematic & quantitative meta-analysis. *Journal of Affective Disorders* **174**:432-440.

Pothuizen, H. H. J., Davies, M., Albasser, M. M., Aggleton, J. P. and Vann, S. D. (2009). Granular and dysgranular retrosplenial cortices provide qualitatively different contributions to spatial working memory: evidence from immediate-early gene imaging in rats. *European Journal of Neuroscience* **30**(5):877-888.

Prasher, D. C., Eckenrode, V. K., Ward, W. W., Prendergast, F. G. and Cormier, M. J. (1992). Primary structure of the *Aequorea victoria* green fluorescent protein. *Gene* **111**(2):229-233.

Pruunsild, P., Kazantseva, A., Aid, T., Palm, K. and Timmusk, T. (2007). Dissecting the human BDNF locus: Bidirectional transcription, complex splicing, and multiple promoters. *Genomics* **90**(3):397-406.

Rabizadeh, S., Oh, J., Zhong, L. T., Yang, J., Bitler, C. M., Butcher, L. L. and Bredesen, D. E. (1993). Induction of apoptosis by the low-affinity NGF receptor. *Science* **261**(5119):345-348.

Radeke, M. J., Misko, T. P., Hsu, C., Herzenberg, L. A. and Shooter, E. M. (1987). Gene transfer and molecular cloning of the rat nerve growth factor receptor. *Nature* **325**(6105):593-597.

Rattenholl, A., Ruoppolo, M., Flagiello, A., Monti, M., Vinci, F., Marino, G., Lillie, H., Schwarz, and Rudolph, R. (2001). Pro-sequence assisted folding and disulfide bond formation of nerve growth factor. *Journal of Molecular Biology* **305**(3):523-533.

Rauskolb, S., Zagrebelsky, M., Dreznjak, A., Deogracias, R., Matsumoto, T., Wiese, S., Erne, B., Sendtner, M., Schaeran-Wiemers, N., Korte, M. and Barde, Y. A. (2010). Global deprivation of brain-derived neurotrophic factor in the CNS reveals an area-specific requirement for dendritic growth. *The Journal of Neuroscience* **30**(5):1739-1749.

Ray, M., Tang, R., Jiang, Z. and Rotello, V. M. (2015). Quantitative tracking of protein trafficking to the nucleus using cytosolic protein delivery by nanoparticle-stabilized nanocapsules. *Bioconjugate Chemistry* **26**(6):1004-1007.

Rios, M., Fan, G., Fekete, C., Kelly, J., Bates, B., Kuehn, R., Lechan, R. M. and Jaenisch, R. (2001). Conditional deletion of brain-derived neurotrophic factor in the postnatal brain leads to obesity and hyperactivity. *Molecular Endocrinology* **15**(10):1748-1757.

Rodríguez-Tébar, A., Dechant, G. and Barde, Y. A. (1990). Binding of brain-derived neurotrophic factor to the nerve growth factor receptor. *Neuron* **4**(4):487-492.

Rodríguez-Tébar, A., Dechant, G. and Barde, Y. A. (1991). Neurotrophins: structural relatedness and receptor interactions. *Philosophical Transactions of the Royal Society of London. Series B: Biological Sciences* **331**(1261):255-258.

Roux, P. P., Colicos, M. A., Barker, P. A. and Kennedy, T. E. (1999). p75 neurotrophin receptor expression is induced in apoptotic neurons after seizure. *The Journal of Neuroscience* **19**(16):6887-6896.

Rudge, J. S., Mather, P. E., Pasnikowski, E. M., Cai, N., Corcoran, T., Acheson, A., Anderson, K., Lindsay, R. M. and Wiegand, S. J. (1998). Endogenous BDNF protein is increased in adult rat hippocampus after a kainic acid induced excitotoxic insult but exogenous BDNF is not neuroprotective. *Experimental Neurology* **149**(2):398-410.

Saarelainen, T., Hendolin, P., Lucas, G., Koponen, E., Sairanen, M., Macdonald, E., Agerman, K., Haapasalo, A., Nawa, H., Aloyz, R., Ernfors, P. and Castrén, E. (2003). Activation of the TrkB neurotrophin receptor is induced by antidepressant drugs and is required for antidepressant-induced behavioral effects. *The Journal of Neuroscience* **23**(1):349-357.

- Sahu, M. P., Nikkilä, O., Lågas, S., Kolehmainen, S. and Castrén, E. (2019). Culturing primary neurons from rat hippocampus and cortex. *Neuronal Signaling* **3**(2):NS20180207.
- Santín, L. J., Aguirre, J. A., Rubio, S., Begega, A., Miranda, R. and Arias, J. L. (2003). c-Fos expression in supramammillary and medial mammillary nuclei following spatial reference and working memory tasks. *Physiology & Behavior* **78**(4-5):733-739.
- Sanyal, S., Sandstrom, D. J., Hoeffler, C. A. and Ramaswami, M. (2002). AP-1 functions upstream of CREB to control synaptic plasticity in *Drosophila*. *Nature* **416**(6883):870-874.
- Sariban, E., Luebbbers, R. and Kufe, D. (1988). Transcriptional and post-transcriptional control of c-fos gene expression in human monocytes. *Molecular and Cellular Biology* **8**(1):340-346.
- Scharfman, H. E., Sollas, A. L., Smith, K. L., Jackson, M. B. and Goodman, J. H. (2002). Structural and functional asymmetry in the normal and epileptic rat dentate gyrus. *The Journal of Comparative Neurology* **454**(4):424-439.
- Schindelin, J., Arganda-Carreras, I., Frise, E., Kaynig, V., Longair, M., Pietzsch, T., Preibisch, S., Rueden, C., Saalfeld, S., Schmid, B., Tinevez, J. Y., White, D. J., Hartenstein, V., Eliceiri, K., Tomancak, P. and Cardona, A. (2012). Fiji: an open-source platform for biological-image analysis. *Nature Methods* **9**(7):676-682.
- Seidah, N. G., Benjannet, S., Pareek, S., Chrétien, M. and Murphy, R. A. (1996). Cellular processing of the neurotrophin precursors of NT3 and BDNF by the mammalian proprotein convertases. *FEBS Letters* **379**(3):247-250.
- Sendtner, M., Holtmann, B., Kolbeck, R., Thoenen, H. and Barde, Y. A. (1992). Brain-derived neurotrophic factor prevents the death of motoneurons in newborn rats after nerve section. *Nature* **360**(6406):757-759.
- Shaner, N. C., Campbell, R. E., Steinbach, P. A., Giepmans, B. N. G., Palmer, A. E. and Tsien, R. Y. (2004). Improved monomeric red, orange and yellow fluorescent proteins derived from *Discosoma sp.* red fluorescent protein. *Nature Biotechnology* **22**(12):1567-1572.
- Shaw, G., Morse, S., Ararat, M. and Graham, F. L. (2002). Preferential transformation of human neuronal cells by human adenoviruses and the origin of HEK293 cells. *The Federation of the American Societies for Experimental Biology (FASEB) Journal* **16**(8):869-871.

Shieh, P. B., Hu, S. C., Bobb, K., Timmusk, T. and Ghosh, A. (1998). Identification of a signaling pathway involved in calcium regulation of BDNF expression. *Neuron* **20**(4):727-740.

Shirayama, Y., Chen, A. C. H., Nakagawa, S., Russell, D. S. and Duman, R. S. (2002). Brain-derived neurotrophic factor produces antidepressant effects in behavioral models of depression. *The Journal of Neuroscience* **22**(8):3251-3261.

Shorey, M. L. (1909). The effect of the destruction of peripheral areas on the differentiation of the neuroblasts. *Journal of Experimental Zoology* **7**(1):25-63.

Silhol, M., Arancibia, S., Maurice, T. and Tapia-Arancibia, L. (2007). Spatial memory training modifies the expression of brain-derived neurotrophic factor tyrosine kinase receptors in young and aged rats. *Neuroscience* **146**(3):962-973.

Singer, W., Manthey, M., Panford-Walsh, R., Matt, L., Geisler, H. S., Passeri, E., Baj, G., Tongiorgi, E., Leal, G., Duarte, C. B., Salazar, I. L., Eckert, P., Rohbock, K., Hu, J., Strotmann, J., Ruth, P., Zimmermann, U., Rüttinger, L., Ott, T., Schimmang, T. and Knipper, M. (2018). BDNF-Live-Exon-Visualization (BLEV) allows differential detection of BDNF transcripts in vitro and in vivo. *Frontiers in Molecular Neuroscience* **11**:325.

Siuciak, J. A., Lewis, D. R., Wiegand, S. J. and Lindsay, R. M. (1997). Antidepressant-like effect of brain-derived neurotrophic factor (BDNF). *Pharmacology, Biochemistry, and Behavior* **56**(1):131-137.

Sklar, P., Gabriel, S. B., McInnis, M. G., Bennett, P., Lim, Y. M., Tsan, G., Schaffner, S., Kirov, G., Jones, I., Owen, M., Craddock, N., DePaulo, J. R. and Lander, E. S. (2002). Family-based association study of 76 candidate genes in bipolar disorder: BDNF is a potential risk locus. *Molecular Psychiatry* **7**(6):579-593.

Skledar, M., Nikolac, M., Dodig-Curkovic, K., Curkovic, M., Borovecki, F. and Pivac, N. (2012). Association between brain-derived neurotrophic factor Val66Met and obesity in children and adolescents. *Progress in Neuropsychopharmacology and Biological Psychiatry* **36**(1):136-140.

Sonoyama, T., Stadler, L. K. J., Zhu, M., Keogh, J. M., Henning, E., Hisama, F., Kirwan, P., Jura, M., Blaszczyk, B. K., DeWitt, D. C., Brouwers, B., Hyvönen, M., Barroso, I., Merkle, F. T., Appleyard, S. M., Wayman, G. A. and Farooqi, I. S. (2020). Human BDNF/TrkB variants impair hippocampal synaptogenesis and associate with neurobehavioural abnormalities. *Scientific Reports* **10**(1):9028.

Squinto, S. P., Stitt, T. N., Aldrich, T. H., Davis, S., Blanco, S. M., Radziejewski, C., Glass, D. J., Masiakowski, P., Furth, M. E. and Valenzuela, D. M., Distefano, P. S. and Yancopoulos, G. D. (1991). TrkB encodes a functional receptor for brain-derived neurotrophic factor and neurotrophin-3 but not nerve growth factor. *Cell* **65**(5):885-893.

Staiger, J. F., Masanneck, C., Bisler, S., Schleicher, A., Zuschratter, W. and Zilles, K. (2002). Excitatory and inhibitory neurons express c-Fos in barrel-related columns after exploration of a novel environment. *Neuroscience* **109**(4):687-699.

Strange, B. A., Witter, M. P., Lein, E. S. and Moser, E. I. (2014). Functional organization of the hippocampal longitudinal axis. *Nature Reviews Neuroscience* **15**(10):655-669.

Suter, U., Heymach Jr., J. V. and Shooter, E. M. (1991). Two conserved domains in the NGF propeptide are necessary and sufficient for the biosynthesis of correctly processed and biologically active NGF. *The EMBO Journal* **10**(9):2395-2400.

Tabuchi, A., Sakaya, H., Kisukeda, T., Fushiki, H. and Tsuda, M. (2002). Involvement of an upstream stimulatory factor as well as cAMP-responsive element-binding protein in the activation of brain-derived neurotrophic factor gene promoter I. *The Journal of Biological Chemistry* **277**(39):35920-35931.

Tang, S. J., Reis, G., Kang, H., Gingras, A. C., Sonenberg, N. and Schuman, E. M. (2002). A rapamycin-sensitive signaling pathway contributes to long-term synaptic plasticity in the hippocampus. *Proceedings of the National Academy of Sciences of the United States of America* **99**(1):467-472.

Tao, X., Finkbeiner, S., Arnold, D. B., Shaywitz, A. J. and Greenberg, M. E. (1998). Ca²⁺ influx regulates BDNF transcription by a CREB family transcription factor-dependent mechanism. *Neuron* **20**(4):709-726.

Tao, X., West, A. E., Chen, W. G., Corfas, G. and Greenberg, M. E. (2002). A calcium-responsive transcription factor, CaRF, that regulates neuronal activity-dependent expression of BDNF. *Neuron* **33**(3):383-395.

Teng, H. K., Teng, K. K., Lee, R., Wright, S., Tevar, S., Almedia, R. D., Kermani, P., Torkin, R., Chen, Z. Y., Lee, F. S., Kraemer, R. T., Nykjaer, A. and Hempstead, B. S. (2005). ProBDNF induces neuronal apoptosis via activation of a receptor complex of p75NTR and sortilin. *Journal of Neuroscience* **25**(22):5455-5463.

Timmusk, T., Belluardo, N., Metsis, M. and Persson, H. (1993a). Widespread and developmentally regulated expression of neurotrophin-4 mRNA in rat brain and peripheral tissues. *European Journal of Neuroscience* **5**(6):605-613.

Timmusk, T., Palm, K., Metsis, M., Reintam, T., Paalme, V., Saarma, M. and Persson, H. (1993b). Multiple promoters direct tissue-specific expression of the rat BDNF gene. *Neuron* **10**(3):475-489.

Tongiorgi, E., Armellin, M., Giulianini, P. G., Bregola, G., Zucchini, S., Paradiso, B., Steward, O., Cattaneo, A. and Simonato, M. (2004). Brain-derived neurotrophic factor mRNA and protein are targeted to discrete dendritic laminas by events that trigger epileptogenesis. *Journal of Neuroscience* **24**(30):6842-6852.

Toni, N., Buchs, P. A., Nikonenko, I., Bron, C. R. and Muller, D. (1999). LTP promotes formation of multiple spine synapses between a single axon terminal and a dendrite. *Nature* **402**(6760):421-425.

Trommald, M., Hulleberg, G. and Andersen, P. (1996). Long-term potentiation is associated with new excitatory spine synapses on rat dentate granule cells. *Learning & Memory* **3**(2-3):218-228.

Tyler, W. J. and Pozzo-Miller, L. D. (2001). BDNF enhances quantal neurotransmitter release and increases the number of docked vesicles at the active zones of hippocampal excitatory synapses. *The Journal of Neuroscience* **21**(12):4249-4258.

Uegaki, K., Kumanogoh, H., Mizui, T., Hirokawa, T., Ishikawa, Y. and Kojima, M. (2017). BDNF binds its pro-peptide with high affinity and the common Val66Met polymorphism attenuates the interaction. *International Journal of Molecular Sciences* **18**(5):1042.

Ultsch, M. H., Wiesmann, C., Simmons, L. C., Henrich, J., Yang, M., Reilly, D., Bass, S. H. and de Vos, A. M. (1999). Crystal structures of the neurotrophin-binding domain of TrkA, TrkB and TrkC. *Journal of Molecular Biology* **290**(1):149-159.

Unger, T. J., Calderon, G. A., Bradley, L. C., Sena-Esteves, M. and Rios, M. (2007). Selective deletion of *Bdnf* in the ventromedial and dorsomedial hypothalamus of adult mice results in hyperphagic behavior and obesity. *The Journal of Neuroscience* **27**(52):14265-14274.

Urfer, R., Tsoulfas, P., O'Connell, L., Shelton, D. L., Parada, L. F. and Presta, L. G. (1995). An immunoglobulin-like domain determines the specificity of neurotrophin receptors. *The EMBO Journal* **14**(12):795-2805.

van Veen, E., Pringle, D. R. and McMahon, M. (2016). P2A-fluorophore tagging of BRAF tightly links expression to fluorescence *in vivo*. *PLoS ONE* **11**(6):e0157661.

Vandenberg, A., Lin, W. C., Tai, L. H., Ron, D. and Wilbrecht, L. (2018). Mice engineered to mimic a common Val66Met polymorphism in the BDNF gene show greater sensitivity to reversal in environmental contingencies. *Developmental Cognitive Neuroscience* **34**:34-41.

Vann, S. D. and Aggleton, J. P. (2003). Evidence of a spatial encoding deficit in rats with lesions of the mammillary bodies or mammillothalamic tract. *The Journal of Neuroscience* **23**(8):3506-3514.

Vann, S. D. and Aggleton, J. P. (2005). Selective dysgranular retrosplenial cortex lesions in rats disrupt allocentric performance of the radial-arm maze task. *Behavioral Neuroscience* **119**(6):1682-1686.

Vann, S. D., Brown, M. W. and Aggleton, J. P. (2000a). Fos expression in the rostral thalamic nuclei and associated cortical regions in response to different spatial memory tests. *Neuroscience* **101**(4):983-991.

Vann, S. D., Brown, M. W., Erichsen, J. T. and Aggleton, J. P. (2000b). Fos imaging reveals differential patterns of hippocampal and parahippocampal subfield activation in rats in response to differential spatial memory tests. *The Journal of Neuroscience* **20**(7):2711-2718.

Vaynman, S., Ying, Z. and Gomez-Pinilla, F. (2004). Hippocampal BDNF mediates the efficacy of exercise on synaptic plasticity and cognition. *European Journal of Neuroscience* **20**(10):2580-2590.

Vogel, C. and Marcotte, E. M. (2012). Insights into the regulation of protein abundance from proteomic and transcriptomic analyses. *Nature Reviews Genetics* **13**(4):227-232.

von Bartheld, C. S., Kinoshita, Y., Pevette, D., Yin, Q. W., Oppenheim, R. W. and Bothwell, M. (1994). Positive and negative effects of neurotrophins on the isthmo-optic nucleus in chick embryos. *Neuron* **12**(3):639-654.

Wan, H., Aggleton, J. P. and Brown, M. W. (1999). Different contributions of the hippocampus and perirhinal cortex to recognition memory. *The Journal of Neuroscience* **19**(3):1142-1148.

Warnault, V., Darcq, E., Morisot, N., Phamluong, K., Wilbrecht, L., Massa, S. M., Longo, F. M. and Ron, D. (2016). The BDNF Valine 68 to Methionine polymorphism increases compulsive alcohol drinking in mice which is reversed by TrkB activation. *Biological Psychiatry* **79**(6):463-473.

Webster, M. J., Weickert, C. S., Herman, M. M. and Kleinman, J. E. (2002). BDNF mRNA expression during postnatal development, maturation and aging of the human prefrontal cortex. *Developmental Brain Research* **139**(2):139-150.

West, A. E., Pruunsild, P., Timmusk, T., Lewin, G. R. and Carter, B. D. (2014). Neurotrophins: transcription and translation. *The Handbook of Experimental Pharmacology* **220**:67-100.

Wetmore, C., Ernfors, P., Persson, H. and Olson, L. (1990). Localization of brain-derived neurotrophic factor mRNA to neurons in the brain by in situ hybridization. *Experimental Neurology* **109**(2):141-152.

Wetsel, W. C., Rodriguiz, R. M., Guillemot, J., Rousset, E., Essalmani, R., Kim, I. H., Bryant, J. C., Marcinkiewicz, J., Desjardins, R., Day, R., Constam, D. B., Prat, A. and Seidah, N. G. (2013). Disruption of the expression of the proprotein convertase PC7 reduces BDNF production and affects learning and memory in mice. *Proceedings of the National Academy of Sciences* **110**(43):17362-17367.

Windisch, J. M., Marksteiner, R., Lang, M. E., Auer, B. and Schneider, R. (1995). Brain-derived neurotrophic factor, neurotrophin-3, and neurotrophin-4 bind to a single leucine-rich motif of TrkB. *Biochemistry* **34**(35):11256-11263.

Woo, N. H., Teng, H. K., Siao, C. J., Chiaruttini, C., Pang, P. T., Milner, T. A., Hempstead, B. L. and Lu, B. (2005). Activation of p75^{NTR} by proBDNF facilitates hippocampal long-term depression. *Nature Neuroscience* **8**(8):1069-1077.

Wosnitzka, E., Nan, X., Nan, J., Chacón-Fernández, P., Kussmaul, L., Schuler, M. and Hengerer, B. and Barde, Y. A. (2020). A new mouse line reporting the translation of brain-derived neurotrophic factor using green fluorescent protein. *eNeuro* **7**:ENEURO.0462-19.

Wu, Y. J., Krüttgen, A., Möller, J. C., Shine, D., Chan, J. R., Shooter, E. M. and Cosgaya, J. M. (2004). Nerve growth factor, brain-derived neurotrophic factor, and neurotrophin-3 are sorted to dense-core vesicles and released via the regulated pathway in primary rat cortical neurons. *Journal of Neuroscience Research* **75**(6):825-834.

Yamamoto, H. and Gurney, M. E. (1990). Human platelets contain brain derived neurotrophic factor. *The Journal of Neuroscience* **10**(11):3469-3478.

Yan, H. and Chao, M. V. (1991). Disruption of cysteine-rich repeats of the p75 nerve growth factor receptor leads to loss of ligand binding. *The Journal of Biological Chemistry* **266**(18):12099-12104.

Yan, Q., Elliott, J. and Snider, W. D. (1992). Brain-derived neurotrophic factor rescues spinal motor neurons from axotomy-induced cell death. *Nature* **360**(6406):753-755.

Yan, Q., Rosenfeld, R. D., Matheson, C. R., Hawkins, N., Lopez, O. T., Bennett, L. and Welcher, A. A. (1997). Expression of brain-derived neurotrophic factor protein in the adult rat central nervous system. *Neuroscience* **78**(2):431-448.

Yang, J., Harte-Hargrove, L. C., Siao, C.J., Marinic, T., Clarke, R., Ma, Q., Jing, D., Lafrancois, J. J., Bath, K. G., Mark, W., Ballon, D., Lee, F. S., Scharfman, H. E. and Hempstead, B. L. (2014). proBDNF negatively regulates neuronal remodeling, synaptic transmission, and synaptic plasticity in hippocampus. *Cell Reports* **7**(3):796-806.

Yang, J., Siao, C. J., Nagappan, G., Marinic, T., Jing, D., Mcgrath, K., Chen, Z. Y., Mark, W., Tessarollo, L., Lee, F.S., Lu, B. and Hempstead, B. L. (2009). Neuronal release of proBDNF. *Nature Neuroscience* **12**(2):113-115.

Yeo, G. S. H., Hung, C. C. C., Rochford, J., Keogh, J., Gray, J., Sivaramakrishnan, S., O'Rahilly, S. and Farooqi, I. S. (2004). A *de novo* mutation affecting human TrkB associated with severe obesity and developmental delay. *Nature Neuroscience* **7**(11):1187-1189.

Zafra, F., Castrén, E., Thoenen, H. and Lindholm, D. (1991). Interplay between glutamate and gamma-aminobutyric acid transmitter systems in the physiological regulation of brain-derived neurotrophic factor and nerve growth factor synthesis in hippocampal neurons. *Proceedings of the National Academy of Sciences of the United States of America* **88**(22):10037-10041.

Zafra, F., Hengerer, B., Leibrock, J., Thoenen, H. and Lindholm, D. (1990). Activity dependent regulation of BDNF and NGF mRNAs in the rat hippocampus is mediated by non-NMDA glutamate receptors. *The EMBO Journal* **9**(11):3545-3550.

Zakharenko, S. S., Patterson, S. L., Dragatsis, I., Zeitlin, S. O., Siegelbaum, S. A., Kandel, E. R. and Morozov, A. (2003). Presynaptic BDNF required for a presynaptic but not postsynaptic component of LTP at hippocampal CA1-CA3 synapses. *Neuron* **39**(6):975-990.

Zangenehpour, S. and Chaudhuri, A. (2002). Differential induction and decay curves of c-fos and zif268 revealed through dual activity maps. *Molecular Brain Research* **109**(1-2):221-225.

Zhang, G., Gurtu, V. and Kain, S. R. (1996). An enhanced green fluorescent protein allows sensitive detection of gene transfer in mammalian cells. *Biochemical and Biophysical Research Communications* **227**(3):707-711.

Appendix I: Statistical Analyses

Figure	Dataset	Shapiro-Wilk Test for Normal Distribution	Test for Equality of Variances	Type of test	Sample size	Comments
3.4C	BDNF WT cortical neurons E18, 11DIV	Control condition: $W = 0.518, p = 1.288 \times 10^{-18}$ + 1 mM 4-AP condition: $W = 0.950, p = 1.49 \times 10^{-4}$ Assumption of normal distribution is violated.	Levene's test $F = 6.170$ $p = 0.014$	2-tailed Mann-Whitney U Test $U = 1061$ $p = 5.568 \times 10^{-33}$	Control condition: 127 + 1 mM 4-AP condition: 127	
4.2C	WT BDNF vs BDNF-GFP BDNF in conditioned media relative to WT BDNF	WT BDNF: N/A	N/A	Independent samples Kruskal-Wallis test $t = -13.500$ $p = 0.002$	WT BDNF: $n = 9$ BDNF-GFP $n = 8$ BDNF-pHluorin $n = 7$ BDNF-P2A-GFP $n = 7$	Bonferroni correction for multiple comparisons; significance deemed by $p < 0.0083$.
	WT BDNF vs BDNF-pHluorin BDNF in conditioned media relative to WT BDNF	BDNF-GFP $W = 0.983$ $p = 0.917$	N/A	Independent samples Kruskal-Wallis test $t = -6.143$ $p = 0.180$		
	WT BDNF vs BDNF-P2A-GFP BDNF in conditioned media relative to WT BDNF	BDNF-pHluorin $W = 0.745$ $p = 0.035$	N/A	Independent samples Kruskal-Wallis test $t = 8.286$ $p = 0.070$		
	BDNF-GFP vs BDNF-pHluorin BDNF in conditioned media relative to WT BDNF	BDNF-P2A-GFP $W = 0.867$ $p = 0.288$	N/A	Independent samples Kruskal-Wallis test $t = -7.357$ $p = 0.118$		
	BDNF-GFP vs BDNF-P2A-GFP BDNF in conditioned media relative to WT BDNF	Assumption of normal distribution is violated.	N/A	Independent samples Kruskal-Wallis test $t = -21.786$ $p = 0.000004$		

	BDNF-pHluorin vs BDNF-P2A-GFP BDNF in conditioned media relative to WT BDNF		N/A	Independent samples Kruskal-Wallis test $t = 14.428571$ $p = 0.00298$		
4.3C	BDNF-myc vs. BDNF-2myc TrkB phosphorylation WT cortical neurons E14.5, DIV5	BDNF-2myc $W = 0.944$ $p = 0.671$	N/A	One sample <i>t</i> -test $df = 6$ $t = -0.631$ $p = 0.551$	WT BDNF $n =$	Bonferroni correction for multiple comparisons; significance deemed by $p <$ 0.0125.
	BDNF-myc vs. BDNF-3myc TrkB phosphorylation WT cortical neurons E14.5, DIV5	BDNF-3myc $W = 0.863$ $p = 0.200$	N/A	One sample <i>t</i> -test $df = 5$ $t = -5.329$ $p = 0.003$	BDNF-2myc $n = 7$	
	BDNF-myc vs. BDNF-4myc TrkB phosphorylation WT cortical neurons E14.5, DIV5	BDNF-4myc $W = 0.902$ $p = 0.385$	N/A	One sample <i>t</i> -test $df = 5$ $t = -5.047$ $p = 0.004$	BDNF-3myc $n = 6$ BDNF-4myc $n = 6$	
	BDNF-myc vs. BDNF-P2A TrkB phosphorylation WT cortical neurons E14.5, DIV5	BDNF-P2A $W = 0.797$ $p = 0.108$ All data passes the assumption of normal distribution.	N/A	One sample <i>t</i> -test $df = 2$ $t = -0.747$ $p = 0.533$	BDNF-P2A $n = 3$	
5.2C	WT vs. Het, body weights (g) Males, 3 – 4-months old <i>Bdnf-P2a-Gfp</i> colony	WT $W = 0.947, p = 0.476$ Het $W = 0.811, p = 5.20 \times 10^{-5}$	N/A	Independent samples Kruskal-Wallis test $t = 6.886$ $p = 0.443$	WT $n = 16$	Bonferroni correction for multiple comparisons; significance deemed by $p <$ 0.025.
	WT vs. Hom, body weights (g) Males, 3 – 4-months old <i>Bdnf-P2a-Gfp</i> colony	Hom $W = 0.689, p = 0.001$ Assumption of normal distribution is violated.	N/A	Independent samples Kruskal-Wallis test $t = 5.044$ $p = 0.677$	Het $n = 32$ Hom $n = 9$	

WT vs. Het, body weights (g) Males, 6 – 7-months old <i>Bdnf-P2a-Gfp</i> colony	WT $W = 0.931, p = 0.347$	N/A	Independent samples Kruskal-Wallis test $t = -22.142$ $p = 0.023$	WT $n = 13$	Bonferroni correction for multiple comparisons; significance deemed by $p < 0.025$.
	Het $W = 0.892, p = 0.002$				
WT vs. Hom, body weights (g) Males, 6 – 7-months old <i>Bdnf-P2a-Gfp</i> colony	Hom $W = 0.879, p = 0.046$	N/A	Independent samples Kruskal-Wallis test $t = -26.685$ $p = 0.018$	Het $n = 35$	
	Assumption of normal distribution is violated.			Hom $n = 15$	
WT vs. Het, body weights (g) Females, 3 – 4-months old <i>Bdnf-P2a-Gfp</i> colony	WT $W = 0.557, p = 0.476$	N/A	Independent samples Kruskal-Wallis test $t = -1.130$ $p = 0.903$	WT $n = 10$	
	Het $W = 0.979, p = 1.7 \times 10^{-5}$				
WT vs. Hom, body weights (g) Females, 3 – 4-months old <i>Bdnf-P2a-Gfp</i> colony	Hom $W = 0.930, p = 0.519$	N/A	Independent samples Kruskal-Wallis test $t = -17.225$ $p = 0.206$	Het $n = 25$	
	Assumption of normal distribution is violated.			Hom $n = 8$	
WT vs. Het, body weights (g) Females, 6 – 7-months old <i>Bdnf-P2a-Gfp</i> colony	WT $W = 0.859, p = 0.149$	N/A	Independent samples Kruskal-Wallis test $t = 7.643$ $p = 0.558$	WT $n = 7$	
	Het $W = 0.887, p = 0.020$				
WT vs. Hom, body weights (g) Females, 6 – 7-months old <i>Bdnf-P2a-Gfp</i> colony	Hom $W = 0.935, p = 0.442$	N/A	Independent samples Kruskal-Wallis test $t = -24.399$ $p = 0.086$	Het $n = 21$	
	Assumption of normal distribution is violated.			Hom $n = 12$	

5.3B	WT vs. Het Hippocampal BDNF levels Relative to WT	Het $W = 0.942, p = 0.674$ Hom $W = 0.968, p = 0.881$ All data passes the assumption of normal distribution.	N/A	One sample <i>t</i> -test df = 5 $t = 0.259$ $p = 0.806$	WT $n = 6$ Het $n = 6$ Hom $n = 6$	
	WT vs. Hom Hippocampal BDNF levels Relative to WT			One sample <i>t</i> -test df = 5 $t = 1.622$ $p = 0.166$		
	WT vs. Het Cortical BDNF levels Relative to WT	Het $W = 0.999, p = 0.938$ Hom $W = 0.816, p = 0.152$ All data passes the assumption of normal distribution.	N/A	One sample <i>t</i> -test df = 2 $t = 1.678$ $p = 0.235$	WT $n = 3$ Het $n = 3$ Hom $n = 3$	
	WT vs. Hom Cortical BDNF levels Relative to WT			One sample <i>t</i> -test df = 2 $t = 1.436$ $p = 0.287$		
5.6	BDNF <i>Bdnf-P2a-Gfp</i> cortical neurons E17.5, 11DIV	Control condition: $W = 0.834, p = 1.043 \times 10^{-8}$ + 1 mM 4-AP condition: $W = 0.890, p = 1 \times 10^{-5}$ Assumption of normal distribution is violated.	Levene's test $F = 110.68$ $p = 1.45 \times 10^{-20}$	2-tailed Mann-Whitney U Test $U = 564$ $p = 1.26271 \times 10^{-24}$	Control condition: 93 + 1 mM 4-AP condition: 93	
	GFP <i>Bdnf-P2a-Gfp</i> cortical neurons E17.5, 11DIV	Control condition: $W = 0.910, p = 1.10 \times 10^{-5}$ + 1 mM 4-AP condition: $W = 0.921, p = 1.30 \times 10^{-5}$ Assumption of normal distribution is violated.	Levene's test $F = 25.83$ $p = 9.23 \times 10^{-7}$	2-tailed Mann-Whitney U Test $U = 621$ $p = 2.519 \times 10^{-23}$	Control condition: 91 + 1 mM 4-AP condition: 92	
6.6	Fos Rostral CA1	Control group: $W = 0.900, p = 0.161$	Levene's test $F = 0.999$	Independent samples <i>t</i> - test	Control group: $n = 12$	

		Experimental group: $W = 0.936, p = 0.339$	$p = 0.329$	$df = 22$ $t = 0.38$ $p = 0.97$	Experimental group: $n = 12$	Full behavioural cohort	
		All data passes the assumption of normal distribution.					
Fos Rostral CA3	Control group: $W = 0.977, p = 0.969$	Experimental group: $W = 0.963, p = 0.829$	Levene's test $F = 0.595$ $p = 0.449$	Independent samples t -test $df = 22$ $t = -0.58$ $p = 0.954$	Control group: $n = 12$		Experimental group: $n = 12$
Fos Rostral DGt	Control group: $W = 0.899, p = 0.152$	Experimental group: $W = 0.941, p = 0.507$	Levene's test $F = 4.639$ $p = 0.042$	Welch's t -test for unequal variances $df = 17.021$ $t = -2.721$ $p = 0.015$	Control group: $n = 12$		Experimental group: $n = 12$
Fos Rostral DGb	Control group: $W = 0.941, p = 0.508$	Experimental group: $W = 0.926, p = 0.338$	Levene's test $F = 4.013$ $p = 0.058$	Independent samples t -test $df = 22$ $t = -0.691$ $p = 0.497$	Control group: $n = 12$		Experimental group: $n = 12$
Fos Caudal CA1D	Control group: $W = 0.894, p = 0.133$	Experimental group: $W = 0.905, p = 0.185$	Levene's test $F = 4.912$ $p = 0.034$	Welch's t -test for unequal variances $df = 19.165$ $t = -0.922$ $p = 0.368$	Control group: $n = 12$	Experimental group: $n = 12$	

		All data passes the assumption of normal distribution.			
Fos Caudal CA1V	Control group: $W = 0.981, p = 0.987$ Experimental group: $W = 0.902, p = 0.169$ All data passes the assumption of normal distribution.	Levene's test $F = 0.645$ $p = 0.430$	Independent samples t -test $df = 22$ $t = -0.519$ $p = 0.609$	Control group: $n = 12$ Experimental group: $n = 12$	
Fos Caudal CA3D	Control group: $W = 0.939, p = 0.486$ Experimental group: $W = 0.880, p = 0.088$ All data passes the assumption of normal distribution.	Levene's test $F = 2.244$ $p = 0.148$	Independent samples t -test $df = 22$ $t = -0.381$ $p = 0.707$	Control group: $n = 12$ Experimental group: $n = 12$	
Fos Caudal CA3V	Control group: $W = 0.945, p = 0.568$ Experimental group: $W = 0.972, p = 0.926$ All data passes the assumption of normal distribution.	Levene's test $F = 2.864$ $p = 0.1$	Independent samples t -test $df = 22$ $t = 0.762$ $p = 0.454$	Control group: $n = 12$ Experimental group: $n = 12$	
Fos Caudal DGt	Control group: $W = 0.962, p = 0.816$ Experimental group: $W = 0.904, p = 0.176$ All data passes the assumption of normal distribution.	Levene's test $F = 2.049$ $p = 0.166$	Independent samples t -test $df = 22$ $t = -0.990$ $p = 0.333$	Control group: $n = 12$ Experimental group: $n = 12$	

	Fos Caudal DGb	Control group: $W = 0.863, p = 0.053$ Experimental group: $W = 0.859, p = 0.047$ Assumption of normal distribution is violated.	Levene's test $F = 1.074$ $p = 0.311$	Mann-Whitney U Test $U = 68.500$ $p = 0.840$	Control group: $n = 12$ Experimental group: $n = 12$	
6.7	Fos Rostral CA1	Control group: $W = 0.875, p = 0.246$ Experimental group: $W = 0.955, p = 0.780$ All data passes the assumption of normal distribution.	Levene's test $F = 0.142$ $p = 0.714$	Independent samples t - test $df = 10$ $t = -0.224$ $p = 0.827$	Control group: $n = 6$ Experimental group: $n = 6$	Reduced behavioural cohort to match BDNF analysis
	Fos Rostral CA3	Control group: $W = 0.911, p = 0.441$ Experimental group: $W = 0.963, p = 0.842$ All data passes the assumption of normal distribution.	Levene's test $F = 0.003$ $p = 0.958$	Independent samples t - test $df = 10$ $t = -0.194$ $p = 0.850$	Control group: $n = 6$ Experimental group: $n = 6$	
	Fos Rostral DGt	Control group: $W = 0.941, p = 0.666$ Experimental group: $W = 0.929$ All data passes the assumption of normal distribution.	Levene's test $F = 7.078$ $p = 0.024$	Welch's t -test for unequal variances $df = 5.725$ $t = -2.0803$ $p = 0.033$	Control group: $n = 6$ Experimental group: $n = 6$	
	Fos Rostral DGb	Control group: $W = 0.853, p = 0.167$	Levene's test $F = 0.201$ $p = 0.663$	Independent samples t - test $df = 10$	Control group: $n = 6$	

		Experimental group: W = 0.936, p = 0.624 All data passes the assumption of normal distribution.		$t = -1.037$ $p = 0.324$	Experimental group: $n = 6$
Fos Caudal CA1D		Control group: W = 0.909, p = 0.461 Experimental group: W = 0.870, p = 0.228 All data passes the assumption of normal distribution.	Levene's test $F = 0.982$ $p = 0.345$	Independent samples t -test df = 10 $t = -0.622$ $p = 0.548$	Control group: $n = 6$ Experimental group: $n = 6$
Fos Caudal CA1V		Control group: W = 0.908, p = 0.454 Experimental group: W = 0.940, p = 0.659 All data passes the assumption of normal distribution.	Levene's test $F = 3.076$ $p = 0.110$	Independent samples t -test df = 10 $t = 0.003$ $p = 0.998$	Control group: $n = 6$ Experimental group: $n = 6$
Fos Caudal CA3D		Control group: W = 0.985, p = 0.960 Experimental group: W = 0.938, p = 0.641 All data passes the assumption of normal distribution.	Levene's test $F = 0.085$ $p = 0.776$	Independent samples t -test df = 10 $t = 0.635$ $p = 0.539$	Control group: $n = 6$ Experimental group: $n = 6$
Fos Caudal CA3V		Control group: W = 924, p = 0.555 Experimental group: W = 0.933, p = 0.601	Levene's test $F = 7.884$ $p = 0.019$	Welch's t -test for unequal variances df = 6.707 $t = 0.640$ $p = 0.544$	Control group: $n = 6$ Experimental group: $n = 6$

		All data passes the assumption of normal distribution.				
	Fos Caudal DGt	Control group: $W = 0.937, p = 0.643$ Experimental group: $W = 0.916, p = 0.478$ All data passes the assumption of normal distribution.	Levene's test $F = 0.511$ $p = 0.491$	Independent samples t -test $df = 10$ $t = -0.465$ $p = 0.652$	Control group: $n = 6$ Experimental group: $n = 6$	
	Fos Caudal DGb	Control group: $W = 0.849, p = 0.190$ Experimental group: $W = 0.765, p = 0.028$ Assumption of normal distribution is violated.	Levene's test $F = 0.534$ $p = 0.482$	2-tailed Mann-Whitney U Test $U = 13.000$ $p = 0.423$	Control group: $n = 6$ Experimental group: $n = 6$	
	BDNF Rostral CA1	Control group: $W = 0.771, p = 0.031$ Experimental group: $W = 0.979, p = 0.946$ Assumption of normal distribution is violated.	Levene's test $F = 1.296$ $p = 0.282$	2-tailed Mann-Whitney U Test $U = 10.000$ $p = 0.200$	Control group: $n = 6$ Experimental group: $n = 6$	
	BDNF Rostral CA3	Control group: $W = 0.967, p = 0.875$ Experimental group: $W = 976, p = 0.928$ All data passes the assumption of normal distribution.	Levene's test $F = 0.155$ $p = 0.702$	Independent samples t -test $df = 10$ $t = 1.233$ $p = 0.246$	Control group: $n = 6$ Experimental group: $n = 6$	Reduced behavioural cohort

BDNF Rostral DGt	Control group: $W = 0.930, p = 0.580$ Experimental group: $p = 0.970, p = 0.893$ All data passes the assumption of normal distribution.	Levene's test $F = 0.421$ $p = 0.531$	Independent samples t - test $df = 10$ $t = 1.188$ $p = 0.262$	Control group: $n = 6$ Experimental group: $n = 6$
BDNF Rostral DGb	Control group: $W = 0.983, p = 0.966$ Experimental group: $W = 0.956, p = 0.789$ All data passes the assumption of normal distribution.	Levene's test $F = 0.119$ $p = 0.737$	Independent samples t - test $df = 10$ $t = 1.165$ $p = 0.271$	Control group: $n = 6$ Experimental group: $n = 6$
BDNF Caudal CA1D	Control group: $W = 0.894, p = 0.342$ Experimental group: $W = 0.850, p = 0.156$ All data passes the assumption of normal distribution.	Levene's test $F = 0.083$ $p = 0.779$	Independent samples t - test $df = 10$ $t = 0.744$ $p = 0.474$	Control group: $n = 6$ Experimental group: $n = 6$
BDNF Caudal CA1V	Control group: $W = 0.965, p = 0.843$ Experimental group: $W = 0.912, p = 0.450$ All data passes the assumption of normal distribution.	Levene's test $F = 0.213$ $p = 0.656$	Independent samples t - test $df = 9$ $t = -0.153$ $p = 0.882$	Control group: $n = 6$ Experimental group: $n = 6$
BDNF Caudal CA3D	Control group: $W = 0.952, p = 0.754$	Levene's test $F = 1.935$ $p = 0.194$	Independent samples t - test $df = 10$	Control group: $n = 6$

		Experimental group: $W = 0.913, p = 0.456$		$t = 0.422$ $p = 0.682$	Experimental group: $n = 6$
		All data passes the assumption of normal distribution.			
BDNF Caudal CA3V	Control group: $W = 0.948, p = 0.720$	Experimental group: $W = 0.978, p = 0.944$	Levene's test $F = 0.055$ $p = 0.820$	Independent samples t -test $df = 10$ $t = -0.353$ $p = 0.732$	Control group: $n = 6$ Experimental group: $n = 6$
BDNF Caudal DGt	Control group: $W = 0.944, p = 0.695$	Experimental group: $W = 0.870, p = 0.227$	Levene's test $F = 0.796$ $p = 0.393$	Independent samples t -test $df = 10$ $t = 1.098$ $p = 0.298$	Control group: $n = 6$ Experimental group: $n = 6$
BDNF Caudal DGb	Control group: $W = 0.938, p = 0.645$	Experimental group: $W = 0.906, p = 0.410$	Levene's test $F = 0.216$ $p = 0.652$	Independent samples t -test $df = 10$ $t = 0.619$ $p = 0.550$	Control group: $n = 6$ Experimental group: $n = 6$
		All data passes the assumption of normal distribution.			